Thermal room modelling adapted to the test of hvac control systems

Peter Riederer

ECOLE DES MINES DE PARIS

CSTB
le futur en construction
SUSTAINABLE DEVELOPM ENT

TU DRESDEN - Institut für Thermodynamik und TGA

N° attribué par la bibliothèque

|__|__|__|__|__|__|__|__|__|__|

Dokumentnummer

|__|__|__|__|__|__|__|__|__|__|

Thesis submitted in November 2001 for the combined degree of

"*Docteur*"	**and**	**"*Doktor-Ingenieur*"**
of the "Ecole des Mines de Paris"		**of the "TU Dresden"**
*Supervisor: Dominique **MARCHIO***		*Supervisor: Gottfried **KNABE***

Defended publicly at the "Ecole des Mines de Paris" by

Peter RIEDERER

28 of January 2002

THERMAL ROOM MODELLING ADAPTED TO THE TEST OF HVAC CONTROL SYSTEMS

Award committee

Jérôme **ADNOT**	ENSMP Paris, France	Committee president
Arthur **DEXTER**	University of Oxford, United Kingdom	Reviewer
Peter **GRUBER**	Siemens, Zug, Switzerland	Committee member
Christian **INARD**	University La Rochelle, France	Reviewer
Gottfried **KNABE**	TU Dresden, Germany	Reviewer
Dominique **MARCHIO**	ENSMP, Paris, France	Committee member
Jean-Christophe **VISIER**	CSTB, Champs, France	Committee member

PREFACE

This PhD is submitted in accordance to the conditions for attaining both the French and the German degree of a PhD, on a co-national basis, in the frame of a statement of the French government from January 18th, 1994.

The research has been carried out in the Automation and Energy Management Group (AGE), Department of Sustainable Development (DDD), at the "Centre Scientifique et Technique du Bâtiment" (CSTB) in Marne la Vallée, France, in collaboration with the "Centre Energétique" (CENERG) at the "Ecole Nationale Supérieure des Mines de Paris" (ENSMP), Paris, France.

The Technical University of Dresden (TUD), Germany has been the partner for the co-national supervision of the work.

This work could not have been completed without the support and help of many people and institutions, for which I am very grateful.

The supervisors have been Dominique MARCHIO from ENSMP and Jean Christophe VISIER from CSTB and I would like to express my gratitude for their guidance, advice and motivation during these three years.

I would like to thank Gottfried KNABE, supervisor from the TUD, for his guidance and effort in order to extend this PhD to a co-national diploma and for having accepted to review this work.

I am especially grateful to Arthur DEXTER for his hospitality, his support and many technical discussions during my visiting period at the University of Oxford, United Kingdom, and who also accepted both to be reviewer of this thesis and member of the award committee.

To Christian INARD from the University of La Rochelle, France, who reviewed this thesis and participated at the award committee, I would also like to express my gratitude.

Many thanks to Peter GRUBER from Siemens, Switzerland, for the fruitful collaboration in the SIMTEST project, for reviewing this thesis and for being member of the award committee.

Thanks also to Jérôme ADNOT, director of the Doctoral program at CENERG who has also accepted to be member and president of the award committee,

I would also like to thank Rofaïda Lahrech and Ahmad Husaunndee for many help and discussions concerning this work; furthermore thanks to Stéphane COUTURIER for the CFD analysis of the EREDIS test room.

I also would like to thank in no particular order:

- *Fabien BRUYAT, CSTB, for his various collaborations and his help,*
- *Jean Pierre QUENISSET, CSTB, for all his help to prepare the EREDIS test room,*
- *Hossein VAEZI-NEJAD and Mireille JANDON, CSTB, for technical discussion,*
- *Pierre RICHARD and Bruno BERTHINEAU, CSTB, for their help and advice,*
- *Jacques RIBERON and Bernard COLLIGNAN, CSTB, for technical discussions,*
- *Chantal PITZALIS and Marlène STRITTER, CSTB, for all administrational support,*
- *Philippe DUCHENE-MARRULAZ, CSTB, for the hospitality at the department of Sustainable Development,*
- *Anne Marie POUGIN,CENERG for all administrational help at the ENSMP,*
- *Renaud GICQUEL and Denis CLODIC, CENERG, for the hospitality at CENERG,*

Finally, I want to thank my parents, my family, my friends and Chay for accepting neglection of social contacts on my part and for supporting me in so many ways.

To my grandmother,

ABSTRACT: Room models, currently used for controller tests, assume the room air to be perfectly mixed. A new room model is developed, assuming non-homogeneous room conditions and distinguishing between different sensor positions.

From measurement in real test rooms and detailed CFD simulations, a list of convective phenomena is obtained that has to be considered in the development of a model for a room equipped with different HVAC systems.

The zonal modelling approach that divides the room air into several sub-volumes is chosen, since it is able to represent the important convective phenomena imposed on the HVAC system. The convective room model is divided into two parts: a zonal model, representing the air at the occupant zone and a second model, providing the conditions at typical sensor positions. Using this approach, the comfort conditions at the occupant zone can be evaluated as well as the impact of different sensor positions.

The model is validated for a test room equipped with different HVAC systems. Sensitivity analysis is carried out on the main parameters of the model.

Performance assessment and energy consumption are then compared for different sensor positions in a room equipped with different HVAC systems. The results are also compared with those obtained when a well-mixed model is used.

A main conclusion of these tests is, that the differences obtained, when changing the position of the controller's sensor, is a function of the HVAC system and controller type. The differences are generally small in terms of thermal comfort but significant in terms of overall energy consumption.

For different HVAC systems the cases are listed, in which the use of a simplified model is not recommended.
KEYWORDS: HVAC control, emulation, simulation, room model, zonal model, sensor position, convective room phenomena, performance assessment of room controllers, energy consumption, graphical programming

RÉSUMÉ: L'étude des régulateurs utilise à ce jour des modèles de zone à un seul nœud d'air. Un nouveau modèle de zone, distinguant les différentes positions possibles du capteur est développé dans cette thèse.

A partir d'une étude expérimentale en chambre climatique et de simulations sur code CFD, on établit la liste des phénomènes thermiques et aérauliques, à prendre en compte lors du développement du modèle pour différents systèmes de chauffage et de climatisation.

L'approche zonale, divisant l'air d'une pièce en plusieurs sous-volumes, est choisie car elle est bien adaptée pour tenir compte des phénomènes convectifs caractérisant les différents systèmes de chauffage et de climatisation. Le modèle de zone est divisé en deux parties : un modèle zonal représentant l'ambiance occupée et un modèle supplémentaire relatif aux emplacements du capteur. Ainsi on peut évaluer les conditions de confort dans la zone d'occupation et l'impact des différentes positions du capteur.

Le modèle est validé pour une cellule test équipée de différents systèmes de chauffage et de climatisation. Une analyse de sensibilité est ensuite menée afin de tester la sensibilité aux paramètres principaux du modèle.

La qualité de la régulation et la consommation d'énergie sont ensuite comparées pour différentes positions du capteur dans une pièce équipée de différents émetteurs et systèmes de climatisation. Les résultats sont comparés à ceux obtenus par un modèle à un nœud d'air.

La principale conclusion de cette thèse est que l'influence de la position du capteur est fortement fonction du système de chauffage et de climatisation et du type de régulateur. Les différences, en général négligeables en terme de confort de l'occupant, peuvent devenir importantes au niveau de la consommation d'énergie.

De ce fait, on peut définir pour quels systèmes de climatisation le modèle à un nœud d'air doit être remplacé par le modèle développé.
MOTS CLEFS: Régulation de température, simulation, modèle de zone, modèle zonal, position du capteur, phénomènes convectifs, performance d'un régulateur, consommation d'énergie, environnement graphique

KURZFASSUNG: In derzeitig für Reglerstudien verwendeten Raummodelle werden die Bedingungen im Raum als homogenes Gemisch betrachtet. Ein neues Modell wird entwickelt, welches unhomogene Raumbedingungen annimmt und zwischen verschieden Positionen des Sensors eines Raumtemperaturreglers unterscheidet.

Unter Verwendung von Messergebnissen und detaillierten Simulationen in Räumen mit unterschiedlichen Heizungs-und Lüftungssystemen wird eine Liste konvektiver Phänomene erstellt, welche bei der Entwicklung eines geeigneten Raummodells beachtet werden müssen.

Die Methode des Zonenmodells, welche die Raumluft in kleinere Volumina unterteilt, wird angewandt, um die charakteristischen konvektiven Phänomene verschiedener Heizungs-und Lüftungssysteme zu berücksichtigen. Das Raummodell beinhaltet zwei Teile: ein Zonenmodel, welches die Bedingungen im Aufenthaltsbereich des Raumes wiedergibt und ein Modell, welches die Bedingungen an verschiedenen Sensorpositionen reproduziert. Auf diese Weise können gleichzeitig der Komfort im Aufenthaltsbereich des Raumes sowie der Einfluss unterschiedlicher Sensorpositionen beurteilt werden.

Das Raummodell wird für einen Testraum mit verschiedenen Heiz-und Lüftungssystemen validiert. Eine Sensibilitätsanalyse der wichtigsten Parameter des Modells wird durchgeführt.

Regelungsqualität sowie Energieverbrauch werden schließlich für unterschiedliche Sensorpositionen in einem Raum mit verschiedenen Heiz-und Lüftungssystemen verglichen. Die Ergebnisse werden außerdem denen von einem vereinfachten Raummodell gegenübergestellt.

Zusammenfassend kann gesagt werden, dass die Differenzen für wechselnde Sensorposition stark vom jeweiligen Heiz- oder Lüftungssystem und aber auch vom Reglertyp abhängig sind. Die Differenz ist zwar oft unbedeutend bezüglich des thermischen Komforts, kann aber signifikant bei Betrachtung des Energieverbrauchs werden.

Für die untersuchten Heiz-und Lüftungssysteme werden die Fälle aufgelistet, in denen von einer Verwendung eines vereinfachten Modells abgeraten wird.
SCHLÜSSELBEGRIFFE: Regelung, Simulation, Raummodell, Zonenmodell, Sensorposition, Konvektion, Regelungsqualität, Energieverbrauch, graphische Programmierung

ABSTRACT

This thesis presents the development of a room model that is adapted to the study of the influence of sensor position on the control of HVAC systems in buildings.

Models, currently used for control studies, are very simplified. They consider the room air as perfectly mixed even when the prevailing conditions are not at all homogeneous. Other models, actually used for comfort studies, are not adapted to control studies since they do not allow the study of dynamic behaviour at small time steps.

The temperature measured by the sensor of a room temperature controller, generally placed outside the occupancy zone of the room, depends on the convective coupling of the room and its HVAC system.

The important phenomena, to be represented in the model, are analysed experimentally and by detailed simulation in this thesis. This analysis brings forward a list of convective phenomena that has to be considered in the development of criteria for the new room model. A phenomenon of negatively buoyant air flow, for example, is observed to be significant for the measurement of a controller's sensor.

Another important issue when testing controllers is the method used to assess the control performance. Since it makes no sense to use very detailed room models, if the method of performance assessment is insensitive to the way in which the room is modelled, both issues must be treated simultaneously.

In order to take into account both important thermal phenomena in a room and constraints of performance assessment of controllers, the zonal model approach, dividing the air of the room into several sub-volumes, is selected and is then adapted to the requirements of controller tests.

A new room model is developed that distinguishes between three typical sensor positions. It is validated for different HVAC systems and operating modes. Sensitivity analysis is carried out for the main parameters of the model.

Controller performance and energy consumption are compared for cases of different sensor positions for a single room equipped with different HVAC systems as well as for a whole building complete with its VAV system and other building services (e.g. sun-blinds, lighting etc.). The results are compared with those obtained using a well-mixed model.

A main conclusion of these tests is that the differences obtained, when changing the position of the controller's sensor, is a function of the HVAC system and controller type. The differences are generally small in terms of thermal comfort but significant in terms of overall energy consumption.

For different HVAC systems the cases are listed, in which a simplified model should not be used.

KEYWORDS

HVAC control, emulation, simulation, room model, zonal model, sensor position, convective room phenomena, performance assessment of room controllers, energy consumption, graphical programming

RÉSUMÉ

Un modèle de zone est développé dans cette thèse. Ce modèle est adapté à l'analyse de l'impact de la position du capteur d'un régulateur de systèmes de chauffage, ventilation, climatisation dans un environnement de simulation graphique modulaire.

Les modèles, couramment utilisés pour l'étude de la régulation, sont très simplifiés. Ils considèrent que l'air dans une pièce est parfaitement mélangé, ce qui ne correspond pas, dans la plupart des cas, à la réalité. Les modèles, utilisés pour l'étude du confort ne sont pas non plus adaptés à l'étude de la régulation qui s'intéresse au comportement dynamique à des pas de temps de simulation faibles. La température mesurée par le capteur est généralement différente de celle de la zone d'occupation et dépend fortement du couplage convectif entre l'air de la pièce et le système CVC installé.

Les phénomènes importants qui doivent être représentés sont déduits de l'expérimentation et de simulations détaillées. Un phénomène d'écoulement à poussée d'Archimède défavorable doit en particulier être représenté.

Une autre question importante pour le test de régulateurs est la méthode retenue pour l'évaluation de la performance d'un régulateur. Il n'est pas cohérent d'utiliser des modèles de zone très détaillés, si l'évaluation du confort n'est pas influencée par le choix du modèle.

L'approche zonale, divisant l'air d'une pièce en plusieurs sous-volumes, est choisie afin de tenir compte des phénomènes convectifs importants. Le modèle développé distingue trois positions typiques du capteur. Ce modèle est validé pour différents émetteurs et systèmes de climatisation et une analyse de sensibilité est menée sur ses paramètres principaux.

La qualité de la régulation et la consommation d'énergie sont comparées pour différentes positions du capteur dans une pièce, équipée de différents émetteurs et systèmes de climatisation, elle même incluse dans un bâtiment équipé d'un système à débit d'air variable. Les résultats sont finalement comparés à ceux obtenus avec le modèle à un nœud d'air.

La principale conclusion de cette thèse est que l'influence de la position du capteur est fortement fonction du système et du type de régulateur. Les différences, en général négligeables en termes de confort de l'occupant, peuvent devenir importantes au niveau de la consommation d'énergie. De ce fait, on peut définir pour quels systèmes de climatisation le modèle à un nœud d'air doit être remplacé par le modèle développé.

MOTS CLEFS: *Régulation de température, simulation, modèle de zone, modèle zonal, position du capteur, phénomènes convectifs, performance d'un régulateur, consommation d'énergie, environnement graphique*

KURZFASSUNG

Es wird ein Raummodell entwickelt, welches die Studie des Einflusses verschiedener Positionen eines Raumtemperatursensors auf die Regelung von Heizungs-, Lüftungs- und Kühlsystemen ermöglicht.

Modelle, derzeitig für Reglertests verwendet, sind größtenteils sehr vereinfacht indem die Raumluft als perfekt vermischt angenommen wird, obgleich dies unter realen Bedingungen keineswegs der Fall ist. Andere Modelle, für Komfortstudien entwickelt, sind für den Einsatz in Reglertests kaum geeignet, da diese ungenügend die dynamischen Zustände im Raum berücksichtigen und außerdem nicht den kleinen Zeitschritten in regelungstechnischen Simulationen angepasst sind.

Der Sensor eines Reglers befindet sich nur in sehr seltenen Fällen im Aufenthaltsbereich des Raumes. Die vom Sensor gemessene Temperatur ist daher ungleich derer im Aufenthaltsbereich und stark von der konvektiven Kopplung zwischen Raum und Heizungs- oder Lüftungssystem abhängig.

Die im Raummodell zu berücksichtigenden thermischen Phänomene werden experimentell und mit Hilfe detaillierter Simulationen analysiert. Eine Liste aller wichtigen Phänomene wird erstellt. Es wird zum Beispiel in vielen Heizfällen eine Warmluftströmung im Bereich des Sensors beobachtet, welche die Messung des Sensors beeinflusst.

Ein weiterer wichtiger Punkt bei der Erstellung eines Raummodells ist die Methode, mit welcher die Qualität der Raumregelung letztendlich beurteilt wird. Da es keinen Sinn macht, ein detailliertes Raummodell zu verwenden, wenn die Reglerklassifizierung nicht oder nur kaum von der Wahl des Raummodells beeinflusst wird, müssen Aspekte der Klassifizierungsmethode und der Sensorproblematik gleichzeitig mitberücksichtigt werden.

Daher wird das Prinzip des Zonenmodells, welches die Raumluft in verschiedene Zonen unterteilt, zur weiteren Entwicklung ausgewählt.

Das neue Modell unterscheidet zwischen drei typischen Sensorpositionen. Es wird für verschiedene Heizungs-und Lüftungssysteme validiert und die Sensibilität bezüglich der wichtigsten Parameter des Modells wird überprüft.

Regelungsqualität und Energieverbrauch werden für unterschiedliche Sensorpositionen, für den Fall eines einzelnen Raums mit verschiedenen Heizungs-und Lüftungssystemen, sowie für ein komplettes Gebäude mit einer variablen Volumenstromanlage und anderer Gebäudetechnik (z.B. Jalousien, Beleuchtung, etc.) verglichen. Die Ergebnisse werden außerdem denen von einem sehr vereinfachten Raummodell gegenübergestellt.

Zusammenfassend kann gesagt werden, dass die Differenzen für wechselnde Sensorposition stark vom jeweiligen Heiz- oder Lüftungssystem und aber auch vom Reglertyp abhängig sind. Die Differenz ist zwar oft unbedeutend bezüglich des thermischen Komforts, kann aber signifikant bei Inbezugnahme des Energieverbrauchs werden.

Für die untersuchten Heiz-und Lüftungssysteme werden die Fälle aufgelistet, in denen von einer Verwendung eines vereinfachten Modells abgeraten wird.

SCHLÜSSELBEGRIFFE

Regelung, Simulation, Raummodell, Zonenmodell, Sensorposition, Konvektion, Regelungsqualität, Energieverbrauch, graphische Programmierung

TABLE OF CONTENTS

LIST OF SYMBOLS

English letter symbols

$\dot{m}$	Flow rate	[kg/s]
A	Surface	[m²]
Ar	Archimedes number (Gr/Re²)	[-]
b	Thickness of plume	[m]
C	Constant for jets or plumes	[-]
cp	Thermal heat capacity of air	[J/(kg K)]
D, d	Thickness, diameter	[m]
E_0	Air entrainment ratio	[-]
f	Weighting factor for temperature in sensor zones	[-]
Gr	Grashof number	[-]
h	Convective heat transfer coefficient	[W/(m² K)]
H	Height	[m]
K, K'	Jet constant	[-]
L	Length	[m]
n	Exponent	[-]
R	Resistance, Radius	[K/W]
Re	Reynolds number	[-]
St	Stanton number	[-]
t	Time	[s]
V	Volume	[m3]
W	Width	[m]
x	Length	[m]
x0	Distance from the fictitious jet origin	[m]
y	Length in y direction	[m]
z	Height	[m]
z_0	Height of the fictitious plume origin	[m]
z_{max}	Penetration of jet	[m]

Greek letter symbols

λ	Conductivity	[W/(mK)]
Δ	Difference	[-]
β	Diffusivity	[m²/s]
Φ	Heat flux	[W]
θ	Temperature difference	[K]
ϑ	Temperature	[°C]
Θ	Weighting factor for temperature in boundary layer	[-]
α	Weighting factor for thermocouple measurement	[-]
δ_P	Penetration of jet	[m]

Subscripts

air	air
BL	boundary layer
cond	conductive
conv	convective, convector
em	emitter
ext, e	external
fresh	fresh air supply
gain	internal heat gain
heavy	heavy wall structure
i	current air sub-volume number
j	sub-volume adjacent to sub-volume i
jet	jet zone
light	light wall structure
mr	mean radiant
p	plume
rad	radiative, radiator
s	resultant
surf	surface
tot	total
transition	transition zone of the wall jet
w	wall
win	window

Matrices and vectors

A	Matrix of heat loss of sub-volumes by heat and mass flow (A1 – A4)
B	Matrix of heat gain of sub-volumes by heat and mass flow (B1 – B3)
C	Matrix of thermal masses of the sub-volumes
D	Matrix defining the outputs of the system
E	Matrix defining the outputs of the system
U	Disturbance vector
X	State vector
Y	Output vector

Abbreviations

AFM	Air Flow Matrix
AHU	Air Handling Unit
ASHRAE	American Society of Heating Refrigerating and Air-conditioning Engineers
BEMS	Building Energy Management System
BL	Boundary layer
CFD	Computational Fluid Dynamics

CSTB	Centre Scientifique et Technique du Bâtiment
CV	Convector
EREDIS	**E**nceinte de **RE**cherche sur la **D**iffusion de l'air et les **I**nteractions **S**ystème-Enveloppe
FCU	Fan coil unit
GRES	Comfort index (G=uniformity of ambience, R=radiative asymmetry, E=temperature difference between feet and head, S=floor temperature)
HVAC	Heating, Ventilating and Air Conditioning
MAXE	Maximum root square error
PMV	Predicted Mean Vote
PPD	Predicted Percentage of Dissatisfied
RMSE	Root mean square error
SIMBAD	Simulator for Building and devices
SV	Sub-volume
UCRES	Comfort index (U=uniformity of ambience, C=air drafts, R=radiative asymmetry, E=temperature difference between feet and head, S=floor temperature)
VAV	Variable air volume system
VL	Virtual Laboratory

INTRODUCTION

The expectation of occupants on indoor comfort is nowadays very high. This results in increasing constraints at the HVAC system in buildings and more and more sophisticated control systems. The latter have to provide the required comfort and to minimise the energy consumption of the HVAC systems.

Various studies have been carried out in order to reduce energy consumption and to improve comfort in buildings.

On the one hand dynamic simulation tools, with hourly time step, are used in studies on energy consumption for simulations on a yearly basis. They assume the conditions in a room as perfectly mixed.

Computational Fluid Dynamics (CFD) models, on the other hand, are used for comfort studies and the prediction of airflow in rooms as they provide detailed conditions in the room. Since CFD calculations are very time consuming, they are mostly used for static problems.

With the control of these systems getting more and more complex and integrating different building services, tools have to be developed in order to provide a new testing environment for the complex controllers.

The SIMBAD building simulator is an example of such a tool and is one step towards such a testing environment. It enables the connection between real control systems such as building energy management systems or room controllers to a virtual building with its HVAC system and different building services (e.g. sun-blinds, lighting, etc.). This "emulation", carried out on a weekly basis, provides then information about the performance of the control system.

The accuracy of the modelling of HVAC systems and building services in existing testing environments has already reached a high level. On the other hand, the modelling of conditions in the rooms of the building is still simplified to some extent. While conduction and radiation modelling is sufficiently detailed, convection modelling is usually poor and often assumes that the air in the room is perfectly mixed. Two main problems arise:

- *Where is a controller's sensor placed and what does it measure?*
- *Where and how is controller performance assessed?*

This thesis deals with the two aspects and presents the development of a room model that is adapted to controller tests and to study the influence of sensor position in building thermal control.

The model will be implemented in a toolbox of dynamic models of HVAC components. This toolbox aims at providing models of components that are "easy to use" and suitable for the design and test of control systems. It is designed in a commercial graphical environment to benefit from its technical computing environment and its readily available user-friendly interface.

In a first chapter, the interest of controller tests by simulation or by emulation is shown. The main objectives for the development of the room model are presented.

In the second chapter of the thesis, the important phenomena, to be represented in the model, are analysed experimentally and by detailed simulation. A large number of controller tests in real test rooms at CSTB and within a European Research project have been analysed in order to obtain criteria for different room geometries and HVAC systems. A list of convective phenomena is gathered for the development of criteria for the new room model.

In a third chapter, criteria for the room model, regarding both sensor measurement and performance assessment, are developed. Taking into account these both main groups of criteria, an appropriated model type for controller tests is chosen for further development.

The fourth chapter deals with the development of the room model. The necessary elements for the model are selected and integrated into the model. The model is validated for a room equipped with different HVAC systems and sensitivity analysis is carried out for the main parameters of the new model.

The last chapter consists of an application of the new model to a single room with different HVAC systems and a whole building, equipped with a VAV system and other building services (e.g. sun-blinds, lighting etc.). Controller performance and energy consumption is analysed for different sensor positions. The results are compared to those obtained using a well-mixed model.

CHAPTER I

CONTEXT AND OBJECTIVES

Controllers of HVAC systems in buildings on the room level (terminal controllers) as well as on the building level (Building Energy Management Systems - BEMS) get more and more sophisticated.

The development and test of these complex control systems raises new questions such as:

- *Where can these complex controllers be tested?*
- *How can the performance of these controllers be evaluated?*

Using virtual laboratories (VL) offers a flexible tool for the development and test of controllers. Various advantages of such a test environment will be explained in a first part of this chapter.

*In different places toolboxes of models of building and **H**eating, **V**entilation and **A**ir **C**onditioning (HVAC) systems are in development in order to provide a tool for the test of controllers of these systems. The models have to be user-friendly, simple and valid. A second part of this chapter lists the rules for the development of the models included in these toolboxes.*

The main question for controller manufacturers, probably the main group of potential users, is the validity of these VL. The main element of any test of thermal building controllers is the room model. While other models have been improved and adapted to control studies, the room model is still very simplified due to the complexity of the phenomena nevertheless it has an important effect on all other parts of the system. A room model, suitable for controller tests, is developed in this thesis.

The main objectives of the thesis are discussed in a third part of this chapter. Starting with an analysis of convective room phenomena, the needs for a new model are studied regarding its use for controller tests.

1. INTRODUCTION TO HVAC BUILDING CONTROL

In modern buildings, HVAC systems as well as lighting/shading systems control the internal conditions such as temperature, humidity, pollutants or illuminance. The systems have to guarantee comfortable and healthy conditions for the occupants in the rooms and, at the same time, reduce energy consumption without creating uncomfortable conditions for the occupants.

The control of the systems is generally represented by a control loop similar to that shown in Figure I - 1.

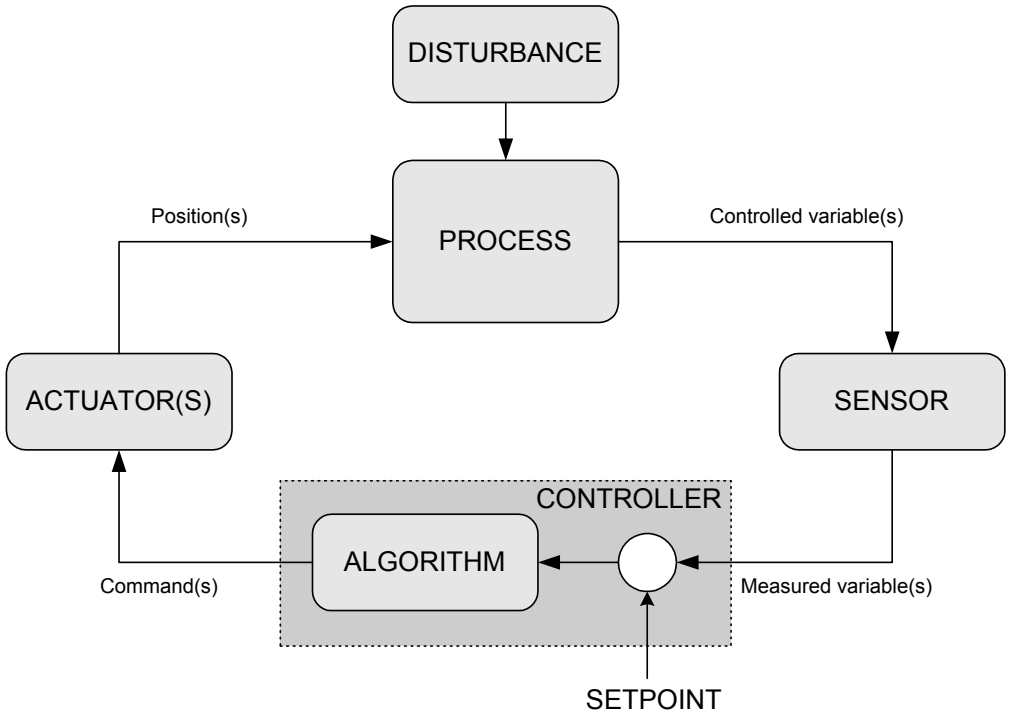

Figure I - 1: General principle of a control loop

The control loop includes a controller, an actuator, the process to be controlled, disturbances of the process and a sensor measuring the controlled variable(s).

The variables measured by the sensor are compared with a set point value. An algorithm outputs a command signal that is transferred via the actuator to the process, disturbed by conditions outside the process. In addition to open loop commands, different closed-loop algorithms can be used ([ASHRAE97], [Knabe92]):

- On/Off controllers
- P controllers (proportional)
- PI controllers (proportional-integral)
- PID controllers (proportional-integral-differential)
- Fuzzy controllers

In the case of HVAC systems, the process can be observed on different levels of the HVAC system (cf. Figure I - 2):

- Control on the room level (e.g. control of the terminal unit of a Variable Air Volume (VAV) system)

  The conditions (e.g. temperature) in the rooms or groups of rooms (building zones) are controlled. The process can either be thermal, flow or lighting phenomena in the rooms. The sensor is placed somewhere in the room and measures conditions as for example temperature or humidity. The actuator is for example a valve, interacting on the hot water flow rate through a radiator.

- Control central unit (e.g. control of the central Air-Handling-Unit of a VAV system)

  The central part of a HVAC system, for example a VAV system, provides the air needed for the conditioning of the zones, distributed to the terminal units of the building zones. Different controllers act on fans, valves, pumps or dampers, installed in the AHU.

- Supervisory control (supervision of the two previous groups)

  Depending on superior criteria (e.g. total building energy consumption or time dependent tariffs), this controller has the possibility of interaction on control signals from the two first levels.

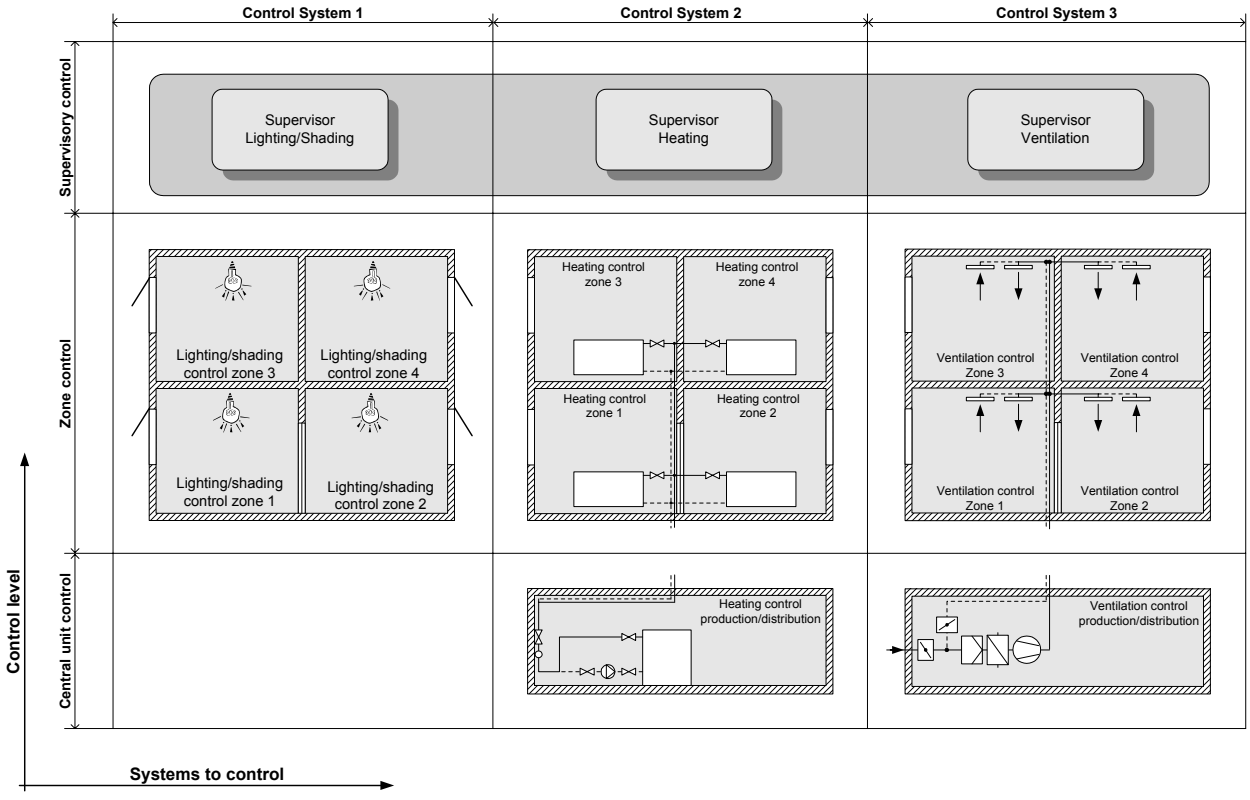

Figure I - 2: Example for different levels of building control

The trend in the development of HVAC controllers changes from optimisation of individual control to the aspects of total building control (e.g. Building Energy Management Systems BEMS).

In recent developments, independent systems controlling different phenomena are combined. In a European research project INTECOM [Husaunndee01], integrated HVAC-shading-lighting

control is developed. Supplementary control interactions are so added between the different systems.

The time range from a new idea to an available product on the market is decreasing more and more, while the complexity of the products increases. This increasing complexity is mostly due to the development and integration of controllers on all levels of building control or even the interaction of control of several building systems.

At the same time, more attention is paid on the comfort in the rooms. The controller(s) has (have) to guarantee comfort conditions in the occupant zone.

For this purpose, testing methods for the controllers have to be developed permitting to test controllers from the early development stage to the final product. The different control systems as well as different levels of the control systems have to be tested separately or combined in order to get detailed information about the performance of the control.

2. TEST OF HVAC CONTROLLERS

Most components of HVAC systems are classified in their performance using standard tests (e.g. EN 215-1 for thermostatic valves). No comparable standards exist to date in order to test and classify control systems, neither for terminal controllers nor for building controllers.

In the following two sections the main questions for testing controllers are raised, on the one hand for terminal controllers and on the other hand for building controllers.

2.1 TEST OF HVAC TERMINAL CONTROLLERS

Room controllers exist for all current HVAC systems as e.g. radiators, convectors or fan coil units. They are characterised by different control algorithms and they use different sensors and sensor positions for the measurement of the variable to control.

The whole system can be divided into the following parts of the control loop (Figure I - 3):

- Room
- Sensor
- Controller
- Actuator (and eventually a valve or a switch)
- HVAC component

A test of such a system raises a large number of questions, partially represented in Figure I - 3, a revised scheme of the control loop:

- what variables should be tested (temperature, humidity, draft, etc.)
- is the controller considered as an independent component or as a combined system including the sensor, the actuator and the valve?
- where and how has the control loop to be divided, if only a part of the control loop is tested?
- what HVAC system (manufacturer and size) is used?
- in what room are the controllers tested (size and type)?
- where is the controller's sensor placed?
- at what position(s) is the performance of the controller assessed?

- how can performance be assessed?
- what test procedure is used ?
- how are the results used for classification of controllers?

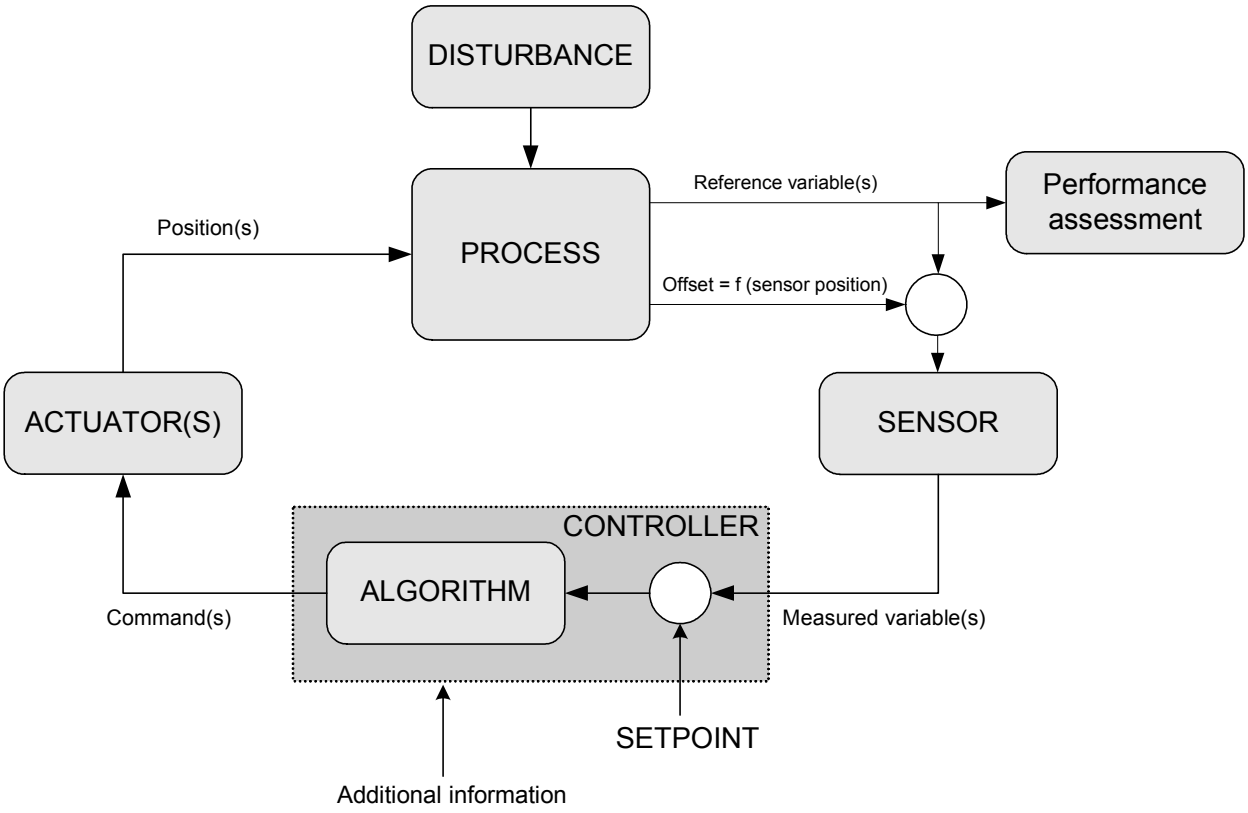

Figure I - 3: Revised scheme of a control loop

2.2 TEST OF HVAC BUILDING CONTROLLERS

While the test of HVAC terminal controllers already raises a certain number of questions, it is even more problematic when HVAC building controllers shall be tested. These complex control systems include a large number of control variables so that their test raises a number of supplementary questions, additional to those of the single room tests.

The aim of particular BEMS systems can be different, from maintaining comfort conditions to minimising energy consumption or taking into account periods of low tariffs. It is thus difficult to define a standard procedure for the performance assessment of this kind of control.

A test of these controllers starting from the criteria of the manufacturer makes more sense. The manufacturer can define his specific test procedure and criteria of evaluation for the improvement of the product.

The tests can principally be carried out using real components or using simulation techniques as compared hereunder.

2.3 REAL TEST ENVIRONMENT FOR CONTROLLER TESTS

The applicability depends on the controller level (cf. Figure I - 2) to be tested. While a test of controllers on the room level is possible in test cells, the test of central or supervisory controllers is very difficult if not even impossible. The more complex the controlled system, the more difficult the test of used control devices is.

In general, a real test provides the following advantages:

- Test of controllers in a real environment,
- Test of the whole control loop (sensor, controller, and actuator).

The disadvantages on the other side are:

- Boundary conditions (surface temperatures, water/air inlet, solar radiation, internal gains,…) are difficult to manage since controller tests create dynamic zone conditions. Repeatability is not guaranteed from one test to another.
- Building parameters (e.g. heavy/light construction) can only be changed with considerable effort and time (new construction would be necessary).
- Disturbances (e.g. occupancy and weather) are difficult or impossible to manage.
- Testing time is very large.
- The test of buildings with several rooms cannot be carried out with a total managing of load profiles (real but unpredictable profiles - no predefined tests possible).
- Enormous measurement effort is necessary for sufficient test monitoring.
- Extremely high testing costs.

Real tests bring visibly many disadvantages. While the use of a real test environment would be possible, with some difficulties, for terminal controllers, it would be very difficult to realise for tests of BEMS controllers.

2.4 USE OF VIRTUAL LABORATORIES FOR THE TEST OF CONTROLLERS

A promising alternative for a real test environment is a virtual laboratory able to test real or simulated controllers in a virtual test environment. Its advantages and inconveniences are studied in the following sections.

2.4.1 PRINCIPLE OF A VIRTUAL LABORATORY

Virtual laboratories use simulation models in order to replace a “real” part of a system by a simulated test environment. Virtual or real controllers can be tested using a virtual laboratory by simulation (whole system is virtual) and by emulation (part of the system is real) respectively. Figure I - 4 shows the principle of the test of real controllers using emulation technique and the two main parts of the virtual laboratory:

- Virtual representation of a part of the system
- An interface which ensures the dialogue between real part and virtual part of the system

The particularity of the virtual laboratory is the use of the "input/output interface". On the one hand the conditions to be controlled (e.g. room temperatures) are transferred from the simulated building e.g. in form of voltages to the controllers (in order to replace the sensor signal). On the other hand the controller commands are transferred to the actuators (real or virtual) and the impact on the building is taken into consideration in the simulation.

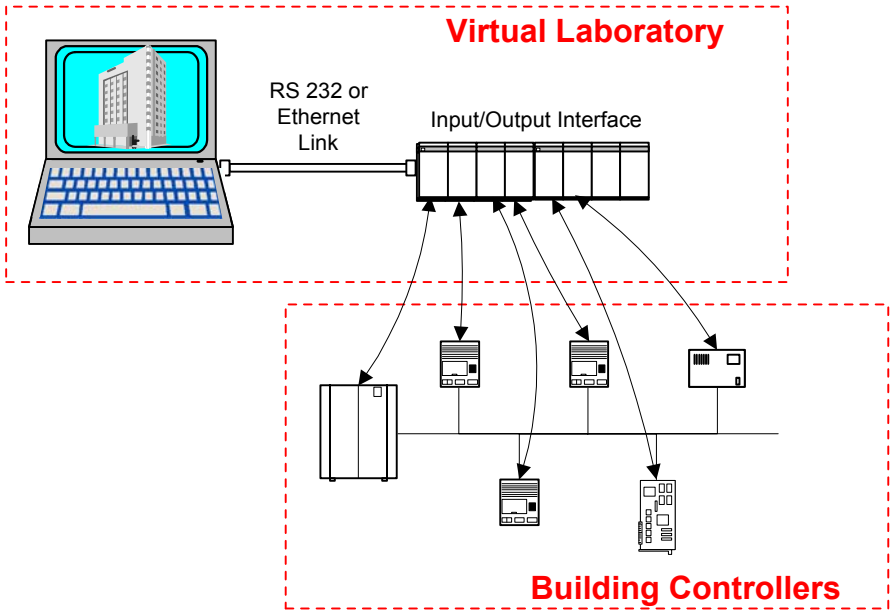

Figure I - 4: Principle of a virtual laboratory used for the test of real building controllers

The run time of the simulation model of the virtual laboratory has to be slowed down in order to permit a test in real time.

In the case of the test of simulated controllers, the input/output interface disappears and the building is directly connected to the controllers.

Controller tests using a virtual laboratory provide an enormous flexibility for the user. Various applications are possible by simulation and by emulation:

- Development of new control strategies or algorithms for different buildings in the virtual laboratory (simulation),
- Optimisation of controller parameters for a given simulated building (simulation or emulation),
- Test of controller prototypes for different simulated buildings (emulation),
- Test of any existing (real) controller for different simulated buildings (emulation),
- Comparison of different controllers for an existing system (simulation or emulation).

2.4.2 CRITERIA OF MANUFACTURERS FOR VIRTUAL LABORATORIES

Since the early 80', the control manufacturers developed their own virtual laboratories for specific purposes. An example is the micro-controller based polyvalent heating system simulator PVHS ([Gruber86]).

In the meantime, computer technology changed dramatically. Commercially available hardware and software of today facilitate the development, implementation and usability of virtual laboratories.

Various simulation models or virtual laboratories exist to date ([Dexter94], [Mathews99], [Haves98], [Hong97], [Husaunndee00], [Kast98], [Osman96], [Vaezi97a], [Visier00], [Wang99]). Their main problem is the restricted usability due to complex models and model parameters that are difficult to obtain. [Hus98] carried out an inquiry with 27 companies on the HVAC field in order to characterise the interest of manufacturers for the use of VL and the criteria important for these VL.

According to the study, 45% of the companies use simulation tools. 17% of the non-users would be interested in simulation, if there was a tool that is suitable to their purposes.

61.5% of the users of simulation tools apply simulation to develop their products without taking into account the interconnection of their product with the system to which they are connected. The rest take into account phenomena of system interaction. This group of users is mainly composed of companies working on the control field where the study of the interactions of their product with the system is of major importance.

Among the users, simulation is actually used for two main purposes: the design (92%) and the test (54%) of products, the principal parts in the development of a product.

The major criteria for used simulation tools are given as:

- Validity of the simulation models
- Easy parametering
- Easy comprehension
- Modularity
- Possibility of modification
- Possible interconnection with other models
- Hybrid simulation (mixing of discrete and continuous models [Stateflow00])

The study showed also the demand of the non-users of simulation tools for the use on PC's.

2.4.3 APPLICATION OF A VIRTUAL LABORATORY TO CONTROLLER TESTS

Compared with a real test environment, the virtual laboratory offers several advantages, reducing enormously many of the problems of controller tests. The advantages are:

- Cheap installation and test,
- Perfect control of all boundary and test conditions by the user,
- Flexible parametering of the test-building concerning structure, size, use, loads, system equipment, …
- Minimisation of test time (simulation),
- Monitoring of test conditions is not limited by sensor number (data acquisition),

- no sensor calibration necessary,
- Perfect test monitoring since all test data are available,
- Easy test automation,
- Possibility of sensitivity analysis for system or controller parameters,
- Possible choice of different representative systems or buildings (e.g. heavy/light structure) and easy adaptation to actual building technology.

On the other hand, the virtual laboratory presents risks that are to be considered:

- Test of controller under unrealistic conditions,
- Error introduced by breaking up of the real control loop (input/output interface),
- Insufficient level of modelling of system components in the control loop (emitter, building model, sensor etc.),
- Risk of false interpretation due to extremely large number of available data.

The last point is in common with controller tests in a real test environment.

To date, virtual laboratories are used in several research projects. Each of them underlines the advantages and large domain of application of the VL:

- SIMTRAIN [Arditi98]: Simulation models are used for training and education on the control field. The training tool can be used from users with various level of knowledge.
- SIMTEST [Lahrech01], A virtual laboratory is used in order to test individual room controllers. The VL consists of a building with only one zone.
- SIMBAD, QUALISIM ([Vaezi91], [Vaezi97b], [Vaezi00], [Riederer01c]), Building Energy Management Systems BEMS and several controllers are tested on a six-zone building.

The listed projects illustrate the large domain of application of a virtual laboratory. On the other hand, if a virtual laboratory is developed for such a large domain of application, the used simulation models have to be suitable to the concerned case.

In the SIMTEST project [http://ddd.cstb.fr/simtest], a test bench for room controllers has been developed. During the project several difficulties appeared due to the test rooms used for validation and due to the use of simplified simulation models, assuming the room air perfectly mixed ([Riederer00]). More suitable but also more complex models can partially solve the observed problems. The testing principle has also been proposed for a new standard for testing HVAC terminal controllers (*[CEN-TC247]*).

In the SIMBAD project on the other hand, the use of more complex models could introduce difficulties to handle the results due to the high number of available data.

Both concerns have thus to be solved simultaneously. The models used have to be able to provide enough data for tests on the room level. For the tests on the building level, solutions have to be provided defining the use of the more detailed information.

2.4.4 RULES FOR THE DEVELOPMENT OF A VIRTUAL LABORATORY

The SIMBAD building and HVAC toolbox [SIMBAD01], developed in the graphical simulation environment Simulink [Simulink98], is already used for virtual laboratories. In [Husaunndee97], [Husaunndee99a] and [Husaunndee99b] rules are developed for such a model toolbox. The rules have to be followed in order to keep the perfect modularity of the models.

All models are developed for the study of controllers. The models have thus to represent the dynamic phenomena with the necessary level of detail for this application.

The model library should be able to provide the user the assessment of:

- Performance of controllers
- Conditions in the occupant zones
- Air quality in the building zones
- Energy consumption of building zones and the whole building

The modularity of the models is based on a definition of interconnections between the models. The interconnections are similar to real interconnections as for example pipes or ducts. The assembly of models corresponds thus to the real system installation. The following vectors have been defined:

- Vector of air (temperature, absolute humidity, pressure, flow rate)
- Vector of water (temperature, flow rate)
- Heat transfer
- Electricity
- Weather data
- Busses containing information or controller commands

All inputs and outputs of the models of the library can be connected using these “standardised” vectors.

Main attention is paid on the parametering of the models. For many available models it is very difficult to obtain all necessary parameters. An approach using two types of models can solve this problem. If detailed information is available, detailed models can be used. As the data provided by the manufacturer catalogues contains only a restricted amount of information, simplified models are used in these cases.

An approach of typical and specific parameters is used. This concept permits the use of pre-defined files that contain all specific parameters. A new user can so obtain valid results without a detailed knowledge of the specific system parameters; however specialists can change them, if necessary.

The models themselves are, if possible, structured following the given rules. The experienced user can so understand the modelled phenomena. Static and dynamic parts of the models are separated, if possible.

In general, the use of pre-processors (e.g. [TRNSYS96]) for the determination of model parameters should be avoided. This makes the model easier to use and the parameters can be changed without difficult transfer of files or information between model environment and pre-processor.

3. MAIN OBJECTIVE AND WORK PLAN OF THE PHD THESIS

The thesis is focussed on the **development of a room model** as a first step towards a representative controller test. It represents the principal part of any test of thermal building control, on the room level and also on the building level.

Existing room models used for controller tests suppose the air in the zone completely homogeneous in temperature and humidity ([Kast98] [Rouvel97], [Vaezi97b]). This reduces some of the problems raised in §2. On the other hand, the coupling of the HVAC system or internal heat gains in the room and the room itself can produce inhomogeneous zone conditions. This has an effect on the result of the test of controllers and is neglected in the case of these simple models.

In [Riederer00], two room models have been tested for their use in control applications. These models were a well-mixed model and a second model with only two air sub volumes. The applicability of these models to controller tests has been shown. However, three main problems appeared while using them:

- the difference between centre and sensor temperature
- the validity of the models when varying emitter loads
- the sensor characterisation

The key points for all these problems are the conditions and phenomena in a room. In Chapter II, as a first step, the **room conditions** for different HVAC systems **are analysed** using a real test room and a "virtual" test room, a detailed Computational Fluid Dynamics (CFD) model. A **large amount of experimental results leads to a list of phenomena** that have to be considered for the development of a room model suitable for controller tests and able to simulate rooms with flexible geometry, type, and equipped with different HVAC systems.

In Chapter III, using the results from Chapter II, the key points of controller test are studied. Existing model types are compared in order to find a model type that is adapted to further development for the use in controller tests where the controller **performance** is **assessed** and the **sensor is placed at realistic positions**.

In Chapter IV, the new room model is developed and integrated in the graphical modelling environment. Validation and sensitivity analysis is carried out.

The development of the room model can be represented by Figure I - 5.

Finally, in Chapter V, the developed model is used in order to analyse the **improvement** of the room model **compared to classic models** in cases of controller tests.

For different HVAC systems, the **influence of the sensor position is analysed**.

The room model as an important part of a complete building is studied in a third part of Chapter V. For a Variable Air Volume (VAV) system, **the impact of the sensor position and model type is studied regarding performance assessment of the controller as well as energy consumption**.

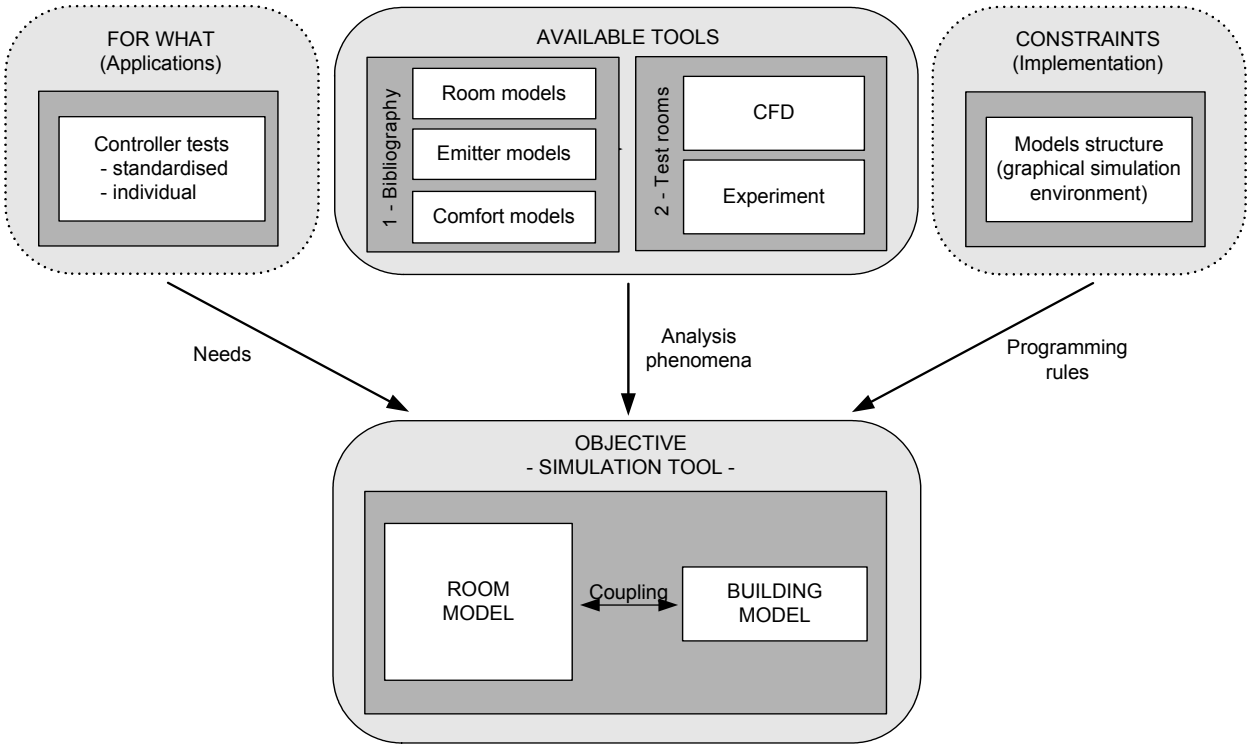

Figure I - 5: Main objectives of the study

4. CONCLUSION CHAPTER 1

An introduction to HVAC control and controller tests has been given. The main question appearing in controller tests have been raised.

The high potential of the use of virtual laboratories for controller tests, compared to tests in a real environment, has been shown. Except some acceptable inconveniences, the VL offers a great number of advantages that make their use very interesting for research laboratories as well as for manufacturers.

The VL permits both the development of new control strategies on the room and on the building level, and the test of controllers (real or simulated). It can also be used for a standardised performance assessment proposed in standardisation committees, e.g. [CENTC247].

The SIMBAD building and HVAC toolbox is an example of a first step towards a virtual laboratory. The structure of all implemented models is adapted to this existing toolbox in order to provide adequate modularity. Rules for structuring the models of the toolbox in the graphical environment and method of parametering of the models are main steps to make models easy to use. The VL becomes thus interesting for various kinds of users.

As a main part of a VL in the test of terminal controllers and of BEMS systems, a new room model is developed in this thesis. [Riederer00] listed problems of existing room models when used for controller tests. Representing the link between the virtual world (system) and the real world (tested controller), it has to be developed in a suitable level of detail considering the needs of a controller test in a virtual laboratory. The needs of the potential users, manufacturers and research laboratories, have to be taken into account as well.

CHAPTER II

ANALYSIS OF PHENOMENA IN A HEATED, COOLED OR AIR-CONDITIONED ROOM

As shown in Chapter I, controller tests with assessment of controller performance raise two main questions:

- *where is a controller's sensor placed and what temperature(s) does it measure?*
- *at which reference position and how is performance assessed?*

In "well-mixed" models both temperatures are identical. The temperature controlled by the zone temperature controller is the same as the temperature used for the performance assessment.

In reality, both temperatures are often different. The difference between both is due to convective phenomena and to the asymmetry of radiation in the room. Controller tests using a simplified model may not be accurate enough.

The asymmetry of radiation can generally be well represented by the use of suitable models for the wall structure (conductive and radiative models). Several models have been tested and studied in previous research ([Brau80], [Roux84]).

On the other hand, convective phenomena have been researched for the issue of comfort in buildings, but never for their importance for controller tests.

In this Chapter, convective phenomena in rooms are studied. Besides their influence on the temperature of the wall structure, they are responsible for any temperature non-homogeneity in a room. The results are used as a basis for the development of a list of criteria (Chapter III) to be considered for the development of models for control studies.

The analysis, carried out mainly in the EREDIS tests cell at CSTB, helps to generalise convective phenomena in a room in order to obtain a simple model, able to represent the most current cases of HVAC systems.

The study is carried out for steady state as well as for transient conditions using measurement and simulation (CFD).

1. GENERAL AIRFLOW PATTERNS IN ROOMS

There are two important positions in a room for the assessment of controller performance: the occupant position and the position near the internal walls, where a controller's sensor is usually placed. The air temperature at both positions depends strongly on the airflow pattern in the zone.

The airflow in a zone can be divided into two main groups:

- ☞ Airflow due to convective sources or air inlets (airflow generators)
- ☞ Airflow at walls (indirect generators)

The first group, convective phenomena from heat sources or air inlets, has been subject of several studies. [Horwarth80], [Inard88], [Bouia93], [Blay93], [Allard90] and [Barles94] studied convective phenomena of radiators and convectors, with and without fresh air supply in the room. [Ngendeku88] and [Maalej94] proposed correlations for stratification in rooms with convective heat sources. [Kherrouf95] and [Peng96] studied a room equipped with a fan coil unit in cooling and heating mode. Several studies are available about isothermal and non-isothermal jets in rooms ([Abr63], [Raj76], [Schw61], [Grim93], [Chen80], [Alb74], [Goldman86], [Kapoor88], [Riberon83] and [Buchmann95]). [Simoneau89] studied the interaction between natural and forced convection (air jet) in rooms.

For the air flow at walls, the problem is different: depending on the temperature difference at the walls and on the general airflow in the room, the airflow can change in direction and flow rate. It is helpful to divide the flow near walls into the following groups:

- ☞ Natural convection boundary layer (no convective heat sources in the room)
- ☞ Negatively or positively buoyant air flow due to air flow "generators" in the room (convective heat sources or non-isothermal ventilation in the room)

The first type of airflow is observed in the case of high temperature differences at the walls combined with the absence of convective heat sources in the room. The boundary layer of natural convection is, in this case, not disturbed by other airflow in the room. [Allard87] studied this phenomenon for the case of a cooled or heated wall.

In the case of convective heat sources in the room, the airflow due to these sources can have a more or less important influence on the airflow at the internal walls of the room.

In the following, typical airflow patterns in rooms are listed as well as the possible phenomena at the internal walls. The given airflow patterns are partly taken from real tests carried out in a European project ([Lahrech01] and [Hediger01]) and from other authors ([Peng96], [Inard88], [Inard90], [Allard87], [Laret80], [Barles94]). Starting with these sources it is tried to generalise the problem for different kind of emitters.

The typical airflow pattern for a room without convective heat sources is shown for the winter case (Figure II - 1) and for the summer case (Figure II - 2):

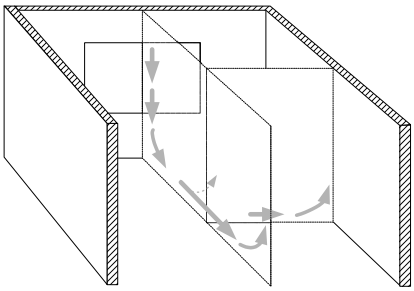

Figure II - 1:General airflow pattern: no air emitter, winter case

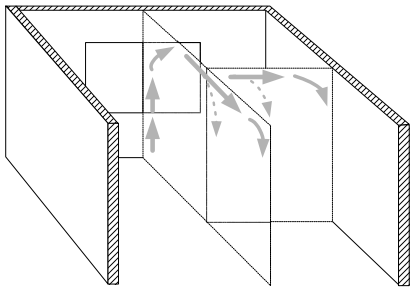

Figure II - 2: General airflow pattern: no air emitter, summer case

The airflow is, in both cases, generated by a temperature difference between the surface temperature of the “external» wall and the room air. The air is cooled (winter case) or warmed up (summer case) at the external wall and a downward (winter case) or upward (summer case) flow is generated. The cold/warm air arrives at the floor or the ceiling and is then distributed towards the other room walls.

If the airflow from the external wall is heated (floor heating) or cooled (chilled ceiling), it is possible that this airflow would be directly mixed to the air at the centre part of the zone instead of arriving at the surrounding walls (dotted flashes in Figure II - 1 and Figure II - 2).

Three other cases, typical for zone conditioning are presented. The are grouped as follows:

- Type 1: emitter placed at external wall emitting heat or blowing air such as convector, radiator or FCU (Figure II - 3 - Figure II - 5)
- Type 2: non-isothermal air introduction from ceiling for example by a VAV system (Figure II - 6 - Figure II - 8)

Besides the types defined beyond, the airflow pattern depends on a second parameter. The airflow created by the source is characterised by:

- positive buoyancy (airflow tends towards the ceiling)
- negative buoyancy (airflow tends towards the floor)

In the two extreme cases, the airflow reaches either the ceiling (positive buoyancy - Figure II - 3 and Figure II - 6) or the floor (negative buoyancy - Figure II - 5 and Figure II - 8) and is distributed to the centre air volume at the walls. In cases of lower buoyancy, the airflow from the source is mixed to the centre air volume before arriving at the walls (Figure II - 4 and Figure II - 7).

The typical airflow pattern of sources of type 1 is shown in Figure II - 3 - Figure II - 5. The group represents different emitters such as convectors, radiators or fan coil units in heating mode (Figure II - 3 and Figure II - 4) or fan coil units in cooling mode (Figure II - 4 and Figure II - 5).

The shown general airflow patterns, created by sources of convective heat or by air introduction, are generating the air flow near the walls. This means, if the general airflow pattern in the zone is known, conclusions can be made on the airflow near the internal walls where the controller sensor is placed.

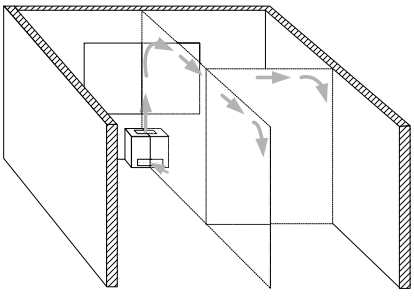

Figure II - 3: Airflow pattern: type 1 – high positive buoyancy forces

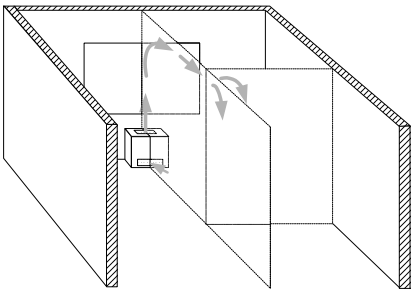

Figure II - 4: Airflow pattern: type 1 – low buoyancy forces

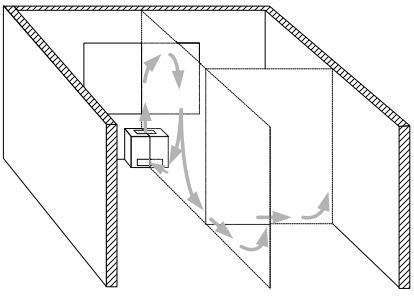

Figure II - 5: Airflow pattern: type 1 – high negative buoyancy forces

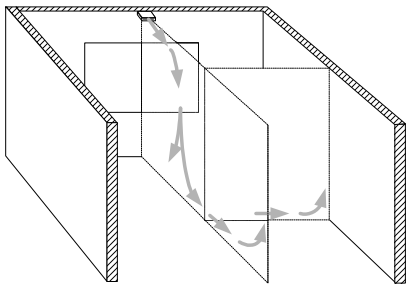

Figure II - 6: Airflow pattern: type 2 – high positive buoyancy forces

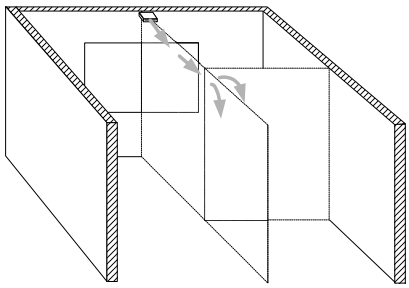

Figure II - 7: Airflow pattern: type 2 – low buoyancy forces

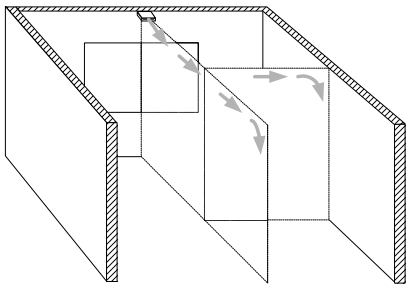

Figure II - 8: Airflow pattern: type 2 – high negative buoyancy forces

The same approach of generalised airflow patterns can be used for the airflow near the walls. In the case of no airflow at all in the room, a standard boundary layer of natural convection will be observed at the walls. The airflow in this boundary layer is a function of the temperature difference between wall and the air temperature.

In the case of a convective source in the room and a boundary layer at the walls, two possibilities for the resulting airflow near the walls exist:

- ☞ the airflow near walls is unfavourable for principal room airflow
- ☞ the airflow near walls is favourable for principal room airflow

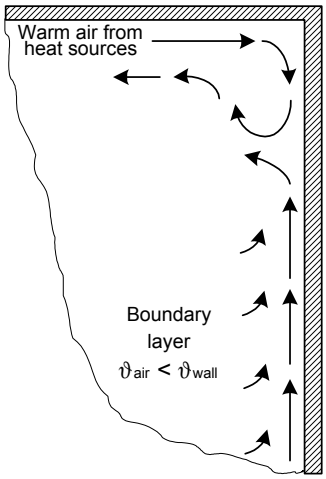

Figure II - 9: Airflow near walls: wall boundary layer unfavourable for zone airflow (zone heating)

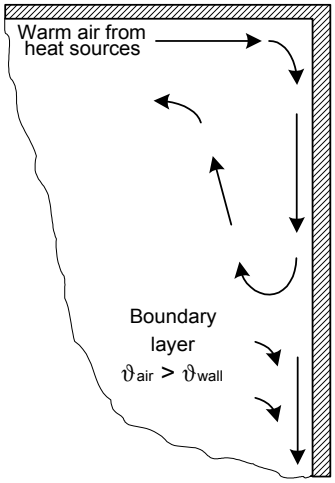

Figure II - 10: Airflow near walls: wall boundary layer favourable for zone airflow (zone heating)

Figure II - 9 and Figure II - 10 show favourable and unfavourable airflow for the example of room heating (high positive buoyancy forces). Figure II - 9 shows the case of a boundary layer unfavourable for the main room airflow. The natural convection along the walls stops the main airflow from a heat source, the warm airflow from the emitter is introduced directly to the upper volume of the room.

In the opposite case, the favourable airflow (Figure II - 10), the warm air from the ceiling is pushed downwards (against buoyancy forces) until a certain maximum height without the opposing force of the natural convection at the wall. [Goldman86] and [Kapoor89] carried out research on this kind of phenomenon. The maximum penetration of the warm air downward is

function of the conditions of the warm airflow at the ceiling and the conditions of the air in the room. This will be shown experimentally in the next section.

The described airflow patterns are only general assumptions. They can be wrong in the following cases:

- High ventilation rates (in this case they have to be assumed as jets and are so air flow generators)
- high internal gains (convective)
- furniture ([Nielsen99] studied the influence of room furniture on the principal air flow)
- complicated types of air introduction (these types are not of interest for controller tests of general HVAC systems)

The influence of each of these error sources on the airflow pattern has to be tested. In general it can be assumed that for heating cases the risk is lower than for cooling cases. A cold airflow near the floor for cooling cases for example is more sensible to furniture or high internal gains.

In the following sections these general phenomena are studied in detail using measurements in a real test room and detailed simulations.

2. DESCRIPTION OF TEST CELL AND MEASUREMENT DEVICES

2.1 THE TEST ROOM

The tests are carried out in the EREDIS (**E**nceinte de **RE**cherche sur la **D**iffusion de l'air et les **I**nteractions **S**ystème - enveloppe) test cell at CSTB (Figure II - 11). The test room is located in a hall with nearly constant temperature conditions. The room is tight enough to prevent significant airflow from the hall.

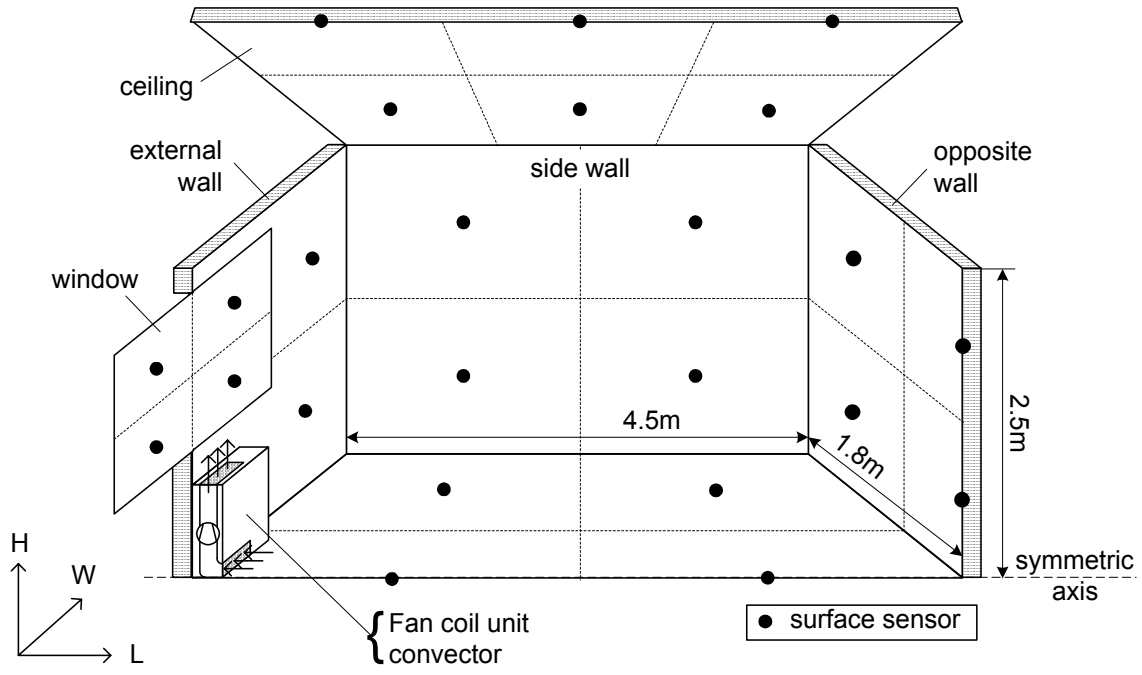

Figure II - 11: Scheme of the EREDIS test room with surface temperature sensors

The symmetrical test room measures 4.5m, 3.6m and 2.5m in **L**ength, **W**idth and **H**eight respectively. It is equipped with a water-flowed metal panel representing an external window that is cooled for winter conditions and heated for summer conditions. The size of this "window" is 1.4m in length and 3m in width. The surface temperature of the metal panel is assumed to be

equivalent to the internal surface temperature of a real window. It has thus to be chosen depending on the internal room temperature during the test and an estimated maximal temperature difference between external and internal conditions.

The construction of walls, floor and ceiling is shown in table 1:

Table 1: Physical properties of the room construction

Surface	Material (Inside → outside)		Thickness [mm]	Density [kg/m^3]	Specific heat [J/(kg K)]	Conductivity [W/(m K)]
Walls	Placoplan 60	Cardboard	8	700	1200	0.14
		Air	60	1.2	1006	0.19
		Cardboard	8	700	1200	0.14
	Polystyrene		100	30	1250	0.035
Floor	Wood		4	400	2700	0.12
	Metal panel		8	7700	470	40
	Water		10	1000	4186	0.56
	Polystyrene		100	30	1250	0.035
	Polyurethane foam		50	50	840	0.031
Ceiling	Wood		4	400	2700	0.12
	Metal panel		8	7700	470	40
	Water		10	1000	4186	0.56
	Polystyrene		200	30	1250	0.035

2.2 EMITTERS AND GAINS IN THE TEST ROOM

Two types of emitter are used for the tests: An electric convector and a fan coil unit (Table 2).

Both emitters are positioned on the symmetrical axis of the test room (Figure II - 11) and at the "external" wall, directly under the heated/cooled metal panel.

The electric convector is assumed to represent all cases of a convective heat source without mechanical ventilation. This means all kind of convectors and radiators (convective part of the radiator). For the tests, a convector with horizontal outlet is chosen.

The fan coil unit is a two-pipe / two-wire model, the air is heated by electrical resistance and cooled by water flowed cooling coil. The outlet air is ventilated only in vertical direction (90° to floor).

Table 2: Characteristics of the emitters and gains used for the tests

Emitters	Power [W]	Length [mm]	Height [mm]	Width [mm]	Ventilation [m^3/h]
Electric convector (CV)	Variable (0-2000)	750	400	100	0
Fan coil unit (FCU) - heating	1200	910	855	265	175 / 270 / 350
Fan coil unit (FCU) - cooling	Depending test	910	855	265	175 / 270 / 350
Internal gains					
Electric convector (CV)	Variable (0-400)	750	400	100	0

Some tests consider internal gains in the zone. They are "simulated" by an electric convector (Table 2). Its heat emission is adjusted depending on the case between 0W and 400W. The position of this convector is between the centre of the cell and the emitter and on the symmetrical axis.

2.3 MEASUREMENT OF SURFACE TEMPERATURES

The sensors, thermocouples of type T (copper/constantan), are integrated in the surfaces at a depth of about 0-0.5 mm from the surface using plaster. The sensors are positioned in the cell considering completely symmetric conditions (Figure II - 11). Only the sensors measuring the window surface temperature are positioned considering non-symmetric conditions (due to water inlet and outlet). The good position of all sensors is checked using an infrared camera (see appendix). The sensors are calibrated with accuracy better than 0.25K.

2.4 TOOLS FOR THE EVALUATION OF CONVECTIVE PHENOMENA IN THE TEST ROOM

Smoke tests are used for the observation of qualitative airflow patterns. Besides this study, measurements are used for quantitative analysis. Computational Fluid Dynamics (CFD) simulation ([Fluent98]) is used as a second qualitative tool. Both tools are described below.

2.4.1 MEASUREMENT OF AIR TEMPERATURES (QUANTITATIVE TOOL)

Two types of sensors are used for the air temperature measurement:

- Platinum-resistance thermometers
- Thermocouples

These two types of sensors are used in order to measure static and dynamic phenomena during the tests. The resistance thermometers (thickness 2mm of glass bulb) are used at the most representative positions (air temperatures at 1.5m height at the centre and at three sensor positions) for the evaluation of the temperature under static test conditions. For measurement under dynamic conditions and for the determination of temperature profiles, thermocouples of type T with a thickness of 0.1 mm are used to keep the response time of the sensor as small as possible (< 10sec.). The position of the sensors depends on the particular test and is indicated in the introduction of each test. For tests of a fan coil unit in cooling conditions, two platinum resistance thermometers are used to measure the inlet and outlet water temperature. In total, 5 resistance thermometers and 47 thermocouples are used to measure the air temperatures in the zone. The sensors are calibrated with accuracy better than 0.05K and 0.25K for resistance thermometers and thermocouples respectively.

The influence of radiation on the accuracy of the measurement is verified as follows: [Peng96] approximately describes the measured temperature by:

$$\vartheta_i = \alpha \vartheta_{air} + (1 - \alpha)\vartheta_{mr} \qquad (1)$$

For the used sensors, the value of α in equation (1) is obtained as 0.65 and 0.93 for resistance thermometer and thermocouple respectively. For a temperature difference between air and radiant temperature of 5K, this results in errors of 1.75K and 0.3K. The difference is due to the emissivities of the two sensor types. Radiation shields are used for the resistance thermometers in order to eliminate the error. The thermocouples are used without shields because they measure correctly the transient effects in the cell. For this, the steady state error can be neglected.

2.4.2 CFD SIMULATION OF AIR TEMPERATURES (QUALITATIVE TOOL)

Detailed simulations are carried out for the case of the fan coil unit (three fan speeds) in cooperation with another CSTB team. The results provide qualitative information about the conditions in the room. Measurements provide the boundary conditions for the model (Figure II - 12). The surfaces are assumed to be uniform in temperature.

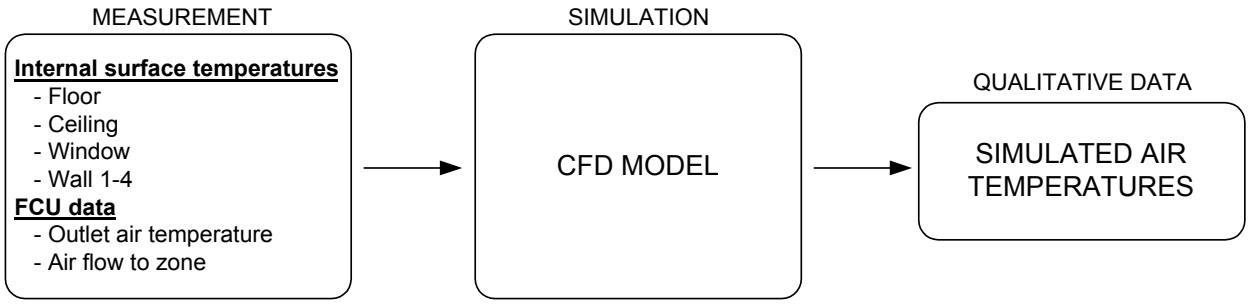

Figure II - 12: Simulation of zone air temperatures with CFD model from measurement data

The jet of the fan coil unit is supposed to be uniform in temperature and in velocity at the outlet of the fan.

A k-ε model is used expressing turbulent diffusivity in terms of the kinetic energy of turbulence k and the dissipation rate of kinetic energy of turbulence ε ([Launder74]).

The standard k-ε model that has been developed for high Reynolds numbers or high turbulence flow. In rooms, low turbulence regions can appear close to the boundaries and can be problematic. [Moser90] proposed thus low Reynolds models for the cases of free and mixed convection.

For this study, a revised k-ε model (k-ε "realisable" [Fluent98]) is used solving equations governing a 3D, turbulent, uncompressible and non-isothermal flow. The grid number is 85000 cells (55-45-35 / L-H-W).

The results are used to show qualitatively the air temperature throughout the room. Especially the temperature profile near the walls and in the comfort zone of the room is studied.

For the simulations, perfect room symmetry is assumed, and only one half of the room is simulated as shown in Figure II - 13 (with the fan coil unit on the left hand).

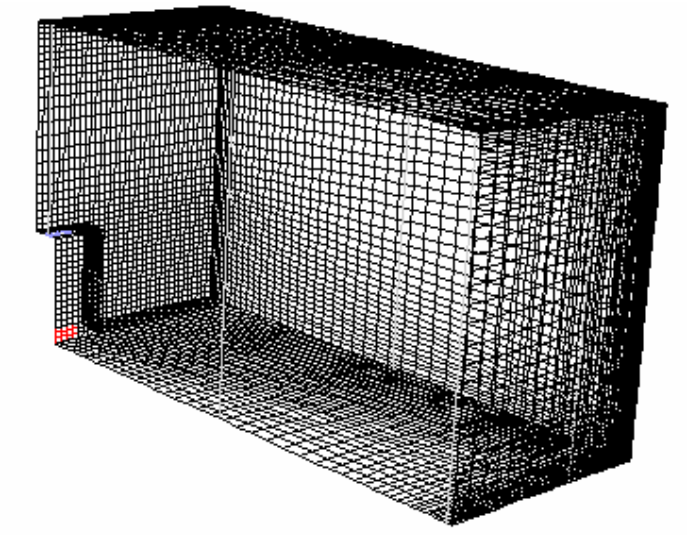

Figure II - 13: Grid of the used CFD model of the EREDIS test cell

3. ANALYSIS OF ZONE CONDITIONS – STEADY STATE PHENOMENA

3.1 OBSERVED AIRFLOW PATTERNS

Smoke visualisation experiments are carried out in the EREDIS test room. They should confirm the general airflow patterns described in §1 of this chapter that have been found in the literature and in preliminary tests in a European project ([Riederer99]).

The results are presented in two-dimensional diagrams since the airflow near the walls besides the external wall is observed to be similar to that shown on the symmetrical axis.

☞ No heating or cooling (cooled or heated window)

The experiments of the case without heating or cooling show the boundary layer at the window (temperature difference between 5 and 20K). At the three internal walls that are neither heated nor cooled (small temperature differences with changing sign), boundary layers are observed. Their direction (upwards or downwards) depends on the sign of the temperature difference between room air and surface of the internal walls (Figure II - 14 and Figure II - 15).

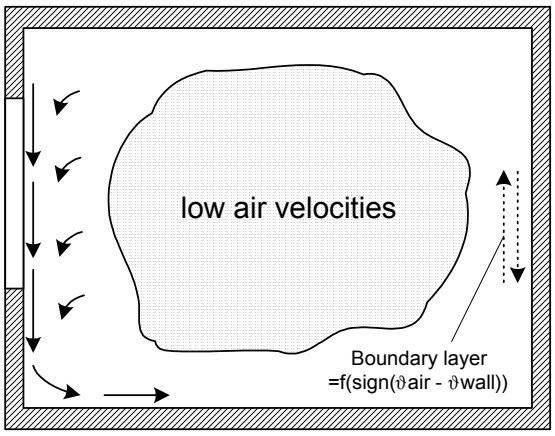

Figure II - 14: Airflow pattern in the EREDIS test room without heating (winter case)

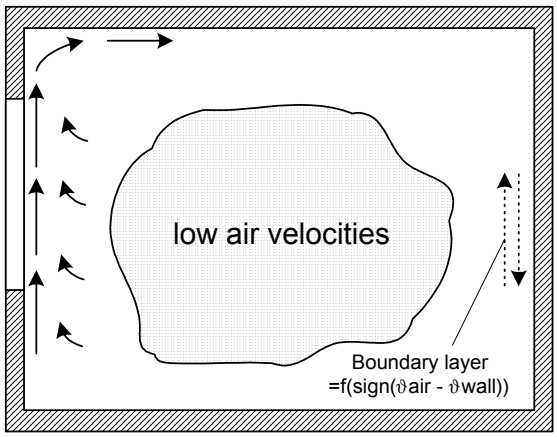

Figure II - 15: Airflow pattern in the EREDIS test room without cooling (summer case)

In the case of a favourable sign of the boundary layer, a slight effect of a wall jet (cf. §1) is observed. This will also be presented in § 3.3.2.

☞ Electric convector and Fan coil unit (heating)

In all heating cases, even for the case of an electric convector with low heat emission (400W), the effect of negatively buoyant flow is observed at the internal walls. In most of the cases, the temperature of the hall around the test room is lower than in the room itself. The boundary layer at the internal walls is, in these cases, in downward direction (Figure II - 16).

Only in some cases an upward boundary layer is observed. In these cases, the warm jet travels only a short distance downward at the internal walls and the warm air is directly injected into the upper air volume of the room. This special case can be observed in a slightly heated room with warm adjacent rooms.

At the external wall, two convective phenomena are observed. Above the emitter a warm jet or a plume is observed. On both sides of the emitter a cold, descending boundary layer is observed transporting cold air to the floor (not represented in Figure II - 16). This is the case in the used test cell, since the emitter has a width of 0.75m while the cold window has a

width of 3m. In the optimal case of emitter sizing ([Bauer99]), the length of the emitter should cover at least the length of the window. This prevents a cold descending boundary layer and only a plume is observed.

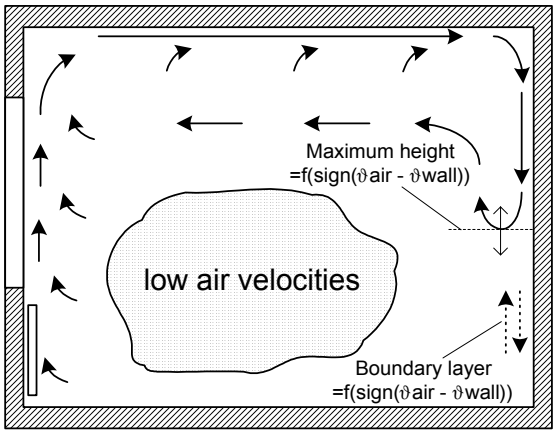

Figure II - 16: Airflow pattern in the EREDIS test room equipped with a heating system – smoke visualisation

☞ Fan coil unit cooling

Depending on the temperature of the cooling coil and the chosen fan speed, different airflow patterns are observed. For high fan speeds, the cold air jet reaches the ceiling and is mixed to the room air after passing along the ceiling until a maximum penetration into the room (Figure II - 17). Theoretically, the cold air jet can reach the internal walls and create a cold downward jet at the internal walls. This case is not realistic since fan coil units work in most cases at low fan speeds; it is thus not studied further.

For low fan speeds and high negative buoyancy of the cold jet (its temperature depends on the control of the valve) against the room air, the jet reaches a maximum height and falls downwards to the floor (Figure II - 18). In this case the cold air at the floor is observed either to rise at the internal walls (favourable boundary layer) or to be injected to the centre room air at lower heights (unfavourable boundary layer).

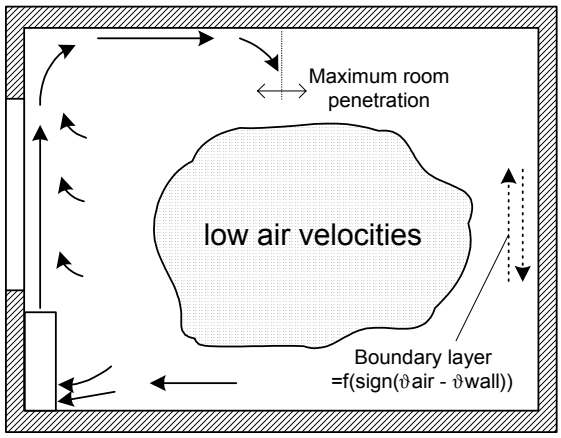

Figure II - 17: Airflow pattern A in the EREDIS test room with a cooling system – smoke visualisation

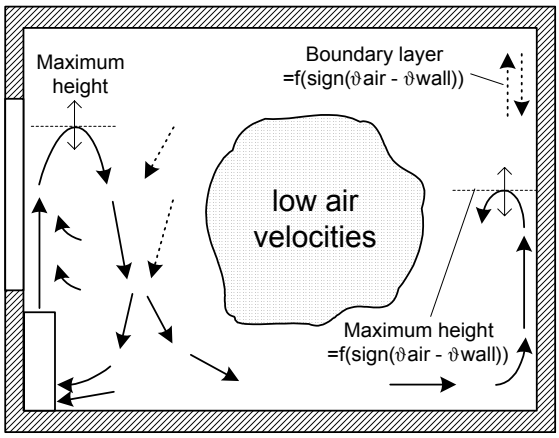

Figure II - 18: Airflow pattern B in the EREDIS test room with a cooling system – smoke visualisation

☞ Observation of the case of negatively buoyant air flow at internal walls

The airflow near the internal walls is shown by smoke visualisation for the hot downward jet with negative buoyancy forces (Figure II - 19). This corresponds to the air flow pattern

shown in Figure II - 16. In the experiments, the jet of warm air is pushed downwards until approximately half of the room height for low fan speeds of the fan coil unit or low heat emission of the electric convector, and nearly down to the floor for higher fan speeds. It is thus possible, that a controller sensor is placed in this warm air jet.

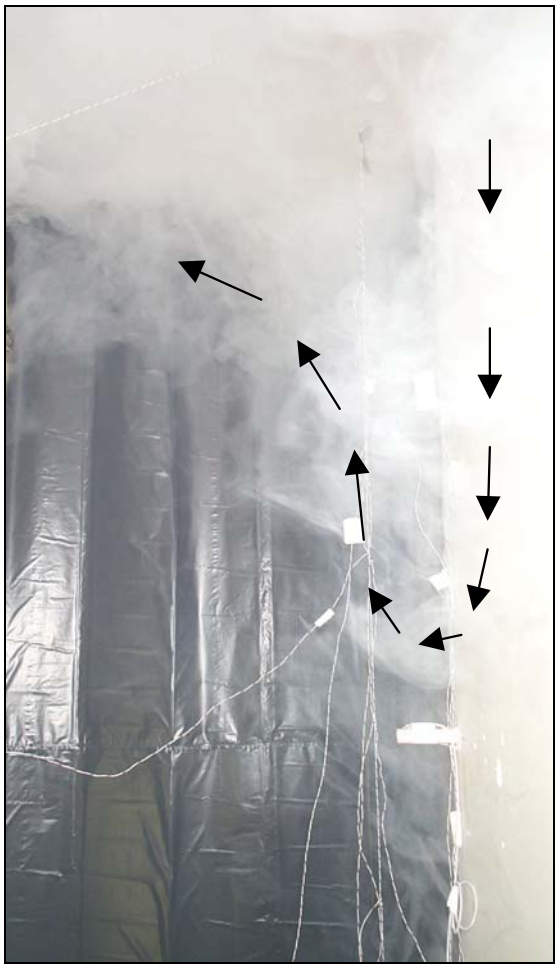

Figure II - 19: Negatively buoyant wall jet in a room equipped with a fan coil unit (speed 1)

3.2 CONDITIONS AT THE OCCUPANTS ZONE

The conditions at the occupant zone can be important for the assessment of controller performance, if the reference position is placed in this zone. The model to be developed should represent these conditions with a suitable precision. Two main aspects are studied:

- horizontal air temperature profile
- vertical air temperature profile (stratification)

Both temperature profiles will give indications about the minimum level of modelling of the occupant zone. It is important for the performance assessment of controllers since the reference position for the evaluation will be placed in this zone.

3.2.1 HORIZONTAL TEMPERATURE PROFILE

The horizontal variation of the temperature throughout the zone is studied. The differences are obtained from four measurement points placed on five horizontal planes in the zone. The maximum difference between the measurements on one horizontal plane is presented in the following.

In the case of the electric convector, no significant temperature differences are observed, except the profile 5cm from the ceiling (Figure II - 20). At this height, the warm plume creates significant differences due to the mixing of the plume at the ceiling and the air from the upper part of the zone. On all other heights the maximum temperature difference is in the order of measurement uncertainty. [Bouia93] studied the horizontal temperature variation for various room conditions and found similar results. Horizontal temperature variation can thus be neglected.

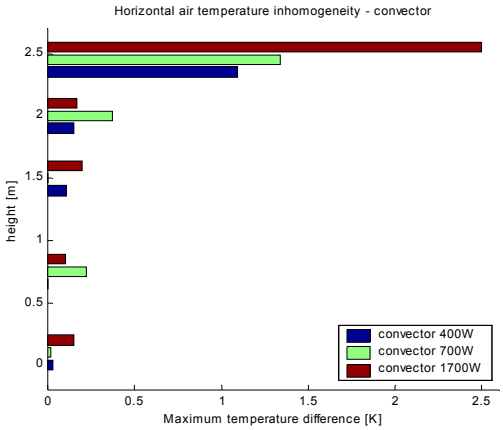

Figure II - 20: Maximum temperature differences on horizontal planes – convector - EREDIS test cell

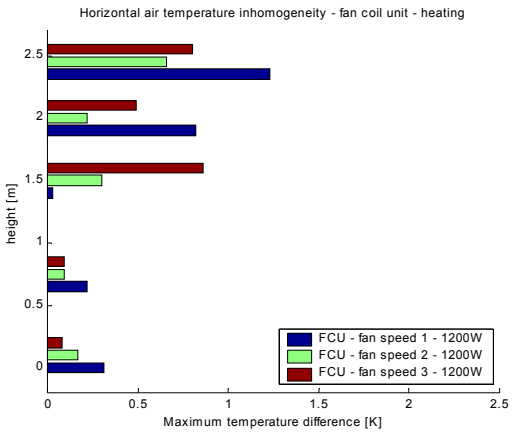

Figure II - 21: Maximum temperature differences on horizontal planes – FCU heating - EREDIS test cell

The fan coil unit test in heating mode shows also very homogeneous temperatures in the lower part of the zone (Figure II - 21). The upper part shows higher temperature differences. This is due to the effect of the negatively buoyant wall jet penetrating to lower room heights for high fan speeds. Since fan coil unit controllers almost work in low fan speeds, this difference can be neglected in our case.

In the cooling case with the fan coil unit (Figure II - 22), the highest temperature differences appear near floor (low fan speed) and ceiling (high fan speed). This shows the presence of the cold jet passing at the floor for lower fan speeds and at the ceiling for high fan speeds. As already mentioned before, fan coil units work mostly at low fan speeds, the non-homogeneity near the floor has to be considered. One measurement point is obviously placed in the cold jet (1m from the fan coil unit). If this jet was modelled separately, the rest of this horizontal plane can be considered to be homogeneous.

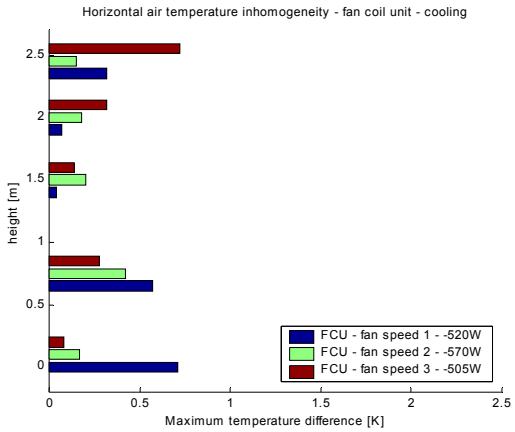

Figure II - 22: Maximum temperature differences on horizontal planes – FCU cooling - EREDIS test cell

The cases of the fan coil unit are also simulated with detailed CFD models. They provide qualitative information about the temperature distribution throughout the room. The temperature is nearly uniform horizontally except the regions near the ceiling where the warm jet passes (Figure II - 23).

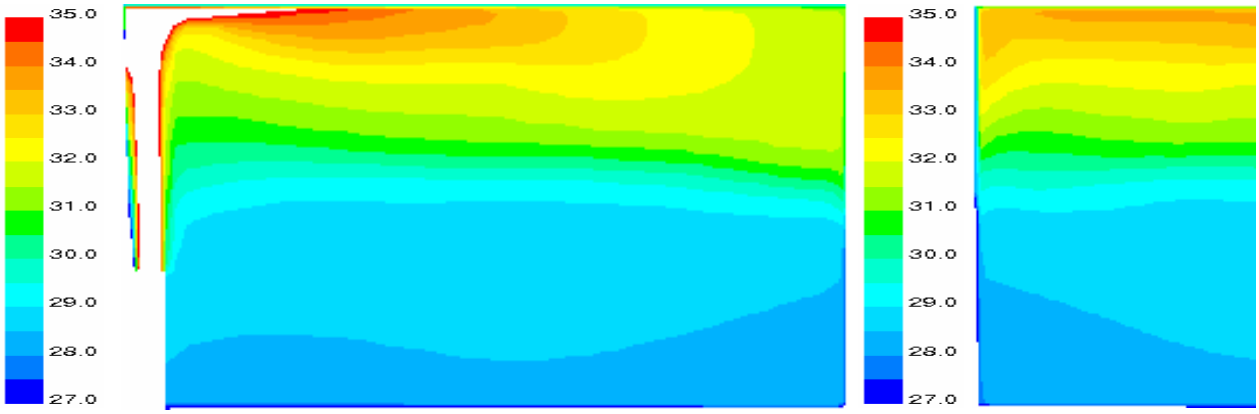

Figure II - 23: Zone temperature on symmetric axis and on vertical cut through centre (FCU, speed 1)

From the obtained results it is concluded that the temperature on different horizontal planes in the zone can be, taking into account the measurement accuracy and the probable accuracy of room simulation models, considered homogeneous in all cases. This excludes local convective phenomena as jets or plumes that have to be represented separately.

3.2.2 VERTICAL TEMPERATURE PROFILE

The vertical temperature profile has an effect on the controller performance since the result will be different depending on the height of the reference position for the performance assessment.

The profiles are studied for three different cases of emitters: convector (pure natural convection) and fan coil unit in heating and cooling mode (forced or mixed convection).

The temperature stratification in the three cases is shown in Figure II - 24 - Figure II - 26.

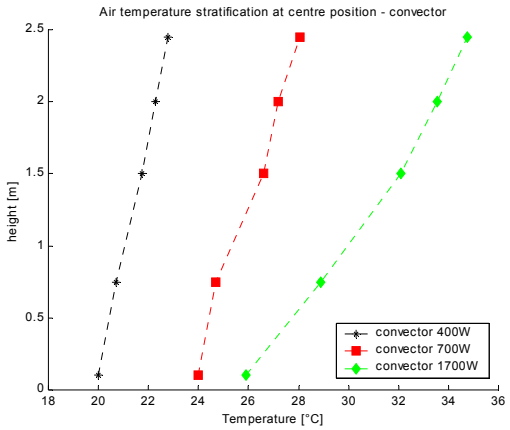

Figure II - 24: Temperature stratification at centre position – electric convector - EREDIS test cell

The results from convector tests (Figure II - 24) show that temperature stratification is nearly linear and increases with the convective heat introduced into the room. This corresponds to results of other authors for cases of heat introduction by natural convection ([Ngendeku88], [Inard88]).

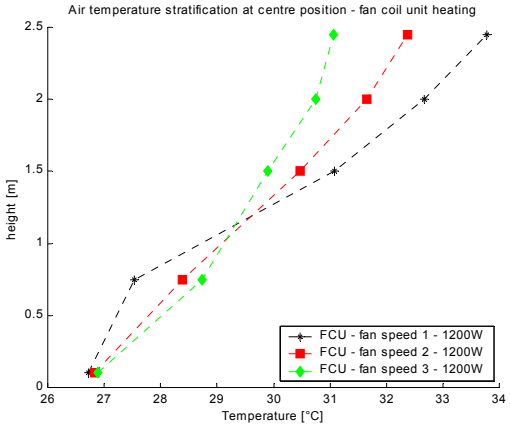

Figure II - 25: Temperature stratification at centre position – fan coil unit – heating - EREDIS test cell

In the heating case of forced convection (Figure II - 25) the stratification is slightly non-linear in the lower part of the zone, but the error introduced by linearization would be low. Stratification decreases with fan speed while mean air temperature is nearly constant (const. heat introduction).

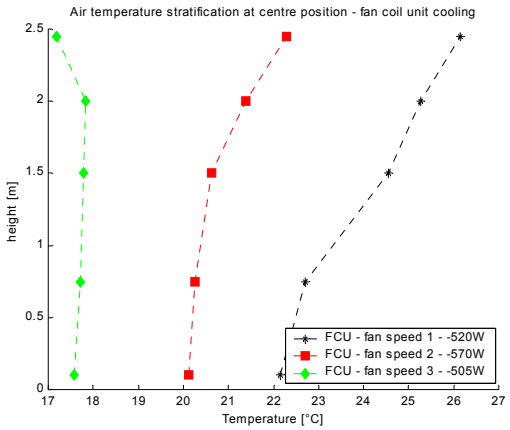

Figure II - 26: Temperature stratification at centre position – fan coil unit – cooling - EREDIS test cell

In the case of the fan coil unit in cooling mode, temperature stratification is also nearly linear. For fan speed 3, the effect of the cold air jet is observed in the upper part of the zone.

Another phenomenon is observed in the cooling cases. Although the cooling power at the fan coil unit is almost the same in all three cases, the mean room temperature decreases with increasing fan speed. This shows the existence of a "bypass" effect at the fan coil unit. For low fan speeds, the cold air from the fan coil unit falls rapidly towards the floor near the fan coil unit without significant mixing with the room air. This air enters then again the fan coil unit. If the controller sensor is placed in the extraction of the fan coil unit, the temperature measured will be lower than the real room temperature. This phenomenon is very important for performance assessment and must be represented in the model.

3.3 CONDITIONS AT SENSOR ZONES

Effects of negatively buoyant air flow have been observed by smoke visualisation at the internal walls. Measurements are thus carried out in order to study the vertical temperature profile following the jet from the ceiling down to the floor. The **air temperature** is measured following two profiles: **centre**-profile and profile at the **opposite wall**. These two temperature profiles can then be compared for the whole room height.

3.3.1 POSITIONING OF TEMPERATURE SENSORS

The distance of the measurement at the wall has to be defined. A preliminary study has been carried out in order to find an appropriated distance for the measurements. Hereby two aspects have to be considered:

- Thickness of a thermal boundary layer without jet or plume influence
- Thickness of a negatively buoyant wall jet

The thickness of a boundary layer without jet or plume influence is generally small. In [Allard87] the flow in these boundary layers is studied. The thickness of such a flow is generally smaller than 5cm. In this case the sensor should be placed at half distance between the wall and the thickness of the boundary layer, probably at 2.5cm from the wall. Since sensor boxes have different geometry, it is possible that the sensor is placed inside or outside the boundary layer. Flow visualisation around sensor boxes has shown that the sensor box does not disturb significantly the flow at the walls. The sensor box was, in all observed cases, inside the airflow in the boundary layer. It can thus be assumed that the sensor measures the mean air temperature of the boundary layer.

On the other hand, if the temperature in a negatively buoyant wall jet has to be measured, the sensor, if placed at the distance appropriated to that appropriated to that for the measurement of the temperature in the boundary layer, is not able to measure the temperature in the jet or plume.

Figure II - 27 shows measured temperature profiles from the wall opposite a convector to the centre of the room at a height of 1.5m. A "relative temperature" is defined for demonstration with 0 as the minimum and 1 as the maximum temperature following the measured temperature profile. At a distance of about 0.02m from the wall the temperature in the jet is identical to the temperature at the centre of the room at the same height. At a distance of 0.05m the temperature has nearly reached its maximum value (at about 0.12m).

This distance of 0.05m is thus chosen for the measurement at all heights. An error will be undertaken in the case of a boundary layer without jet or plume influence, but a measurement closer to the wall would introduce an error in the measurement of the jet temperature.

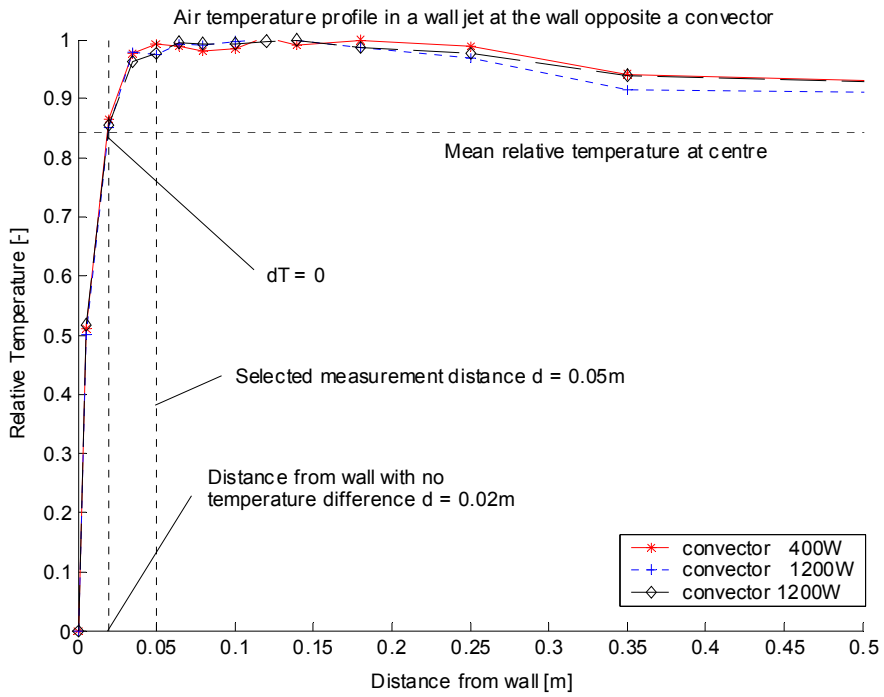

Figure II - 27: Relative temperature in a negatively buoyant wall jet - selection of measurement point

Figure II - 28 shows the positions of the temperature sensors for this study. At the centre, the temperature profile is measured using 5 sensors. At the opposite wall, the profile is measured at 13 or 5 points, depending on the case.

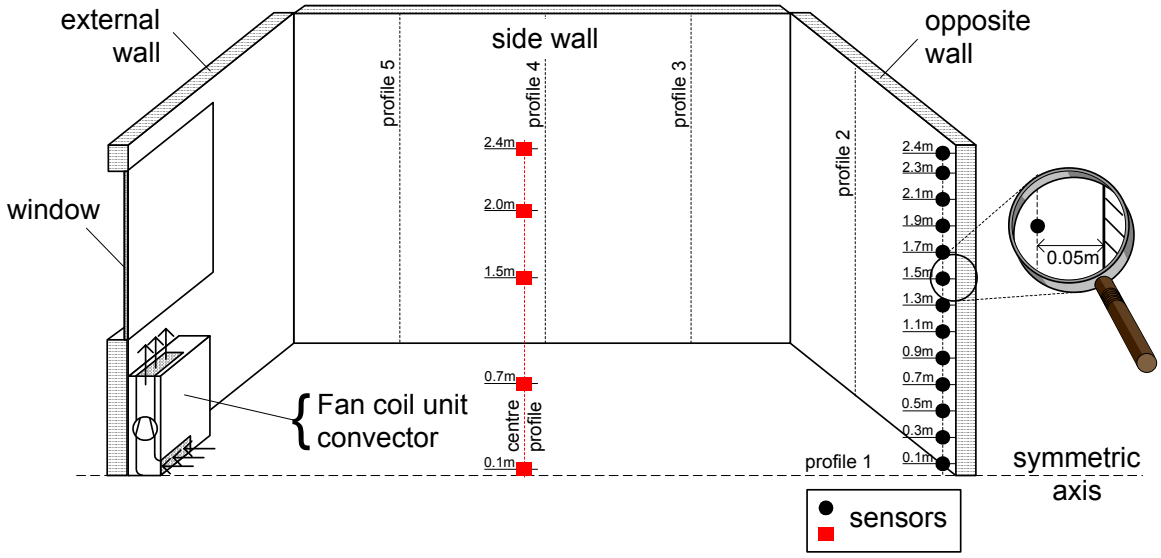

Figure II - 28: Measurement of the temperature profile at the centre and near the opposite wall

The measurements are carried out for different cases that are important for controller studies:

- Room without convective heat sources
- Heating systems
- Cooling systems

These cases should prove the general assumptions about airflow phenomena near walls (for different boundary conditions) and show the order of magnitude of temperature difference created by these phenomena.

3.3.2 ROOM WITHOUT CONVECTIVE HEAT SOURCES

This case is particularly important for ON/OFF controllers or for a time period without heating or cooling.

The only heat sources are surrounding surfaces, internal and external walls, floor and ceiling. They create boundary layers of natural convection with upward or downward flows depending on the sign of temperature difference between room air and wall.

Two cases are studied, winter and summer case. While the boundary layer in the winter case transports cold air to the floor (Figure II - 29 and Figure II - 30), warm air is transported to the ceiling in the summer case (Figure II - 31 and Figure II - 32). The figure on the left indicates the airflow pattern observed in the corresponding case.

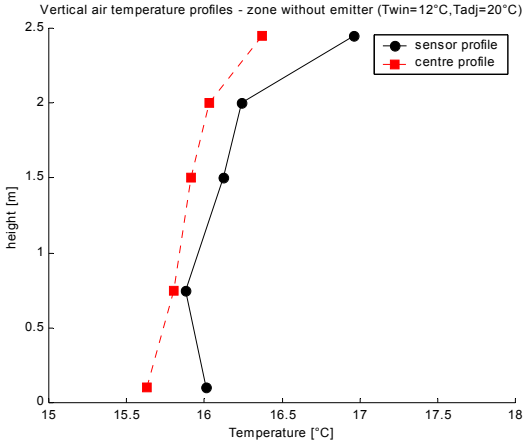

Figure II - 29: Temperature profiles at centre and sensor position for the case without heating (winter case) - EREDIS

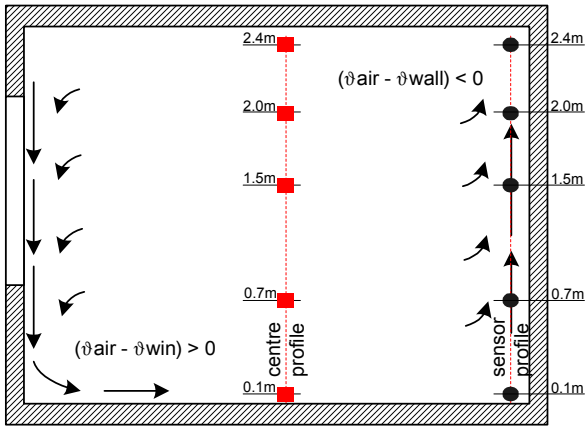

Figure II - 30: Qualitative airflow pattern in the winter case - EREDIS

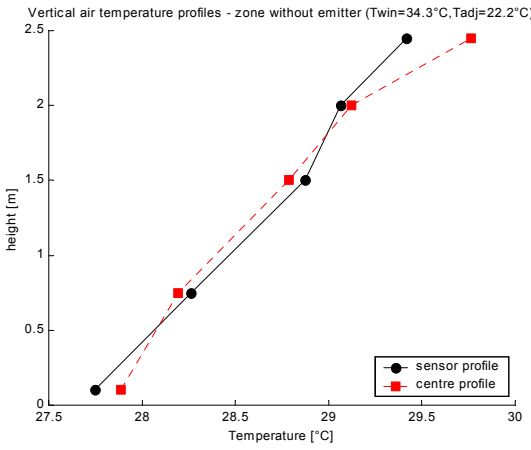

Figure II - 31: Temperature profiles at centre and sensor position for the case without cooling (summer case) - EREDIS

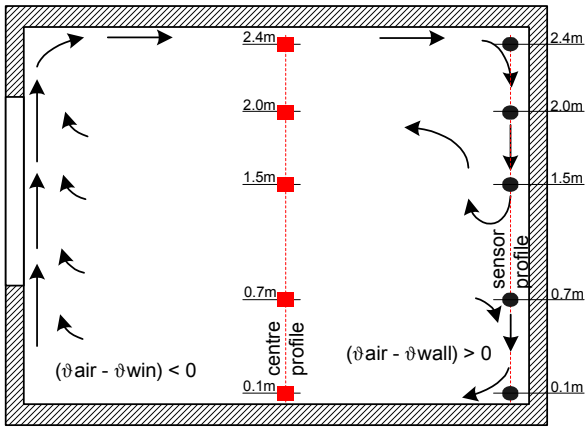

Figure II - 32:Qualitative airflow pattern in the summer case - EREDIS

A boundary layer of natural convection is observed all over the internal walls for the winter case. Since the temperature difference ϑ_{air} - ϑ_{wall} is negative, air is transported upwards.

In the summer case a very slight effect of negatively buoyant air flow is observed. The warm wall jet at the wall opposite the emitter, created by natural convection at the window, travels

downwards. The warm air penetrates to a relatively low room height due to the very small temperature difference between warm air from the ceiling and room air.

In principal, the effects should be the same for both cases since the phenomena are the same. Probably the smaller temperature differences and the position of the window close to the ceiling are responsible for the difference in the results.

3.3.3 AIR DISTRIBUTION AT CEILING – HEATING SYSTEMS

In the case of heating systems, the warm air from plumes or jets rises to the ceiling and entrains air from the room into the flow. As shown qualitatively in §3.1, the warm air is then pushed downwards and the flow changes its direction at a point of maximum room penetration. The temperature measurement shows this phenomenon clearly for the convector (Figure II - 33 and Figure II - 34).

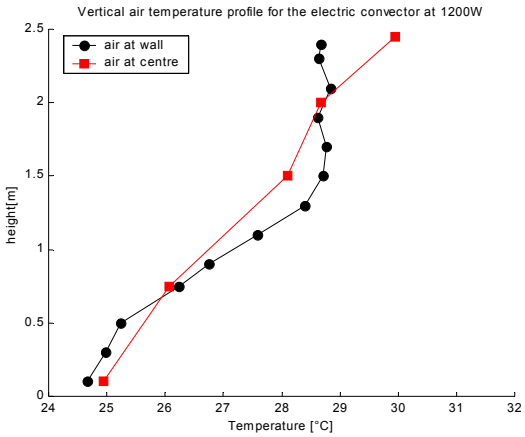

Figure II - 33: Vertical temperature profile - convector – favourable boundary layer - EREDIS

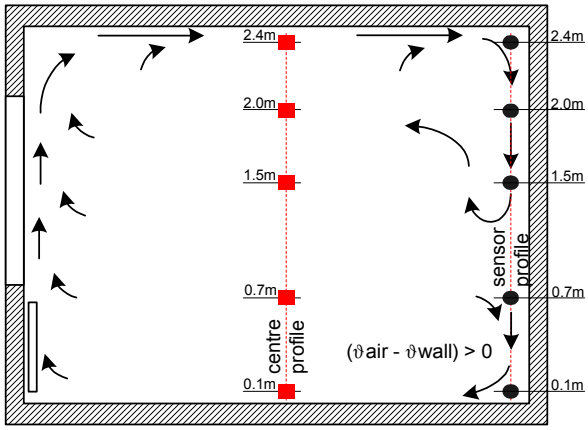

Figure II - 34:Qualitative airflow pattern with a convector – favourable boundary layer

The warm jet can clearly be distinguished in this case. While the centre temperature profile is nearly linear all over the room height, the jet keeps a constant temperature until a certain height. The jet temperature at the top of the opposite wall is lower than at the centre since the warm jet passes at this point at the ceiling and is still mixed with room air.

In the middle zone, the temperature near the wall changes quickly due to a big part of the jet leaving towards the centre part of the room.

In the lower part of the room, the temperature near the wall falls down the centre temperature. This indicates a boundary layer of natural convection. The temperature of the air near the wall is now between surface- and centre air temperature.

In all test cases, the boundary conditions at the internal walls are favourable for the wall jet. In a real case, if the adjacent zones are on a higher temperature, an unfavourable boundary layer can be observed reducing the penetration of the warm wall jet.

3.3.4 AIR DISTRIBUTION AT FLOOR – COOLING SYSTEMS

The problem is generally the same as in the heating case. The only difference is that the cooling load can be due to two phenomena that create more variable boundary conditions (surface temperatures) as in the heating case:

☞ Load by high external and adjacent temperatures

In the case of higher external temperatures the boundary conditions at the internal walls will always be favourable for a cold upward jet.

Figure II - 35 and Figure II - 36 show the case of high external temperatures representing the only cooling load of the room. The boundary layer is, as seen in both figures, favourable and a cold wall jet is pushed upwards until more than half of the room height. The cold air passing at the floor at the centre profile is colder than at the same height at the opposite wall. This is the first indicator for the existence of the negatively buoyant wall jet. In the upper part, the temperature near the wall is higher than the centre temperature and thus between centre air temperature and the temperature of the adjacent zones (20.8°C). This is exactly the same case as for the heating system with the wall jet of opposing buoyancy.

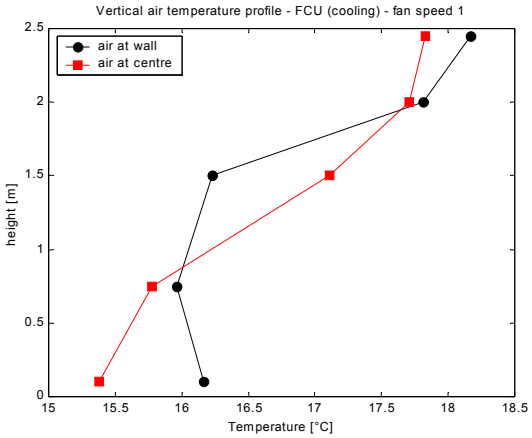

Figure II - 35: Vertical temperature profile; cooling case – favourable boundary layer - EREDIS

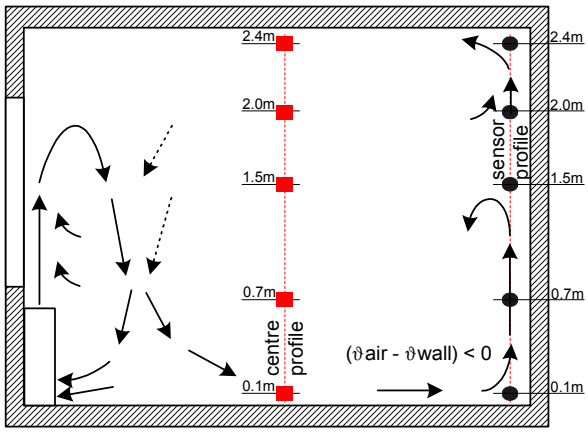

Figure II - 36: Qualitative airflow pattern in the cooling case – favourable boundary layer

☞ Case of high external temperature

In this case, the boundary conditions of the jets at the internal walls can be either favourable or unfavourable.

Figure II - 37 and Figure II - 38 show one possible case. The test is carried out without internal gains. Only a warm window introduces the cooling load and creates an upward boundary layer at the window.

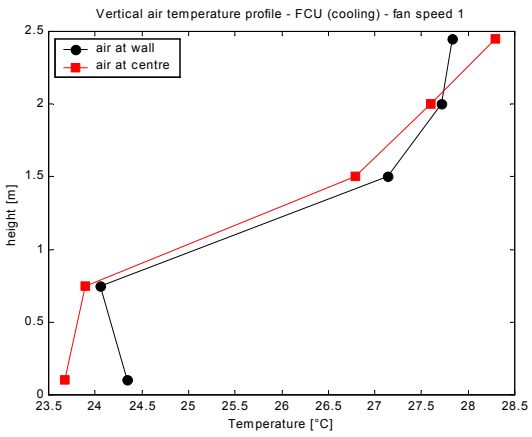

Figure II - 37: Vertical temperature profile; cooling case – unfavourable boundary layer - EREDIS

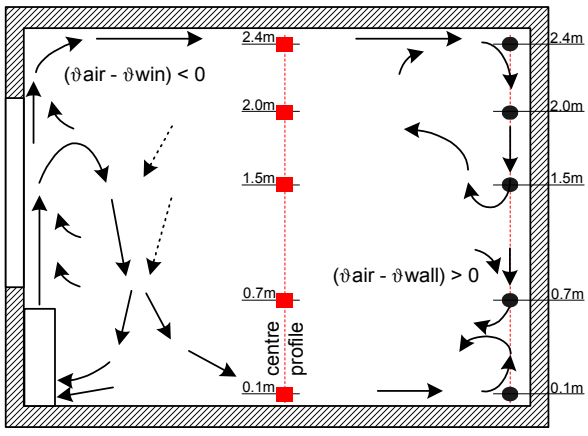

Figure II - 38: Qualitative airflow pattern; cooling case – unfavourable boundary layer

This warm flow passes along the ceiling and is pushed downwards, as a negatively buoyant wall jet. At the same time the cold jet from the fan coil unit falls towards the floor. Since the boundary conditions from the adjacent zones impose a downward boundary layer at the internal walls, the cold jet at the floor is stopped already in the lower part of the internal walls.

The study of the vertical temperature profile near walls has not been carried out for different positions around the internal walls. This will be analysed in the following section. The phenomena observed at the opposite wall are studied on three-dimensional effects for the example of the heating case.

3.4 STUDY OF FLOW AROUND A CONTROLLER SENSOR

3.4.1 STUDY ON 3-D EFFECTS OF THE FLOW IN SENSOR ZONES

The existence of the jet around the internal walls is showed qualitatively by CFD simulation results, by infrared pictures of the surrounding walls and by measurement at strategic points for the heating case. The aim of this part of the study is to check if the negatively buoyant wall jet represents mainly a two-dimensional effect opposite the emitter or if significant three-dimensional effects exist.

The study is carried out for the case of the fan coil unit in the EREDIS test cell. Results are presented for the low fan speed since they represent the general case.

Starting from the fan coil unit placed below the window, the warm air reaches the ceiling. From this point on, the jet spreads at the ceiling. Figure II - 39 shows qualitatively the temperature distribution obtained by CFD simulation on a horizontal plane 5 cm from the ceiling surface.

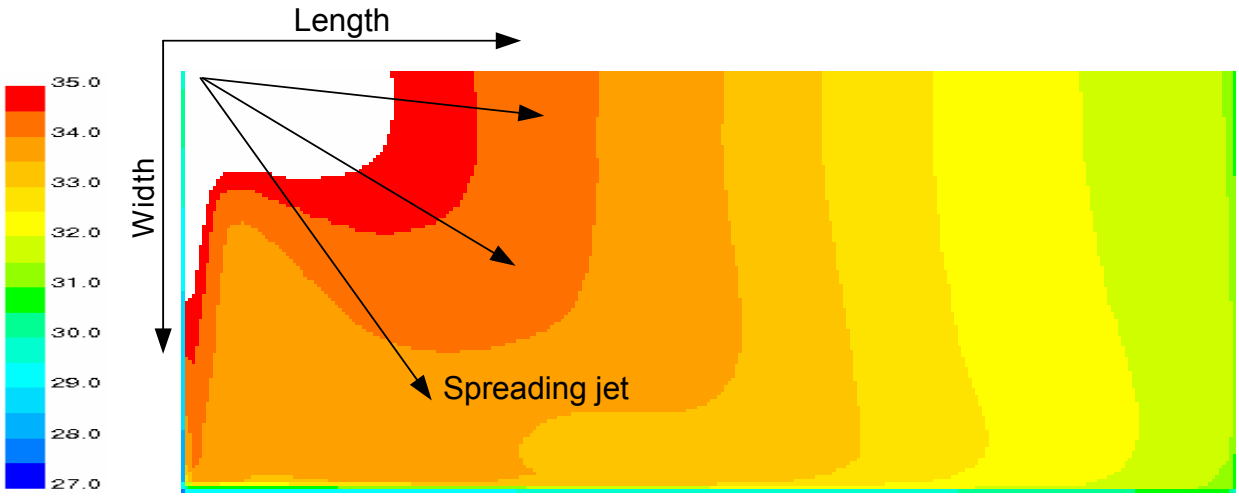

Figure II - 39: Temperature profile in a warm ceiling jet at 5cm from the ceiling (FCU, speed 1)

The isotherms of the warm air layer show approximately circles around the injection point of the jet into the ceiling (white spot on the top of the figure). This means that the temperature of the jet arriving at the internal walls is approximately a function of the distance between the point of the jet introduction into the ceiling layer and the jet entry from the ceiling layer into the air volume near the internal walls. The decrease in temperature is due to heat exchange at the ceiling and to mixing of the jet air with air from the room.

Once arrived at the upper corners at the internal walls, the warm jet is pushed downwards along the internal walls. As already shown by measurement, a negatively buoyant wall jet exists at the

opposite wall. Figure II - 40 shows the temperature in this wall jet around the internal walls at a distance of 5 cm from the internal walls.

The horizontal air temperature profile near the wall is nearly constant for the lower and intermediate regions of the room. Small differences at the top of the walls where the temperature is that of the ceiling jet and thus function of the distance from the fan coil unit (Figure II - 39). Near the cold window, the effect of the descending boundary layer is observed. A part of the warm air from the ceiling is carried with this boundary layer to lower parts of the room.

Generally there exists a three-dimensional effect due to the dispersion of warm air at the ceiling. This effect changes the conditions at the "origin" of the wall jet at the top of the internal walls. The wall jet is characterised by a higher temperature close to the emitter (side wall) and by a lower temperature at the opposite wall. This increases the buoyancy forces against the room air. The wall jet of higher temperature at the side wall is thus pushed less than at the opposite wall and the three-dimensional effect is diminished.

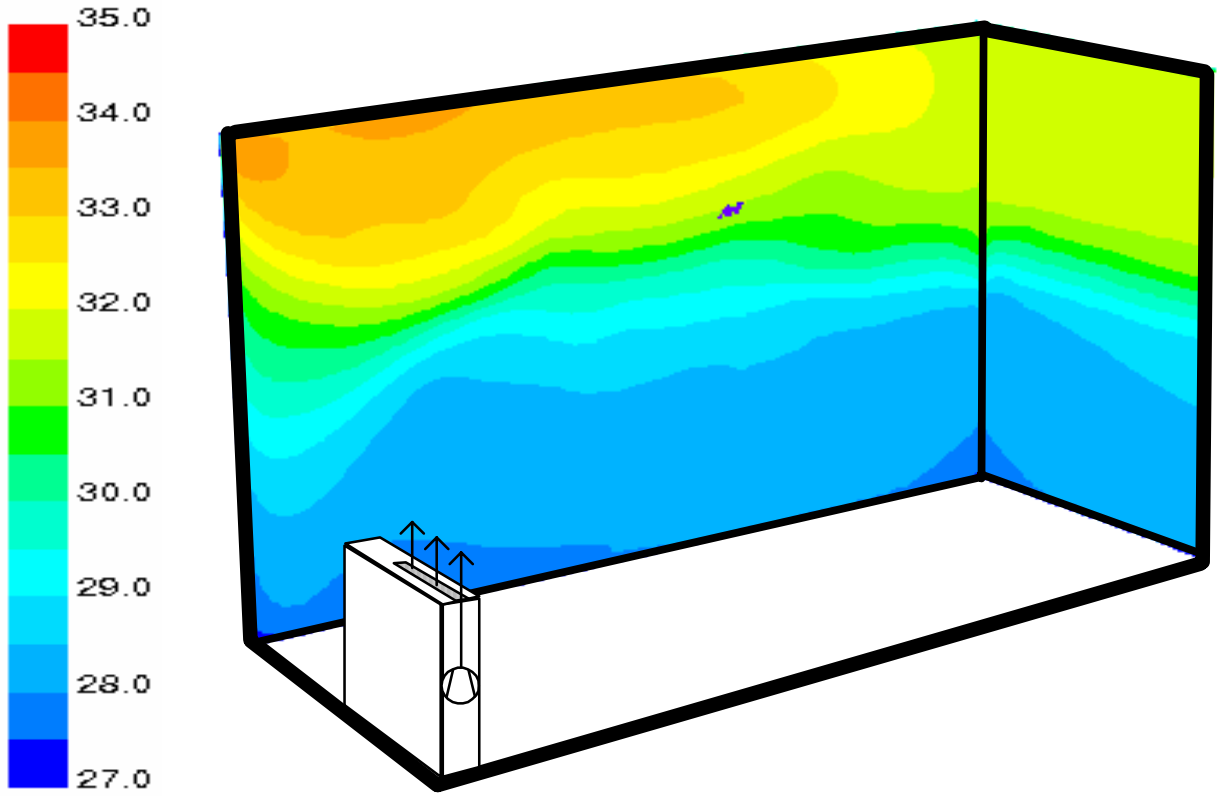

Figure II - 40: Simulated temperature profile 5cm from walls and ceiling for the fan coil unit (fan speed 1)

In infrared measurements, the surface temperature of the walls is visualised. Since the temperature of the air in the boundary layer influences the surface temperature, the result of an infrared measurement can be taken as an indicator for the air temperature near the wall. Figure II - 41 shows the temperature profile for the case of fan speed 1.

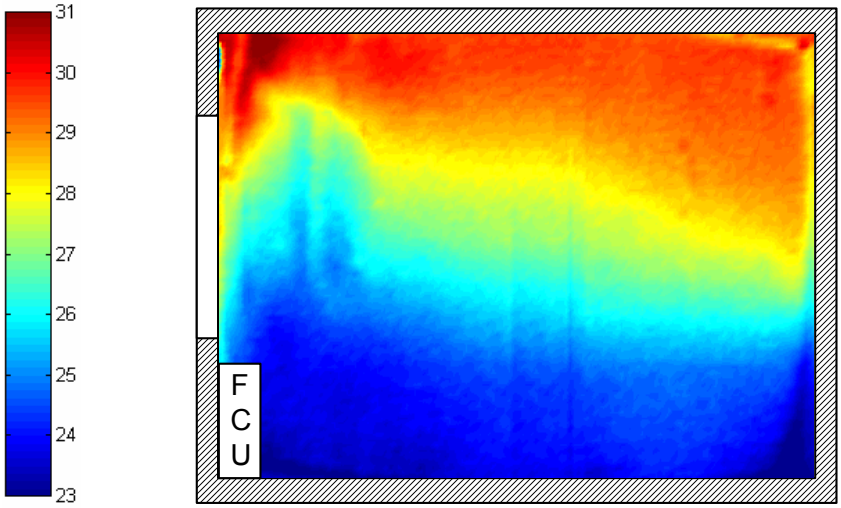

Figure II - 41: Surface temperature (infrared meas.) of wall next to emitter, FCU – heating; fan speed 1

The fan coil unit is positioned at the left hand of the picture. The wall jet reaches a slightly higher penetration height next to the opposite (right) wall. Close to the external wall (left) the temperature close to the ceiling is higher and the jet penetration is thus smaller due to higher buoyancy forces. The results from infrared measurement are different from the CFD simulation results for the part close to the window (left side). This difference is on the one hand due to a small glass window placed in the side wall at this point. On the other hand, the results from infrared measurement are influenced by radiation from the cold window (reflection at side wall).

As seen before, the maximum penetration height is, for the observed cases, approximately half of the zone height. The measurement of five temperature profiles at the internal wall surfaces as well as the measurement of the air temperature at 1.5m at each of these profiles will give further information. The profiles as well as measurement points are shown in Figure II - 42.

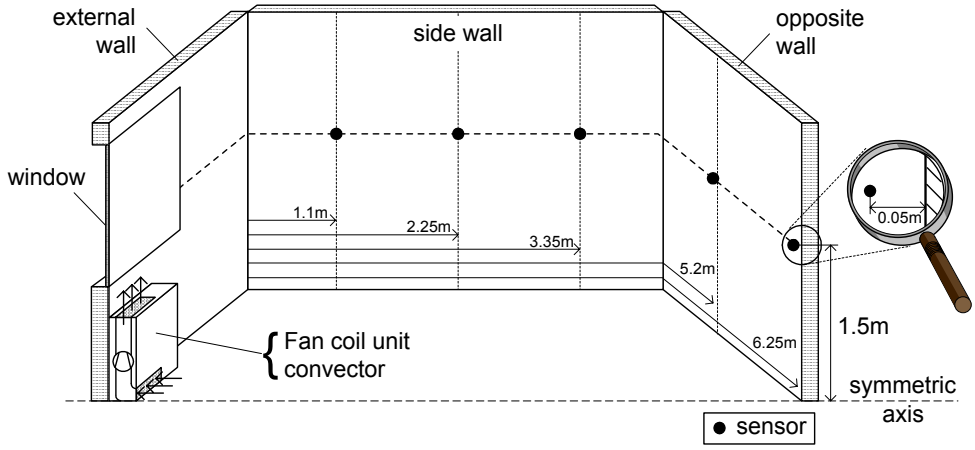

Figure II - 42: Principle of the measurement of the temperature profiles along the internal walls

Five profiles of surface temperature as shown in Figure II - 42 are plotted in Figure II - 43.

The warm wall jet is observed at the positions of 3.35m, 5.2m and 6.25m. At the positions closer to the emitter, the effect of the wall jet is slight or does not exist. This means that the warm air is pushed down, along the internal walls, at about half of the length of the walls next to the emitter. This phenomenon depends on the geometry (relation length/width) of the room and the width of the emitter related to the width of the room.

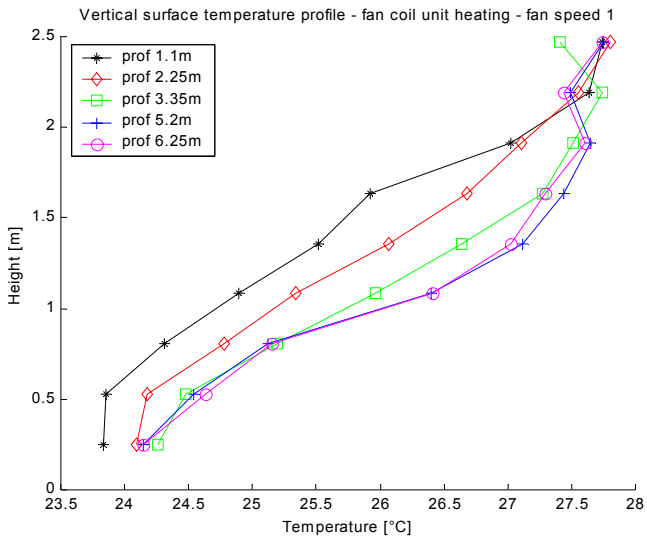

Figure II - 43: Wall surface temperature (infrared meas.), FCU – heating; fan speed 1- EREDIS

For long rooms, the part of the side wall with the negatively buoyant wall jet will be greater. If the room is short, it is possible that the wall jet is only observed at the wall opposite to the emitter. In this case, the relation between room length and width is 1.25.

The air temperature at the five points at 1.5m height above floor and at 5cm from the surface, as indicated in Figure II - 42, is then compared to the centre air temperature at the same height (Figure II - 44). The results are shown for all fan speeds.

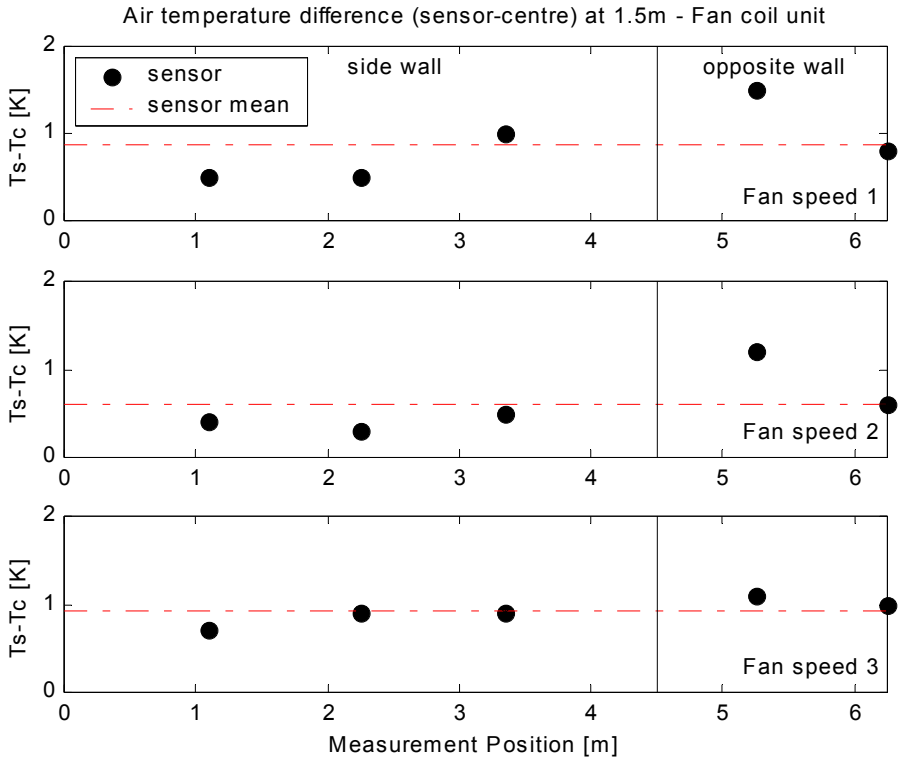

Figure II - 44: Measured temperature difference between centre and sensor position at 1.5m height (fan coil unit) - EREDIS

The temperature difference between the air near the wall and the air at the centre is positive for all measured points. The mean value of the difference between near-wall temperature and centre temperature is shown in Figure II - 44.

The difference is, for all cases increasing from the first point near the external wall to the other points. This proves that the effect of the negatively buoyant wall jet is measurable at all three internal walls. The effect is smaller at the side walls and near to the external wall where the difference is smaller than the mean difference. At the opposite wall, the highest temperature difference is observed. Measurements with a convector at different heat emissions are also carried out and show the same phenomenon.

The obtained results of air temperatures fit well with the measurement carried out using the infrared camera.

Since the difference at the opposite wall is similar to the mean difference of all measurement points around the internal walls, a more detailed analysis is carried out for the point 6.25m at the opposite wall and on the symmetric axis. This study gives further information about the sensitivity of the negatively buoyant wall jet on convective heat emission for the convector case or fan speed for the fan coil unit case.

3.4.2 STUDY OF THE FLOW IN THE NEGATIVELY BUOYANT WALL JET FOR THE EXAMPLE OF HEATING SYSTEMS

The analysis is grouped into two steps treated in the following.

- ☞ Study of the wall jet temperature profile at different heights

  The thickness of the wall jet is studied in this part in order to get information if the controller sensor is placed inside or outside the wall jet.

  The temperature profiles near the wall for different heights obtained by simulations show the airflow (Figure II - 45). Near the ceiling, the air temperature decreases the more the jet approaches the opposite wall. Then, at a lower level, the wall jet appears, visible by a maximum of the curves near the wall. At heights lower than the maximum penetration height, the airflow is characterised by a typical boundary layer under free convection conditions.

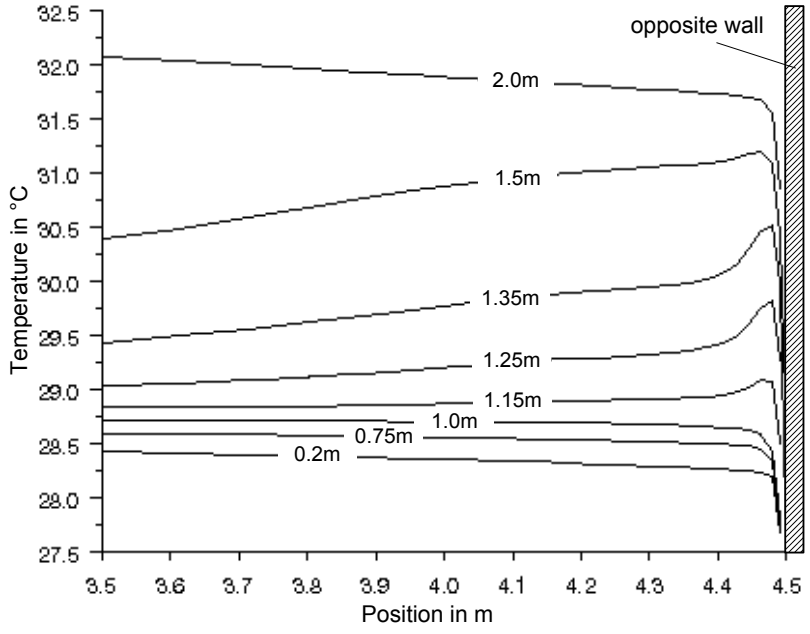

Figure II - 45: Air temperature profile in the wall jet at different heights (fan speed 1) - CFD simulation

The thickness of the jet is about 10cm. Measurements showed higher values. However, even considering the CFD results, the controller sensor box is generally placed in this warm air layer. In the lower part, where the boundary layer appears, the sensor is placed in the boundary layer of natural convection.

☞ Study of the vertical wall jet profile at 5cm from wall surface

The sensitivity of the wall jet for a change in heat emission or fan speed is studied. It can be possible that the sensor is, depending on the heat emission, placed either in the warm wall jet or in the boundary layer at the wall.

The temperature is plotted for different heat emissions and for different fan speeds for the convector and the fan coil unit respectively (Figure II - 46 and Figure II - 47).

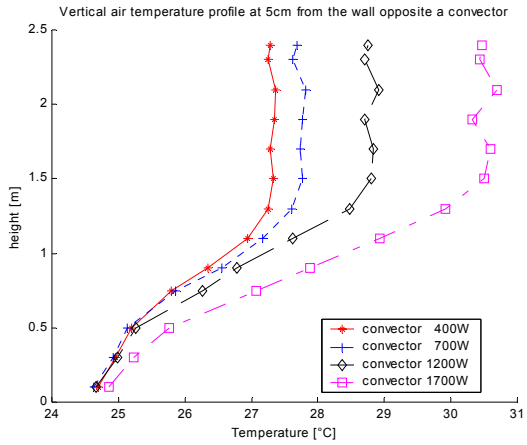

Figure II - 46: Measured stratification of sensor air temperature for an electric convector - EREDIS

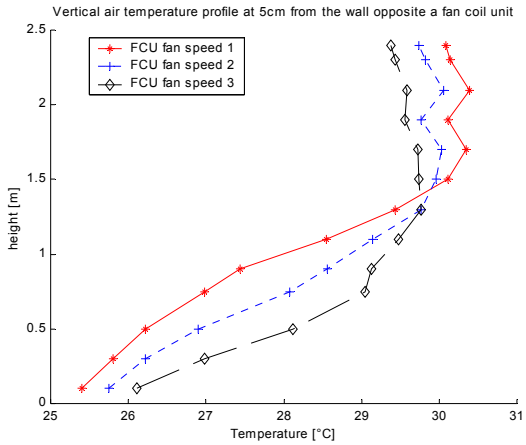

Figure II - 47: Measured stratification of sensor air temperature for a fan coil unit - EREDIS

All cases, even at small heat emission, show qualitatively the phenomenon of the wall jet. An upper jet region is characterised by nearly constant temperature following the jet. Then, from this point on, the temperature near the wall decreases with height. This indicates mixing with the air from the centre of the room. At a certain height, the slope of the temperature curve near the wall changes again. This indicates the end of mixing of the near-wall region with the centre air. The height of penetration depends on emitted power and fan speed. At the end of the jet, the maximum penetration depth is achieved and the temperature in the jet is identical with the temperature at the centre profile.

Rules for the calculation of the phenomenon, depending on the Archimedes number, will be given in the modelling chapter. In general, the jet velocity and the temperature difference between centre and jet at the "origin" of this jet are characteristic for the problem. Depending on the values of both variables, the jet penetrates more or less the air volume near the internal walls. For example in the case of the fan coil unit, the higher fan speed increases the initial jet velocity and thus the penetration depth. For the case of the electric convector, the increase of heat emission does not increase sensibly the initial jet flow rate (see description of convective phenomena in Chapter IV) but increases the temperature difference between jet and centre and diminishes thus the penetration depth.

3.5 CONCLUSION ON STEADY STATE PHENOMENA

There is **very little horizontal temperature variation** throughout the room. Near the walls, especially at the internal walls, the temperature is not homogenous due to phenomena of a natural convection boundary layer or a phenomenon of negatively buoyant air flow.

Vertical **Temperature stratification** is observed in all cases. The stratification is approximately linear. Its magnitude depends on the convective heat sources in the room.

A **negatively buoyant wall jet**, depending on the jet or plume of the emitter, is observed at the internal walls for heating and cooling cases. Its development depends on the boundary conditions at the internal walls and the conditions at the origin of the wall jet. In the heating case the negatively buoyant wall jet is observed in most cases. In the shown cooling cases, room furniture, occupants or equipment will probably disturb or even stop this phenomenon. Main attention will thus be paid on the heating case where these factors have only little influence on the development of this kind of jet.

Measurements in steady state conditions show a division of the air near walls into three different zones. These zones have been shown by detailed measurement and by CFD simulation. The zones are: An upper zone with constant air temperature, an intermediate zone with rapidly changing temperature (transition zone) and a lower zone with the characteristics of a boundary layer with natural convection (Figure II - 48). These zones are similar for heating or cooling cases.

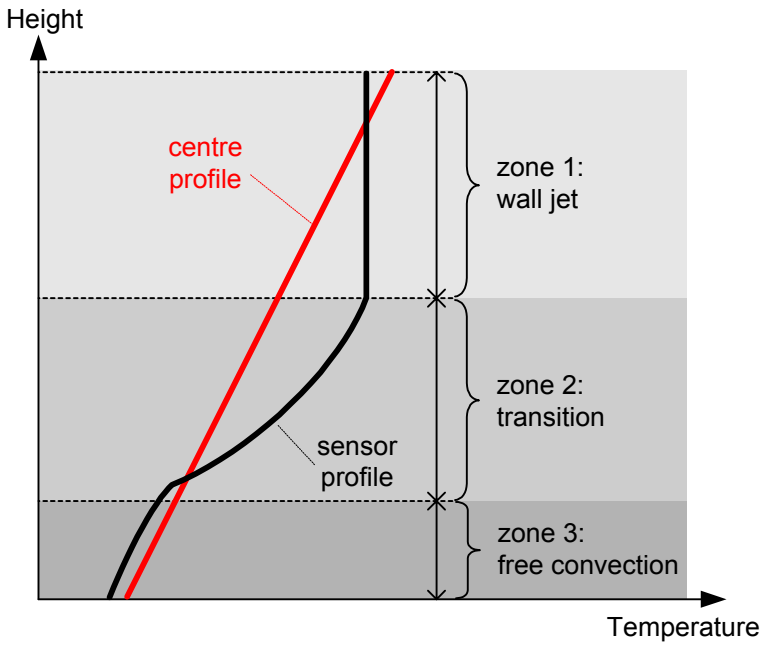

Figure II - 48: Qualitative comparison between centre air and near-wall air temperature profile

Depending on the zone in which the controller sensor is positioned, the sensor will measure a temperature different from the temperature at the centre and at the same height.

The phenomenon of the negatively buoyant wall jet has been studied on all internal walls of the test room. While the phenomenon is clearly visible at the wall opposite the emitter, it disappears slightly at positions closer to the emitter.

4. ANALYSIS IN TRANSIENT CONDITIONS

4.1 GENERAL TRANSIENT PHENOMENA

The dynamic phenomena depend on the airflow in the room. Since the dynamics are principally introduced by changes in the heat emission of the emitter or gains, they can be estimated from the steady state airflow pattern: in the heating case the air layer at the ceiling has a fast temperature response, since all warm air from the emitter passes there. In the upper zone of the negatively buoyant wall jet, the temperature response is still fast. It decreases then slightly in the transition zone, where it is still faster than at the same height at the centre. In the lower part of the wall zones, the boundary layer, the temperature response is slower than at the centre at the same height, due to the coupling to the wall surface with slow temperature response.

4.2 MEASUREMENT OF TRANSIENT PHENOMENA

The phenomena in transient conditions are shown for two kinds of test, the switching on of the emitter and the switching off. As in the steady state measurements, the heating case is presented representatively for the cooling case. The air temperature profile at the opposite wall is taken as representative for the sensor temperature profile, following the results from steady state tests.

For each measurement point, a relative temperature is defined as follows:

$$\vartheta_{rel,i}(t) = \frac{\vartheta_i(t) \; - \; \vartheta_{\min,i}(0 \le t \le t_{end})}{\vartheta_{\max,i}(0 \le t \le t_{end}) \; - \; \vartheta_{\min,i}(0 \le t \le t_{end})} \qquad (2)$$

Using this relative temperature, the evolution of the temperature profiles at centre and sensor position can easily be compared.

4.2.1 SWITCHING ON

In the test presented, a fan coil unit is used as HVAC system. A step in the fan speed from off to low fan speed is carried out. At the same time the electrical heater in the fan coil unit is switched on. Figure II - 49 shows the evolution of the temperatures at the centre profile at different heights.

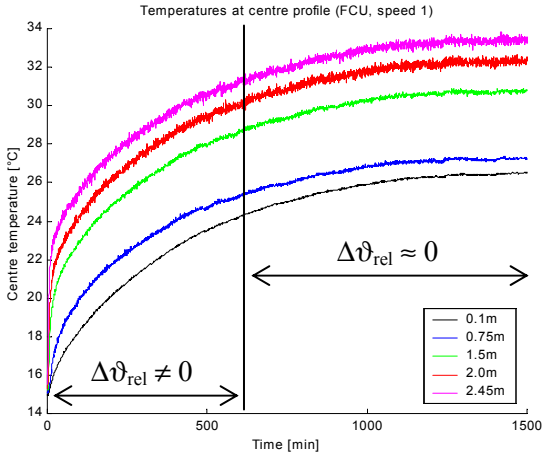

Figure II - 49: Evolution of air temperatures at centre profile (test OFF → ON) - EREDIS

The steady state conditions are reached after more than 24 hours, the test time is thus reduced in the following way:

The time, interesting for this study, is the time where a difference between the response at centre and at sensor position exists. The relative temperatures of both temperature profiles are thus compared. After 600 minutes no measurable difference exists between both relative temperatures. For the following analysis, the test time is reduced to this time ($t_{end,\ new}$ = 600min) and the new relative temperatures are calculated using equation (2).

Two main questions are studied in this part:

- ☞ Evolution of the temperature profiles depending on time
- ☞ Evolution of relative temperatures depending on time

The evolution of the temperature profiles at centre and at sensor position shows quantitatively the real temperature differences between centre and sensor temperatures and, qualitatively, if the two profiles change harmoniously. The evolution of the relative temperature profile shows the response of the profiles to the step carried out. Figure II - 50 shows the real temperature profiles:

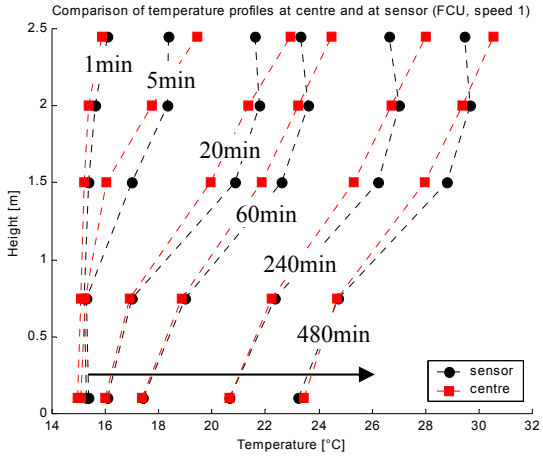

Figure II - 50: Evolution of centre and sensor temperature profile (test OFF → ON) - EREDIS

The temperature profiles at centre and at sensor position at 480min correspond principally to the profiles in the steady state case. Figure II - 50 shows a harmonic evolution of both profiles and the faster response in the upper part of the room. A more detailed comparison of the response of the two profiles can not be carried out with the temperature profiles. Therefore, the relative temperature profile is used which permits a better visualisation of the differences. In Figure II - 51 the evolution of the relative temperatures at the centre profile is shown.

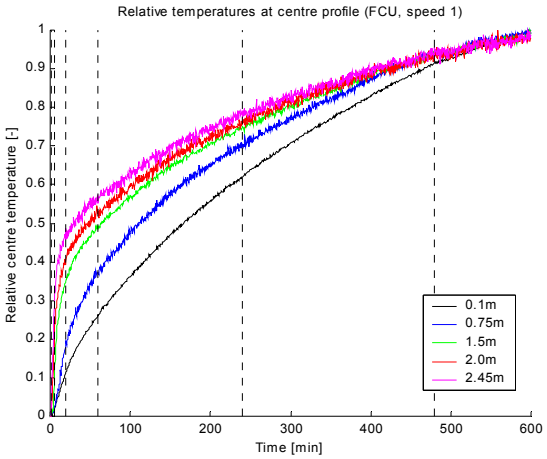

Figure II - 51: Evolution of relative temperature at centre profile (test OFF → ON) - EREDIS

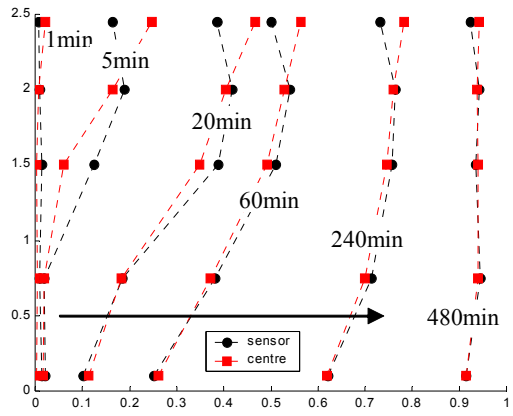

Figure II - 52: Evolution of centre - sensor relative temperature profile (test OFF → ON) - EREDIS

The response in the higher part of the zone is clearly faster compared to the lower part. The dotted lines in Figure II - 51 indicate the times used for the plot of the temperature and relative temperature profile shown in Figure II - 50 and Figure II - 52.

In Figure II - 52, besides the upper part with "fast" temperature response and the lower part with "slow" temperature response, the dynamic effect of the negatively buoyant wall jet is visible. The warm jet reaches about half of the room height and rises, while leaving the jet, to the upper part of the room. The relative temperature at the sensor profile at the heights, where the negatively buoyant wall jet appears, responds faster than the relative temperature at the centre position and at the same height. Other tests with different fan speeds or with the electric convector as emitter prove that the biggest difference in the response of both profiles of relative temperature is always at the end of the wall jet.

A difference in the relative temperatures appears after the step. The difference is important for the period of 0 to 20 minutes. At 20 minutes, the difference between relative temperature at the two profiles at 1.5m is still 15% (reference: centre position).

The dynamic difference is thus important especially for ON/OFF controllers where this kind of step appears more often. If the temperature sensor of an ON/OFF controller is placed in the jet zone, an anticipatory effect will appear improving the performance of the controller. In the other case, if the sensor is placed in the zone of boundary layer below the end of the jet, the opposite effect can appear.

4.2.2 SWITCHING OFF

The fan coil unit is switched off in this test from fan speed 1 to the OFF position. The wall jet will thus disappear quickly and the conditions at the walls are characterised by natural convection. Figure II - 53 and Figure II - 54 show the evolution of the temperatures at the centre profile and the evolution of the temperature profile at centre and at sensor position respectively. The same test time is chosen as for the first test (OFF → ON).

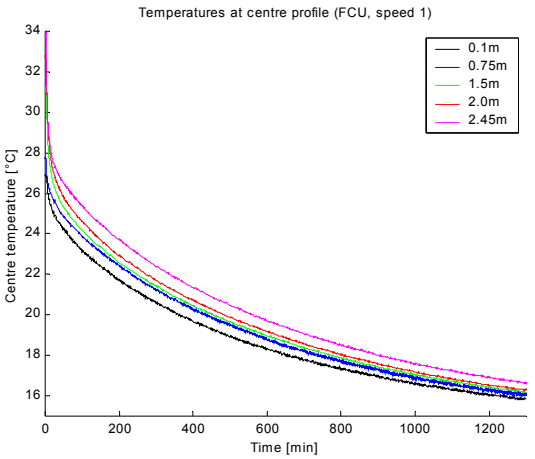

Figure II - 53: Evolution of air temperatures at centre profile (test ON → OFF) - EREDIS

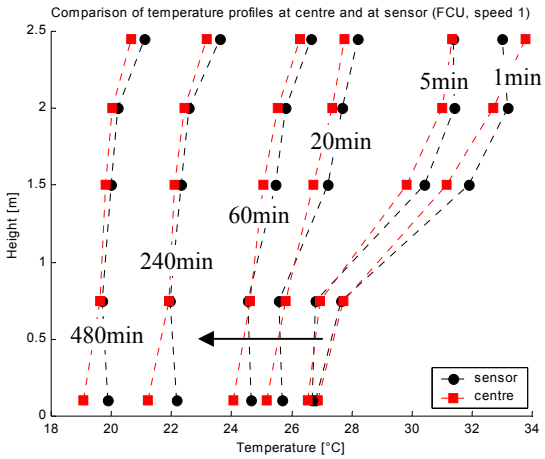

Figure II - 54: Evolution of centre and sensor temperature profile (test OFF → ON) - EREDIS

The difference between sensor and centre temperature profile disappears more and more. The stratification decreases as well and reaches a minimum value of about 1K at the end of the test.

Figure II - 55 shows the evolution of the relative temperatures at centre position. An upper zone with a quick response and a lower zone with a slow response are visible. The responses in the

upper zone and in the lower zone are nearly homogeneous. The difference is due to the transport of air from the upper part to the lower part by the cold boundary layers at the walls.

This difference can be very important for controller studies if the sensor is placed in the upper part or in the lower part.

Figure II - 56 shows the evolution of centre and sensor relative temperature profile. Contrary to the switch-on test no important differences between both profiles of relative temperature are visible. Even if the complete temperature difference between t=0 and $t=t_{end}$ is the same in the switch-on test and in the switch-off test, the two profiles can be assumed to be identical. The reason for this is that the difference in the response is distributed all over the test period while the difference appears rapidly in the switch-on test (time of jet development).

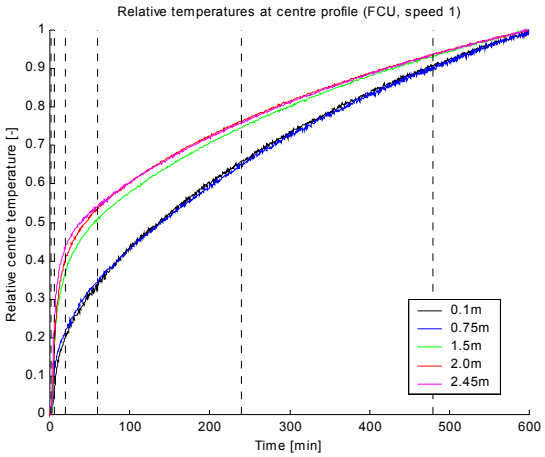

Figure II - 55: Evolution of relative temperature at centre profile (test ON→OFF) - EREDIS

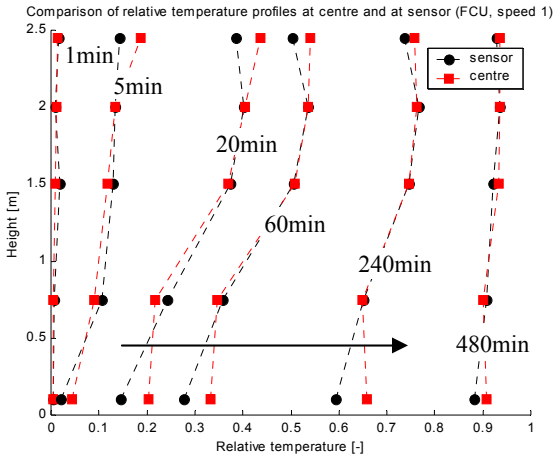

Figure II - 56: Evolution of centre - sensor relative temperature profile (test ON→OFF) - EREDIS

4.3 CONCLUSION TRANSIENT PHENOMENA

In most cases of zone heating, the case of a negatively buoyant wall jet is observed. This case can also be observed for cooling, but this case is very sensitive to the temperature difference at the walls and has thus not been treated. Two main dynamic phenomena in the zone exist for these cases:

☞ Differences in dynamic behaviour of temperature in the upper and the lower part of the zone:

These differences are principally the same for the heating case and for the cooling case. In the centre part the following two phenomena exist:

One zone collects the air from the boundary layers and has thus a slow temperature response (lower zone for winter case/cold boundary layers and upper zone for summer case/warm boundary layers).

In the other zone, all warm or cold air from the emitters is injected. The fast dynamics of this zone is only slowed down by mixing with the air of the second zone.

☞ Differences in dynamic behaviour of temperature at centre position and near walls:

In the case of a warm or cold wall jet, the temperature response is faster than at the corresponding height at centre position (switching on).

In the case that no jet exists at the walls, a boundary layer of natural convection is developed. The temperature dynamics in this boundary layer is slightly slower than in the centre air volume at the same height (switching off).

5. CONCLUSION CHAPTER II

Starting with general analysis of air flow in rooms from the literature and from a number of tests carried out for a European research project ([Lahrech01]), more detailed measurements have been carried out in the EREDIS test room at CSTB. The analysis of phenomena has been carried out using measurement and CFD simulation. The principal airflow patterns in the room and the conditions throughout the zone have been shown. The following phenomena were observed:

- ☞ *An air flow generator defining the principal air flow pattern in the room. This air flow generator can be divided into three cases:*
  - *room with air flow characterised by high positive buoyancy forces*
  - *room with air flow characterised by low positive or negative buoyancy forces*
  - *room with air flow characterised by high negative buoyancy forces*

  The impact of these flow cases on the conditions in the centre zone as well as in the near-wall air volumes (sensor zones) has been shown.
- ☞ *At the occupant zone it is observed that:*
  - *there is very little horizontal temperature variation outside jet and plume regions,*
  - *there is vertical temperature stratification, approximately linear in most of the cases studied. It can be non-linear in the case of bad design.*
- ☞ *The airflow near the walls is either characterised by natural or by mixed convection. In heating cases a negatively buoyant air flow is observed at the wall. The downward travel of this jet or plume depends on the temperature difference between the room air and the surface at the corresponding wall (favourable or unfavourable boundary layer).*

The last point can be very important for controller studies since the sensor is generally placed near the walls. The conditions near the wall differ, depending on the flow characteristics, in steady state regime as well as in their dynamic behaviour from the conditions at the occupant zone. This case can thus be a critical point for controller studies.

Finally in has been observed, that, even for emitters with plumes and low air velocities, a significant effect on the conditions at the sensor position can exist.

After this analysis, the new model should thus represent:

- *the variable temperature stratification in the room*
- *the variable temperature difference between the regions near the internal walls and at the centre of the room*

The model should be able to predict these two points in steady state and in transient conditions.

CHAPTER III

ANALYSIS OF EXISTING ROOM MODELS AND DEFINITION OF CRITERIA FOR A NEW MODEL

This chapter gives answers to two main questions:

- *Which are the criteria for the new model for controller studies?*
- *Which type of model is appropriated to satisfy the criteria?*

A first part of this chapter analyses criteria for the development of a new room model. These criteria are divided into general criteria and criteria for the test of controllers. The latter are characterised by three main aspects: the assessment of the performance of a controller, the position of the controller's sensor and the phenomena defining the measurement of a controller's sensor.

The main existing model types are then presented in a second part of this chapter. As the main part of the complete room model with its convection, radiation and conduction, different models of room convection, well-mixed models, zonal models, CFD models and lumped parameter models are studied.

Models of conduction and of radiation are briefly listed. They are not a main concern of this thesis, but since they are coupled with the convective model, a suitable type has to be chosen for both conduction and radiation.

Using the developed criteria in this and the previous chapter, the existing model types are discussed for the use in controller studies. An appropriated type for the convection model is selected for further development.

1. CRITERIA OF A NEW ZONE MODEL

1.1 GENERAL CRITERIA FOR THE MODEL

1.1.1 OPTIMISED DETAIL OF ROOM MODEL

Models for controller studies have generally to be simplified in order to allow fast dynamic simulations. At the same time, simplifications risk to create sensible errors in the simulation results. The principal objective in the development of a new room model is thus to find "the" optimal degree of precision for the model.

Generally there exist three groups of models:

- Room models for energy studies
- Room models for studies of comfort or/and airflow in rooms
- Room models for control studies

The first group needs fast dynamic simulations while keeping a defined minimum of precision. The simulation time step is in the order of an hour permitting long-term simulations in the order of a year.

The second group concerns mainly steady state simulations for the determination of airflow in rooms and for comfort assessment. The restriction of this type of model to steady state cases is due to the available computational resources. With the fast improvement of computational resources these studies are more and more extended to the simulation of transient cases or quasi-transient cases. However, the simulation of a complete building or even a zone using CFD room models remains unrealistic.

The third group of room models that is treated in this work is actually similar to the first group. The main difference is that these models have to be suitable for the use for simulations with a short time step in the order of seconds to be compatible with the test of controllers (e.g. time-proportional or PID).

The aim is to find an optimum degree of accuracy for room models of the third group. This degree of accuracy is within the two other model groups (Figure III - 1). As shown in the previous chapter the temperature depends generally on the position in the room. If the user wants to consider different possible positions of the controller sensor and the occupants of the room, the degree of detail of the convection model has to match this new demand. At the same time the degree of detail has to be kept at a minimum level (Figure III - 1).

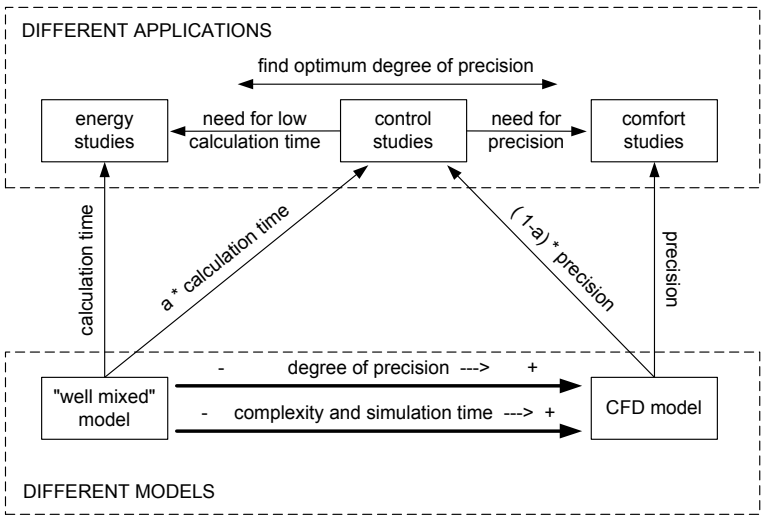

Figure III - 1: Use of a room model depending on the application

This degree of detail is chosen, considering all of the specific criteria developed, in the following sections.

1.1.2 USE OF AVAILABLE AND SIMPLE MODEL PARAMETERS

The use of available and simple parameters is one of the main issues of the development of the room model. It has to be usable either by simulation specialists carrying out simulation studies of control systems or by users having only a basic knowledge of system modelling. Detailed CFD models for example would be unusable for the second group of users. The knowledge, necessary to find an appropriated turbulence model, grid size or other parameters in order to obtain satisfying results, is very high. Already problematic, depending on the simulated case, in steady state conditions, the use of CFD simulation for transient cases is even more difficult and until now, very little work is done on this field.

A good mixture between complexity of parameters and model detail has to be found.

1.1.3 VALIDITY OF THE MODEL

The user of the new model should be able to carry out simulations for different room geometry, different use of the room or with different envelop construction (light or heavy construction). The models have thus to be as general and as flexible as possible. Models using physical laws seem interesting in this case since they permit, in certain limits, the extrapolation of the model. This is possible if all particular convective phenomena that are represented in the model (e.g. in a zonal model) are valid over a range, as large as possible.

The models have to be robust. Convergence and quality of the results is absolutely necessary since the test can not be repeated several times. A minimum of complexity is thus needed in order to reduce the number of iterations needed and thus the probability of convergence.

1.2 CRITERIA REGARDING TEST OF CONTROLLERS

The test and evaluation of a control system is a delicate problem in real conditions as well as in simulated conditions. Several simplifications or choices have to be undertaken in order to guarantee reasonable results. These choices are discussed in the following sections.

For a better understanding, the principle of a controller test bench is shown in Figure III - 2. The figure shows the interactions between the particular elements of the test bench. As shown in the figure, major problems appear on the room level and its links with the other elements of the test bench.

Three links appear in Figure III - 2 connecting the room model to the rest of the test bench. The links are:

- Link from actuator/emitter to the room model
- Link between room model and controller sensor (defined by position and measurement of the controller sensor)
- Link between room model and performance assessment module (defined by method and location of performance assessment)

These links are studied in the following section in order to develop the criteria for the new room model.

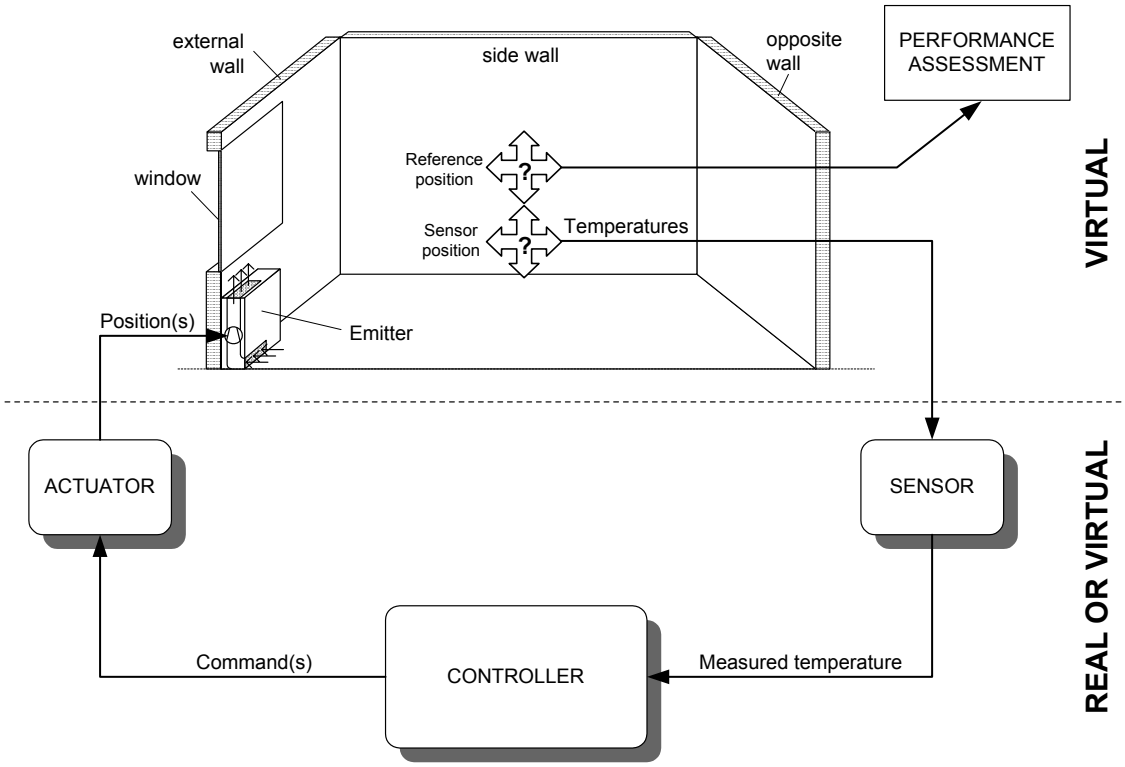

Figure III - 2: Principle of controller test and performance assessment

1.2.1 LINK BETWEEN ACTUATOR/EMITTER AND ROOM

This connection to the room can be of different type, depending on the test bench. It consists in a position of a valve or a damper interacting on water or airflow or a relay interacting on an electric resistance integrated in the emitter system. There is no direct connection between the actuator and the room. Both are coupled by an emitter system that influences the room conditions. The important link from the actuator side in Figure III - 2 is thus the coupling between the emitter and the room. This has been analysed in Chapter II, where the main convective phenomena have been studied.

1.2.2 LINK BETWEEN THE ROOM AND THE CONTROLLER

1.2.2.1 Position of the controller sensor in the room

If the conditions are homogeneous throughout the room, this point can be neglected. In all other cases the location of the sensor has, at least theoretically, an effect on the simulation results. Even if the controller is assumed to control the conditions at the occupant zone, it is, in real cases, placed at one of the internal walls at the same height, where the room conditions are controlled. This means that the sensor can be, depending on the airflow pattern in the room, placed either in a boundary layer of natural convection or in a jet or plume from an air diffuser or an emitter. For this reason the developed model should include the modelling of the air volumes where the sensor is usually placed. Figure III - 3 shows the possible positions of a room controller sensor in the example of a VAV system with a slot diffuser.

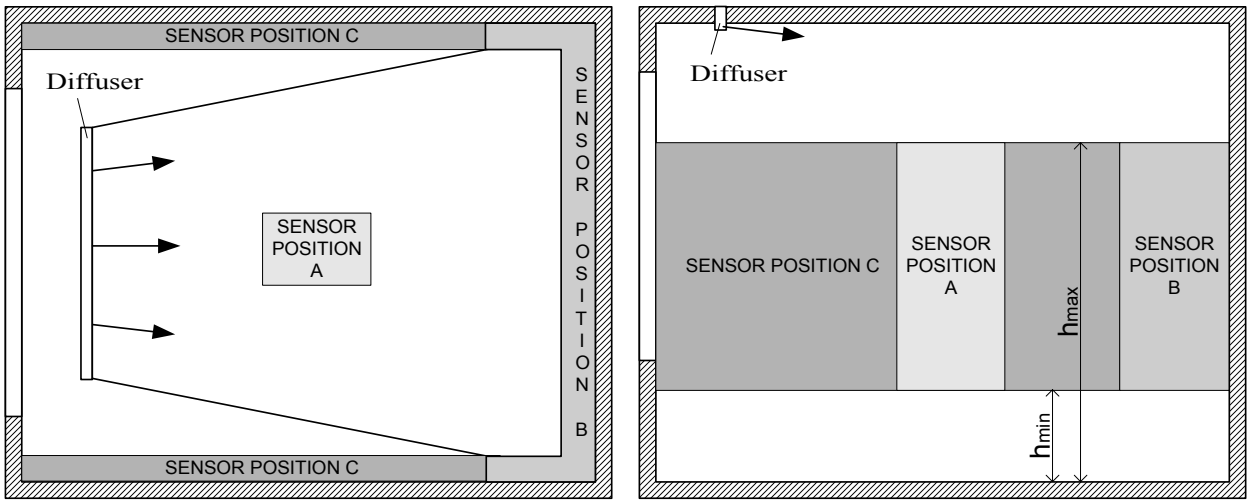

Figure III - 3: Possible positions of a controller sensor in the case of a standard room - example VAV system

As shown in Chapter II, the air conditions next to the internal walls show the same qualitative tendency all around the internal walls. This is true for cases with emitters located at lower levels in the zone. In these cases, the jet or plume spreads at the ceiling level and guarantees relatively homogeneous conditions around the internal walls. For cases of ventilation or air conditioning by the ceiling (VAV system with diffusers), the jet spreads depending on the diffuser characteristics. The spread of the jet defines two different regions near the walls that exist besides the "optimal sensor position" (sensor position A) at the centre:

- inside the possible trajectory of a jet (sensor position B)
- outside the possible trajectory of the jet (sensor position C)

These three sensor positions (A, B and C) have to be represented by the new room model in order to study the influence of these positions on controller test results.

1.2.2.2 Measurement of a controller sensor

The measurement of a controller's sensor is also a major problem in controller tests. The position of the sensor in the sensor box, the design of the sensor box and "hardware", integrated in the sensor box (convective and radiative heat emission of electronics), affect the result of sensor measurement. The measurement depends on all radiative, convective and conductive characteristics of sensor, sensor box and room. Even if it is assumed that the sensor is not affected by the electronic part that is integrated in the sensor box, the parts of convective, conductive and radiative measurement have to be known. Figure III - 4 shows the principal interactions between zone and sensor and the sensor with itself.

The observed phenomena can be divided into four main groups:

- Internal heat transfer inside the sensor box
- External heat transfer at the outside of the sensor box
- Phenomena of inertia of sensor and sensor box
- Airflow through the sensor

Each of these phenomena depends themselves on several factors that are described hereunder.

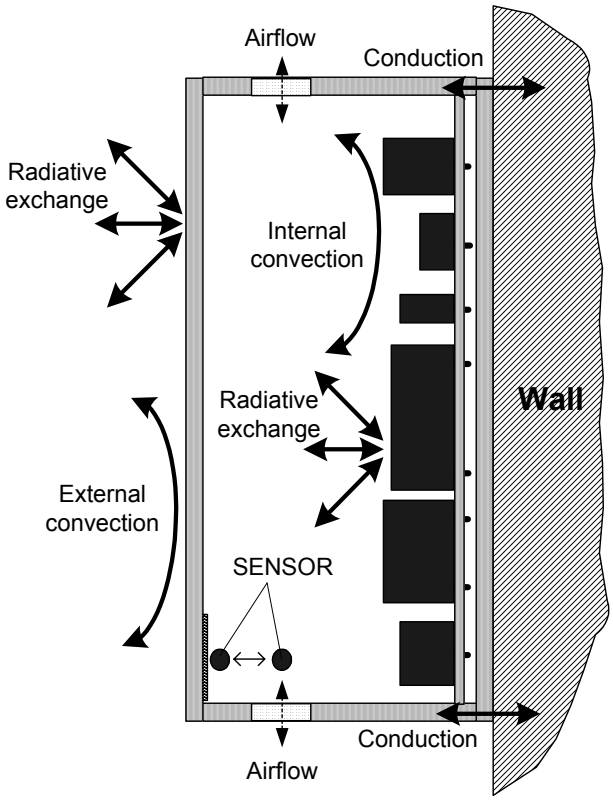

Figure III - 4: Typical heat and mass flows in and around the box of a controller sensor

The internal heat transfer inside the sensor box depends on different factors as:

- Mean radiant temperature at sensor position inside the sensor box
- Radiative properties of inside the sensor box
- Air temperature at sensor position inside the box
- Convective heat exchange coefficient at sensor inside the box (function of the airflow inside the box)

On the other hand, the external heat transfer around the sensor box depends as well on some other parameters that are:

- Mean room radiant temperature at position of the sensor box
- Radiative properties of the sensor box and its environment
- Air temperature at the position of sensor box
- Convective heat exchange coefficient around the sensor box (function of the airflow around the box)

The airflow through the sensor depends on the following points:

- Airflow around sensor box (depends on zone airflow and box design)
- Construction of sensor box (depends on box design: air inlets and outlets?)
- Internal heat sources generating air movements upwards (if controller is integrated in the box)

The phenomena of inertia depend on box structure and position of the sensor in the box. The sensor is, in general, placed either at a thin metal plate inside the wall of the sensor box, or in the

air volume inside the sensor box (Figure III - 4). The inertia of the "sensor system" depends thus either on the first or all of the following parameters:

- sensor mass
- mass of metal layer
- mass of box wall

The interaction of the general zone airflow and the internal convection can be a critical point in the design of a sensor box. The sensor is generally positioned in the box in order to measure the temperature around the sensor box. This would be the lower part of the sensor box since internal heat sources generate an upward airflow and the aspirated air at the bottom of the box passes at the sensor. In the case of an inverted airflow due to the interaction of internal and external airflow (downward airflow) it can be possible that the sensor measures a temperature that is highly influenced by the internal heat sources of the sensor box.

The important phenomena that have to be provided from the room model (depending on the degree of detail of the sensor model) are those of the groups "external heat transfer" and "airflow through the sensor". A too low degree of detail of the zone model limits the possible degree of detail of the sensor model since, in this case, the necessary inputs for the model can not be provided. However, the degree of detail of both models should be reduced to a minimum.

Another phenomenon can appear for modern controllers. Some controllers containing the sensor and some electronic equipment (bus etc.) in the same box create an own convective heat. To avoid an influence of this convective heat flow, the sensor is positioned in the lower part of the sensor box. In cases of wall jets or plumes, this proper convective air flow created by the electronic equipment risks to be inverted. If this is the case, the heat emitted by the electronics can influence the sensor measurement.

1.2.2.3 Conclusion on necessary outputs for sensor measurement

The room model has to provide the following outputs in order to characterise the conditions around the controller's sensor:

- Mean room radiant temperature at position of sensor box
- Air temperature at position of sensor box
- (Eventually the air velocity around the sensor box)

These two (three) outputs have to be known for the three sensor positions A, B and C in order to study the influence of sensor position on the controller test result.

1.2.3 LINK BETWEEN THE ROOM CONDITIONS AND PERFORMANCE ASSESSMENT

Two main key points have to be distinguished while assessing the performance of a controller. The position(s) where the performance is assessed, as well as the variable(s) considered at this position for the assessment.

1.2.3.1 Position of performance assessment

If the conditions are homogeneous throughout the room, no position has to be defined, where performance should be assessed.

The position of performance assessment affects the test results in a similar way as the position of the controller sensor. It has thus carefully to be defined. A realistic position is the zone of occupancy and a height where optimal comfort should be achieved. On the other hand one can argue that a controller can only be judged on the state variable it is controlling. This question demands a decision, if the controller should better be classed as a separate element or if the

combination of controller and sensor is considered for the test. In this latter case the distinction between sensor location and position of performance assessment seems to be necessary. The question of position of performance assessment is also linked to the state variable(s) considered for the performance assessment that will be treated in the next section.

1.2.3.2 State variable(s) or index for performance assessment

A choice of a specific index can lead to conclusions that are not general. At the same time, simplified room models do not provide all necessary data for the calculation of comfort indices. This requires assumptions that have an influence on the results (e.g. air velocity). Different methods are currently used in order to classify controllers depending on their ability to control room conditions. While in [Lahrech01] the resultant temperature is proposed for performance assessment, [Fisk81] proposes the use of a "mean error square" that is more related to comfort indices. In the tests they carried out they considered the room conditions as homogeneous. In reality, with non-homogeneous conditions, other problems appear. Other approaches for the selection of state variables could be necessary. Generally, the following variables or indices can be considered for the performance assessment:

- Temperature in general (air, radiant or resultant)
- mean square error of temperature (air, radiant or resultant)
- several comfort indices obtained from detailed room conditions

In all cases it has to be studied, if the criteria for necessary controller performance are consistent with the thermal sensation of the occupant. It does not make sense to introduce controller performances that could not be distinguished by the occupant due to thermal sensation of the occupant. The three groups will be studied in the following for their application as performance index in controller studies. A basic introduction in mechanisms of control of body temperature is given before a discussion of the different performance indices.

1.2.3.2.1 Control mechanisms in the human body

The human body is exposed to different ambient conditions [Fang98]. Depending on these conditions, the body exchanges energy with its environment. Several authors describe the principal mechanisms of control and heat exchange in the human body ([Fanger67], [Fanger70], [Hardy49], [Rapp67],[Gagge67]). In [ASHRAE97] these mechanisms are overviewed. A general overview on the mechanisms is shown in Figure III - 5, taken from [Hensen91].

Two aspects are described in the following, since they have a major effect on the sensitivity of occupants in transient conditions.

Thermoreceptors in the body

More than 100000 thermal sensors are integrated in the human body to permit an efficient control of the body temperature (Figure III - 5). Skin thermoreceptors are placed at the skin at about 1/10mm of the external surface. Other sensors are in the internal organs and also in the brain, especially the hypothalamus. Thermoreceptors exist for cold and for warm sensations. Both of them send signals to the brain containing two kinds of information:

- Temperature difference from the “normal” temperature (frequency of signals depending on the temperature difference)
- Temporal temperature gradient of the variable environment temperature (frequency of signals depending on the temporal temperature gradient)

The number of sensors for cold sensation is about 10 times higher than for warm sensation. This might be due to the fact that cold conditions can be more dangerous for people than warm conditions. The sensibility of the sensors is about 0.004°C for warm sensors and 0.001 for the cold ones ([Hensel51]).

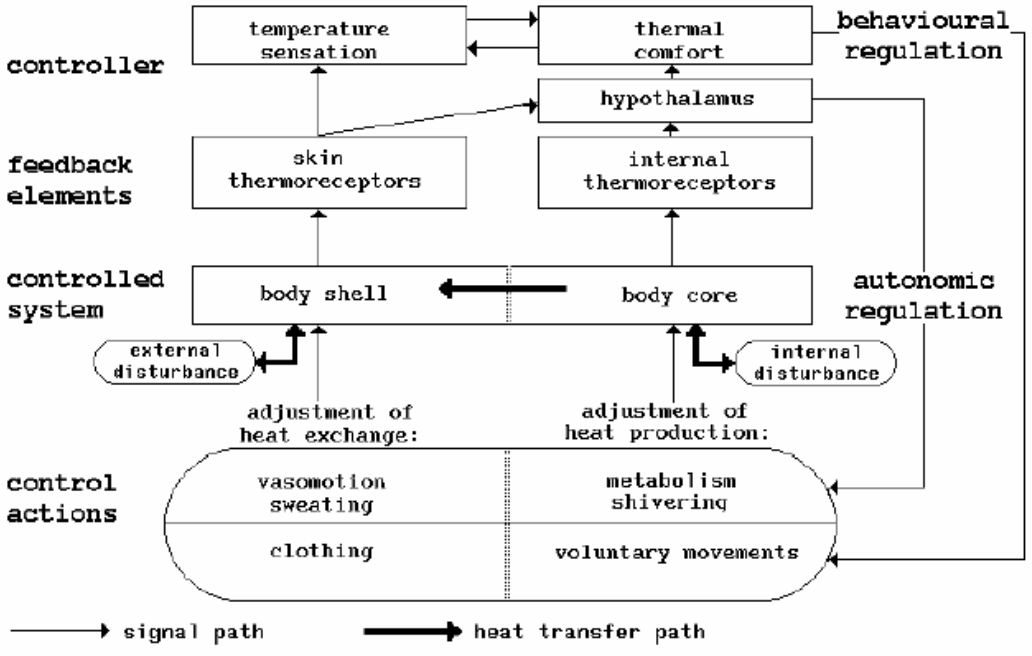

Figure III - 5: Schematic diagram of autonomic and behavioural temperature in man (from [Hensen1991])

Actions controlling the core temperature

The body uses different mechanisms (Figure III - 5) to react on temperature variations of the thermal environment and to keep the "core" temperature at a set point of about 37°C (+/- 0.4K day/night).

If the temperature is too high:

- The blood flow through the skin is increased. This increases the skin temperature and thus the temperature difference between skin and the environment (convective heat transfer).
- If the first mechanism is not sufficient, the body begins to sweat. Evaporative effects increase now the heat loss at the skin surface.

If the temperature is too low:

- The blood flow is decreased to decrease the temperature difference between body and environment.
- In a second step, shivering sets in to stimulate the muscles and to generate heat.

A very detailed knowledge about these phenomena is necessary in order to analyse the comfort of a person in a room.

1.2.3.2.2 Thermal comfort of building occupants

Comfort in general is the result of a subjective reaction (psychological and physiological) on objective, measurable values, for example the air temperature in a room. The standard [ISO7730] defines thermal comfort as « That condition of mind which expresses satisfaction with the thermal environment ». Many experiments have been carried out in order to get sufficient information about the sensation of a person in his thermal environment. Comfort is related to two types of factors, factors related to the person and factors related to its environment. They are listed in the following:

Factors related to the person:

- Position and activity
- Clothing
- Sex, size and age
- Day to day variations [ASHRAE97]
- Seasonal and circadian rhythm
- Individual factors (variation between individuals, variation between the behaviour of the same individual on different occasions or variation in response to successive stimuli by the same individual on the same occasion)

Factors related to the environment:

- Temperature, velocity, turbulence and humidity of the ambient air
- Mean radiant temperature at the position of the occupant
- Asymmetry of radiation at the position of the occupant

These factors are general, they have to be considered in local form since neither the person can be treated as a uniform body nor the environment is completely homogeneous outside a person. [ISO7730] gives ranges of acceptability for the factors related to the environment.

[ASHRAE97] proposes a scale for thermal sensation in order to classify the sensation of people in different environments and to standardise them (Table 3).

The values are commonly used for comfort studies in order to quantify a “mean” sensation of a person in an environment.

Table 3: ASHRAE thermal sensation scale

Numerical Code	Sensation
+3	Hot
+2	Warm
+1	Slightly warm
0	Neutral
-1	Slightly cool
-2	Cool
-3	Cold

A large number of authors studied the thermal sensation of occupants in order to correlate thermal sensation with scales as proposed in Table 3. This research has been mainly carried out in steady state conditions. Different indices have been developed:

- Predicted Mean Vote (PMV) index ([Fanger73]),

- Predicted Percentage of Dissatisfied (PPD) index ([Fanger72]),
- UCRES index integrating phenomena of temperature (U), air velocity (C), asymmetric radiation (R), temperature stratification (E) and floor temperature (S) ([Ribéron90]),
- GRES index, a simplified UCRES index ([François92]) neglecting the variable influence of air velocities.

While the first two indices refer to a certain point in the room or to mean values, the third and fourth one refer to a spatial distribution in the occupant zone (e.g. temperature stratification).

Some research has been carried out in transient cases. Several authors developed transient models of the regulatory responses of the body to its environmental conditions and related them as well to similar comfort scales as shown in Table 3 ([Stolwijk70], [Gordon74], [Gagge71], [Hardy61]).

Other work has been carried out experimentally in order to study the human sensitivity to transient temperatures ([Griffins74], [Sprague70], [Wyon71], [McIntyre74], [Wyon73], [Nevins75], [Rohles80], [Berglund78], [Rohles85]). The results of these studies do not permit an absolute clear conclusion since the results contradict partially. [Hensen90] gives an overview about all this research carried out for cyclic, step and ramp temperature changes and presents as main conclusions:

- the knowledge concerning thermal comfort in transient conditions is still limited
- for cyclic changes, the guidelines by ASHRAE's standard 55-1981 can be considered which state: "*If the peak variation in operative temperature exceeds 1.1K, the rate of temperature change shall not exceed 2.2K/h. There are no restrictions on the rate of temperature change if the peak to peak is 1.1K or less*".
- It is stated that there is "*no evidence ... found why the limit for cyclical changes would not be valid for temperature drifts and ramps as well"*.
- Clothing insulation has a negligible effect on thermal sensitivity during temperature changes
- Humidity fluctuations, when inside the range of 20% to 70%, have no significant effect
- Comfort decreases with increasing air turbulence

[Knudsen90], using results from experiments with steps from neutral to warm and from neutral to cold conditions, states that temperature variations are felt immediately for both steps. Contrarily to steps from neutral to warm conditions, steps from neutral to cold conditions are characterised by an overshoot in thermal sensation before adjusting to the steady state value after about 30 minutes. He also observed that for steps from uncomfortable to comfortable conditions thermal acceptability is reached faster than for steps in the opposite sense. Other authors as for example [Kubota91] have also observed this overshoot.

In the following sections, different possible state variables or indices are compared regarding their adaptation as index for performance assessment during the controller tests.

1.2.3.2.3 The use of temperature as performance index

Using temperature as performance index represents the simplest approach since this temperature is generally direct output of any room model. No further assumptions have to be made to convert the simulation results into a performance index, which is a meaningful, physical index and includes only objective parameters.

The used temperature can be the air temperature, the mean radiant temperature or better the resultant (operative) temperature at the specified position (see §1.2.3.1).

On the other hand this index does not relate directly to the comfort of the occupants. Even if the controller is able to maintain the room conditions inside a "zone of thermal comfort" ([ASHRAE97]) the performance is not monitored as perfect. Depending on how the index is treated in the following, this problem can be avoided by introducing a classification as used in [Lahrech01] or the standard proposal [CENTC247], shown in Table 4.

Table 4: Classification table for controller test

CLASS	Control Accuracy		Set point accuracy
1	$\leq$0,5 K	&	$\leq$1 K
2	$\leq$1,0 K	&	$\leq$2 K
3	$\leq$2,0 K		not applicable

Table 4 introduces two performance indices:

- Control accuracy (amplitude of temperature oscillation)
- Set point accuracy (difference between mean temperature and set point temperature)

The control accuracy can be given as total or half peak to peak amplitude of temperature. The latter makes its definition closer to that of the other two indices described below.

By fixing the borders in the classification table it is possible to match with the definition of a zone of thermal comfort with a minimum of complaints.

This fixing of borders in the classification table introduces a subjective point into the method. On the other hand the classification table permits to keep the test results (classes 1-3) on a simple, physical basis.

1.2.3.2.4 The use of temperature mean error square as a performance index

As for the case where temperature is used as performance index, the mean error square or root mean error square of temperature demands in a first step to define which temperature is used (air, radiant or resultant temperature).

[Fisk81] presents this index as a criterion adapted to the assessment of performance, since it is "*one of the easiest measures of error to compute in control design and relates to both the mean value of the PPD and to the probability of occupants taking unprompted action to change their thermal environment*". The author demonstrates that the square error of resultant temperature is approximately proportional to PPD index. In the study the mean error square has been found a good indicator for the response of individuals on transient ramp changes.

If this criterion is supposed to be similar to PPD indices the user risks to interpret the result equivalent to a comfort index. A quantitative interpretation can be deceptive since it ignores a large number of assumptions made on thermal comfort of an individual, especially in transient cases. In this case it would perhaps be better to use PPD with all precautions necessary for this index (see §1.2.3.2.5).

1.2.3.2.5 The use of comfort indices as performance index

Several comfort indices have been listed in §1.2.3.2.2. If the experimental results in transient conditions are considered, the main question that has to be solved before using a comfort criterion is, if the temperature changes during the controller tests are within the maximum ranges of validity obtained by experiment. If the ranges listed in §1.2.3.2.2 are coherent with the maximum temperature during a controller test steady state criteria can be used without precautions. In the opposite case the use of transient models could be of interest if these take into account the overshoot in thermal sensation, observed from several authors (see §1.2.3.2.2).

Preliminary tests could be carried out in order to get an idea of the ranges of slope of temperature change during the tests. These tests are difficult to evaluate since the slope of temperature depends on HVAC system, room geometry and other factors.

On the other hand, since the assessment of comfort demands several factors of the thermal environment in a room, the high level of detail of the room model would be necessary. The assessment of comfort integrates conditions in the room such as air velocity that is only obtained using a CFD model. Other factors as for example clothing and activity of the occupant have to be chosen. These assumptions for the performance assessment of a controller would thus also represent a subjective result.

PPD and PMV indices consider either local or mean conditions at the occupant zone. They can thus be applied for well-mixed models as well as for more detailed models. When more detailed models are used, a new question appears, if local PPD values or mean values on a fixed domain should be considered. If local values are used, the question of the reference position for performance assessment has to be solved.

The use of the UCRES or the GRES profiles would simplify this problem. They characterise the conditions in the occupant zone. Since they consider partially the problem of non-isothermal conditions at the occupant zone, the problem of local or mean values is already solved. On the other hand, these indices provide even more results that have to be converted into some kind of classification as well. This conversion would finally, as for all other indices, introduce a factor of subjectivity in the test result.

1.2.3.3 Conclusion on performance assessment

Different performance indices have been presented. Each of them has its particularities. The indices using the definition of comfort have all been developed for steady state conditions. An application to transient conditions with temperature variations introduces new factors of uncertainty.

All mentioned indices for performance assessment need particular information about the room conditions and so different outputs of the room model. They are listed in Table 5:

Method	Air temperature	Mean radiant temperature	Temperature Stratification	Surface temperatures	Air velocity
Temperature	X	X			
Error square	X	X			
PMV/PPD	X	X			X
UCRES	X		X	X	X
GRES	X		X	X	

Table 5: Necessary outputs of a room model

The indices PMV, PPD and UCRES need the knowledge of the air velocity at the position in the room where performance is assessed.

The other indices need generally the room air temperature and the mean radiant temperature and in the case of UCRES and GRES also the temperature stratification and the surface temperatures.

The new model has to be able to cover the main outputs in order to give the user the possibility to use different performance indices. However, the output of the velocity seems unreasonable since therefore CFD models would be necessary.

2. ANALYSIS OF EXISTING ROOM MODELS

Room models exist with different levels of complexity: from simple "well mixed" models with one air node representing the whole air volume in the room to complex computational fluid dynamic (CFD) models solving the equations of conservation of mass, momentum and energy. The models can be divided into five main groups:

- Well-mixed models (model of convection)
- CFD models (model of convection)
- Zonal models (model of convection)
- Lumped parameter models (model of room including envelope)
- Model using identification (convection model or room model)

The simple well-mixed models on the one hand are commonly used to study the energy consumption in buildings ([TRNSYS96], [DOE89], [Clarke85], [Redares86]).

CFD models, on the other hand ([Phoenics91], [Fluent98]), are used for comfort studies and the prediction of airflow in rooms because they provide detailed information about the conditions in the room. Since CFD calculations are very time consuming, they are mostly used for steady state problems. To date, transient phenomena are rarely studied ([Ratnam98], [Lin00]).

Zonal models represent an intermediate type of model, between well-mixed models and CFD models. They divide the room air into a reduced number of air sub-volumes. Although they have mainly developed for the study of comfort and thus for the steady state case, they have also been used for the simulation of transient cases ([During94], [Musy99a]).

For control purposes, mostly lumped parameter models are used ([Klinger99], [Rouvel97], [Laret80], [Haves98], [Osman96], [Kast98]). Only in some rare cases, zonal models or, very rarely, CFD models with several simplifications have been used (Peng96], [Ratnam98]). But these cases are limited to one specific case. They are not generic and can hardly be reused for other zones or emitters.

The first three types of models are only models for the room convection. They have to be coupled with a model of the room envelope (conduction) and a model of the thermal radiation in the room. Different types of envelope models are currently used:

- Lumped parameter wall model
- Finite difference model
- Nodal wall model

Heat exchange by radiation can either be modelled by using:

- Mean radiant temperature node,
- Walton's method ([Walton80]),
- Other radiation models ([Özisik83])

The modelling of the envelope and radiation has been subject of various studies. They are thus not treated here in detail. Only in the case of lumped parameter models the envelope modelling is shown here since convection, radiation and conduction is coupled in these models.

In the following sections the different types of convection models are presented.

2.1 MODELS OF CONVECTION

2.1.1 WELL-MIXED MODELS

This type is frequently used for the study of energy consumption in buildings. The air in the room is considered to be perfectly mixed in temperature and all other properties as e.g. humidity, pollutants as well. Figure III - 6 (left) shows the heat exchanges in the well-mixed model. The phenomena of heat exchange in the case of the well-mixed model are:

- external air supply (fresh air, inter-zonal air exchange, air conditioning system)
- Convective heat exchange at internal surfaces (walls, floor, ceiling)
- Convective heat exchange at internal heat sources (emitters, other heat sources as occupation, electric equipment, …)

All heat exchange is assumed to be between the boundary conditions and the mean temperature node in the room. Figure III - 6 (right) shows the corresponding electrical representation.

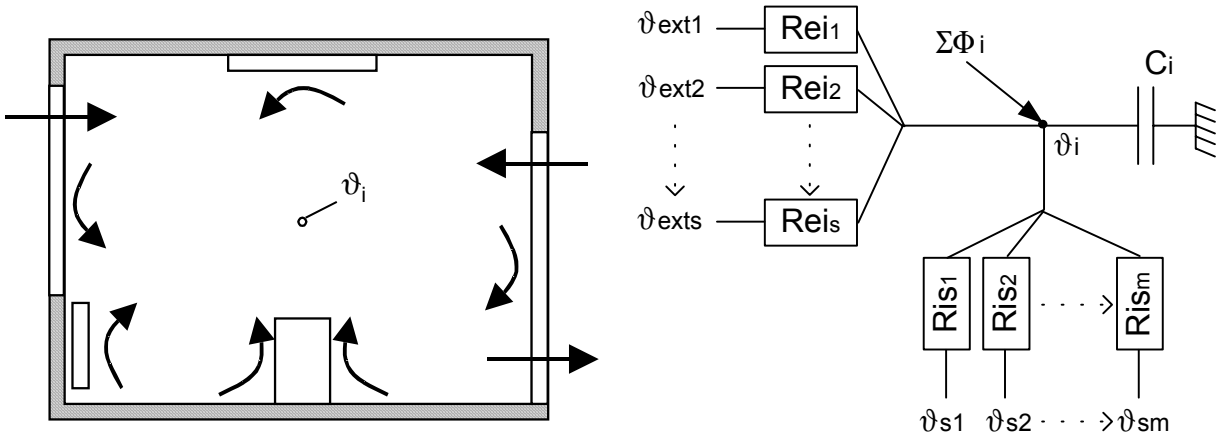

Figure III - 6: Heat exchanges in the well mixed model (left) and electrical representation (right)

The system is described by the equation of energy conservation:

$$\rho V_i C_p \frac{d\vartheta_i}{dt} = \sum_1^m \Phi_{conv} + \sum_1^s \Phi_{j,i} - \sum_1^s \Phi_{i,j} + \sum_1^q \Phi_{Gains} \qquad (3)$$

where

m is the number of internal surfaces, s the number of sources of air exchange and q the number of convective heat sources in the zone.

Due to the simplification of homogeneous conditions no information about temperature distribution is available in this type of model.

2.1.2 COMPUTATIONAL FLUID MODELS

Since this type of model is unrealistic for the use in control studies, only a short overview is given here.

Using computational fluid models, the room air is divided into a large number of finite elements or volumes. In each of the cells the equations of mass, momentum and energy are solved in order to obtain the conditions throughout the room. Due to the high number of cells the computational effort is very high and fast simulations or even a real-time simulation are, to date, impossible for three-dimensional cases.

In [Beausoleil01a] and [Beausoleil01b] a first step for the integration of building simulation is undertaken. One zone of the building is there simulated in detail while the detail in all other zones is kept on a low level. In [Ratnam98] a "quasi-transient" CFD model is applied to the transient study of a control loop. [Lin00] carried out a real transient simulation of a room equipped with a chilled ceiling system. Due to the enormous calculation time this kind of model is unusable in our case. [Peng95] carried out CFD simulations for the generation of a simplified CFD model with fixed flow fields.

CFD models need the use of a turbulence model. The choice of this type of model is, even for specialists, still difficult, and depends on the case treated. Various simulations have been carried out in order to recommend the use of turbulence models for particular cases of HVAC systems.

2.1.3 ZONAL MODELS

In zonal models, the internal zone air volume is divided in several sub-volumes ([Hemmi67], [Bouia93], [Wurz95], [Peng96], [Musy99b]). Contrarily to CFD models, only the equations of conservation of mass and of energy are solved. The Navier-Stokes equations are not considered. The airflow between the sub-volumes has to be calculated by correlation or other simplified method (pressure calculation).

This type of model has been developed in order to characterise the comfort in a zone while keeping the model as simple as possible. The main purpose has been to represent the conditions at the occupant zone of the room. Figure III - 7 shows the principle heat and mass exchange between the sub-volumes and boundary conditions.

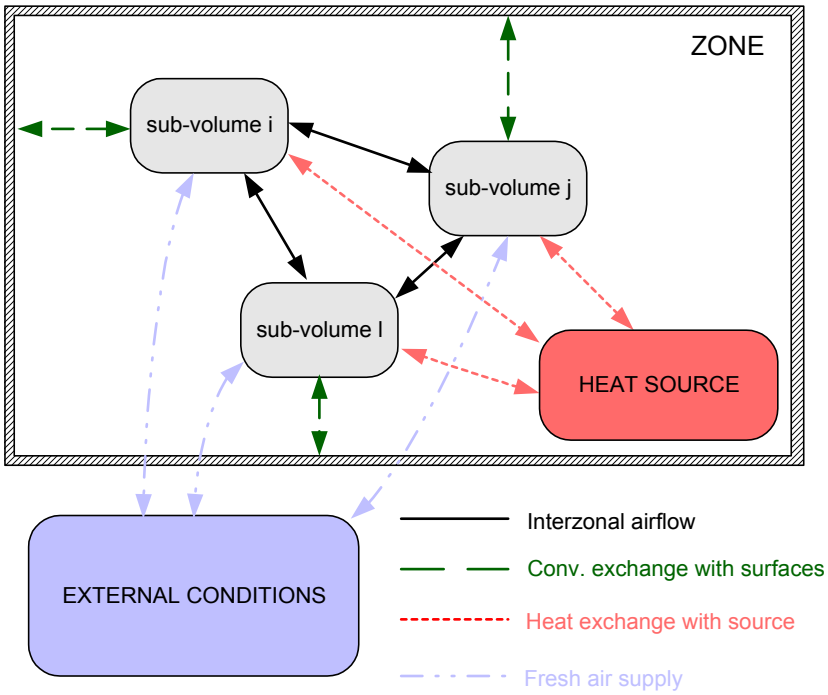

Figure III - 7: Principle of a zonal model

The following heat and mass transfers appear in a zonal model:

- Airflow between sub-volume i and sub-volume j
- Convective heat exchange of sub-volume i with adjacent surface A_k
- Airflow between sub-volume i and external conditions (fresh air supply or ventilation)
- Heat source in sub-volume i

The flow rates are obtained from correlations, the equations of momentum have thus not to be solved. The correlations can be of one of the following types:

- Correlation for the flow rate in plumes and jets
- Correlation for the flow rate in boundary layers (free convection)
- Correlation for the flow rates between air volumes due to temperature differences

The heat balance on one air sub-volume is:

$$m_i\, c_p \frac{d\,\vartheta_i}{d\,t} = \sum_{j=1}^{l} \dot{m}_{j,i}\, c_p\, \vartheta_j \; - \sum_{j=1}^{l} \dot{m}_{i,j}\, c_p\, \vartheta_i \; + \sum_{k=1}^{m} h_{i,k}\, A_{i,k}\, (\vartheta_{A,k} \; - \; \vartheta_i) + \sum_{r=1}^{s} \dot{m}_{ext;r,i}\, c_p\, \vartheta_{ext,r} \; - \sum_{r=1}^{s} \dot{m}_{ext;i,r}\, c_p\, \vartheta_i \; + \sum_{p=1}^{q} \Phi_p \tag{4}$$

where
l is the number of sub-volumes, m is the number of internal surfaces, s the number of sources of external air exchange and q the number of convective heat sources in the zone.
One of the inconveniences of the zonal model approach is that the principal airflow pattern in the zone has to be known in order to guarantee reasonable results.

Several authors have developed zonal models for a room equipped with a convective heat source, such as a convector or a radiator, below a cold window. [Lebrun70] proposed first, to divide the air volume in the room into several air sub-volumes, depending on their flow phenomena (Figure III - 8). [Horwarth80], after analysing experimentally the main convective phenomena in a room heated by a radiator, the plume of the radiator and the boundary layer at the external wall, developed a zonal model with an upper zone and a lower zone, working in transient conditions (Figure III - 9). The boundary layers at all walls have been assumed as natural convection cases.

[Laret80] developed an analytical model, based on steady state conditions, able to calculate the temperature profile at the centre of the room (Figure III - 10). This model has also been extended, after some simplifications, to the transient case.

[Inard88] developed a model for a room with a convector or a radiator including the plume and boundary layer phenomena in free convection. The occupant zone is modelled with three zones (Figure III - 11).

[Ngendeku88] developed a model using the principle of heat exchangers in order to calculate the heat transfer at the walls. He also included a re-circulation in the upper part of the room (Figure III - 12).

[During94] studied the use of zonal models for transient conditions (Figure III - 13). He increased the number of air sub-volumes to 12. The transient analysis was, in his case, focussed on long time periods (simulation of several days). Short time dynamics, important in controller studies, have not been treated. The dynamic phenomena studied in this case were thus mainly the

dynamics of the envelope elements. A second, similar model for the case of a heated floor has also been developed.

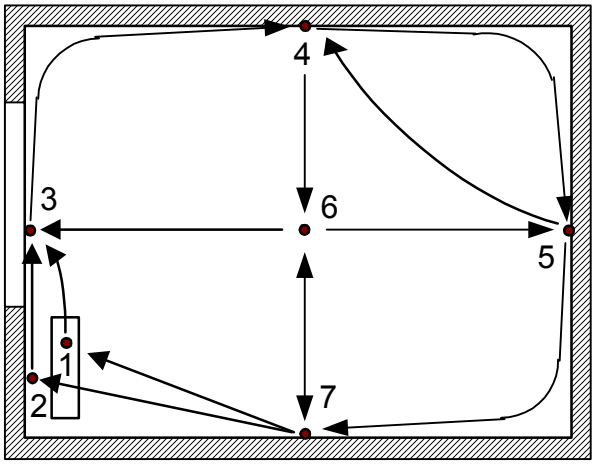

Figure III - 8: Zone with radiator/convector ([Lebrun70])

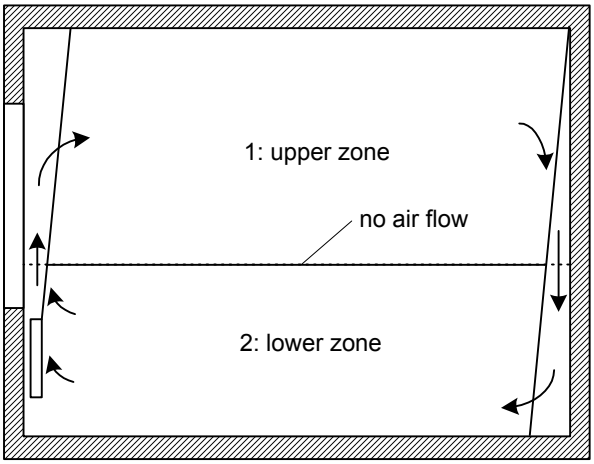

Figure III - 9: Zone with radiator ([Horwarth80])

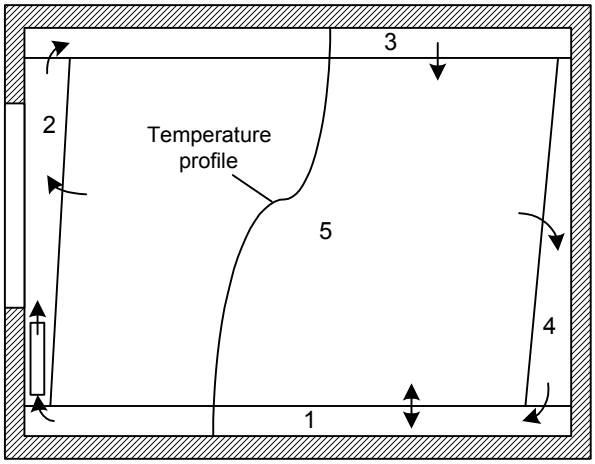

Figure III - 10: Zone with heater ([Laret80])

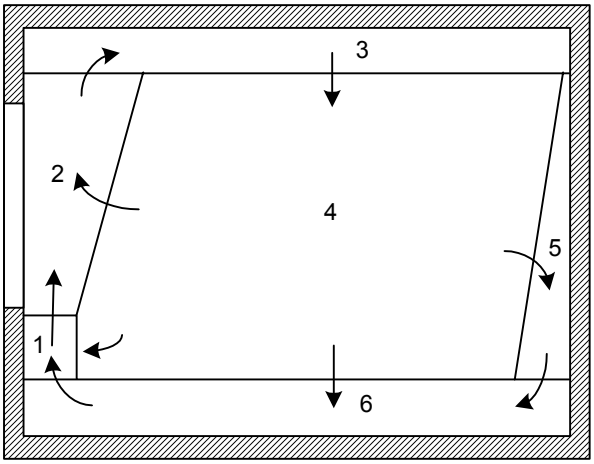

Figure III - 11: Zone with convector/radiator ([Inard88])

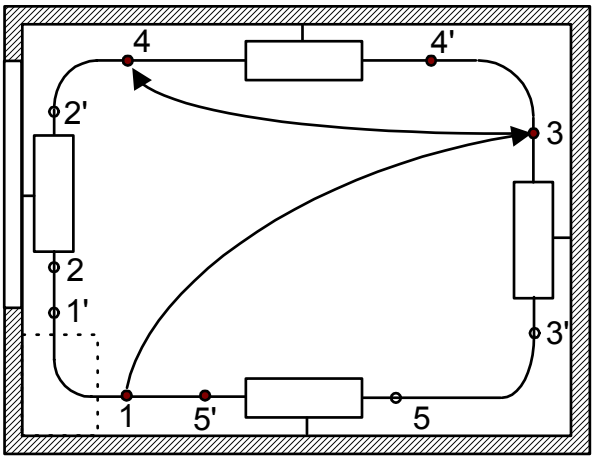

Figure III - 12: Zone with convector/radiator ([Ngendeku88])

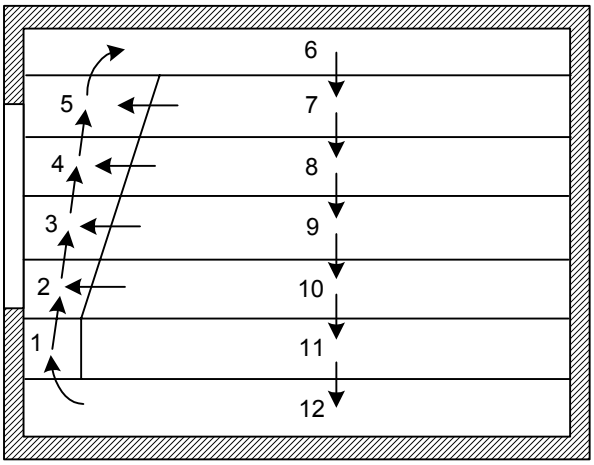

Figure III - 13: Zone with radiator/convector ([During94])

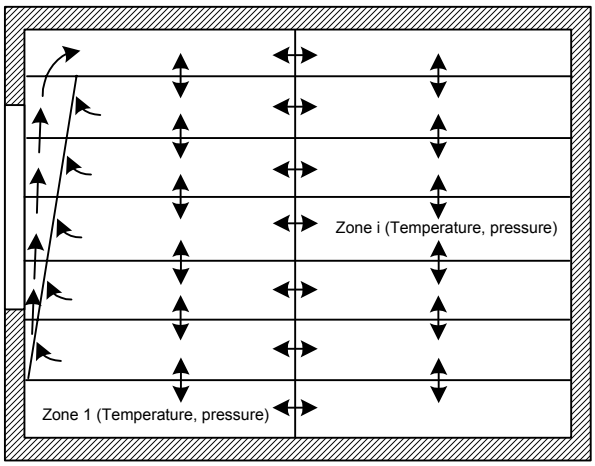

Figure III - 14: General zonal model (based on pressure laws and correlations) (since 1985)

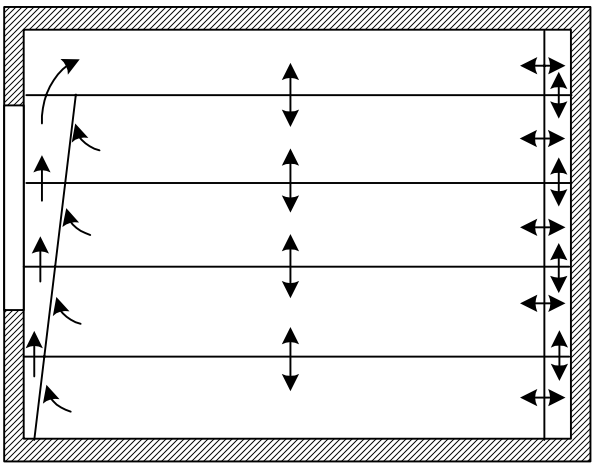

Figure III - 15: General zone model of Togari [Togari93]

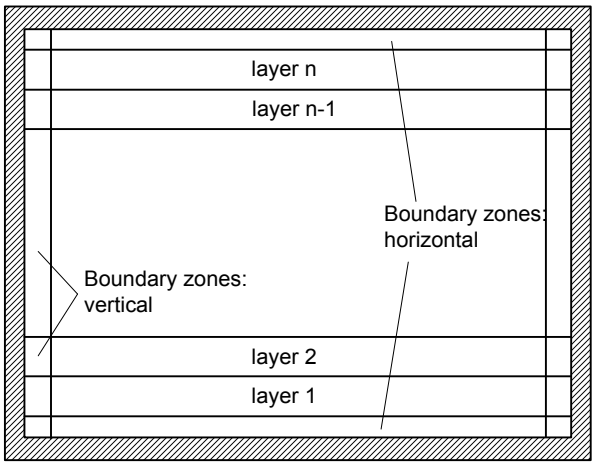

Figure III - 16: Zone with natural convection ([Hutter81])

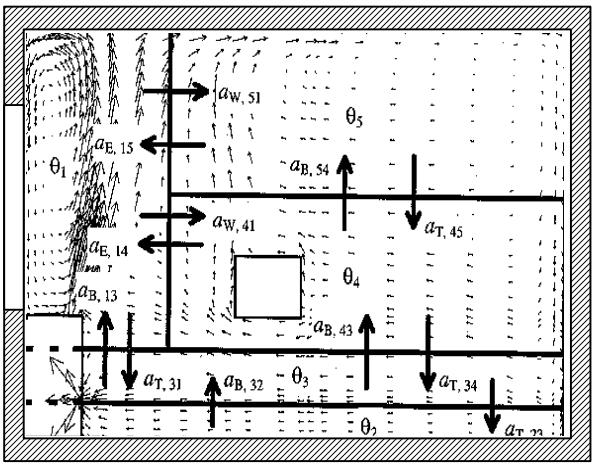

Figure III - 17: Zone with fan coil unit and heat source ([Peng96])

[Fauconnier85] developed a zonal model where the mass transfer between the zones is obtained from correlations based on pressure differences. Bouia [Bouia93], Wurtz [Wurz95] and Musy [Musy99a] continued this work and developed models with flexible zones as shown in Figure III - 14.

A model presented by [Togary93], similar to Inards model [Inard88] and with higher number of zones, is extended to the use for different emitters or ventilation (Figure III - 15). It can be used also for air conditioning with divers jets and also in transient conditions.

Hutter ([Hutter81]) presented a zonal model for natural convection. This model uses a variable number of horizontal air layers (Figure III - 16) and represents also the zones of natural convection near the walls.

Peng [Peng96] developed a first zonal model for control studies for a fan coil application based on pre-simulations in CFD for controller studies (Figure III - 17). However, since the sensor was, in his case, placed at the air extraction of the fan coil unit, it was not necessary to model convective phenomena around the sensor (wall jet). The main assumption in his modelling is that the airflow in the zone does not change and is only a function of the fan speed of the fan coil.

The zonal model principle has been more and more generalised. But all of these models have been optimised in order to represent well the conditions at the centre of the zone. The modelling of thermal effects near walls was of lower importance. The boundary layers at the wall have thus

all been represented by expression for free convection. Either correlation of vertical flat plates has been used or correlation obtained in test rooms with heated or cooled surfaces. The results of these approaches are in good agreement if the boundary layers are one of the main engines of the airflow in the room. This is the case for high temperature differences between room air and the surfaces. On the other hand, phenomena of negative buoyancy are more difficult to handle. The measurements carried out in Chapter II to characterise the phenomena in the air volumes near the wall show that in many cases negative buoyancy governs the flow near the internal walls.

Some of the presented models have been used in the transient case. But except for the model of Peng, all of them have been validated for long term simulations (e.g. [During94]), since they have been developed for the study of energy consumption.

2.1.4 SIMPLIFIED MODELS USING SUPPLEMENTARY IDENTIFICATION OR CORRELATION

This model type is typical in the control field. By identification with measurements, the necessary phenomena can be modelled. The system can then be represented as a state space model with the parameters obtained by identification with experimental results.

This concept could be interesting due to the possibility to represent the observed phenomena while keeping the model at a minimum level of detail. [Maalej95], for example, presents correlations for temperature stratification in rooms for different heat sources. Correlation or identification could also be used to represent differences between sensor and centre temperature.

However, identification or black box models have the disadvantage that they are only valid within the range of conditions they are based on. Extrapolation outside this range given by the identification process is risky compared to physical models as for example zonal models.

2.2 MODELS OF CONDUCTION

There are four basic types of wall models:

- Lumped parameter model: they have the advantage of a low number of parameters. A set of a few parameters describes the system. A lumped parameter model can integrate all layers of one envelope element (e.g. wall), all elements of the envelope of a room or the whole room model (convection, conduction and radiation in a room). The latter is currently used to simulate rooms in controller studies. In the same way, one or more envelope elements can be modelled as a lumped parameter model. This modelling permits fast simulations since the system is reduced to a fist order system. The model can be described as by thermal-electrical analogy. Several authors ([Laret80], [Roux84]) studied this type of model and found acceptable agreement with more detailed models.

- Finite difference model: it is based on the spatial and temporal discretisation of the equation of conduction. The model can be used in one or more-dimensional representation ([Özisik83]).

- Nodal wall model: the wall is divided into n equivalent sub-layers of a wall, each characterised by a thermal capacitance. The capacitances connected with resistances equivalent to the inverse of the thermal conductivity. The nodal model is equivalent to the finite difference model with second order approximation ([Roux84]).

- Transfer-Function models: the coefficients of the transfer function are calculated in a “pre-processing” program. The model is currently used in simulation programs for the study of energy consumption ([TRNSYS96]).

2.3 MODELS OF RADIATION

There are different types of radiation models that are only described briefly since their detail of modelling has a lower importance on the studied problem as the modelling of convective phenomena. The three main types are:

- model using one mean radiant temperature node:

  All radiative heat exchange between the internal room surfaces and external radiation is calculated using a fictitious mean radiant temperature node. Due to the simplification using a mean temperature node, an error is introduced depending on the temperature differences between the surfaces. The error can be neglected for small temperature differences. The heat balance uses a simplified radiative heat transfer coefficient.

- model using the mean radiant temperature nodes of all surfaces surrounding the treated surface ([Walton80]):

  The second model type uses different fictitious radiant temperature nodes. For each surface element, the mean radiant temperature of all other surfaces exchanging long wave radiation with this element is calculated. Solar radiation and radiation from equipment has to be injected to the different radiant temperature nodes. This model represents an improvement of the first model using a mean radiant temperature since it considers only the temperatures of all other surfaces for the balance at the concerned surface. A simplified radiant heat transfer coefficient is used in the heat balance on each surface.

- models using view factors:

  The view factors between the different internal surfaces are calculated. The view factors are then introduced into the heat balances of each surface element. [Özisik83] lists some methods of radiation modelling based on view factor theory.

2.4 LUMPED PARAMETER ROOM MODELS

This model type “lumps” a number of parameters together, in order to obtain a model, as simple as possible, able to represent the necessary phenomena in a room. This can be the room air that is generally treated as well-mixed or the different layers of a wall or even different walls or surfaces. Figure III - 18 shows an example of a lumped parameter model representing the air temperature ϑ_i, a resultant temperature ϑ_s (mix between mean radiant and air temperature) and a wall temperature ϑ_w ([Riederer00]).

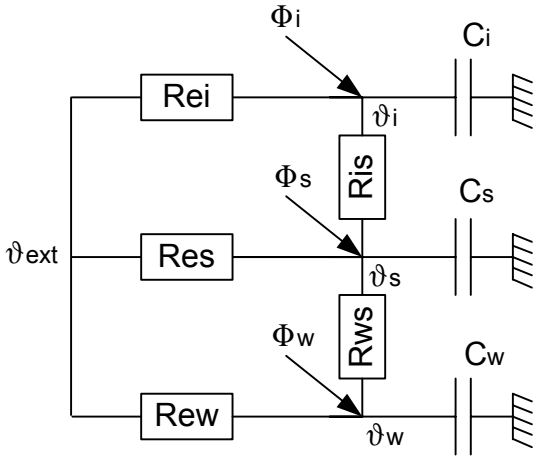

Figure III - 18: Example for a lumped parameter model with 3 capacitors and 5 resistances (R5C3)

[Laret80] developed a model representing only a resultant temperature in the zone. This results in a very simple model structure and the elimination of non-relevant outputs of a model. On the other hand, the use of these models is limited since they only represent the minimum of information.

2.5 CONCLUSION ON ROOM MODELS

Convective models:

Only few detailed room models have been developed for control analysis. None of these models would be able to represent the phenomena of negative buoyancy at the internal walls that have been observed in Chapter II. Zonal models seem to deal well with this problem since they have a great flexibility while keeping a rather simple description of the system. Figure III - 19 and Figure III - 20 show, qualitatively, the error of the well-mixed model and one of the existing zonal models (supposing natural convection near walls) respectively while predicting temperature at the sensor zones.

While the well-mixed model is not able at all to predict stratification, except with a supplementary module that calculates stratification as a function of emitter and emitted heat, the zonal model predicts an average stratification in the room. In the case of natural convection at the internal walls the zonal model would give satisfactory results. In the case of negative buoyancy at the internal walls, the model will not be able anymore to predict well the conditions near the walls. The error will increase in this case and will depend on the negatively buoyant air flow near the walls.

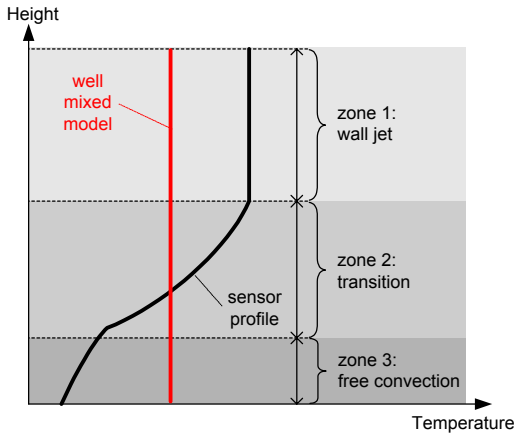

Figure III - 19: Qualitative error for the well-mixed model for the case of negative buoyancy

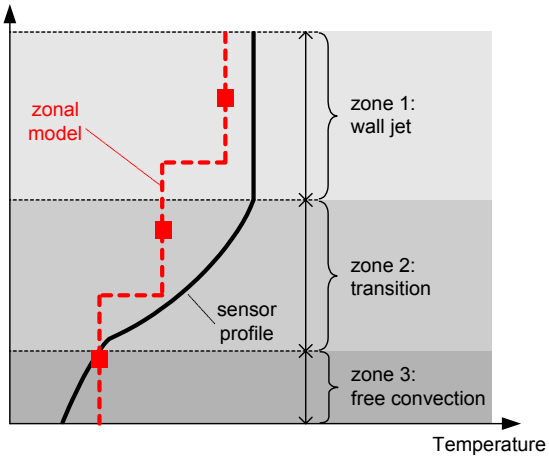

Figure III - 20: Qualitative error for the zonal model for the case of negative buoyancy

Radiation model and convection model:

Radiation models and conduction models of different complexities have been listed. These model types have been researched in various studies and are not studied here.

For further specification of the necessary convection model, criteria are developed regarding the use of the room model for controller studies.

2.6 CONCLUSION ON MODEL CRITERIA

The new room model should be a good mixture of low simulation time, accuracy and detail. Zonal models have been found to match this specification. The room model has to be based on simple and available parameters while the validity and the robustness of the model is guarantied.

The model has to represent the conditions at three possible sensor positions: at the centre of the room, in the jet trajectory of an emitter and in a boundary layer of natural convection. A sensor model will then use the corresponding temperature around the controller sensor.

For the performance assessment of a controller, two main questions appear concerning a reference position of the assessment and the index to use in the assessment. The selection of an index is problematic since all indices need "subjective" assumptions, the result of a controller test can thus vary from one index to the other.

A comparison of different room models is carried out using qualitative classification in Table 6.

The values in Table 6 are estimated regarding the possibilities of the different model types.

While the well-mixed model is characterised by good results in the upper part of the table (general characteristics, parametering and validity) it is not able to predict most of the interesting outputs offered by the CFD models. CFD models on the other hand, supposing perfect knowledge of their use, obtain good results in the model outputs but have bad results in the upper part, general characteristics, parameters and validity.

Identification models are interesting from the point of view of their general characteristics since they are simple and offer fast simulation runs. Also the outputs of interest could probably be well predicted. Since the phenomenon of the negatively buoyant wall jet is a very non-linear phenomenon this kind of model would bring high uncertainties when used for other zone geometry or for other zone use.

Table 6: Criteria for the development of the zone model

		Model types			
Groups of criteria	Specific criteria	**Well mixed**	**Improved well mixed**	**Zonal**	**CFD**
General characteristics	Possibility of real time simulation	YES	YES	YES	?
	Calculation time	++	++	+	--
	User level	Low	Low	Intermediate	Very high
Model Parameters	Low number of parameters	++	+	+	--
	Low user level for parameterisation	++	+	+	--
	Complexity and coherence of initial and boundary conditions	++	++	o	--
Model Outputs Performance Assessment	Mean room air temperature	o	o	+	++
	Mean radiant temperature at occupant zone	Depends on wall modelling			
	Horiz. temperature variation at occupant zone	n.a.	+	+	++
	Vert. temperature variation at occupant zone	n.a.	+	+	++
	Air velocities at occupant zone	n.a.	-	o	++
Model Outputs Sensor measurement	Horiz. temperature variation at sensor positions	n.a.	-	o	++
	Vert. temperature variation at sensor positions	n.a.	o	+	++
	Air velocities at sensor positions	n.a.	o	o	++
	Mean radiant temperature at sensor positions	Depends on wall modelling			
Validity	Validity for different zone type (heavy/light)	Depends on wall modelling			
	Validity for different geometry	?	?	?	++
	Validity for different zone use	?	?	?	++
++ very good + good o satisfying - sufficient -- insufficient n.a. not available					

Zonal models can be seen as a good compromise in all three main groups of criteria. While they permit real time simulation, even with a longer simulation time as simple models, they are, depending on the correlations used, also valid for other room geometry and uses. Most of the outputs of interest can be predicted with acceptable accuracy.

3. CONCLUSION CHAPTER III

The general scheme of a controller test bench has been discussed in order to obtain all necessary criteria for the model to develop. Considering the results obtained in Chapter II, the new model has to represent three possible sensor positions. These are at the centre of the room, near the walls in the possible trajectory of a jet or plume of the emitter and near the wall outside the trajectory of any jet or plume.

The measurement of the controller sensor at these three positions has been found to introduce supplementary factors of uncertainty and has a main influence on the test results. The existing phenomena in and around a sensor box are listed in order to prepare a simplified modelling of the sensor including its box.

When a controller is tested, its performance should be assessed concerning its ability to keep the room conditions at a certain value. In more detailed room models, where different temperatures are available, this needs the definition of a reference position where the performance is assessed. The point at the centre of the zone is proposed even if the controller does not control on this temperature when the sensor is placed near the walls.

Performance assessment is based on the selection of a state variable or index that indicates the performance of room control. Temperature, error square of temperature and different comfort indices are discussed. Since all of them need sooner or later in the assessment process basic assumptions of the user, they all include a subjective part. The results can thus differ depending on the assumptions made. It is proposed to use resultant temperature as performance index for the studies in the application chapter (Chapter V). A comparison between some of the mentioned performance indices is given in a last part of Chapter V.

A review of existing models shows the advantages and inconveniences of the presented room models. Zonal models are shown to be the most usable and flexible of the different room models for the application in controller studies. They can be developed in order to represent the complex conditions in the sensor zones. They provide, coupled with models of the envelope, the necessary outputs for the sensor measurement and performance assessment.

For the envelope model, a simple model using one fictitious node of radiant temperature and a nodal conduction model are chosen. The number of elements to be represented will be chosen according to the structure of the convection model developed in the next chapter.

CHAPTER IV

MODEL DEVELOPMENT

In this chapter a new room model is developed, taking into account the criteria developed in the previous two chapters.

The development of the convective room model can be divided into five parts:

- *System definition and division of the room into sub-volumes*
- *Bibliography and selection of correlations for convective phenomena*
- *Development of the model with implementation of the selected correlations*
- *Implementation of the model in the graphical environment*
- *Model validation and sensitivity analysis for representative cases*

The conductive and radiative aspects of the room model are obtained from literature. They are structured and implemented in the graphical environment to be consistent with the convective model of the room.

1. SYSTEM DEFINITION AND GENERAL EQUATIONS OF THE CONVECTIVE ROOM MODEL

The following vectors of air temperatures, wall surface temperatures, temperatures of external air supply (by a ventilation or air conditioning system) and convective heat sources define the system of a zonal room model:

$$\vartheta_{air,i} = \begin{pmatrix} \vartheta_{air\ 1} \\ \vdots \\ \vartheta_{air\ i} \\ \vdots \\ \vartheta_{air\ l} \end{pmatrix} \qquad \vartheta_{A,k} = \begin{pmatrix} \vartheta_{A1} \\ \vdots \\ \vartheta_{Ak} \\ \vdots \\ \vartheta_{A\,m} \end{pmatrix} \qquad \vartheta_{ext,r} = \begin{pmatrix} \vartheta_{ext,1} \\ \vdots \\ \vartheta_{ext,r} \\ \vdots \\ \vartheta_{ext,s} \end{pmatrix} \qquad \Phi_{conv,\,p} = \begin{pmatrix} \Phi_{conv,1} \\ \vdots \\ \Phi_{conv,p} \\ \vdots \\ \Phi_{conv,q} \end{pmatrix}$$

with

l : number of air sub-volumes i

m : number of surfaces k

r : number of sources of external air supply s

q : number of convective heat sources p

The representation of the external temperatures allows the model to have different types of air exchange with external volumes. These can be an air conditioning system, air infiltration from exterior or air exchange between rooms.

The energy balance for each air sub-volume i of the system is:

$$\begin{aligned} m_i\, c_p\, \frac{d\,\vartheta_i}{d\,t} = & \sum_{j=1}^{l} \dot{m}_{j,i}\, c_p\, \vartheta_j \; - \sum_{j=1}^{l} \dot{m}_{i,j}\, c_p\, \vartheta_i + \sum_{k=1}^{m} h_{i,k}\, A_{i,k}\, (\vartheta_{A,k} - \vartheta_i) \\ & + \sum_{r=1}^{s} \dot{m}_{ext;r,i}\, c_p\, \vartheta_{ext,r} \; - \sum_{r=1}^{s} \dot{m}_{ext;i,r}\, c_p\, \vartheta_i \; + \sum_{p=1}^{q} \Phi_p \end{aligned} \tag{5}$$

The sub-volumes j exchange air with the flow rate $m_{i,j}$ with the actual sub-volume i.

The energy balance includes six terms of heat and mass exchange:

- Air flow leaving sub-volume i towards sub-volumes j,
- Air flow entering sub-volume i from sub-volumes j,
- Convective heat exchanged at internal surfaces A_k,
- Air flow entering sub-volume i from external volume r,
- Air flow leaving sub-volume i towards external volume r,
- Convective heat injected from source p to sub-volume i.

The steady state flow balance on a sub-volume i is given by:

$$\sum_{j=1}^{l} \dot{m}_{j,i} \; + \sum_{r=1}^{s} \dot{m}_{ext;r,i} = \sum_{r=1}^{s} \dot{m}_{ext;i,r} \; + \sum_{j=1}^{l} \dot{m}_{i,j} \tag{6}$$

The balance includes air flow between the air sub-volume i and the adjacent air sub-volumes j of the system as well as the air flow between the sub-volume i and external conditions r.

The system consists thus of l equations for the energy balances and l equations of flow balances. If the flow rates between the room and the exterior is supposed to be known, there are l unknown air temperatures and (l x l - l) unknown flow rates, since there exists no flow between the sub-volume i and itself. The total of unknown variables is thus l^2.

Supplementary equations have to be used in order to determine the air flow rate through the sub-volumes. Correlations, characterising the air flow through and between the sub-volumes "generating" air flow in the room. They will be selected in the following section. Together with the l mass balances on each sub-volume they furnish the l^2 unknown flow rates.

The l unknown temperatures can then be obtained solving the l energy balances of equation (5).

2. DIVISION OF THE ROOM INTO SUB-VOLUMES

With the proposed division of the room air into sub-volumes, one model is able to represent all emitter types of interest. The only difference lies in the selection of correlations suitable to each case of HVAC system. The systems of interest are:

- Radiators and convectors
- Fan coil units (heating and cooling mode)
- VAV system with ceiling diffusers (heating and cooling mode)
- Emitters, integrated in the envelope

The analysis of air flow in a room for different emitter in Chapter II shows the possibility to divide the room, for all selected HVAC systems, in sub-volumes of the following types:

- Jet or plume from a radiator, convector or a fan coil unit
- Jet at ceiling
- Phenomena of mixed or natural convection at the internal walls
- Boundary layers at the external or internal walls
- Centre (occupied) part of the room

The selected sub-volumes are presented in Figure IV - 1 to Figure IV - 4in a plan view and two section views AA and BB, indicated in the three dimensional view in Figure IV - 1. For the representation of vertical temperature gradients the room is divided into a number of horizontal air layers. The figures show also the possible air flows between the sub-volumes of the room. In the model development, a number of 3 horizontal layers is chosen as an example. A higher number can also be chosen with the result of higher calculation effort. In this thesis all descriptions will be based on the division into 3 horizontal air layers.

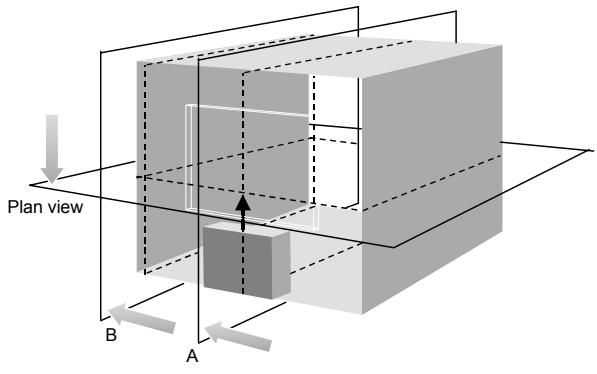

Figure IV - 1: 3D- view of the room

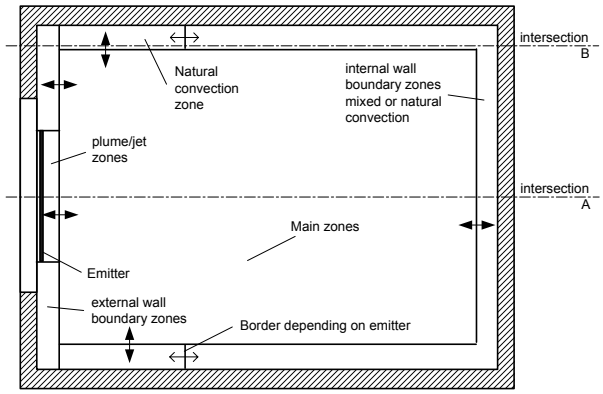

Figure IV - 2: Plan view of the room division

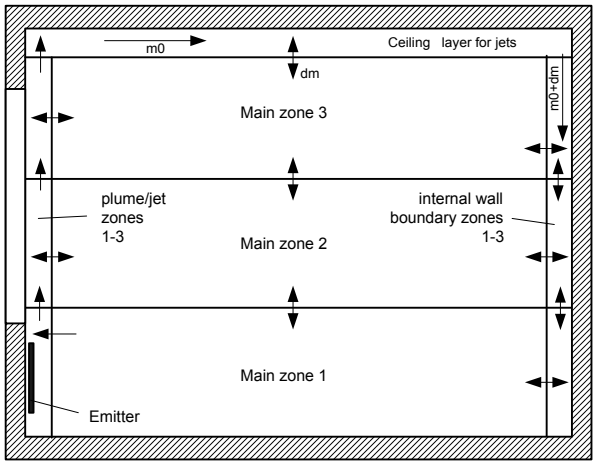

Figure IV - 3: Section AA through the room

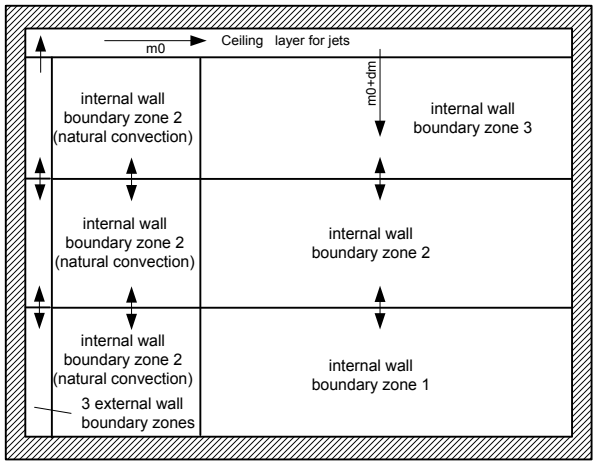

Figure IV - 4: Section BB through the room

The border between the zone of natural convection and negative buoyancy at the internal walls (Figure IV - 2 and Figure IV - 4) depends on the HVAC system installed in the room. For the emitters studied in chapter II the border is close to the external wall so that there is only a small zone of natural convection. For cases of a VAV air diffuser mounted at the ceiling the zone of natural convection can be larger, depending on diffuser length and type. This zone of natural convection can be very important for cases of high temperature stratification (e.g. VAV ceiling diffuser in heating mode) since this is the only zone that transports warm air from the upper room part to the lower one. It is thus responsible for temperature stratification in the room.

The sub-volumes of negative buoyancy at the internal walls can either represent natural, mixed convection or both. While phenomena of negative buoyancy are observed at the upper part of the walls, a boundary layer of natural convection is observed at lower heights, depending on the maximum travel of the negatively buoyant air flow.

The jet zone at the ceiling (Figure IV - 3 and Figure IV - 4) represents the phenomena of ceiling jets (for a VAV ceiling diffuser) or a "jet" at the ceiling, created by a plume arriving from a radiator, a convector or by the jet of a fan coil unit. This jet provides the necessary boundary conditions for the calculation of the negatively buoyant air flow at the internal walls.

No sub-volumes representing the zones of plumes from internal gains are considered since the temperature in these zones is not of interest. However, the plume from these heat gains has to be considered for the flow balances in the main air volumes and the ceiling air layer.

A cold air layer can exist where a cold air layer is observed near the floor (e.g. fan coil unit in cooling mode). A sub-volume, similar to that near the ceiling, could represent this phenomenon. The air volume near the ceiling has been added to the model in order to estimate the "boundary" conditions of a wall jet at the internal walls. The same phenomenon can be observed at the floor with a negatively buoyant wall jet. However, due to better mixing of this cold jet with the air of the lower main zone and due to a, mostly unfavourable, boundary layer at the internal walls, this zone has not been added to the model.

The room model has thus a total number of 13 air sub-volumes. With this zone division any of the mentioned emitter types can be modelled with satisfying representation of the phenomena and providing all necessary outputs for controller studies.

The division into zones will be fixed for all cases and the user will not have the possibility to change this parameter. The zone division is selected to represent all the studied phenomena for rooms of normal size. Attention has to be paid in the case of atriums or halls, since higher horizontal temperature differences can appear. The model can be used but no information will be available concerning horizontal temperature variations. Other models, dividing the main volume in several smaller sub-volumes [Musy99a] are more adapted in this case. However these models have been developed for comfort studies and would have to be adapted for controller studies.

3. STUDY AND SELECTION OF CORRELATIONS FOR CONVECTIVE PHENOMENA

In this section the correlations, required to solve all flow balances, are studied and selected for the use in the zonal room model. The correlations are given for the types of flow that can appear in a room equipped with the selected HVAC systems. The correlations of interest are:

- Wall plume from a radiator or a convector
- Free plume from heat gains
- Wall jet of a fan coil unit in heating mode
- Wall jet of a fan coil unit in cooling mode
- Ceiling jet of an air conditioning system
- Airflow near walls for natural convection (boundary layer)
- Airflow near walls characterised by negative buoyancy

Correlations of these phenomena are hereunder explained and evaluated, regarding their use in the room model.

3.1 AIRFLOW IN PLUMES

Plumes can be divided into two parts: wall plumes and free plumes. Figure IV - 5 gives a schematic representation of the phenomena in a plume of a heat source.

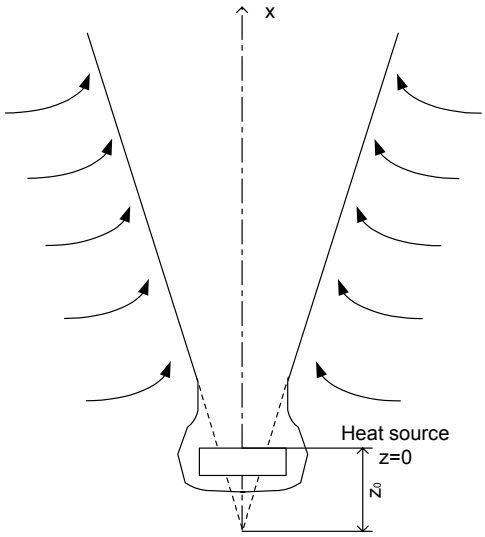

Figure IV - 5: Schematic representation of plume flow over a heat source

The temperature difference between the surface of the heat gain (that can be an emitter, an occupant or equipment in the room) and the air around the heat source create density differences between the air in contact with the heat source and the surrounding room air. As a result, the warmer, lighter air above the heat source rises toward the ceiling and entrains surrounding air into the plume. The description of the flow inside the plumes and between plumes and their environment is given in the following paragraphs. For any plume a fictitious origin z_0 can be defined where the air flow rate is zero.

3.1.1 RADIATOR PLUMES

Radiators emit heat by convection and by radiation. Depending on the surface temperature of the radiator, heat is exchanged by long wave radiation with the surfaces of the room. The relation between radiative and convective part of the heat emission depends on type and geometry of the

radiator.

Several authors analysed the flow in radiator plumes. [Horwarth80] studied the air flow due to a radiator. He suggested a correlation for the air flow rate at the height of the radiator:

$$\dot{m}(H_{Rad}) = 0.015\ H_{Rad}\ L_{Rad}\ (\vartheta_{SR} - \vartheta_{Air})^{0.4} \qquad (7)$$

The air flow rate in the plume can then be calculated using the following correlation, valid for heat losses at the window less than one third of the convective output of the radiator:

$$\dot{m}(z) = \dot{m}(H_{Rad}) \left(\frac{z - z_0}{H_{Rad} - z_0} \right)^{4/5} \qquad (8)$$

[Inard88] studied the air flow in plumes of radiators and of convectors. He suggested a correlation providing the air flow rate following the plume:

$$\dot{m}(z) = C_{plume}\ \Phi(z)^{1/3}_{conv}\ (z - z_0) \qquad (9)$$

where Φ(z) corresponds to the heat flow in the plume depending on the height (it is in fact the emitted convective heat diminished by the heat losses following the plume [Inard90] and the stratification in the room). However, the correlation is quite insensitive to the variation of the convective heat with height (third root). The constant for the plume C_{conv} is given to 9.51 10^{-3} with a maximum error of about +/- 5% for different radiator types, geometries and heat emissions. The fictitious height z_0 (cf. Figure IV - 5) is given to about 0-0.3m.

Since [Horwarth80] analysed the flow only for one type and size of a radiator, the second correlation is chosen.

3.1.2 CONVECTOR PLUMES

A plume, similar to that of the radiator develops beyond the convector. Since there is only a very low radiative heat emission, the major part of the heat is injected into the room by convection and the plume air flow rate is higher than for a radiator.

[Barles92] suggested correlations characterising the air flow rate in a convector plume. The thickness of the plume is given by:

$$b = \frac{2\,E_0}{\sqrt{\pi}} \left[1 + \frac{St\ \left(1 + \lambda^2\right)^{1/2}}{3\ \lambda\ E_0} \right] (z - z_0) = C_{conv1}\ (z - z_0) \qquad (10)$$

The maximum velocity in the plume is given by:

$$U_m = \left[\frac{6\ \lambda\ \left(1 + \lambda^2\right)^{1/2}}{3\ \lambda \left(Cf + \sqrt{2}\ E_0\ St\ \left[2\left(1 + \lambda^2\right)\right]^{1/2} \right)} \right]^{1/3} \left(\frac{\phi(z)\ g\ \beta}{\rho\ c_p} \right)^{1/3} = C_{conv2}\ \phi(z)^{1/3} \qquad (11)$$

and finally the flow rate in the plume by:

$$\dot{m} = \frac{\sqrt{\pi}}{2}\ \rho\ U_m\ b = C_{conv3}\ U_m\ b = C_{conv}\ \phi(z)^{1/3}\ (z - z_0) \qquad (12)$$

[During94] gives the values of λ, C_f and St as 1.0, 0.01 and 0.005 respectively. [Musy99b] gives values of λ varying between 0.84 and 1.0 for isothermal wall and adiabatic wall respectively.

Since its value has only a small importance on the result in air flow rate, the value of 1.0 is chosen here.

The values for the entrainment ratio E_0 and the fictitious height z_0 have a greater influence on the air flow rate. For E_0 [Inard97] proposes values of 0.08 for a convector with vertical air outlet and 0.14 for a convector with horizontal air outlet. The resulting constants $C_{conv\ 1}$ - $C_{conv\ 3}$ using these values and a fictitious height z_0 of 0.3m are given in Table 7:

Table 7: Constants for the correlation of a convector plume

Convector type	E_0	Z_0	$C_{conv\ 1}$	$C_{conv\ 2}$	$C_{conv\ 3}$	C_{conv}
Vertical outlet	0.08	0.3	0.093	0.084	1.064	0.0083
Horizontal outlet	0.14	0.3	0.161	0.070	1.064	0.012

[During94] gives values for E_0 and z_0 for the two convector types, for different heat emissions and for two convector lengths. For convectors with vertical outlets the values of E_0 vary between 0.07 and 0.11 and those of z_0 between 0.278 and 0.498, resulting in a final maximum difference in the constant C_{conv} of 9.9%. For the case of a convector with horizontal air outlet, E_0 is given between 0.11 and 0.17 and z_0 between 0.23 and 0.388, resulting in a maximum difference of 8.9% for the constant C_{conv}.

For convectors with horizontal air outlet, a phenomenon of detachment of the jet from the wall can appear. [Bouia94] observed this phenomenon. For lower heat emission and small temperature differences between the room air and the window, the plume of this kind of convector attaches at the window from a certain height on. In cases of higher heat emission it is even possible that the plume does not attach at the window until reaching the ceiling. However, for cases of moderate heat emission, which is generally the case in controller studies, and for small temperature differences between the room air and the window this phenomenon does not appear. It is thus not considered for further modelling.

3.1.3 FREE PLUMES

Convective heat gains in the zone, such as from electric equipment or room occupants, create plumes, transporting air toward the ceiling. Since these plumes are generally not at the walls, they entrain air all around the plume interface. The air flow in these plumes is thus higher than for the wall plumes of emitters. This can be very important to estimate the stratification in a room, especially for cases where no other air flow generators exist. At the same time, since there are generally several sources of internal gains, the air flow from gain plumes can be the most important factor for the internal room conditions. [Kofoed91] gives the air flow rate in a free plume to:

$$\dot{m}(z) = 0.0061\ \Phi(z)_{conv}^{1/3}\left(z - z_0\right)^{5/3} \qquad (13)$$

[Fitzner96] gives a correlation depending on the diameter of the heat source:

$$\dot{m}(z) = 0.006\ \Phi(z)_{conv}^{1/3}\left(z - d\right)^{5/3} \qquad (14)$$

[Crawford62], [List82] and [Morton58] give other expressions for plume characteristics. [Crawford62] suggests an expression relating the flow rate to the 4th root of the emitted heat, different to the others proposed. The correlation given by [Kofoed91] is chosen since it is very similar to that proposed for convectors and radiators. A general correlation will be used in the following to represent all these plumes. The fictitious height z_0 in the relation depends strongly on the heat source and the height of the source above floor. For reasons of simplicity the same

height is chosen for z_0.

A factor of uncertainty for the calculation of air flow rate in plumes is the number and position of the heat sources. [Bjørn95] studied this phenomenon. He concluded that two sources with a distance Δx smaller than 0.1m can be considered as one joint heat source. When the distance Δx between two heat sources is larger than about 1m they can be considered as two separate sources, the air flow rate is thus higher.

3.1.4 GENERAL REPRESENTATION FOR PLUMES

The selected plume correlations of radiators, convectors and internal gains will, in the model, be represented by the following expression:

$$\dot{m}(z) = C_{plume}\ \Phi(z)_{conv}^{1/3} \left(z - z_0 \right)^{n_{plume}} \qquad (15)$$

The constants are chosen depending on the plume type. They are given in Table 8.

Table 8: Constants for the correlation of different plumes

Type	z_0	C_{conv}	n_{plume}
Convector with horizontal air outlet	0.3	0.012	1
Convector with vertical air outlet	0.3	0.0083	1
Radiator	0.1	0.0095	1
Heat Gain (free plume)	0.3	0.0061	5/3

For all types of plumes the accuracy of the correlation is estimated to +/-5% of the flow rate.

3.2 AIRFLOW IN JETS

3.2.1 OVERVIEW AND DEFINITIONS

In a room, various types of jets can appear. Generally, two main groups have to be distinguished:

- Isothermal jet
- Non-isothermal jet

Depending on shape, type and direction each of the two groups of jets is characterised by:

- Shape: e.g. plane, rectangular, cylindrical or radial
- Type: Free in a room or attached at a surface
- Direction: Vertical, horizontal or inclined

The equations, required for the selected HVAC systems (fan coil units and VAV systems), are discussed. While the FCU system is characterised by a mostly non-isothermal vertical surface jet, the VAV system is characterised by a horizontal, non-isothermal jet (only horizontal ceiling jets have been selected for the room model).

Main attention is paid on the equations determining flow rates in the jet since they are necessary for the zonal room model.

For reasons of simplification, only plane jets with a high aspect ratio (diffuser width to length) as well as radial diffusers (VAV ceiling diffuser) are treated, both in the two dimensional case. Figure IV - 6 shows the schematic representation of a plane jet.

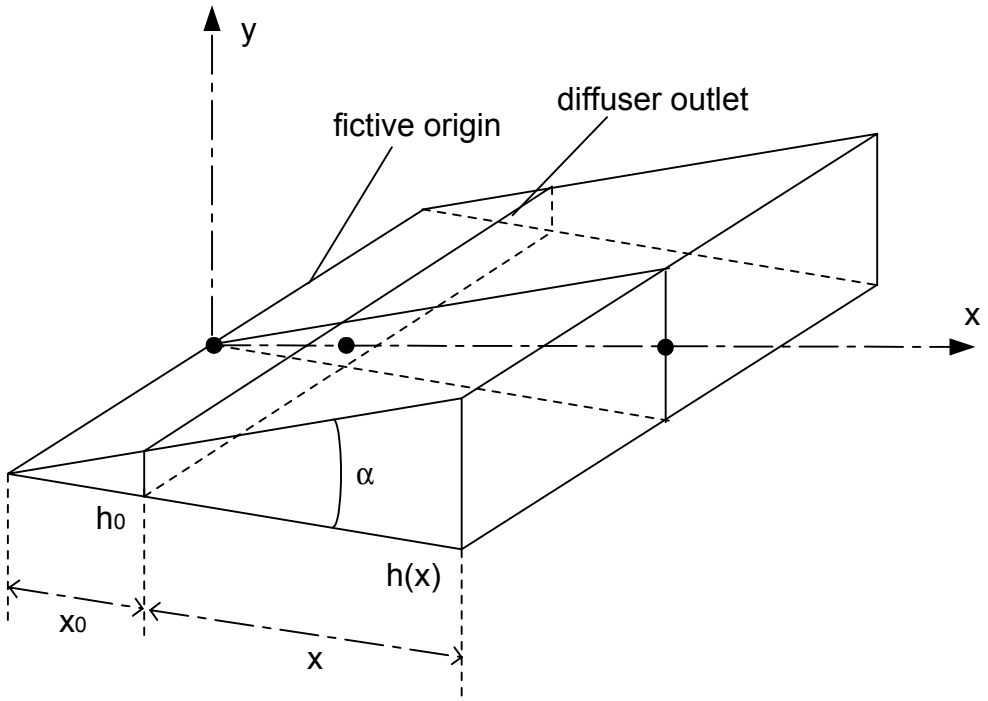

Figure IV - 6: Scheme of the plane jet with definitions

Attention has to be paid on the fictitious origin, x_0 from the diffuser outlet. This fictitious origin is different for the jet height and for the flow rate. In Figure IV - 6 the height is represented. The relationship between these two fictitious origins can be found from the velocity and flow equations.

Figure IV - 7 shows the scheme of the radial ceiling diffuser. Different to the plane diffuser the outlet is placed at a distance of R_0 from the centre of the diffuser. As for the plane jet a fictitious origin has to be calculated.

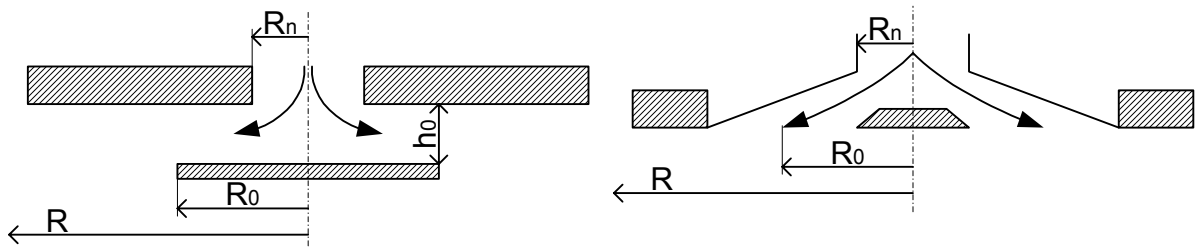

Figure IV - 7: Radial ceiling diffusers

The equations describing the different jets are presented in the following paragraph.

3.2.2 ISOTHERMAL JETS

Isothermal jets are described by identical equations whether the jet is in vertical or in horizontal direction. Thermal buoyancy effects do not influence the jet travel.

3.2.2.1 Jet zones and centre-line jet velocity

The ASHRAE Handbook [ASHRAE97] provides information about air flow in jets for several different types of air diffusers.

Generally the jet can be divided into four characteristic zones (Figure IV - 8).

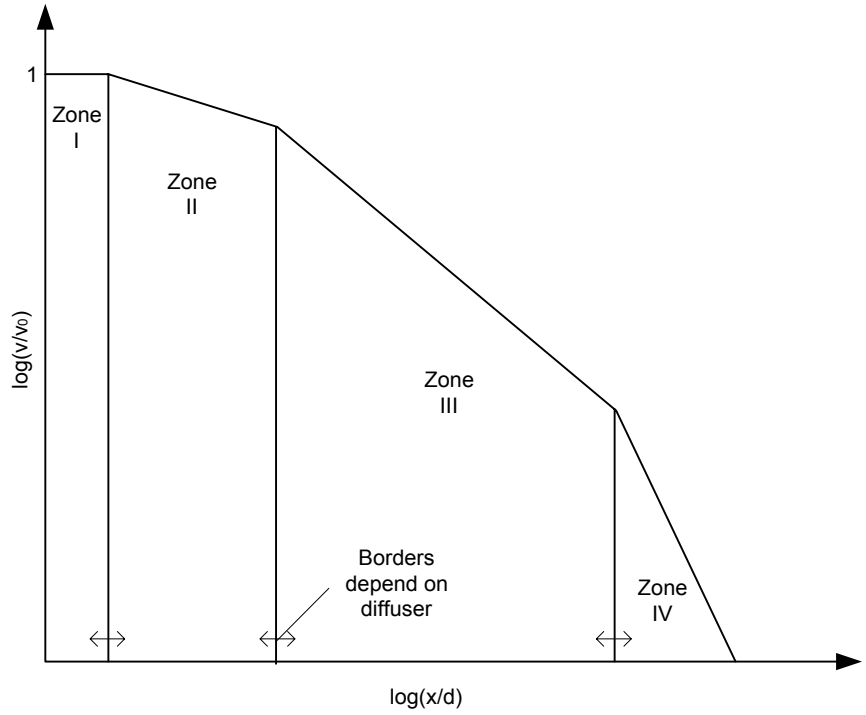

Figure IV - 8: Zones of expansion of a jet

The relationship between the centreline velocity and the distance from the outlet of the diffuser are given below for rectangular diffusers with high aspect ratios:

- First zone (core zone)

  The centreline velocity and flow rate remain nearly unchanged; the length of the first zone is of order four times the slot width and can thus be neglected.

- Second zone: the centreline velocity of the jet is given by:

$$\frac{v_x}{v_0} = \sqrt{\frac{K' d_0}{(x + x_0)}} \qquad (16)$$

  where v_0 is the centreline velocity at the outlet of the diffuser, and d_0 is the width of the outlet. x_0 is the distance of the outlet to the fictitious origin of the jet, x is the distance from the diffuser outlet. The length of the second zone depends on the type of diffuser and outlet parameters.

- Third zone: the centreline velocity is in linear relationship to the distance from the outlet and is given by:

$$\frac{v_x}{v_0} = \frac{K' d_0}{(x + x_0)} \qquad (17)$$

The length of the third zone is between 25-100 times the slot width d_0, depending on diffuser geometry ([ASHRAE97]).

- Fourth zone: the jet velocities decrease rapidly depending on the condition of the ambient air (velocity and turbulence). This zone is not considered in the model of the jet used in this study since it appears at large distances from the outlet and due to a low number of references treating this case ([Madison95], [Weinhold69]).

A radial diffuser is a particular case. Figure IV - 7 shows two kinds of radial air diffusers. The geometry can be complex, depending on the particular type. [Koestel57] presented equations describing the velocities in a jet from a radial diffuser.

$$\frac{v_R}{v_0} = \frac{\sqrt{K \frac{h_0}{r_0} \cos\alpha \left[K \frac{h_0}{r_0} \cos\alpha + 1 \right]}}{\frac{\sqrt{R(R - R_0)}}{R_0}} \qquad (18)$$

K is a constant defining the length of the constant velocity core in terms of the width h_0 (K=4 in [Koestel57]). Or after defining a constant C_{radial}, this simplified expression:

$$\frac{v_R}{v_0} = \frac{C_{radial}}{\frac{\sqrt{R(R - R_0)}}{R_0}} \qquad (19)$$

The square root of both expressions in the denominator gets close to R/R_0 for $R>>R_0$. [Koestel57] observed a jet deflection of about 25° for the radial jet.

Jets from diffusers with a high aspect ratio (such as slot diffusers) and small diffuser widths are generally characterised by a larger length of the second zone. Jets from radial diffusers or diffusers with a larger diffuser width have a very short second zone. As shown by [Koestel57] they are better characterised by the equations for the third zone type. They can approximately be represented by equation (17) from the ASHRAE handbook [ASHRAE97] gives standard values for the constant K' in (1) and (3) for several types of diffuser, including radial diffusers.

In the case of surface jets, which is particularly the case for fan coil units and for the ceiling diffusers selected for this work, the values of the constants K' are approximately those of free jets multiplied by $\sqrt{2}$.

3.2.2.2 Velocity profile

The transversal velocity profile in the jet is generally assumed as a Gauss error function, approximated by the following equation:

$$\left(\frac{y}{y_{0.5v}} \right)^2 = C_{jet,tr} \log\left(\frac{v_x}{v} \right) \qquad (20)$$

where $y_{0.5\ v}$ is the y-ordinate with the velocity reduced to half of the centreline velocity at the same distance from the outlet. This velocity is generally represented by a linear function C_U x. [Rajaratnam76] proposed a constant C_U characterising this function. Its value varies between 0.07 and 0.12, depending on the diffuser characteristics. This corresponds to a total angle α of divergence of a jet from about 20° to 24° (with an average of 22°). For the jet constant $C_{jet,tr}$,

[Rajaratnam76] and [ASHRAE97] propose values of -0.693 and -0.303 for second zone and third zone respectively. These constants result in a mean velocity v_{mean} of 0.34 and 0.41 times the centreline velocity. This corresponds to a difference of the mean velocity of 18.7%.

For the second zone jet the factor of mean velocity is smaller than for the third zone jet. On the other hand the factor of divergence is bigger for the second zone jet than for the third zone jet. The differences remain thus smaller than the variation of each factor considered separately.

3.2.2.3 Air flow rates

The entrainment ratio into a jet is very important for the development of a zonal room model.

The flow rates in jets are given in [ASHRAE97] for the case of a long slot with high aspect ratio, corresponding to a **free jet** with second zone characteristics:

$$\frac{\dot{m}_x}{\dot{m}_0} = \sqrt{2}\,\frac{v_0}{v_x} \qquad (21)$$

where $\dot{m}_0$ is the flow rate at the outlet of the diffuser and $\dot{m}_x$ the flow rate at the distance x of the outlet.

For circular free jets and third zone jet characteristic the following relation is given:

$$\frac{\dot{m}_x}{\dot{m}_0} = 2\,\frac{v_0}{v_x} \qquad (22)$$

The correlations are given for free jets. In the **case of surface jets**, as already mentioned in §3.2.2.1 about jet velocity, the jet constant K' has to be multiplied by $\sqrt{2}$. Since air is only entrained from one interface, the rate of entrainment is approximately half of that of a free jet. The flow rate in equations (21) and (22) has thus to be divided by 2 in the case of a surface jet.

[Musy99b] gives the flow in the isothermal, plane jet for the second jet zone. The flow is obtained from integration of the transversal velocity profile of a plane jet, approximated by a Gauss error function ([Abramovich63], [Rajaratnam76]) for one side of the symmetry axis, and considering the evolution of the maximum jet velocity as a function of the distance from the outlet:

$$\frac{\dot{m}_x}{\dot{m}_0} = C_{jet\,type}\; C_U\; K_V \sqrt{\frac{(x+x_0}{d_0}} \qquad (23)$$

The constant $C_{jet\ type}$ is calculated as 1.054 for the wall jet and 2.13 for the free jet. The constants C_U and K_V are derived from results from [Rajaratnam76] and are 0.074 and 3.67 respectively for the wall jet and 0.0109 and 2.62 for the free jet. As a result the flow rate in a free plane jet is approximately twice the flow rate in a surface plane jet. The result using (23) is similar to that obtained using (21) with the values suggested by [ASHRAE97].

[Regenscheit58] presents a summary of results for flow rate in the second zone of plane free and surface jets. While proposing an equal law for the free jet, the equation for the plane jet is given as:

$$\frac{\dot{m}_x}{\dot{m}_0} = \sqrt{2}\sqrt{\left(\frac{x+x_0}{\frac{2\,h_0}{m}}\right)^{3/4}} \qquad (24)$$

where m is a constant corresponding to the mixing between jet air and room air. Besides the

exponent, different to that of the free jet, the equation assumes the core length (=$2h_0$/m) of the jet twice as long as for the free jet.

3.2.3 NON ISOTHERMAL JETS

Non isothermal jets appear for all cases selected for the model. While the jet of a fan coil unit is in vertical direction, the jet of the selected ceiling diffusers is horizontal. Both types, the vertical as well as horizontal jet will be treated in the following. In both cases the buoyancy can have a different effect on the jet and changes the flow characteristics compared to the characteristics in isothermal conditions.

3.2.3.1 Horizontal jets

For the selected HVAC systems the horizontal jet appears at the ceiling for the VAV ceiling diffusers but also for the fan coil unit, where the jet reaches the ceiling. In the heating case the jet will attach at the ceiling. In the cooling case, when the jet reaches the ceiling, the jet can separate from the ceiling.

In the case of plumes from convectors, radiators or even internal heat gains, the warm air will also pass by the ceiling and entrain air from the centre part. No jet as defined before will appear in this case. However, since the plume passes along the ceiling, an expression is needed in order to describe the air entrainment in this flow. Probably the flow characteristics are similar to the third or fourth zone of a jet, the plume zone.

In all cases of interest the surface jet is of interest. Equations for the trajectory and temperature of free, non-isothermal jets are given in [Davies75] or [Grimitlyn93].

In the heating case, the trajectory will follow the ceiling and the jet characteristics will thus be similar to those for the isothermal jet.

In the cooling case the Coanda effect will influence the trajectory. While [Wilson70] showed similar profiles of temperature and velocity in these jets, the Coanda effect will affect the trajectory and air entrainment of the jet. The equations for trajectory can thus not be used.

Other equations determining the position of jet detachment from the surface due to buoyancy forces are given in [Kirkpatrick91], [FranceAir91] or [Marchal99]. They could be interesting for the case of a horizontal VAV diffuser near the ceiling or the fan coil unit in cooling conditions. In the first case, the VAV diffuser, a detachment of the jet, before reaching the internal walls, is generally avoided in the design process. The calculation of the point of detachment of the jet from the surface is thus only worthwhile in the case of a bad system design.

In the case of the fan coil unit in cooling conditions a calculation of the point of jet detachment is very risky since the jet already changes its characteristics when reaching the ceiling making the use of the given correlations very uncertain. Regarding the low level of detail of the needed model the calculation of the point of detachment is only more or less suitable.

The use of the correlations for horizontal ceiling jets will be explained in the corresponding paragraphs about the use of the correlations.

3.2.3.2 Vertical jets

The characteristics of vertical, non-isothermal jets are of interest for the jet from a fan coil unit. In this case, the jet has positive buoyancy for the heating case. The jet is thus accelerated. In the opposite case, the jet velocity is reduced faster as in the isothermal case. It is even possible that the jet flow changes its direction for cases of high negative buoyancy.

The non-dimensional Archimedes number (also number of Richardson) is used in this case to quantify the influence of buoyancy forces on the flow. It is defined as:

$$Ar = \frac{Gr}{Re^2} = \frac{g\,\beta\,\Delta\vartheta\,d}{v^2} \qquad (25)$$

[Grimitlin93] proposes equations for temperature and velocity in vertical, non-isothermal jets.

The laws proposed by [Chen80] for accelerated jets divide the jet in three characteristic zones as in the isothermal case. He found similar behaviour to that of the isothermal case in the first jet zone. In the second zone, the buoyancy forces are of the same order as the forces by velocity, the Archimedes number appears in the equation for velocity. In the third zone, the buoyancy forces dominate the flow.

[FranceAir91] lists equations for non-isothermal jets, introducing also the Archimedes number into the jet equations.

Considering the diversity of correlations for this type of jet a comparison between the isothermal jet model and results of CFD simulations of a room equipped with a fan coil unit is carried out for the heating case.

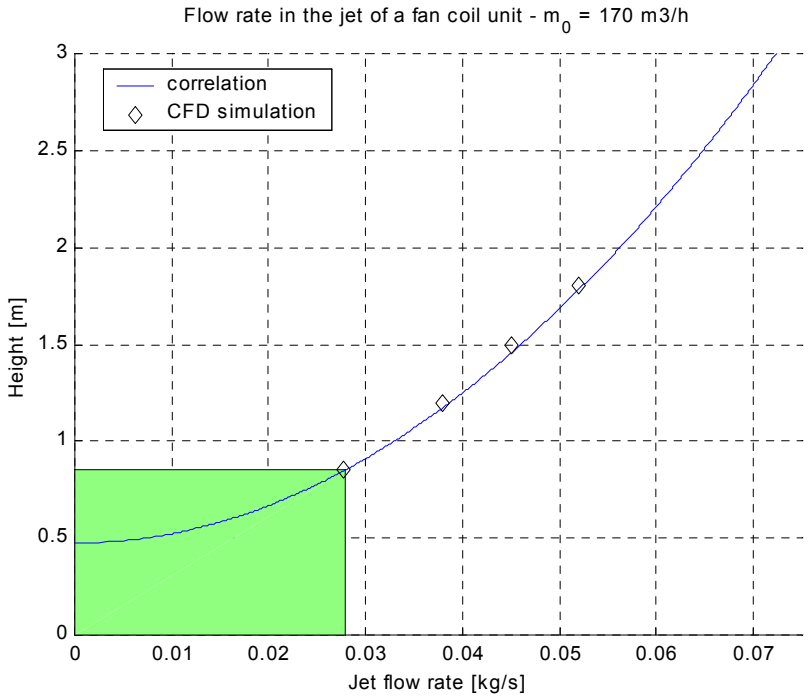

Figure IV - 9: Flow rate in the jet of a fan coil unit

The lowest fan speed (175m^3/h) is chosen since in this case the buoyancy effect is most important. The results of the CFD simulations carried out in chapter II are used. From the CFD results, the flow above the fan coil unit is integrated at four different heights (0.85m, 1.2m, 1.5m and 1.8m). The equation for the first zone of an isothermal jet is compared with the results from detailed simulation. Figure IV - 9 shows the comparison of both flows. The constant in the jet correlation has been found as 4.5. This corresponds to the proposed values in [ASHRAE97].

For higher flow rates, the correlation will also be valid since the importance of buoyancy decreases with increasing outlet velocity.

In the cooling case the phenomena will be different. As already observed in chapter II, the jet can change the flow direction for cases of low fan speed. The equations of [Grimitlyn93] can be used in this case to evaluate the centreline velocity following the jet trajectory. Another correlation can be found to calculate the maximum jet travel before achieving the point of flow inversion that is given as:

$$\delta_p = 0.68\, d_0 \frac{K_V^{4/3}}{K_T^{2/3}} Ar_0^{-2/3} \qquad (26)$$

[Kapoor88] and [Goldman86] investigate the same case in order to obtain information about maximum jet travel for free jets and for wall jets. For wall jets they propose an expression characterising the heat transfer at the walls following the jet. For the case of an adiabatic wall they propose a maximum jet travel of:

$$\delta_p = 4.5\; d_0\; Ar_0^{-0.4} \qquad (27)$$

For the case of an isothermal wall they propose the following expression introducing a factor that considers the temperature difference between the room air and the surface. The maximum jet travel is then:

$$\delta_p = \left(4.1 - 5.9\frac{\theta_S}{\theta_0}\right) d_0\; Ar_0^{-\left(0.4 + 0.9\frac{\theta_S}{\theta_0}\right)} \qquad (28)$$

where θ_S is the temperature difference between the wall and the room air related to the temperature between jet and the environment at the outlet and θ_0 the temperature difference between jet and room air related to the temperature between jet and the environment at the outlet.

The entrainment of this kind of jet is difficult to assess. For reasons of simplicity and to keep the same expression for all jet cases, the isothermal correlation for air flow is chosen.

3.2.4 GENERAL REPRESENTATION FOR JETS

All jets in the room model will be represented by the equation for an isothermal jet:

$$\frac{\dot{m}_x}{\dot{m}_0} = C_{flow}\left(\frac{(x + x_0)}{K' d_0}\right)^{n_{jet}} \qquad (29)$$

The constants are chosen depending on the jet type. [ASHRAE97] gives standard values for the values of K'.

For a given diffuser the K' can also be calculated from ratings data using equation (29). The throw data (length and velocity) is used to define the characteristic curve of velocity. The velocity at the outlet of the diffuser v_0 has to be calculated either from geometrical data or from dynamic pressure. Latter is more adapted since it is valid for complex geometry.

The following values are generally available for diffusers concerning airflow and for different flow rates:

- Pressure drop through diffuser
- Air flow rate
- Throw (0.75/0.5/0.25m/s)
- Geometrical data (more or less detailed since geometry can be complex)

Figure IV - 10 shows the result of this method. The constant is calculated from the three throw values and for different outlet velocities. The velocity calculated using equation (29) is then compared with the data available from manufacturer.

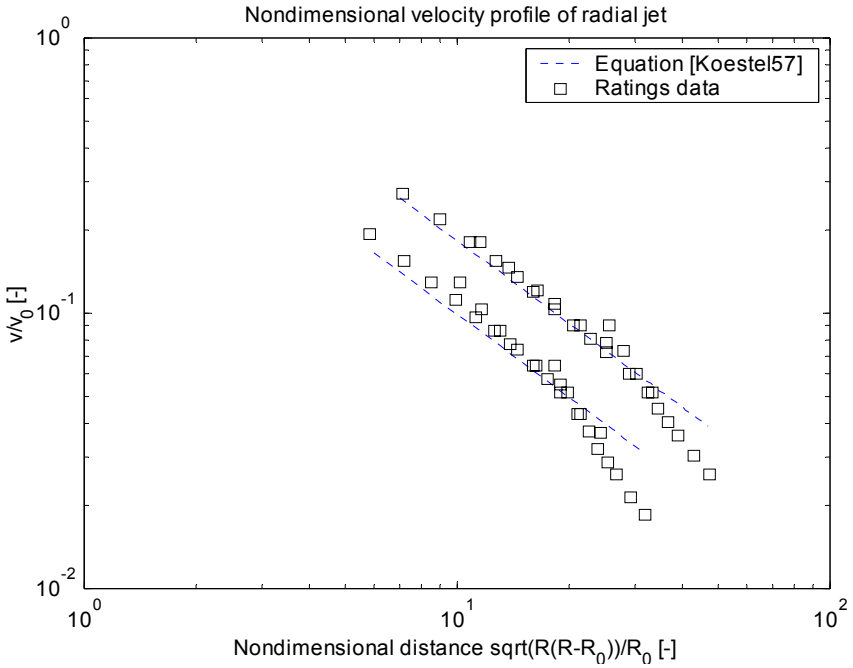

Figure IV - 10: Velocity profile from equation (7) and from ratings data

In the case of the ceiling jet/plume for the emitters as convector, radiator or fan coil unit, the jet constant K' is estimated from [ASHRAE97] for third zone jets.

The constants used for the different jets are listed in Table 8.

Table 9: Constants used for correlation (29) for the different jets

Type	K'	C_{flow}	n_{jet}
Jet fan coil unit	Ratings data	$1/\sqrt{2}$	0.5
VAV slot diffuser at ceiling	Ratings data	$1/\sqrt{2}$	0.5
VAV radial diffuser at ceiling	Ratings data	$1/\sqrt{2}$	1
Ceiling jet/plume in the heating case	4	$1/\sqrt{2}$	1

In the case of jets the modelling error undertaken is very difficult to estimate. When standard values are chosen the error can be significant. When rating data is used, the uncertainty is reduced. For the ceiling jet/plume, the value is only a rough estimation while considering a third zone jet flow characteristic.

In the case of the fan coil unit in cooling conditions, equation (27) is used in order to estimate the maximum upward jet travel before changing the direction of flow and falling toward the floor. The jet equation for air entrainment is used up to this limit in order to quantify the extent of jet mixing with ambient air.

3.3 AIRFLOW AT INTERNAL WALL SURFACES

The air flow at a wall can either be characterised by natural convection or by mixed convection or by both. When jets or plumes reach the wall, the air is then distributed downwards, along the internal walls. The descending air is characterised by negative buoyancy. When no jet or plume exists, the case of natural convection is observed. Both cases will be treated in the following.

3.3.1 NATURAL CONVECTION

This case is generally assumed in classic zonal models. A boundary layer of natural convection transports air upward or downward due to temperature differences between the surface and the surrounding air. The higher the temperature differences are the more air is transported since the buoyancy forces are higher.

[Allard87] analysed the air flow characteristics in boundary layers. For the flow rate he proposed the following expression relating the flow rate to the temperature difference between the wall and the air.

$$\dot{m}(z) = C_{BL} \left(\vartheta_{Surf} - \vartheta_{Air}\right)^{n_{BL}} z \qquad (30)$$

He proposes values of 0.004 and 1/3 for the constant C_{BL} and n_{BL} respectively.

[Laret80] proposes the same expression with the constants 0.0043 and 1/3.

Figure IV - 11 compares different equations relating flow rate in the boundary layer to the temperature difference ([Horwarth80], [Allard87], [Laret80]). The flow rate is calculated per meter height and per meter length.

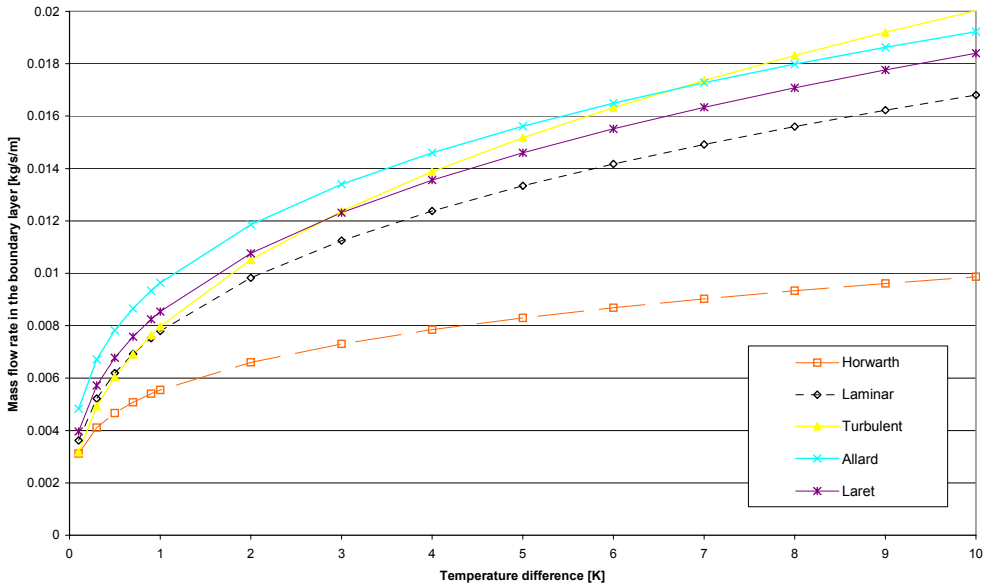

Figure IV - 11: Flow rate in a boundary layer for varying temperature difference

The equation given by [Horwath80] shows a significant difference. All others are very similar, that of [Laret80] is thus chosen for the model.

The mean temperature in the boundary layer can be calculated approximately by integrating the velocity profile in the boundary layer on the thickness of the boundary layer.

The temperature in the boundary layer is between the temperature of the surrounding air and the surface temperature. Considering temperature and velocity profiles obtained for laminar or turbulent flow in the boundary layer, the mean temperature in the boundary layer can be, independent of the height in the room, obtained by the integration of the flow:

$$\overline{\vartheta}_{bound} = \frac{\int_0^{\delta_t} w(y)\,\vartheta_{bound}(y)\,dy}{\int_0^{\delta_t} w(y)\,dy} \qquad (31)$$

After integration, the mean temperature of the flow in the boundary layer can approximately be given by:

$$\overline{\vartheta}_{bound} = \Theta\, \vartheta_{air} + (1 - \Theta)\, \vartheta_{wall} \qquad (32)$$

where Θ is a weighting factor indication the influence of the air temperature on the mean temperature in the boundary layer. The calculation leads to slightly different factors for laminar and for turbulent flow.

$\Theta \approx 0.6$ for laminar flow

$\Theta \approx 0.75$ for turbulent flow

Measurements of Eckert and Jackson [Eckert51] and Allard [Allard87] considered turbulent flow for the boundary layers.

3.3.2 NEGATIVELY BUOYANT FLOW

The case of negatively buoyant flow at the internal walls has been shown in Chapter II as an important phenomenon for controller studies. If, for the walls, the classic boundary layer is assumed (as done to date), the effect of a warm, negatively buoyant wall flow, created from a HVAC system, is neglected. As shown in Chapter II the sensor can be in this warm jet. This affects the transient temperature response as well as the steady state temperature at this point.

[Goldmann86] and [Kapoor88] studied experimentally the negatively buoyant jet for the problem of fires in buildings. In their experiments, they introduced a jet of hot air downward into a room (Figure IV - 12). In the case of an adiabatic wall they proposed the following correlation for a negatively buoyant wall jet:

$$\delta_p = 4.5\, D\, Ar_0^{-0.4} \qquad (33)$$

Where δ_p is the penetration depths of the jet, D the thickness of the outlet of the jet and Ar_0 the Archimedes number at the diffuser outlet. The test arrangement used in their studies is shown in Figure IV - 12:

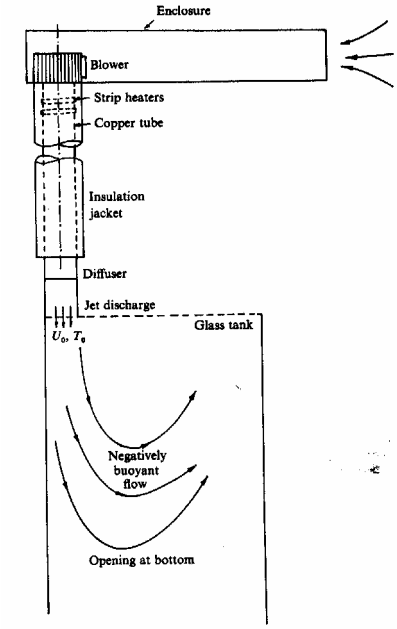

Figure IV - 12: Experimental arrangement used by [Kapoor88] and [Goldmann86]

In the test the thickness of the jet at the inlet is known. This is not the case for the negatively buoyant flow at walls to be treated here. The thickness of this jet has to be estimated. The sensitivity of this parameter will be studied in the validation part.

Different from the test carried out by [Goldmann86] and by [Kapoor88] are also the conditions at the diffuser. In their case, the aim was to get information about the behaviour of fires in buildings. The temperature differences are thus much higher than in the case of a heated or cooled room. Table 10 shows the conditions of the experiments of both authors. Grashof, Reynolds and Archimedes numbers are given for the two cases as well as values, estimated for the case of standard heating conditions with an electric convector.

Table 10: Comparison of the experimental conditions with estimated values in a heated zone

$\vartheta_0 - \vartheta_{amb}$ [°C]		$\vartheta_s - \vartheta_{amb}$ [°C]		v_0 [m/s]		Gr x 10^{-6} [-]		Re [-]		Gr/Re² [-]		Author
50	128	-3	25	0.4	1.1	9	10	950	3400	0.08	1	Kapoor
30	60	0	0	1	1.8	2	10	1000	5000	≥0	1	Goldmann
0.1	3	-5	5	0.05	0.8	0.5	30	500	5000	0.01	5	Zone heating

As shown in the table, the conditions are different in both cases. While the temperature difference between the jet air and the room is much smaller in the case of heating, the temperature difference at the walls is of a similar order. The second is only used for the correlation of the isothermal wall (28). The velocity at the top of the jet depends on the estimation of the jet thickness. In this case it is estimated to 0.15m. The resulting Archimedes number is from a wider range as in the tests of [Kapoor88] and [Goldmann86]. The range of the Archimedes number in this case has been from about 0 to a maximum of 1. Figure IV - 13 shows the obtained values for the penetration distance as a function of the Archimedes number found by [Goldmann86].

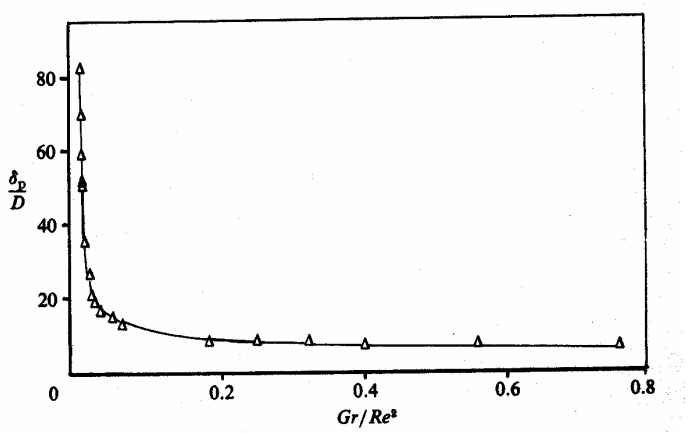

Figure IV - 13: Variation of the penetration distance δ_p with the Archimedes number (taken from [Goldmann86])

The difference between the range of boundary conditions from the tests and the heating case (Figure IV - 13 and Table 10) is discussed using a simple example of a heated zone:

A standard zone has a height of about 2.5 to 5m. The initial jet thickness is assumed to be within the range of 0.1 to 0.3m. The maximum value of δ_P/D in this case is thus 50 (for the jet penetrating the whole room height of 5m and the jet thickness of 0.1m at the inlet). All higher values of δ_P are not of interest since the wall jet penetrates in this case down to the floor. The minimum Archimedes number to be considered in the case of a heated zone (δ_P /D = 50) is thus about 0.02. This value is in the range of the experimental results. In the other extreme case, the

high values of the Archimedes number, the problem is different. The value of δ_P /D can nearly be considered constant for high Archimedes numbers (Figure IV - 13). In other words, if the Archimedes number is higher than in the experimental range of [Goldmann86], the value is nearly independent of the Archimedes number. Furthermore, for this extreme case, the maximum jet travel is very small compared to the room height (and the height of one sub-volume of the zonal model); the error is thus not relevant.

No correlation has been found concerning the flow characteristics of the jet near a wall. [Musy99b] provides an equation for flow rate and temperature for free jets. The results in temperature, using this correlation, did not fit with results obtained by measurement. The correlation is thus not used.

[Kapoor88] gives a correlation for the heat exchange at the wall following the jet:

$$\overline{Nu}_D = (10.3 - 13.4\theta_S)\, Ar^{-(0.19+0.32\theta_S)} \qquad (34)$$

where θ_S is the temperature difference between the wall and the room air related to the temperature between jet and the environment at the outlet.

The wall jet can be divided into two parts: an upper part where the heat exchange coefficient is high and is about 4W/m²/K and a lower part where the heat exchange coefficient is close to zero. The upper part with the high heat exchange has been found to be approximately 70% of the total jet travel given by (27). The low heat exchange in the lower part can be explained by the fact that, at the limit between the two parts, nearly all jet air has left the jet and joined the room volume. In the lower jet part, only a small amount of air continues until reaching the maximum penetration distance. The velocities have been found to be very low (by smoke visualisation in chapter II) in the EREDIS test cell. This explains the low heat exchange coefficients. The CFD simulations showed the same tendency. The division into these two parts can also be seen at the temperature profile showed for example in Figure II - 46 and Figure II - 47. A change in the slope of the temperature profile of the jet indicates this phenomenon. In the test in the EREDIS test cell the division into the upper and the lower part is obtained to approximately 60%, with only small variation.

3.4 CONVECTIVE HEAT TRANSFER COEFFICIENTS AT THE INTERNAL ROOM SURFACES

A large number of correlations are available characterising the heat transfer coefficient at the internal room surfaces. Depending on the emitter and the flow characteristics, correlations relating temperature difference or Reynolds number to the heat transfer coefficient.

[Awbi98] proposes correlations for convective heat transfer coefficients for all internal room surfaces in the case of natural convection. [Wallentén99] studied heat transfer coefficients in furnished and unfurnished rooms for a room with a radiator. [Beausoleil99] proposes correlations for heat transfer coefficients for the case of negatively buoyant air flow. Simple expressions are selected in the following for the new room model since all results are similar. The differences will not have an important impact on the results of controller tests.

[During94] gives an expression for the plume of a convector. The following linear approximation is used for this case:

$$h_{plume} = 4 + 2\frac{\phi_{convector}}{2000} \qquad (35)$$

In the case of the jet of a fan coil unit, a constant value of 5W/(m² K) is used.
For the vertical surfaces, the following expression is used [Lebrun78]:

$$h_{wall} = 3\ (\vartheta_{air} - \vartheta_{wall})^{1/3} \qquad (36)$$

For the floor, the constant value of 2W/(m² K) is used in all cases.
High values are generally observed at the ceiling. For the convector case, [Inard88] proposed the

following expression:

$$h_{ceill} = 3\,(\vartheta_{air} - \vartheta_{ceil})^{2/3} \qquad (37)$$

The same expression is used for other cases as e.g. the VAV ceiling diffusers since it has been found to be of similar order [Beausoleil99].

3.5 CONCLUSION ON CORRELATIONS

The study of correlations has permitted to select suitable correlations for the integration into the zonal room model. Expressions have been found for plumes and jets as well as for the convective heat transfer coefficients.

On the other hand, the available correlations for flow of negative buoyancy at the internal walls have been found to be not adapted or not existent. As shown in Figure IV - 14 the zonal model needs the knowledge of the air flows $\dot{m}_1$ and $\dot{m}_2$ between the sub-volumes at the internal walls.

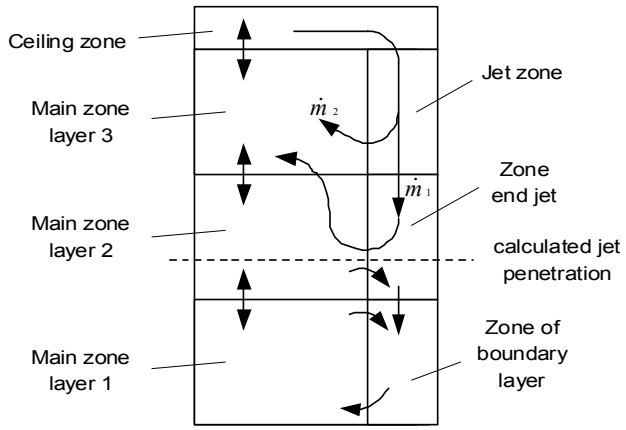

Figure IV - 14: Air flow in the sub-volumes at the internal walls in the case of negatively buoyant flow

This means, that a solution has to be found for the part of the negatively buoyant wall jet for the development of a zonal room model. It will be developed in the next section.

4. DEVELOPMENT OF THE CONVECTIVE ROOM MODEL

This section shows the development of the convective room model. Main concern is the implementation of the phenomenon of the negatively buoyant flow at the internal walls into the zonal room model. Two possibilities are considered to deal with this problem. Either the flow is estimated by identification from the measurements in a test room corresponding to Figure IV - 14 and the zonal model includes all sub-volumes, or a separate model is developed in order to estimate the temperature in the concerned sub-volumes. The latter is chosen for further development, since more detailed measurement would be necessary to obtain correct identification results.

The development can thus be divided into three parts:

- Division of the zonal model into two parts of sub-volumes
- Development of the zonal room model
- Development of a model representing the conditions in the sensor zones

4.1 DIVISION OF THE SUB-VOLUMES IN TWO PARTS

A new structure, different to that described in §2, is developed since the correlations for air flow found in the literature are not adapted for the sensor sub-volumes where negatively buoyant flow phenomena can appear. However, the temperatures in all zones indicated in §2 have to be provided, the solution proposed is thus to divide the model into two main parts:

- Classic zonal model using flow and energy balances
- Additional part of the model estimating the conditions in the different sensor sub-volumes

The first part, a simplified zonal model (Figure IV - 15), integrates all zones where correlations are available. The outputs of this model are the conditions in the main air sub-volumes, the temperature in the plume or jet above the emitter placed at the external wall and the temperature of the ceiling jet (when existing). For all these zones correlations are available in order to obtain the air flow. The energy balance shown in equation (5) can be solved. The conditions in the main sub-volumes are then used for the assessment of the performance of the controller.

As shown in Figure IV - 15 the boundary zones at the external and internal walls are not considered. Only the plume or jet at the wall, a ceiling air layer and three horizontal air layers are represented in this zonal model.

The second part of the model consists in a separate module describing the conditions in the sensor zones (Figure IV - 16). This module uses the temperatures and obtained in the simplified zonal model for the calculation of the temperatures in the sensor zones.

A second reason for this division of the model into two main parts, besides the unavailability of suitable correlations, is the need for modularity of the models. The division into two parts permits to use the simple zonal model separately in cases where the sensor is placed at the centre. When the sensor is positioned in one of the typical sensor zones at the internal walls, both models can be used as a coupled model.

When superposing Figure IV - 15 and Figure IV - 16 the representation of Figure IV - 2 to Figure IV - 4 is obtained.

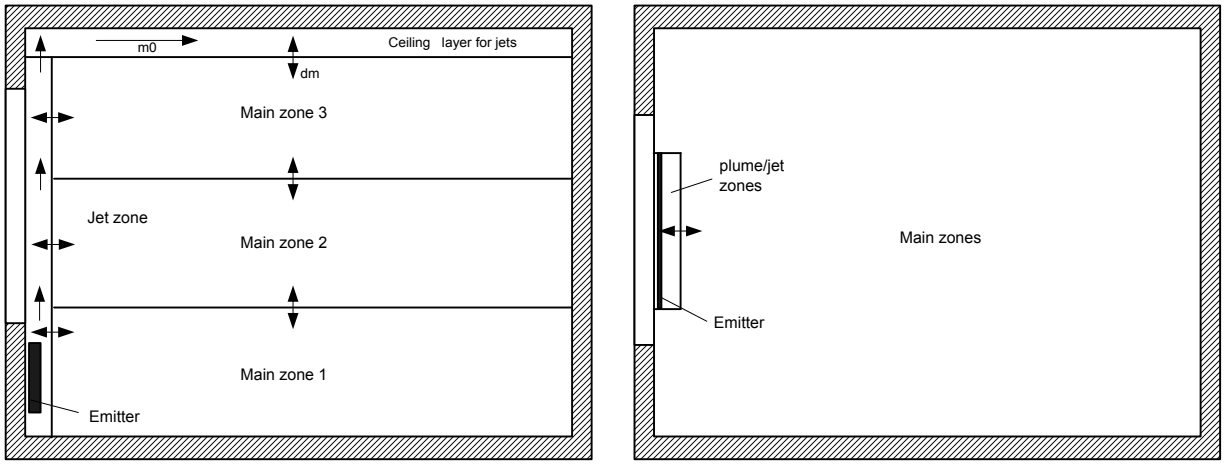

Figure IV - 15: Division into sub-volumes of the simplified zonal model (left: section view, right: plan view)

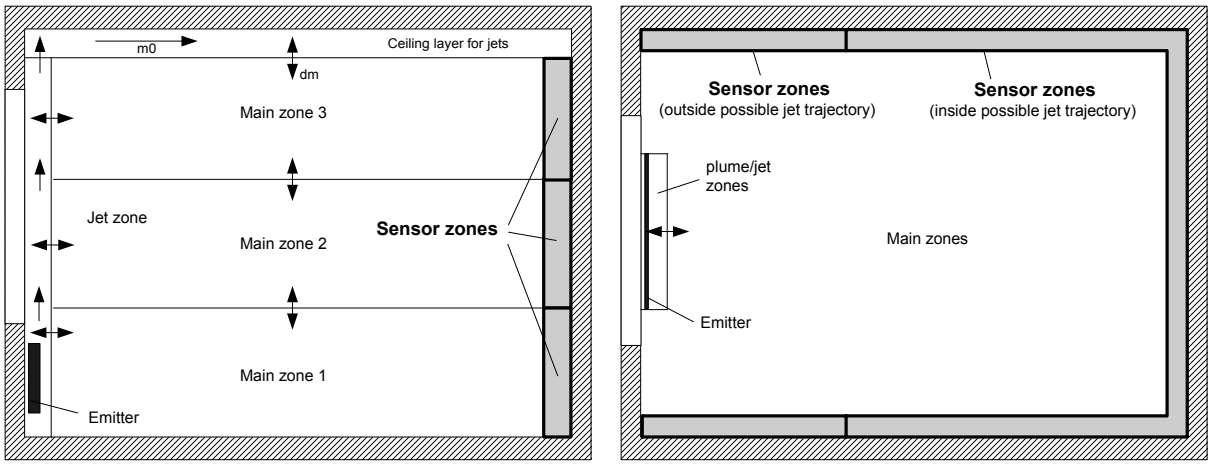

Figure IV - 16: Division into sub-volumes of the module "sensor conditions" (left: section view left, right: plan view)

4.2 DEVELOPMENT OF THE SIMPLIFIED ZONAL MODEL

4.2.1 GENERAL STRUCTURE OF THE MODEL

As shown in Figure IV - 15, the zonal model is divided into five sub-volumes. For each of them, energy and air flow balance is solved.

The selected correlations for air flow are now used to calculate the air flow between these five sub-volumes. A matrix containing the flow rates between the different sub-volumes is constructed. In general form it is:

$$\textit{Main flow matrix}: \quad \begin{array}{c} \\ SV_1\ out \\ \vdots \\ SV_i\ out \\ \vdots \\ SV_l\ out \end{array} \begin{array}{c} \begin{array}{ccccc} SV_1\ in & \cdots & SV_i\ in & \cdots & SV_l\ in \end{array} \\ \begin{pmatrix} 0 & \cdots & \dot{m}_{1-i} & \cdots & \dot{m}_{1-l} \\ \vdots & \ddots & & \ddots & \vdots \\ \dot{m}_{i-1} & & 0 & & \dot{m}_{i-l} \\ \vdots & \ddots & & \ddots & \vdots \\ \dot{m}_{l-1} & \cdots & \dot{m}_{l-i} & \cdots & 0 \end{pmatrix} \end{array}$$

The correlations are then used to fill the matrix. For each phenomenon an Air Flow Matrix (AFM) with the same dimension is constructed. All flow matrices are finally added in order to obtain the resulting matrix of flow rates.

4.2.2 DEFINITION OF THE PARTICULAR AIR FLOW MATRICES

4.2.2.1 Air flow due to emitter plume or positively buoyant fan coil unit jet

The plume from an emitter or the jet from a fan coil unit entrains air from the three main volumes into the jet zone (sub-volume 5). The resulting flow is then injected into the ceiling zone (sub-volume 4). These phenomena are shown in Figure IV - 17 in form of the air flow scheme (left) and the corresponding air flow matrix. All of the convective gain from a convector or a radiator or the fan coil unit is injected to the jet volume (5).

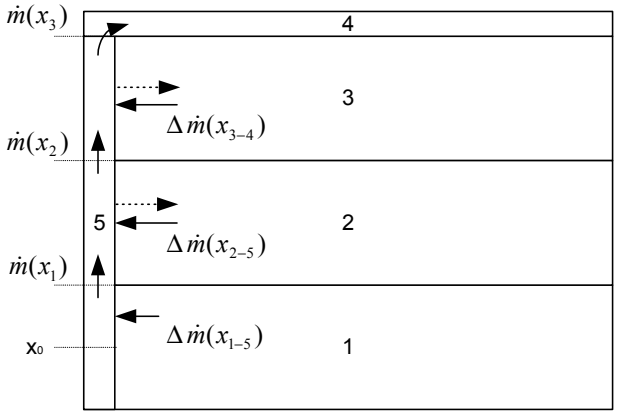

$$AFM_{Plume/Jet} = \begin{bmatrix} 0 & 0 & 0 & 0 & \dot{m}_{J:1-5} \\ 0 & 0 & 0 & 0 & \dot{m}_{J:2-5} \\ 0 & 0 & 0 & 0 & \dot{m}_{J:3-5} \\ 0 & 0 & 0 & 0 & 0 \\ 0 & 0 & 0 & \dot{m}_{J:5-4} & 0 \end{bmatrix}$$

Figure IV - 17: Use of the plume/jet correlation in zone 4

For high heat exchange at the external wall or window and for low heat emissions of the emitter, it is possible that the temperature in the jet zone falls below the temperature in the main zones. In this case, the plume will not continue to rise and the plume air will be injected into the main zone with the closest temperature. This is shown by the dotted lines in Figure IV - 17.

When the emitter is switched off and no plume or jet exists, this zone works as a zone of a boundary layer with natural convection. The same principle as in §4.2.2.5 is applied.

4.2.2.2 Air flow due to negatively buoyant fan coil unit jet

Different to the previous case, the jet is characterised by negative buoyancy forces. The jet can, in this case, reach the ceiling for high fan speeds or for low temperature differences (Figure IV - 18). On the other hand, the jet can reach its maximum travel before reaching the ceiling and the cold jet will fall towards the floor. This case can create a "bypass" effect around the fan coil unit: the fan coil extracts room air into the coil. The cooled air leaving the diffuser falls then towards the floor and is again part of the air extracted by the fan coil unit.

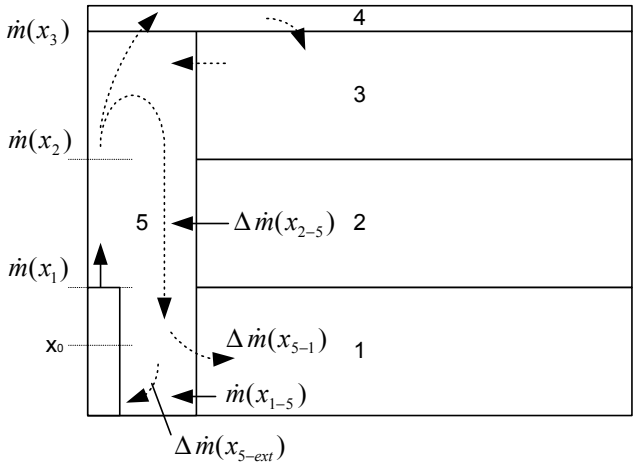

$$AFM_{Jet-cold} = \begin{bmatrix} 0 & 0 & 0 & 0 & \dot{m}_{J:1-5} \\ 0 & 0 & 0 & 0 & \dot{m}_{J:2-5} \\ 0 & 0 & 0 & 0 & \dot{m}_{J:3-5} \\ 0 & 0 & 0 & 0 & 0 \\ \dot{m}_{J:5-1} & 0 & 0 & \dot{m}_{J:5-4} & 0 \end{bmatrix}$$

Figure IV - 18: Air flow for the case of the cold fan coil jet

The two possible trajectories of the jet considered as illustrated in Figure IV - 18, are:

- The jet does not reach the ceiling and falls back down towards the floor. The model assumes in this case that the jet, while entraining air until its maximum height, injects one part of its flow rate into the lower air volume (sub-volume 1). The other part rests in the jet zone (sub-volume 5). This is only a very rough estimation, since an accurate calculation is very difficult.
- The jet reaches the ceiling (sub-volume 4) and is then injected to the upper main volume without reaching the internal walls

The matrix shows all possible flows. Depending on the air flow between the jet volume and the main volumes (5-1;4) only one of the air flows contains the jet flow. The others are zero.

4.2.2.3 Air flow in the ceiling jet

The ceiling jet can either be the continuation of the jet or plume from the emitter placed at the external wall or the jet of the VAV system ceiling diffuser. Air is entrained into the jet sub-volume (4) from the upper main volume 3. The sum of the flow at the origin of the jet and of the entrained air over the travel of the jet is injected into the upper main volume 3 (Figure IV - 19):

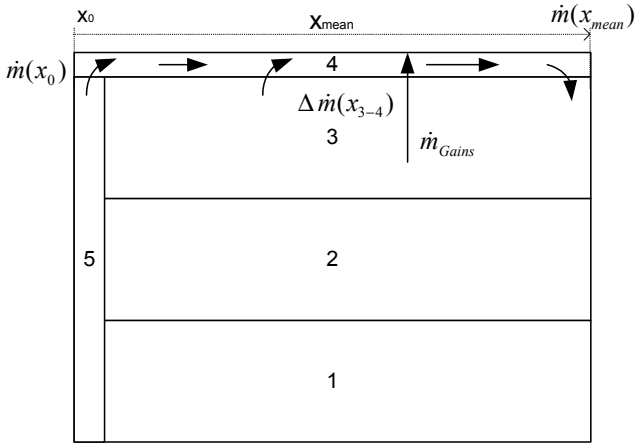

$$AFM_{ceiling} = \begin{bmatrix} 0 & 0 & 0 & 0 & 0 \\ 0 & 0 & 0 & 0 & 0 \\ 0 & 0 & 0 & \dot{m}_{C:3-4} & 0 \\ 0 & 0 & 0 & 0 & 0 \\ 0 & 0 & 0 & 0 & 0 \end{bmatrix}$$

Figure IV - 19: Air flow due to the ceiling jet

The air entrainment depends on the position of the origin of the jet. In the case of the continuation of the jet of an emitter at the external wall, the jet spreads to approximately all directions (cf. Chapter II, §3) and air is entrained over the mean length of jet travel as shown in Figure IV - 20. In the case of a jet of a VAV slot diffuser, the position of the diffuser defines the length of the jet before reaching the internal walls. The mean length is only calculated for the horizontal angle of divergence of the jet. When a radial ceiling diffuser, mounted at the centre of the ceiling, is used, the length of the jet is the mean distance to all walls.

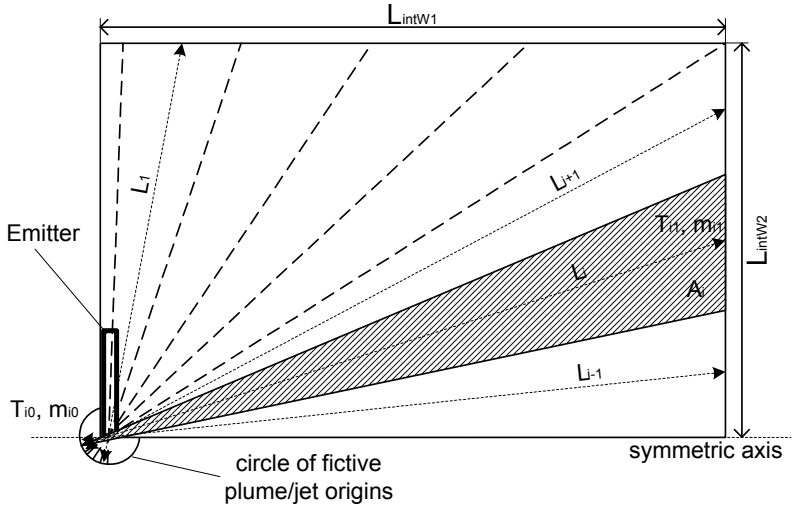

Figure IV - 20: Calculation of mean jet entrainment length

4.2.2.4 Air flow due to plumes from internal heat gains

Internal heat sources create a warm air from the heat source upward. In cases with low turbulence in the air at the occupant zone, this warm air rises toward the ceiling while entraining air from the occupant zones. Only in cases of a jet creating highly turbulent flow (e.g. cold jet

from VAV ceiling diffuser that does not reach the internal walls) the heat of the convective source is mixed directly with the room air due to the high turbulence.

For the first case, where a plume is developed over the heat source, air is entrained from the three main sub-volumes into the plume flow (Figure IV - 21) and the convective gain of the heat source is injected to the upper sub-volume (4). The corresponding air flow matrix contains the air flow transported from the three main sub-volumes (1-3) to the ceiling sub-volume (4).

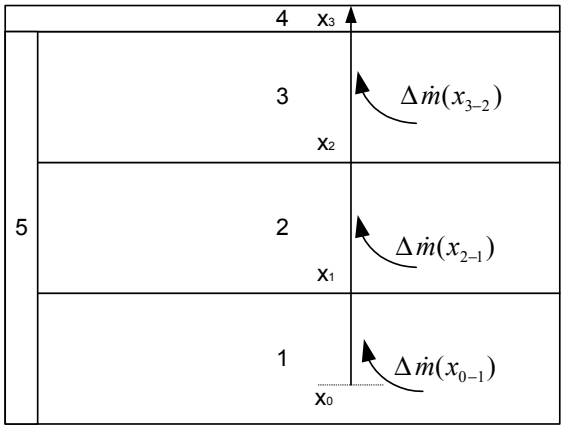

$$AFM_{Gains} = \begin{bmatrix} 0 & 0 & 0 & \dot{m}_{G:1-4} & 0 \\ 0 & 0 & 0 & \dot{m}_{G:2-4} & 0 \\ 0 & 0 & 0 & \dot{m}_{G:3-4} & 0 \\ 0 & 0 & 0 & 0 & 0 \\ 0 & 0 & 0 & 0 & 0 \end{bmatrix}$$

Figure IV - 21: Air flow due to plumes from internal heat gains

In the second case, where the flow in the main part of the room is highly turbulent, this air flow matrix is a zero-matrix and the heat gain from the source is injected to all volumes.

4.2.2.5 Air flow due to the boundary layer at the external surfaces

The boundary layer at the external surface transports air between the main volumes (Figure IV - 22).

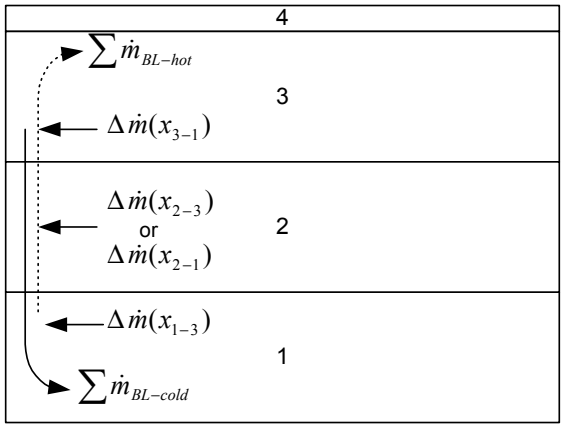

$$AFM_{ext\ wall} = \begin{bmatrix} 0 & 0 & \dot{m}_{BL:1-3} & 0 & 0 \\ \dot{m}_{BL:2-1} & 0 & \dot{m}_{BL:2-3} & 0 & 0 \\ \dot{m}_{BL:3-1} & 0 & 0 & 0 & 0 \\ 0 & 0 & 0 & 0 & 0 \\ 0 & 0 & 0 & 0 & 0 \end{bmatrix}$$

Figure IV - 22: Air flow due to the boundary layer at the external surfaces

In order to simplify the model, a mean temperature is used for the calculation of the temperature difference between the room air and the surface. The flow in the boundary layer can be upward or downward, depending on the sign of the temperature difference.

The corresponding air flow matrix contains amount of air flow transported from the two lower volumes for an upward boundary layer flow and from the two upper volumes for a downward boundary layer flow. The ceiling layer is not assumed to participate at this kind of air flow.

4.2.2.6 Air flow due to a boundary layer of natural convection at the internal walls

This case corresponds to the previous one, the boundary at the external wall (Figure IV - 23). Natural convection can either be the case at the part of the wall outside the possible jet trajectory

(VAV slot diffuser) or for cases where no heat gains from a HVAC system or gains exist. The length of the internal wall is therefore divided into two parts: One part of the wall without jet influence and a second one where the jet can have an influence. The partition of these two parts is variable and is detected as a function of HVAC system and load. The air flow matrix in this case is shown in Figure IV - 23.

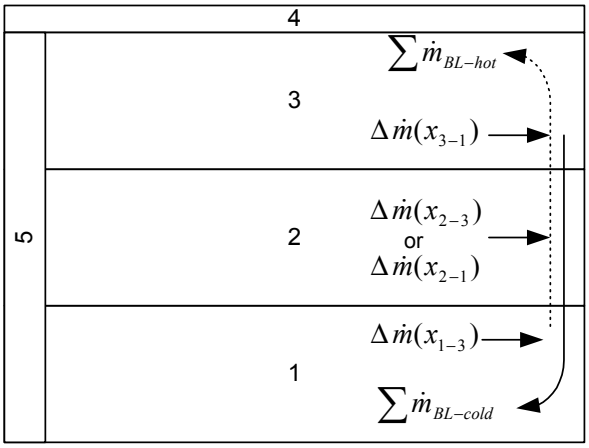

$$AFM_{\text{int}\,WJ} = \begin{bmatrix} 0 & 0 & \dot{m}_{BL:1-3} & 0 & 0 \\ \dot{m}_{BL:2-1} & 0 & \dot{m}_{BL:2-3} & 0 & 0 \\ \dot{m}_{BL:3-1} & 0 & 0 & 0 & 0 \\ 0 & 0 & 0 & 0 & 0 \\ 0 & 0 & 0 & 0 & 0 \end{bmatrix}$$

Figure IV - 23: Air flow due to the boundary layer at the internal surfaces

4.2.2.7 Air flow due to negatively or positively buoyant air flow at the internal walls

Two different cases of air flow can appear: either the jet or plume from the ceiling is cold (Figure IV - 24) or warm (Figure IV - 25).

The cold jet can exist for the VAV system. If the temperature difference between the wall and the room air is not too large, this jet will flow downwards, attached at the wall, along the wall towards the floor. For high temperature differences a boundary layer in the opposite (upward) direction would probably make the jet detach from the wall. Since the walls are considered internal (with adjacent temperatures close to the room temperature), this phenomenon is neglected and the cold jet is assumed to stay attached at the walls. While travelling to the floor this jet entrains air from the main volumes. The flow matrix in this case of the cold jet is given in Figure IV - 24.

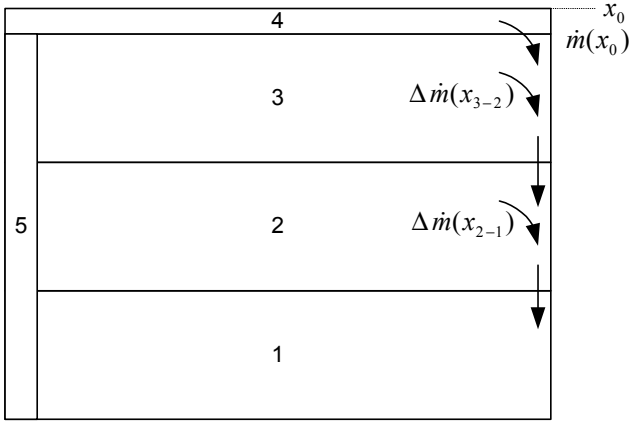

$$AFM_{\text{int}\,WJ\ pos} = \begin{bmatrix} 0 & 0 & 0 & 0 & 0 \\ \dot{m}_{BLM:2-1} & 0 & 0 & 0 & 0 \\ \dot{m}_{BLM:3-1} & 0 & 0 & 0 & 0 \\ \dot{m}_{BLM:4-1} & 0 & 0 & 0 & 0 \\ 0 & 0 & 0 & 0 & 0 \end{bmatrix}$$

Figure IV - 24: Air flow due to a positively buoyant wall jet at the internal walls

In the case of the warm jet from the ceiling, the jet is characterised by negative buoyancy forces. The jet will reach a maximum downward travel and will then reverse its flow direction and rise again to the upper main volume (Figure IV - 25). As mentioned previously the air flow characteristics in this jet are not well known for this case.

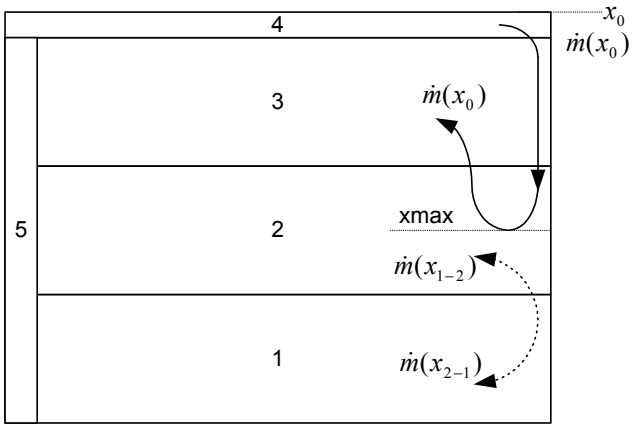

$$AFM_{\text{int}WJ\,neg} = \begin{bmatrix} 0 & \dot{m}_{BLM:1-2} & 0 & 0 & 0 \\ \dot{m}_{BLM:2-1} & 0 & 0 & 0 & 0 \\ 0 & 0 & 0 & 0 & 0 \\ 0 & 0 & \dot{m}_{BLM:4-3} & 0 & 0 \\ 0 & 0 & 0 & 0 & 0 \end{bmatrix}$$

Figure IV - 25: Air flow due to the negatively buoyant wall jet at the internal walls

The vertical jet penetration into the room can be calculated using equation (33). Its calculation from the available data will be explained in §4.2.4. If this maximum travel is larger than the room height, the buoyancy forces of the jet are too low to make the jet rise back towards the upper main zone. In this case the air is assumed to be injected to the lower air volume. The air flow matrix is identical to that for the cold jet. In the case that the maximum downward travel is lower than the room height, the jet is thus assumed to rise again to the upper main volume without entraining air from the lower zones. Below the end of the wall jet a boundary layer of natural convection can appear, if the jet does not penetrate until very low heights. The corresponding air flow matrix can thus contain also flow rates considering a natural convection boundary layer below the jet zone (Figure IV - 25).

4.2.2.8 Air exchange with external conditions or the HVAC system

The model has to take into account different kinds of air exchange with external conditions. This can be the HVAC system (including fan coil unit), inter-zonal air exchange or opening of windows. Two supplementary air flow matrices are necessary to take these air flows into account. The matrices have the size (l,s) where s is the number of external air supplies.

4.2.3 CONSTRUCTION OF THE FINAL AIR FLOW MATRIX AFM

All air flow rates in the "generator" zones are known with this procedure. However, the air flow balance is generally not satisfied since there can be air flow between the main volumes. For solving these flow rates all flow matrices AFM_i (see previous paragraphs) are added:

$$AFM = \sum AFM_i \qquad (38)$$

The sum of the lines (flow leaving sub-volume) and rows (flow entering sub-volume) is compared. A correcting flow matrix is defined including the errors in the flow balance. This correction matrix corresponds to the resulting flow between the main sub-volumes (1-3) and is finally added to the previous matrix AFM.

The resolution of the system of heat balances will be shown in the section of the model implementation.

4.2.4 ESTIMATION OF THE MAXIMUM DOWNWARD TRAVEL OF NEGATIVELY BUOYANT AIR FLOW AT THE INTERNAL WALLS

The air flow of the ceiling jet is composed of three particular air flows:

- Jet or plume from jet/plume zone or from VAV ceiling diffuser

- Plume from internal gains
- Air entrained into the ceiling jet

This corresponds to the sum of the incoming flow to the ceiling volume (3), given by the sum of the rows of the ceiling sub-volume in the air flow matrix AFM. The sum of these particular air flows will, when arriving at the internal walls, flows downward along the internal walls until arriving a maximum penetration into the room. A virtual outlet of this wall jet is thus defined (cf. x_0 in Figure IV - 25). For equation (33) the jet velocity at this virtual outlet has to be known. It is calculated using:

$$v_0 = \frac{\dot{m}_{ceiling}}{\rho_{air}\, d_0\, L_{wall}} \qquad (39)$$

where d_0 is the estimated thickness of the downward jet at the top of the wall and L_{wall} is the length of the part of the internal walls where the ceiling jet appears. This length depends on the HVAC system used and is given by:

- the length of the internal walls for an emitter placed at the external wall (cf. 2 $L_{intW\ 1+2}$ in Figure IV - 20),
- the sum of the lengths of the internal and external walls for the VAV radial diffuser,
- the part of the internal walls affected by the ceiling jet (either with the angle of divergence given by the manufacturer or from standard values given in [ASHRAE97]) for a VAV slot diffuser.

The conditions at the fictitious jet origin are:

- the mean velocity at the top of the walls by equation (39),
- the temperature of the ceiling sub-volume 4.

The thickness of a virtual jet diffuser placed at this point has to be estimated. The sensitivity of the estimation of this thickness will be studied in the validation part.

The Archimedes number in equation (33) is based on the temperature difference between the air at the virtual diffuser and the room air. Stratification in the room makes the definition of this room air temperature difficult. An iterative process is thus used in order to obtain a mean air temperature surrounding the wall jet. The air temperature around the wall jet is assumed to be the mean temperature at the centre of the room for the height of the top of the room until the height where the wall jet ends.

4.2.5 CALCULATION OF HEAT TRANSFER IN THE ZONAL MODEL

The ceiling exchanges heat with the ceiling air sub-volume. The floor exchanges heat with the lower main sub-volume and the sub-volume of plume or jet of an emitter exchanges heat with the window(s) or the external wall.

The heat exchanged with the walls is essentially taken into account in the zonal model, even if the calculation of sensor temperatures is carried out separately. Therefore each of the main sub-volumes exchanges heat at the internal and external walls.

In the case of the external wall, natural convection is assumed in any case since the controller sensor is not placed at this wall and the real temperature at this position is not of interest. Depending on the direction of the boundary layer, the heat exchange of the whole external surface (excluding the part in contact with the plume/jet zone) is assumed to be with the main sub-volume where the air flow in the boundary layer is directed to. This means that, in the case of an upward boundary layer (summer case) all convective heat exchange takes place between the external surface and the upper main sub-volume. In the opposite case the heat exchange is assumed between the external surface and the lower main sub-volume. The heat exchange with the external surface considers a mean temperature of the part of the external surfaces (wall and window(s)) not covered by the plume or the jet weighted by the area of the wall and the window.

In the case of the internal walls, the heat exchange of the room air with the surfaces is, due to lower temperature differences, less than at the external wall and the window. Even if the air flow rate passing along the internal walls is considered in the flow balances, each main sub-volume is assumed to exchange heat with the internal walls at the corresponding interface.

4.3 DEVELOPMENT OF A MODULE ESTIMATING THE TEMPERATURE IN THE SENSOR ZONES

4.3.1 DIVISION OF THE SENSOR ZONES INTO THREE CHARACTERISTIC ZONES

The temperature in the sensor zones has been studied in Chapter II. As already mentioned in Chapter II, the case of negatively buoyant flow is only treated in heating mode. In the cooling case, positively buoyant flow is assumed.

It has been observed that the conditions at the wall for the case of negatively buoyant flow can be divided into three main parts:

- Pure jet/plume zone
- Transition zone
- Boundary layer zone

The lowest temperature is the temperature in the boundary layer at the wall near the floor, the highest that in the upper jet/plume zone. The temperature in the sensor zones will always be between these two limits.

Furthermore it has been found that, in terms of temperature, the temperature is nearly constant in the upper jet zone. This zone has a height of approximately 60-70% of the total jet travel, which is defined as the length of the jet where the temperature difference between the jet and the room air is reduced to 1% of the initial value. This includes also the transition zone. In this zone the temperature decreases with height until the temperature has reached the value of the temperature in the boundary layer at the wall.

In all sensor zones outside the jet trajectory, the temperature is between the temperature of the wall surface and the surrounding room air. Its value can be approximated by expression (32).

This information about the temperature in the three zones at the internal walls allows us to describe the temperature in the sensor zones when the temperatures in the sub-volumes 1-4 of the simplified zonal model as well as the maximum downward travel of the jet are known (previous section).

The temperature in all sensor zones can be estimated using the following expression:

$$\vartheta_{sensor} = f_{jet}\,\vartheta_{jet} + f_{transition}\,\vartheta_{transition} + f_{BL}\,\vartheta_{BL} \qquad (40)$$

where f_{jet}, $f_{transition}$ and f_{BL} are weighting factors defining the influence of each of the three zones on the sensor temperature.

As an example, the temperature in the upper jet zone is obtained with a factor $f_{jet}=1$ and both other factors as zero. The temperature in the transition zone is obtained with the factor $f_{transition}=1$ and the others zero etc.

The unknown element in equation (40) is the temperature in the transition zone which will be treated in §4.3.2.

4.3.2 FUNCTION FOR THE TEMPERATURE IN THE TRANSITION ZONE OF THE WALL JET

With the information available from the simplified zonal model, the temperature at the sensor position can be estimated easily. The missing temperature in the transition zone is evaluated using the results of the EREDIS experiments (Chapter II) and the results from [Kapoor88].

A linear function is defined in order to obtain the temperature in the transition zone. This

simplifies the evaluation of the temperature in the sensor sub-volumes, which do not correspond to the jet zones of the negatively buoyant wall jet, observed in the tests. With this function, the temperature can later be calculated for the zones in the module "sensor conditions", for any maximum penetration distance of the wall jet.

The temperature in the transition zone of the wall jet is approximately linear with height (Figure IV - 26). This permits to correlate the temperature in the transition zone to the two borders of the transition zone (Figure IV - 26): The temperature of the jet, ϑ_{jet}, at the height (h_{zone} - 0.6 δ_P) and the temperature of the room ϑ_{jmain} at the corresponding height (h_{zone} - δ_P).

The temperature in the transition zone is then expressed by:

$$\vartheta_{transition}(h) = K_1 h + K_2 \qquad (41)$$

With this element, the vertical profile of the temperature in the sensor zone, affected by a negatively buoyant air flow can be estimated over the whole height of the room.

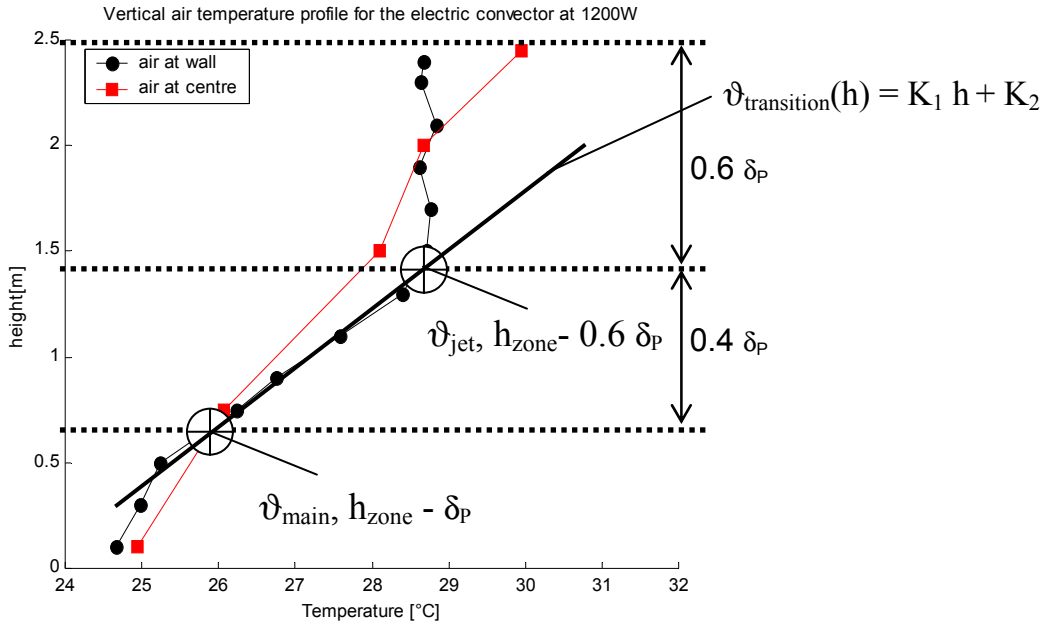

Figure IV - 26: Definition of the function for the temperature in the zone of transition of the wall jet

The temperature in the sub-volumes at the sensor positions and at the same height as the main zones in the simplified zonal model has to be calculated. This allows a direct comparison of the temperature in the main sub-volumes and the sensor sub-volumes.

A mean temperature has thus to be calculated for the sub-volumes characterising the sensor position.

4.3.3 CALCULATION OF THE TEMPERATURE IN THE SENSOR ZONES

The main difficulty of the calculation is the variable penetration of the wall jet. The three heights of the sensor zones are defined with the same height as the zones from the zonal model (Figure IV - 15).

The superposition of the zones from the zonal model and the module "sensor conditions" gives the same structure as the proposed zonal model in Figure IV - 2 - Figure IV - 4.

The estimation of the temperature in these zones is explained in the following.

The wall jet can penetrate to different heights in the room. The influence of the three jet zones on the temperature in the sensor zones is thus variable. A division in characteristic cases is proposed in order to deal with this problem. Depending on the penetration distance of the jet, six cases are

defined indicating the maximum jet travel compared to the particular heights of the sensor zones h_{vol}. The two borders dividing the jet into three typical zones (jet - transition - boundary layer) are used as indicators for the six cases. The cases are presented in Figure IV - 27:

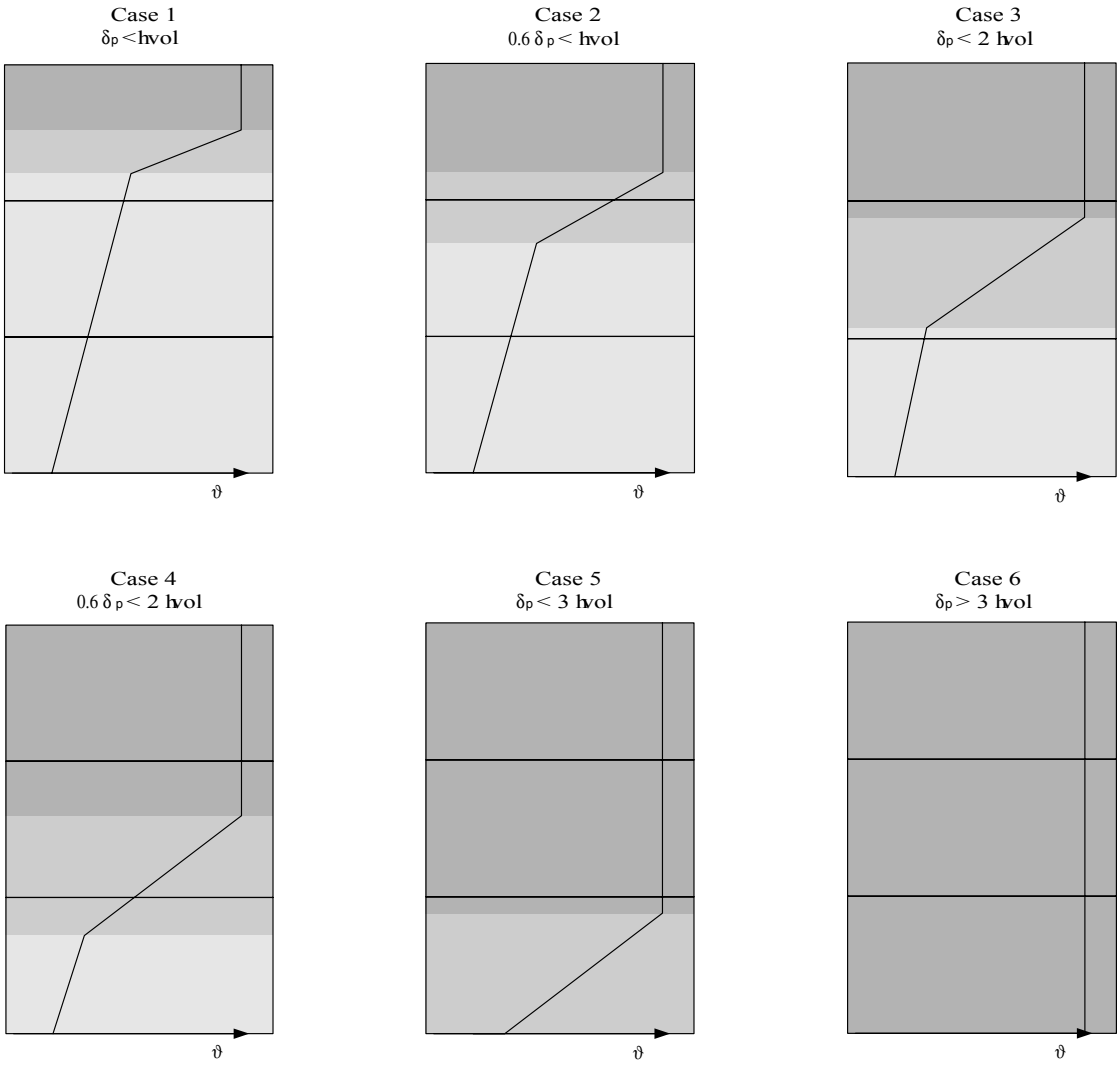

Figure IV - 27: Temperature in the negatively buoyant wall jet - 6 typical cases

The case of natural convection in all zones is not represented here. It is defined as case 7 and assumes the factor of the boundary layer as 1 one for all zones.

For each case the factors f_{jet}, $f_{transition}$ and f_{BL} are defined as shown in Table 11:

Table 11 Weighting factors for the calculation of the temperature in the sensor zones

	Upper sensor zone			Mean sensor zone			Lower sensor zone		
Case	f_{jet}	$f_{transition}$	f_{BL}	f_{jet}	$f_{transition}$	f_{BL}	f_{jet}	$f_{transition}$	f_{BL}
$\delta_P < h_{vol}$	$0 \le f \le 1$	$0 \le f \le 1$	$0 \le f \le 1$	0	0	1	0	0	1
$0.6\ \delta_P < h_{vol}$	$0 \le f \le 1$	$0 \le f \le 1$	0	0	$0 \le f \le 1$	$0 \le f \le 1$	0	0	1
$\delta_P < 2\ h_{vol}$	1	0	0	$0 \le f \le 1$	$0 \le f \le 1$	$0 \le f \le 1$	0	0	1
$0.6\ \delta_P < 2\ h_{vol}$	1	0	0	$0 \le f \le 1$	$0 \le f \le 1$	0	0	$0 \le f \le 1$	$0 \le f \le 1$
$\delta_P < 3\ h_{vol}$	1	0	0	1	0	0	$0 \le f \le 1$	$0 \le f \le 1$	0
$\delta_P > 3\ h_{vol}$	1	0	0	1	0	0	1	0	0

Each weighting factor corresponds to the part of the height of **one** sensor zone occupied by the corresponding phenomenon: jet zone, transition zone or Boundary layer zone (Figure IV - 28). The values are thus between zero and one for all factors and the sum of the three factors is 1 for each sensor zone.

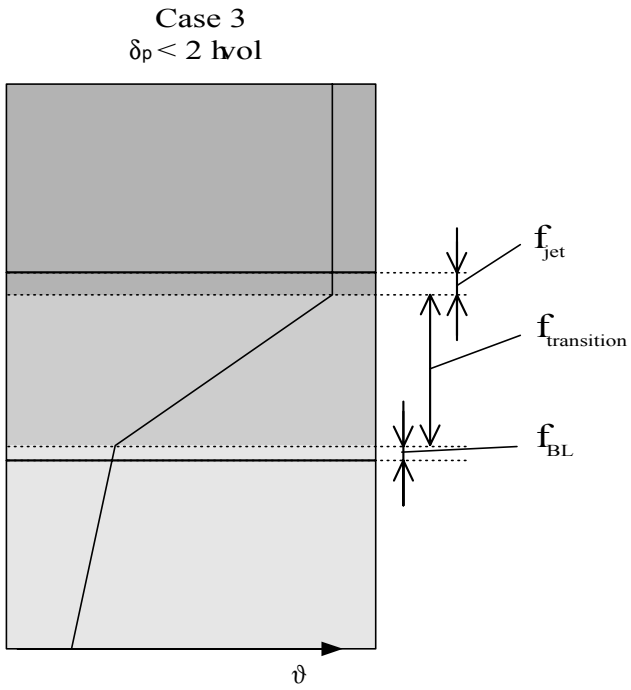

Figure IV - 28: Definition of the weighting factor for the calculation of sensor temperatures

For each sensor volume where the transition zone appears, the mean temperature of this part of the transition zone is calculated using the function defined in (41).

The temperature of the boundary layer is calculated using equation (32). The case of turbulent flow is assumed ($\theta = 0.7$). This principle is also used to calculate the temperature at the positions outside the possible jet trajectory.

Equation (40) is then applied in order to calculate the temperatures in the sensor zones.

4.4 CONCLUSION MODEL DEVELOPMENT

A modular model has been developed to represent at the same time the temperature in the occupant zone of a room, important for the assessment of controller performance, and the temperature at the positions of the controller sensor, necessary to represent the measurement of the controller sensor.

The model is divided into two parts:

- Zonal model of room convection
- Module for the estimation of the temperature in the sensor zones

The superposition of both modules gives information about all room temperatures.

The zonal model can be used separately when the sensor position is in the zones of occupancy. The model gives more detailed information about the room conditions compared to a well-mixed model. At the same time the convective heat exchange at the room surfaces is better represented than in the well-mixed model. Convective phenomena as for example bypass effects due to recirculating air when using a VAV system (heating case) or a fan coil unit (cooling case) are considered. This was not possible with a well-mixed model, which is currently used for controller studies.

The module for the estimation of the temperature at different sensor positions can be used, coupled to the zonal model. It permits to study the influence of sensor position on the control result.

The separation of both modules reduces the necessary number of sub-volumes in the zonal model and reduces thus simulation time.

The division into sub-volumes can also be carried out with lower or higher level of detail, depending on the needs. It is for example possible to combine a zonal model with only one main zone (instead of the three) to the sensor module with three zones.

The calculation procedure for the coupled model is as follows:

1. definition of heat and mass balances for the sub-volumes of the zonal convection model (c.f. §1)
2. definition of the air flow matrix of the zonal convection model as shown in §4.2.2-§4.2.3
3. solution of heat and mass balances for the zonal convection model
4. estimation of the maximum downward travel from §4.2.4
5. calculation of the coefficients of the linear function of the temperature in the transition zone following §4.3.2
6. calculation of the mean temperatures in the sensor zones following §4.3.3

If the zonal model is used as stand-alone model, only points 1-3 are treated.

5. IMPLEMENTATION OF THE ROOM MODEL IN THE GRAPHICAL SIMULATION ENVIRONMENT

The room model is divided into three main parts:

- Model of zone convection
- Model of the room envelope
- Model of radiation

The development of the model of the envelope and the model of radiation is not a main concern in this work. It has been developed using classic approaches and a selection of a model has been

carried out in Chapter III. Neither the development nor the implementation will be shown here.

The room model is structured in the graphical environment, following [Husaunndee99b], in order to:

- Implement the model into the SIMBAD building and HVAC toolbox
- Maximise the modularity of the model which is one of the the main principles in this toolbox
- Minimise the user knowledge regarding parameterisation

All models are thus, whenever it is possible, developed as individual modules to use the modularity, main advantage of the graphical simulation environment. The masking of the modules helps the user to understand and to use the models. Intelligent masking permits to choose between individual parameterisation and the use of predefined parameter initialisation files.

5.1 FIRST LEVEL: THE ROOM MODEL

The first level of the room model specifies the main inputs and outputs (Figure IV - 29).

The inputs of the model can be grouped into four parts:

- Radiation from exterior
- Temperatures outside the room (external and adjacent zones)
- Gains from heat sources (emitter, occupants or equipment)
- Air entering the room (HVAC system, infiltration or inter-zonal air flow)

The main groups of outputs are:

- Room air temperatures
- Internal surface temperatures
- Air leaving the room (HVAC etc.)

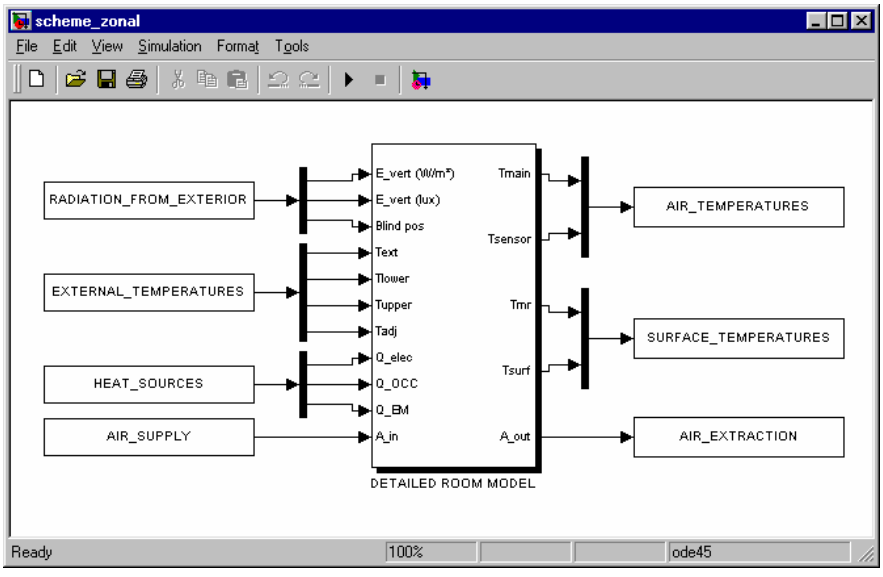

Figure IV - 29: Room model with principal inputs and outputs

The parameter mask of the main model asks for the general characteristic of the room (Figure IV - 30).

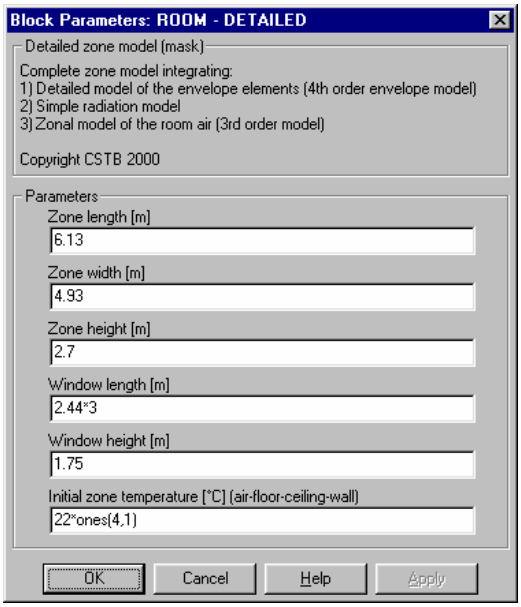

Figure IV - 30: Main parameters of the room model

Parameters, specific for the models on the second level are specified on these levels. This second level divides the model into the models of convection, radiation and envelope (Figure IV - 31).

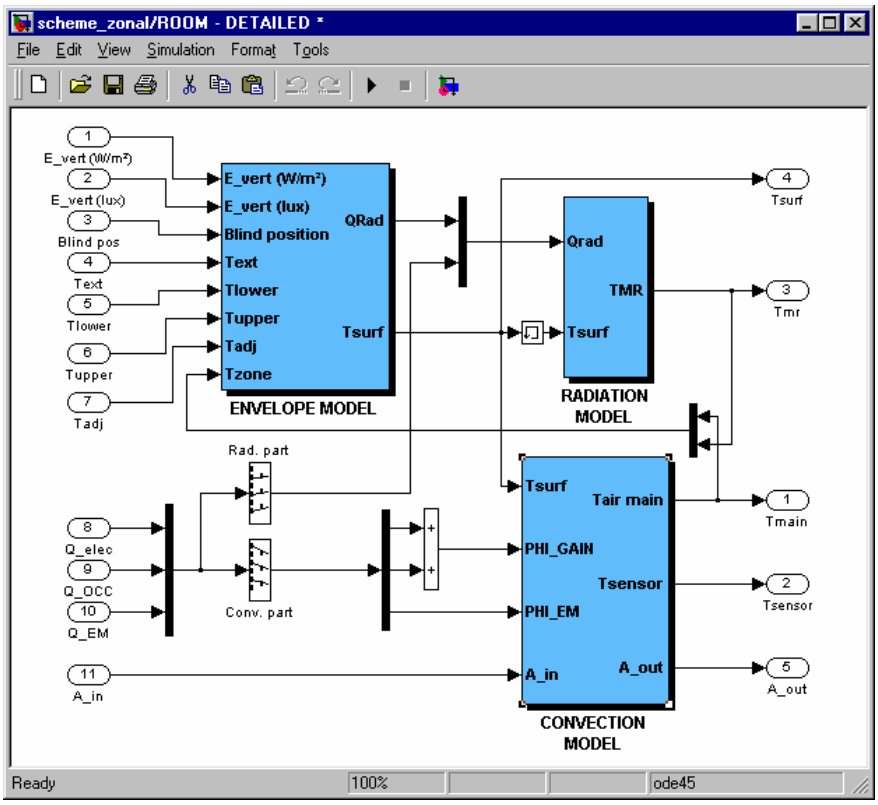

Figure IV - 31: Main parts of the room model: convection, conduction and radiation model

The gains from the emitter, occupants or from internal equipment are split into their radiative and the convective part. These both parts are inputs into the model of radiation and the model of convection. The implementation of the latter model is demonstrated in the following sections.

All three blocks of models are developed respecting the modularity of the SIMBAD library where they are implemented in. The models can be connected in different configurations: the number of surface elements can be changed depending on the simulated case. The model of convection can also be changed from the zonal model to a simple well-mixed model in cases

where low accuracy is acceptable. The particular wall models as well use the principle of modularity.

5.2 MODEL OF CONVECTION

The convection model includes the two modules that have been developed in §4 of this chapter. For reasons of modularity they are divided into two separate blocks in the simulation environment (Figure IV - 32).

The coupling between both modules consists in

- vector with the air temperatures from the zonal model
- vector with the two coefficients of the linear function for the temperature in transition zone of the jet, the maximum penetration distance and the case as shown in §4.3.3.

The main output of the convection model is the temperatures in the main sub-volumes (from the zonal model) and the temperatures in the sensor zones (from the module of sensor temperatures).

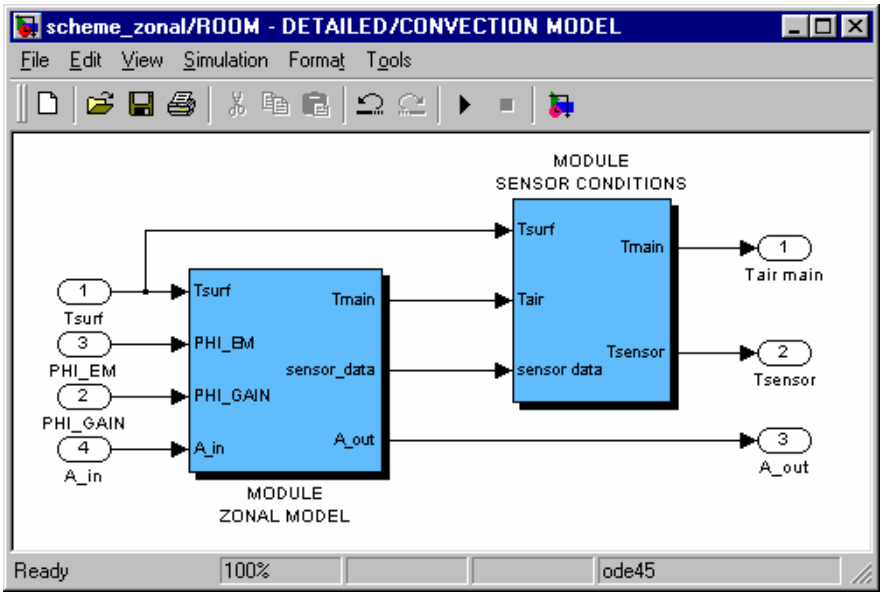

Figure IV - 32: Zonal model of convection with zonal model and sensor module

5.2.1 THE ZONAL MODEL

5.2.1.1 State space representation

The zonal model, developed in §4.2, is represented in the graphical environment.

The heat balance of the l sub-volumes the system as introduced in equation (5) is written in the state space form:

$$\dot{X} = AX + BU \tag{42}$$

and

$$Y = CX + DU \tag{43}$$

The system of heat balances on the sub-volumes can be represented by the first term. The second term for the outputs corresponds to the second module "sensor conditions" and will be treated separately.

The system of heat balances can be rewritten as:

$$C \frac{d \vartheta_{air}}{d t} = (A_1 - A_2 - A_3 - A_4) \vartheta_i + B_1 \vartheta_{A,k} + B_2 \vartheta_{ext,r} + B_3 \Phi_{conv,p} \quad (44)$$

Defining the following matrices and vectors:

The transposed state vector X:

$$X = \left[\vartheta_{air\,1} : \vartheta_{air\,i} : \vartheta_{air\,l}\right]^T \quad (45)$$

The transposed disturbance vector U:

$$U = \left[\vartheta_{A-1} : \vartheta_{A-k} : \vartheta_{A-m}, \vartheta_{ext-1} : \vartheta_{ext-r} : \vartheta_{ext-s}, \Phi_{conv-1} : \Phi_{conv-p} : \Phi_{conv-q}\right]^T \quad (46)$$

The matrix A containing the coefficients for leaving heat fluxes:

$$A = C^{-1} (A_1 - A_2 - A_3 - A_4) \quad (47)$$

The matrix B containing the coefficients of entering heat fluxes

$$B = \left[\left[C^{-1} B_1\right]\left[C^{-1} B_2\right]\left[C^{-1} B_3\right]\right] \quad (48)$$

With these definitions the system represents by equation (42). The second part, equation (43) corresponds to the sensor module and is treated in §4.3.

This implementation includes the following steps and definitions:

- Development of the heat balance of the system (conservation of energy),
- Restructuring of equation (5) in matrix form,
- Construction of matrices A and B from A_1 - A_4 and B_1 - B_3 representing the following phenomena:

  A_1 : Matrix of flow rates entering into sub-volume i from of other sub-volumes j (AFM),

  A_2 : Diagonal matrix of flow rates leaving from sub-volume i to other sub-volumes j,

  A_3 : Diagonal matrix of heat transfer numbers representing the leaving heat flux by convection at the internal room surfaces,

  A_4 : Diagonal matrix of flow rates leaving to external conditions due to ventilation, air conditioning or air exchange between adjacent zones

  B_1 : Matrix of heat transfer numbers representing the incoming heat flux by convection at the internal room surfaces,

  B_2 : Diagonal matrix of flow rates entering from external conditions (see A_4)

  B_3 : Matrix defining the injection of convective heat from emitters or gains
- Construction of the matrix C with the capacitive masses of the sub-volumes
- Construction of the disturbance vector U
- Construction of the state vector X

5.2.1.2 Sub-volumes with high and low inertia

The air sub-volumes will have various levels of inertia, depending on the volume of the sub-

volume and the air flow transferred through the sub-volume.

The zones of air flow generators have a very low inertia compared to the sub-volumes with less air flow. The latter are generally the main sub-volumes, where smaller flow rates are observed compared to their capacitive mass. The jet zones for example are characterised by a small capacitive mass but high flow rates, due to the entrainment of air from the main sub-volumes.

The sub-volumes are thus divided into those with high and those with low inertia. This division is carried out assuming the jet zones to have low inertia and main zone high inertia. A division, depending on the flow-dependent inertia of the sub-volume would guarantee converging results for a given time step but would bring more complexity at the same time.

The equation for the sub-volumes with low inertia is solved as a steady state heat balance. For the others with high inertia the differential equation of energy conservation will be solved. As a result, simulations can use larger time steps due to the higher time constant of the system.

When dividing into sub-volumes, those with low inertia are:

- Jet/plume zone
- Ceiling zone

For the other sub-volumes, the three main zones, the differential equation is solved.

The steady state balances for the jet zones are solved:

$$X_{HI} = -inv(A_{HI}) \cdot (B_{LI}\, U + A_{HI-LI}\, X_{LI}) \tag{49}$$

New vectors have to be defined to simplify the problem. The state vectors are constructed starting with the sub-volumes of low inertia. Then, the sub-volumes with high inertia are added. Using this method, the matrices A and B as well can be divided into two parts, one "steady state part" and one "transient part".

The state vector X is now defined by:

$$X = [X_{LI}, X_{HI}] \tag{50}$$

The matrix A_{HI} includes now the sub-matrices $A_{HI\text{-}LI}$ and A_{HI}:

$$A = \begin{bmatrix} A_{1-1} & \cdots & A_{1-i} & \cdots & A_{1-l} \\ \vdots & \ddots & & \ddots & \vdots \\ A_{i-1} & & A_{i-i} & & A_{i-l} \\ \vdots & A_{HI-LI} & & A_{HI} & \vdots \\ A_{l-1} & \cdots & A_{l-i} & \cdots & A_{l-l} \end{bmatrix} \tag{51}$$

And the matrix B includes the sub-matrix B_{LI}:

$$B = \begin{bmatrix} B_{1-1} & \cdots & B_{1-i} & \cdots & B_{1-l} \\ \vdots & \ddots & & \ddots & \vdots \\ B_{i-1} & & B_{i-i} & & B_{i-l} \\ \vdots & \ddots & B_{HI} & \ddots & \vdots \\ B_{l-1} & \cdots & B_{l-i} & \cdots & B_{l-l} \end{bmatrix} \tag{52}$$

The implementation in the graphical environment is shown in Figure IV - 33:

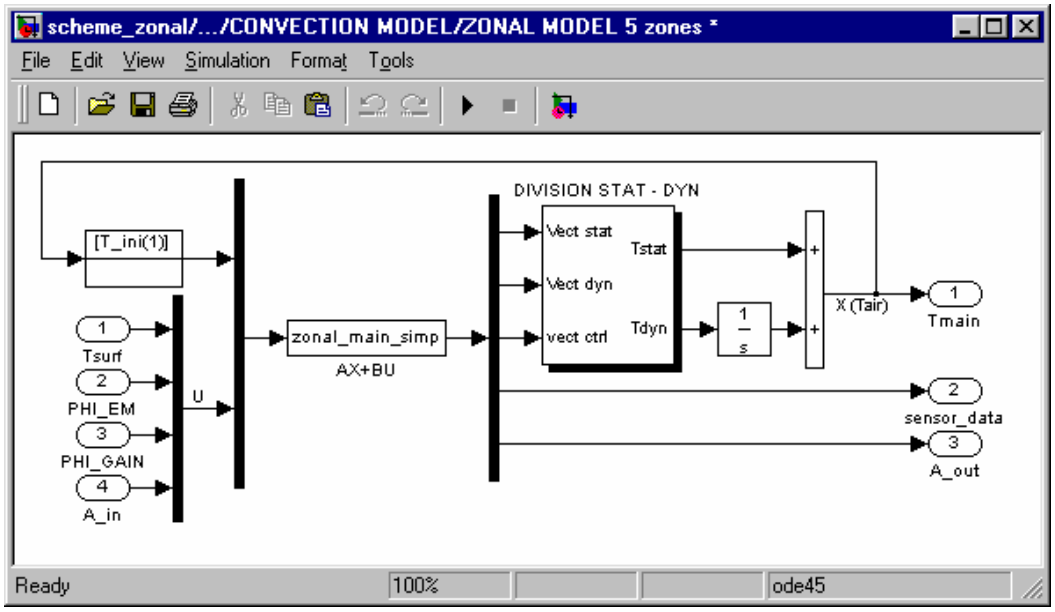

Figure IV - 33: Implementation of the simplified zonal model in the graphical environment

Usually, the matrices A and B are constant. In this case the matrices contain the flow rates between the sub-volumes which are variable. The block "zonal_main_simp" in Figure IV - 33 carries out the construction of the matrices and outputs a vector of the dynamic states as well as a vector of the calculated steady state temperatures. A third vector "vect_ctrl" indicates if the heat balance of the sub-volume is solved as steady state balance (value 0) or as differential equation (value 1). This permits to add the results of static and dynamic calculation and to output the combined state vector of the system.

5.2.2 THE SENSOR MODULE

The second part of the convection model determines the temperatures of the sensor zones starting from the solution of the system represented by equation (42).

The sensor module is an additional module defining the outputs of the model given by equation (43).

The different cases for the variable downward travel of the wall jet at the internal walls make the output matrices C and D variable. In the graphical environment this equation can be represented in another way, using the simplicity of the graphical environment. Figure IV - 34 (top) shows the implementation of the sensor module.

Each of the blocks "Case 1-7", equivalent to the cases defined in the development part (§4.3), contains the calculation procedure for the temperatures in the sensor zones. In each of these blocks the temperature in the sensor zones is calculated using equation (40), shown in Figure IV - 34 (bottom), and the necessary information from the zonal model. These are the temperatures of the main air sub-volumes, the coefficients for the function of the temperature of the transition zone, the maximum jet travel and the number of the case. In the left part of the block the three factors F_{jet}, $T_{transition}$ and F_{BL} are calculated. The temperatures in the three zones are calculated in the centre part. Note that the name of the maximum downward travel δ_P is replaced by z_{max} in Figure IV - 34.

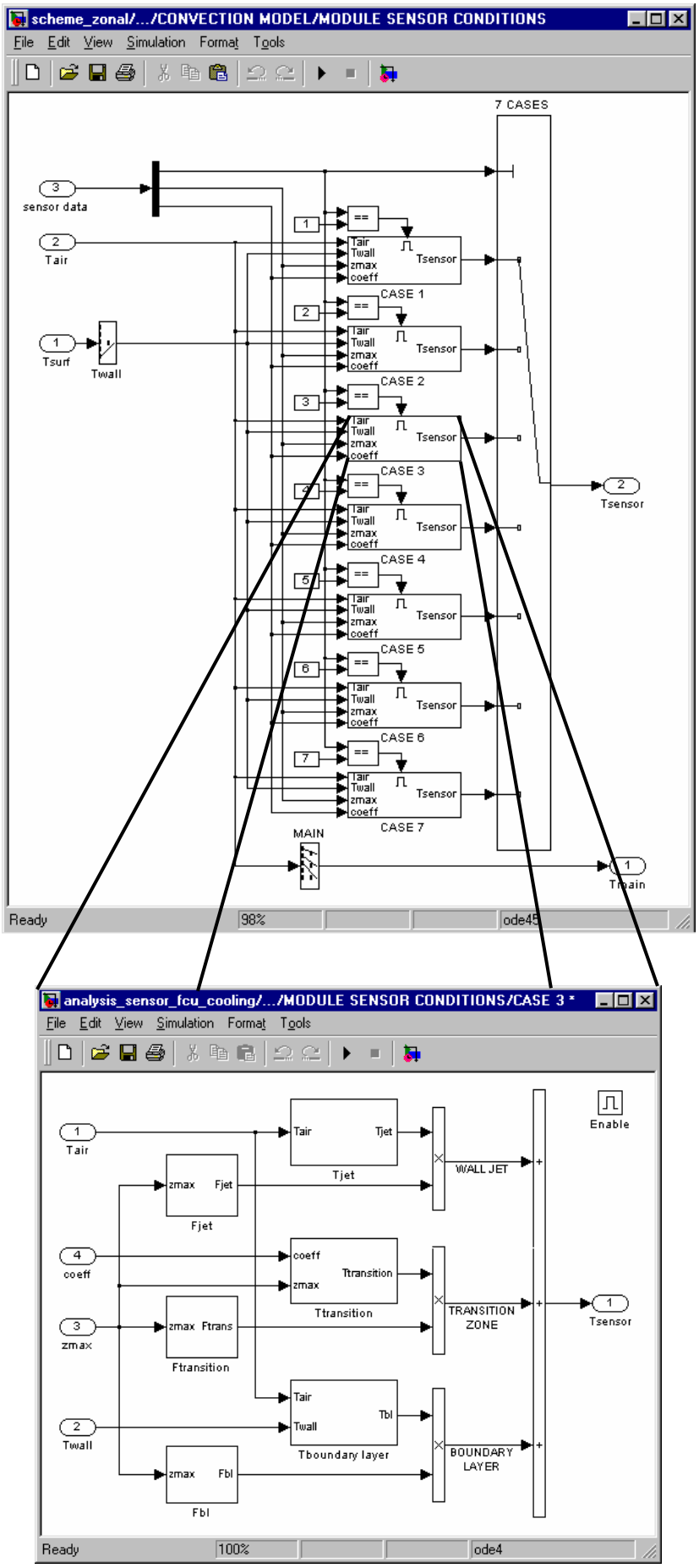

Figure IV - 34: Implementation the equation for sensor temperature (example: case 3)

5.3 CONCLUSION MODEL IMPLEMENTATION

The developed structure uses the modularity of the simulation environment. The division into three main models for convection, radiation and conduction permits the combination of different models, for example the use of different convection models, which have only to be changed in the existing model.

The zonal convection model can either be used as an independent model for controller tests where the sensor is placed at the centre of the room or as a coupled model together with the module for the estimation of the temperature in the sensor zones.

6. EXPERIMENTAL VALIDATION OF THE ROOM MODEL

The developed room model is validated for several cases. Since detailed measurement of room conditions including a temperature profile at the internal walls (sensor zones) is only available for the tests carried out in the EREDIS test cell, the complete model is validated for these cases.

Validation with the sensor module is carried out for the following emitters:

- Electric convector
- Fan coil unit (heating)
- Fan coil unit (cooling)

The tests are identical to those used in Chapter II for the quantitative analysis of phenomena in rooms. All tests are carried out in open loop conditions. The test data is described in each of the three validation parts. Comparisons for a long period are not of main interest for control studies. The comparisons are thus carried out for a period of one hour.

All comparisons are based on the same principle:

- Comparison of the air temperature profile at the centre position (performance assessment)

  The comparison of the centre temperature permits on the one hand the verification of the temperature profile, necessary for the performance assessment. On the other hand it is an indicator for the heat losses of the room model. If the centre temperature is significantly different from the measured value, the modelled room has a heat loss different from the real room. This influences the heating or cooling demand of the HVAC system. The load of the HVAC system has an important effect on the transient behaviour of a HVAC system. The result of a controller test by simulation is directly influenced by the difference of load between real room and simulated room. This phenomenon has been observed in [Riederer00]. It has been shown that the introduction of a second temperature node can improve the results.

- Comparison of the temperature difference between centre and sensor air temperature profile

  A direct validation of the sensor temperature profile would not make sense. For the use in controller studies only the difference between both is of interest since the value of this difference decides whether the controller is acting on the centre temperature (for no difference) or on a temperature directly influenced by the HVAC system or the wall.

  The accuracy of the measurement of this temperature difference seems high to the difference to be represented. However, since several sensors have been used to quantify the temperature difference (two at centre and four near the walls), the risk of a high error is small. The particular measurements at centre and sensor zones as well as the average of both groups of measurements (centre and sensor positions) show all the same tendency and only very small differences.

Only if both of these two criteria are valid a controller test in a real room is comparable with that in a simulated room. The following sections will use these two criteria for the validation of the developed room model.

6.1 CASE 1: ELECTRIC CONVECTOR

In the tests of the electric convector, a step of the heat emission of the convector from zero to a final value is carried out. Three test series are carried out in order to test the validity of the model for three different heat emissions, 400W, 700W and 1200W.

The test cell is described in Chapter II. The boundary conditions during the tests are shown in Table 12.

Table 12: Test conditions for the convector tests

TEST	Heat emission [W]	External temperature		Window temperature	
		ϑ [°C]	$\Delta\vartheta$ [+/-K]	ϑ [°C]	$\Delta\vartheta$ [+/-K]
CV1	400	14.6	0.3	15.6	0.8
CV2	700	15.2	0.1	16.2	0.4
CV3	1200	13.4	0.4	15.9	0.7

The boundary temperatures during the test are the surface temperature at the cooled wall (window) and the temperature outside the test room. Their mean values are given for the period of the simulations in Table 12. For the simulations the time-dependent measured values are considered.

A first order model of an electric convector is used in order to obtain the heat emission of the emitter after switching on the electricity supply of the convector.

The comparison of the centre temperature is shown in Figure IV - 35, Figure IV - 37 and Figure IV - 39 for the three cases CV1, CV2 and CV3. The temperatures at the heights of the three main sub-volumes of the zonal model are compared with measurement. The positions of the temperature sensors in the measurements are not identical with the heights of the sub-volumes of the model; it has thus been interpolated between the measured temperatures supposing a linear temperature profile between each measurement point.

The comparison of the temperature difference between centre and sensor profile is only carried out at three time steps. These time steps are indicated in Figure IV - 35, Figure IV - 37 and Figure IV - 39 and are 10 minutes, 20 minutes and 45 minutes. This type of presentation provides probably more information as the comparison of the difference for one height as a function of time.

The comparison includes the temperature response of the air temperatures in the room and the temperature level during the period. Previously it has to be mentioned that the comparison of the temperature response between measurement and in simulation is strongly influenced by the time constant of the electric convector. The used model of the emitter is a first order with a fixed time constant of 200 seconds. In reality, the convector is either switched on or off, by an ON/OFF controller or for example by a time-proportional controller (P, PI or PID). In the tests, the voltage is modulated in order to obtain the needed heat output. The time constant of the electrical resistance of the convector is thus different for each simulation case.

In the following, the results of the three tests are shown (Figure IV - 35- Figure IV - 40).

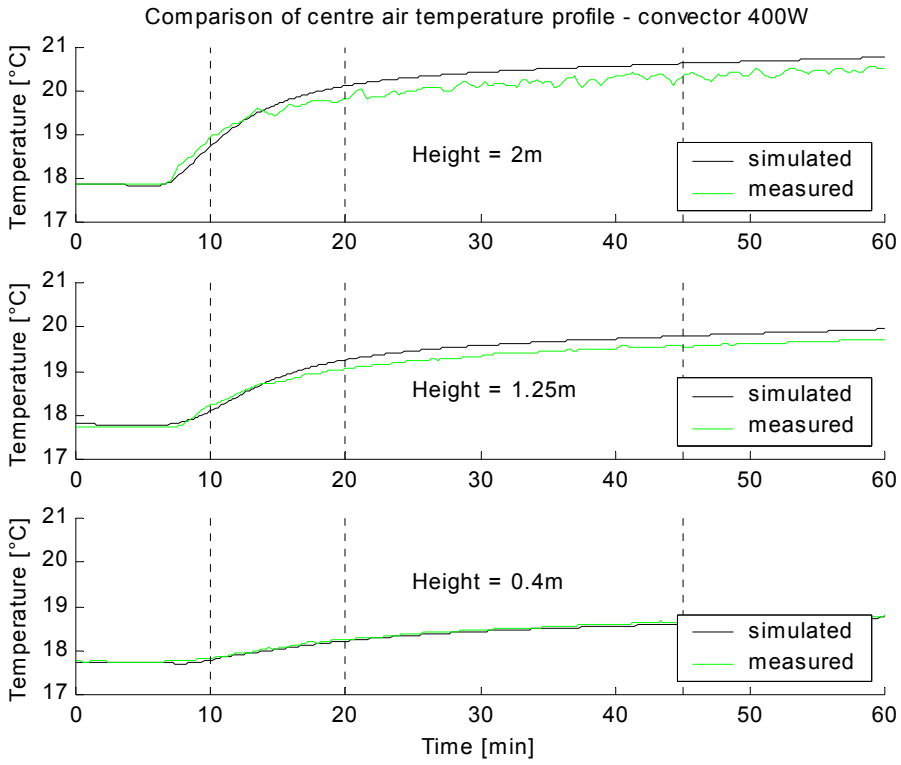

Figure IV - 35: Validation of the room model for the electric convector - centre temperature - 400W

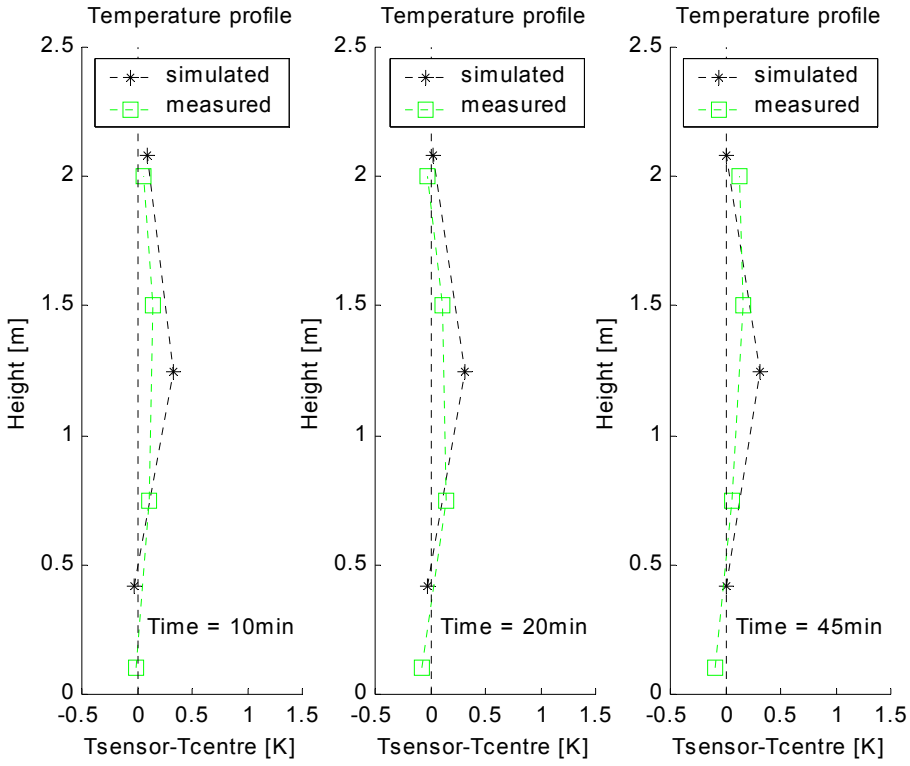

Figure IV - 36: Validation of the room model for the electric convector - sensor temperature - 400W

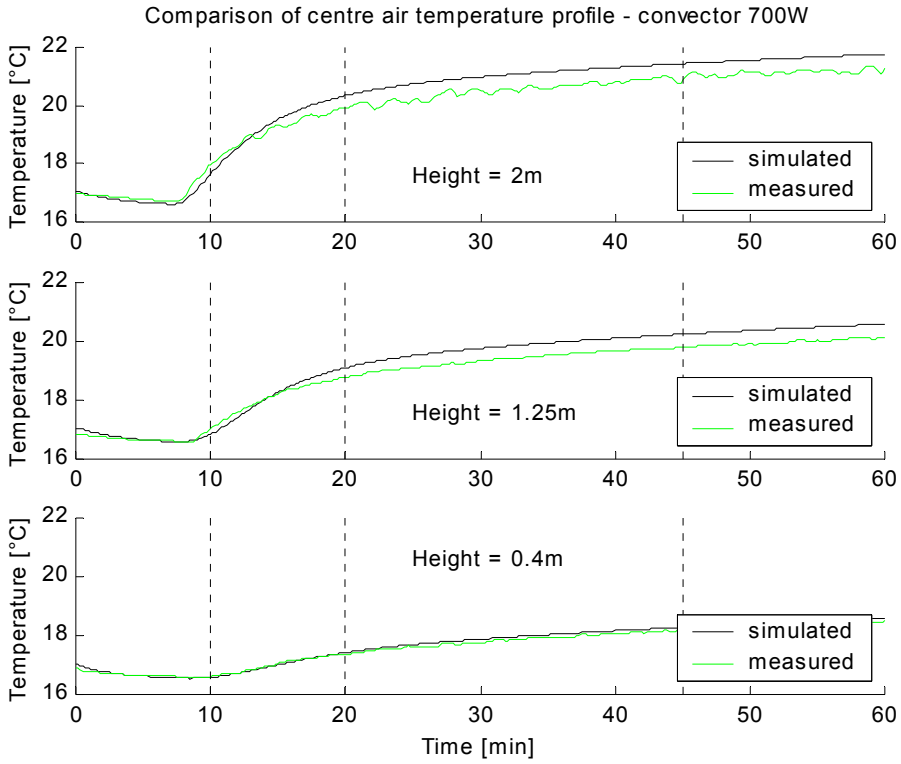

Figure IV - 37: Validation of the room model for the electric convector - centre temperature - 700W

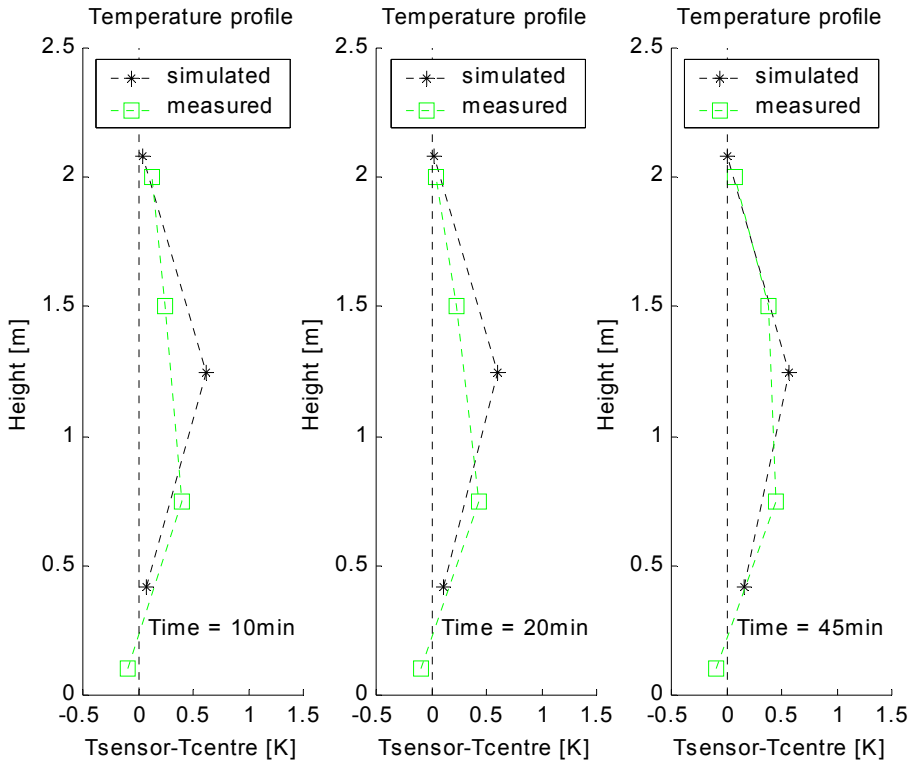

Figure IV - 38: Validation of the room model for the electric convector - sensor temperature - 700W

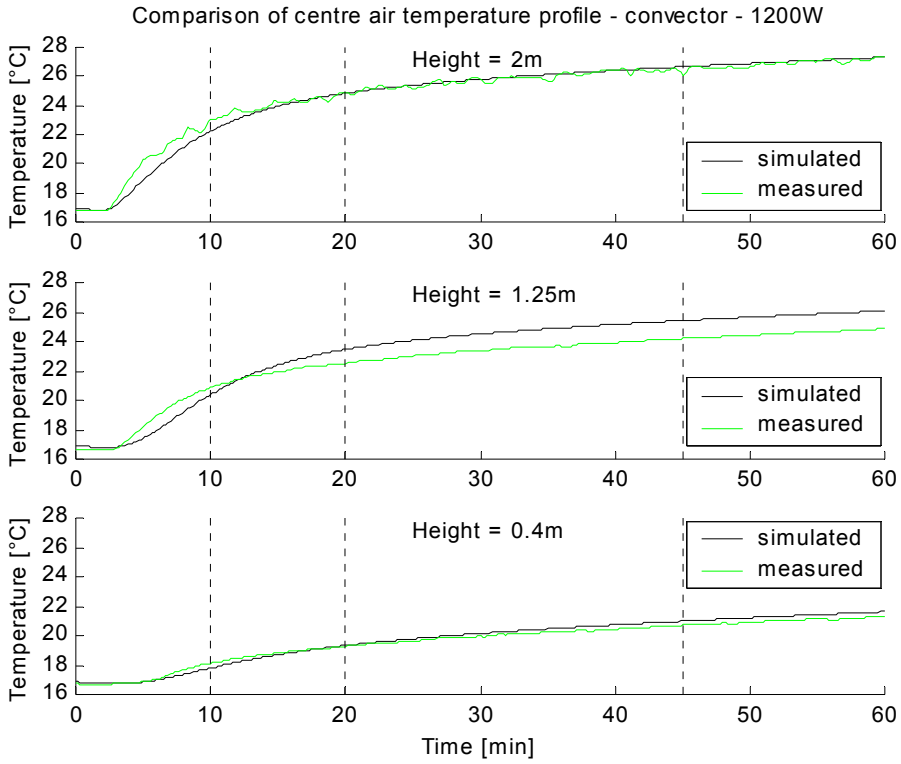

Figure IV - 39: Validation of the room model for the electric convector - centre temperature - 1200W

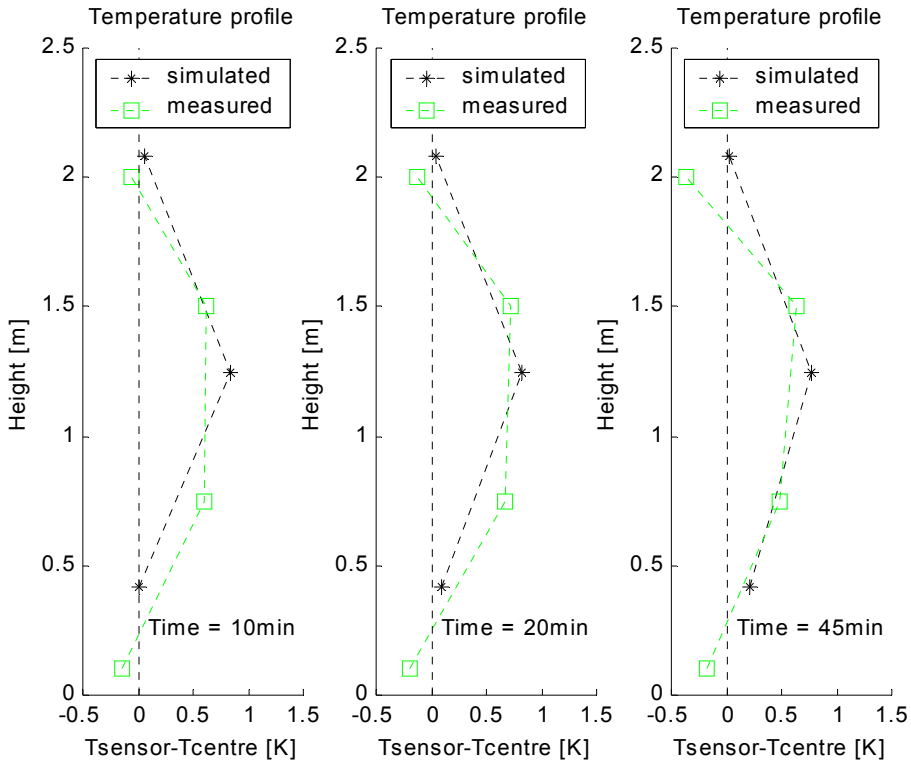

Figure IV - 40: Validation of the room model for the electric convector - sensor temperature - 1200W

Before the step:

Before the step, the comparison of the centre temperatures shows very good agreement in all three test cases. This is not surprising since the temperature difference between internal and external conditions is very small.

Temperature response after the step:

The temperature response at the centre profile shows good agreement with measurements for the two first cases with lower heat emissions (CV1 and CV2) at all three heights. In the last case, CV3, a difference is observed in the upper and the mean sub-volume of the room while the response is acceptable for the lower sub-volume. The difference is probably due to the time constant of the convector which has been estimated in the simulation.

Temperature level in the "quasi-steady state conditions":

At the end of the period all three cases show slightly higher temperatures than the measurements. The convective heat transfer coefficients have been fixed to standard values. This could be a reason for the difference. An error in the heat transfer at the window has a great impact on the heat balance on the room. However, with a temperature difference between measurement and simulation never passing 1K the model can be judged as acceptable for all these cases.

Difference between sensor and centre temperature profile

The comparison of the temperature difference between sensor and centre temperature gives the following results:

The temperature difference is small at the upper sub-volume. This is well represented in the model. The comparison in the lower sub-volume shows good agreement as well, however it has to be mentioned that the measurement has been carried out at 5cm from the wall. The thickness of the boundary layer is generally smaller than this value. The real value of the temperature difference will thus be different as given here. In the case of these tests the wall temperature has been lower than the air temperature; the temperature difference would thus be negative. On the other hand, since the model supposes an isothermal wall with a homogeneous temperature, the temperature difference would also be negative if the wall temperature was modelled correctly.

In the mean volume, the temperature difference is difficult to compare. The heights do not correspond between measurement and model. However the results agree very well for the third case. In the cases of lower heat emission and applying linear interpolation (see Figure IV - 36, Figure IV - 38 and Figure IV - 40), the difference is slightly overestimated. §6.4 shows a method in order to reduce the risk of an overestimation.

6.2 CASE 2: FAN COIL UNIT IN HEATING MODE

In the tests of the fan coil unit a step of the heat emission of the electric resistance in the coil from zero to a certain value is carried out. Two tests are carried out in order to test the validity of the model for two different fan speeds, the lower and the medium speed. The high fan speed is not compared since with most of the control strategies it appears only in extreme cases. The stratification has been shown less significant for the high fan speed. If the model is valid for the cases with the lower fan speed, it will also be acceptable for the high fan speed.

The fan coil unit is described in Chapter II. The boundary temperatures during the test are the surface temperature at the cooled wall (window) and the temperature outside the test room. Their mean values are given for the period of the simulations. For the simulations the measured values are considered. All necessary boundary conditions are shown in Table 13.

Table 13: Test conditions for the fan coil tests - heating mode

TEST	Fan speed	Air flow rate	External temperature		Window temperature	
	[1-3]	[m^3/h]	ϑ [°C]	$\Delta\vartheta$ [+/-K]	ϑ [°C]	$\Delta\vartheta$ [+/-K]
FCU1H	1	170	20.4	0.3	11.1	0.6
FCU2H	2	270	19.5	0.1	10.4	0.6

As for the electric convector, a first order model of the electric resistance is used in order to obtain the heat emission of the coil after switching on the electricity supply of the coil.

The temperature from measurement has also been interpolated in order to match the heights of the model nodes. The time steps for the comparison of the temperature difference between sensor and centre profile are 10 minutes, 20 minutes and 45 minutes.

Before the step:

As for the convector tests, there is only little difference between modelled room and real room. The temperature gradient from external to internal conditions is too small to observe significant differences.

Temperature response after the step:

Figure IV - 41 and Figure IV - 43 show, for both tests, the comparison of the temperature profile at the centre position of the room. Identical with the convector tests a slight difference in the temperature response if observed. It is difficult to assess the impact of the time constant of the electric resistance and of the room modelling on this difference.

Temperature level in the "quasi-steady state conditions":

Also in this case the temperature inside the room is higher in simulation than in measurement. The difference is higher in the case of medium fan speed. Probably the choice of the convective heat transfer coefficient at the ceiling (warm ceiling layer) but also for the vertical surfaces, especially at the window) is not correct for this case. Since the model uses only fixed heat transfer coefficients for the different loads, this slight difference has to be accepted.

Difference between sensor and centre temperature profile:

Figure IV - 42 and Figure IV - 44 show the results of this comparison. In the upper sub-volume, the measurements show a positive difference between the sensor and the centre temperature. This value is underestimated in the simulation.

At a lower height, the comparison is acceptable, with the restrictions given in the comparison for the convector case.

At mean height, good agreement is observed. In the first case of low fan speed, the difference is slightly underestimated. In the second case, the difference seems correct.

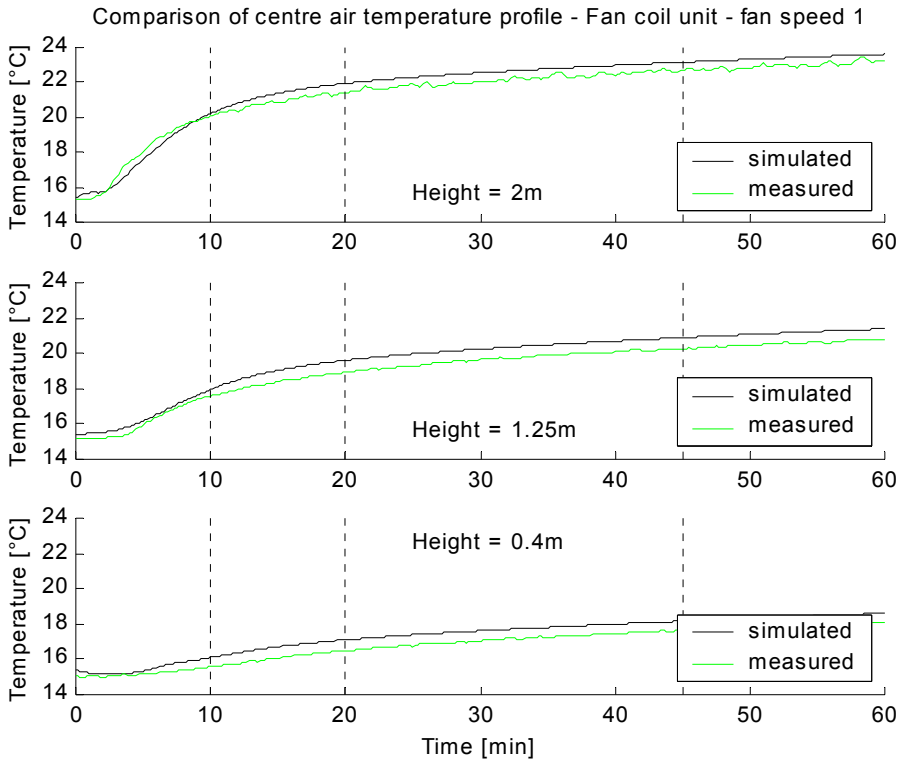

Figure IV - 41: Validation of the room model for the fan coil unit - centre temperature - fan speed 1

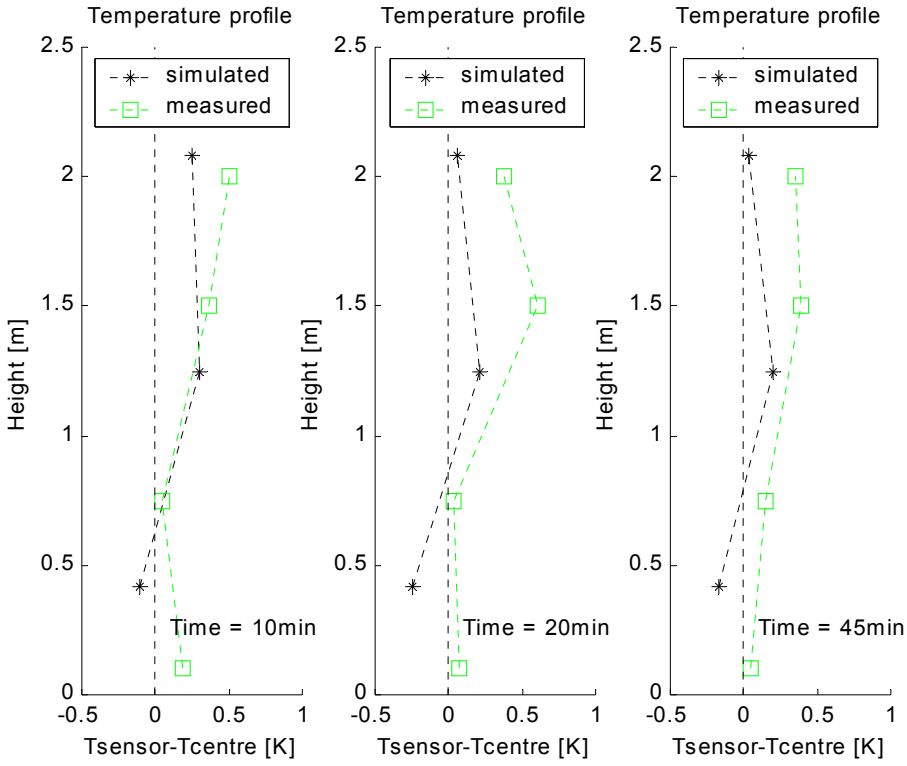

Figure IV - 42: Validation of the room model for the fan coil unit - sensor temperature - fan speed 1

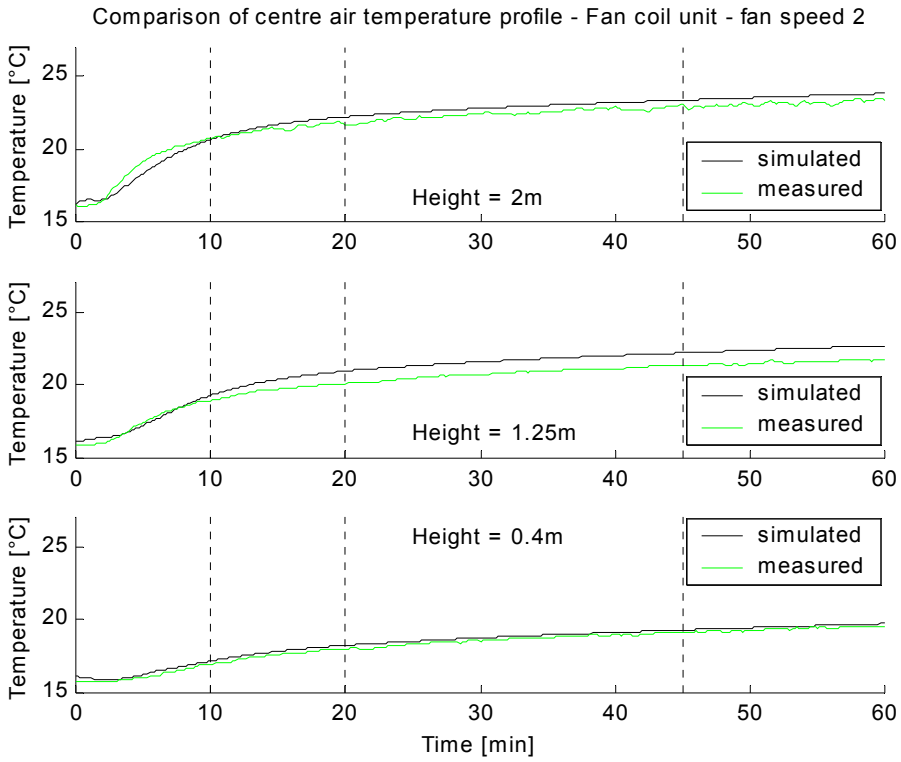

Figure IV - 43: Validation of the room model for the fan coil unit - centre temperature - fan speed 2

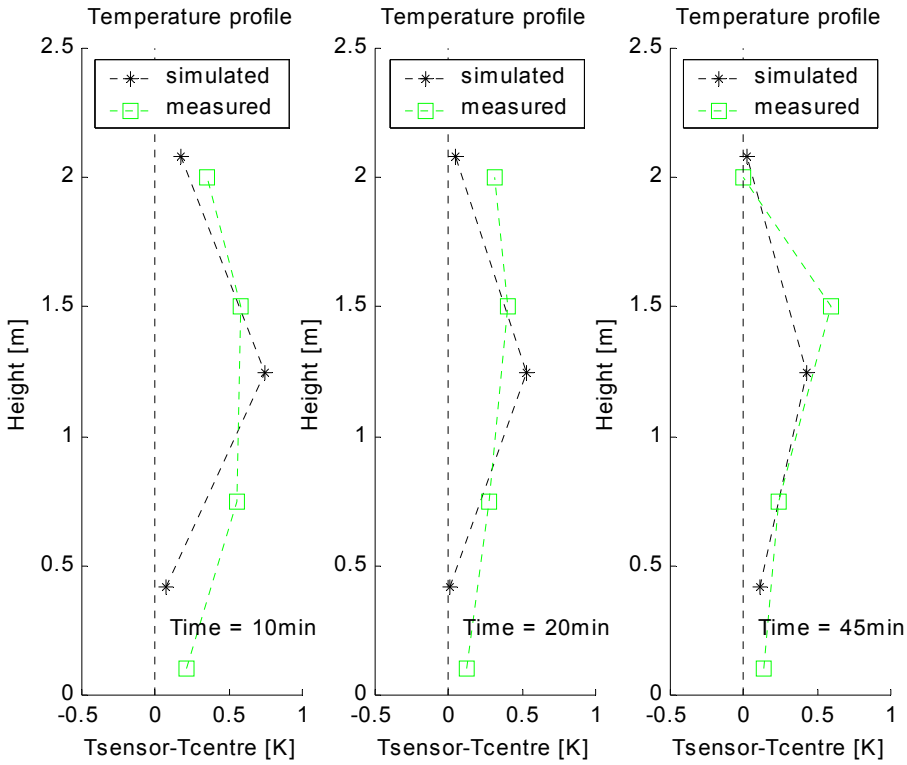

Figure IV - 44: Validation of the room model for the fan coil unit - sensor temperature - fan speed 2

6.3 CASE 3: FAN COIL UNIT IN COOLING MODE

In the cooling tests of the fan coil unit, a step in the water flow rate of the cooling coil is carried out while the fan speed is kept constant during the test. Two tests are carried out in order to test the validity of the model for two different fan speeds, the lower and the medium speed. The high fan speed is not compared since with most of the control strategies it appears only in extreme cases. In the case of standard controllers, the fan works only in the low fan speed.

The fan coil unit is described in Chapter II. The boundary temperatures during the test are the surface temperature at the heated wall (window) and the temperature outside the test room. Their mean values are given for the period of the simulations. The boundary conditions are shown in Table 14.

Table 14: Test conditions for the fan coil tests - cooling mode

TEST	Fan speed	Air flow rate	External temperature		Window temperature	
	[1-3]	[m^3/h]	ϑ [°C]	$\Delta\vartheta$ [+/-K]	ϑ [°C]	$\Delta\vartheta$ [+/-K]
FCU1C	1	170	22.3	0.1	34.2	0.2
FCU2C	2	270	22.7	0.1	31.1	0.4

The inlet temperature of the water is 12°C, the water flow rate after the step is 0.08kg/s.

A detailed model is used for the model of the cooling coil. The model uses a detailed geometrical description of the coil in order to calculate heat transfer coefficients as well as inertia of the coil for the coil dynamics. The model has been validated in [Husaunndee98] for exactly the same fan coil unit regarding static and transient temperature of the outlet air and water. The model is a first order.

The temperature from measurement has also been interpolated in order to match the heights of the model nodes. The time steps for the comparison of the temperature difference between sensor and centre profile are 10 minutes, 20 minutes and 45 minutes.

Before the step:

There is a difference in the temperature level between measurement and simulation. The higher temperature differences between internal and boundary conditions combined with the fixed convective heat transfer coefficients cause this error. The difference is, in all cases, less than 1K.

Temperature response after the step:

This part is particularly challenging for the room model. The quality of the results depends on the fan speed and the temperature difference at the outlet of the diffuser. Depending on these two variables, the cold jet reaches, for higher fan speeds (and higher air velocities) and even for high temperature differences, the ceiling and falls, from there, into the main sub-volumes. For lower fan speeds and high temperature differences at the outlet, the jet can change its direction, before reaching the ceiling. The jet will then fall back downwards while entraining room air. As mentioned in the development part, this phenomenon poses a major problem, not only in the steady state case, but even more in the transient case. This can be seen in Figure IV - 45 (low fan speed). Just after the step, the jet still reaches the ceiling. At a certain time, the jet starts to fall back down towards the floor. At this point, the air flow from the jet is not more injected into the ceiling, but to the jet volume itself and to the lower main volume. This effect is, in the model, very non-linear. The temperatures in the lower and in the mean volume in Figure IV - 47 show this phenomenon. Nevertheless, the non-linearity is, in this case, still acceptable since the temperature variation does not exceed 0.5K. In closed loop simulations, when the controller is

directly affected by this non-linearity, the result could be unacceptable.

Besides this phenomenon of non-linearity, the temperature response is quite satisfying, after the adjustments shown in §4.2.2.2, for the lower and for the mean air volume (Figure IV - 45 and Figure IV - 47). The temperature in the upper volume is not acceptable from the modelling point of view. But since the temperature at this height does not have an influence on the assessment of controller performance, this result can be accepted.

Temperature level in the "quasi-steady state conditions":

The temperatures in the two lower sub-volumes are in very good agreement with the measurements. In the upper zone, a maximum temperature difference of about 1K is observed. If a comfort model as for example the UCRES model is used, this difference is important. For other methods of performance assessment this error has little influence since the performance will be assessed at a lower height.

Difference between sensor and centre temperature profile:

In the first test (Figure IV - 46) the results are in good agreement with measurements for the upper and the mean air volume. In the lower volume the difference is bigger in simulation as in reality. Firstly the cold jet falls, in this case of the low fan speed, down to the lower volume.

In reality the jet passes then along the floor towards the walls. The temperature of the cold air at the floor increases on its travel to the walls, due to mixing with the mean air volume and due to convective heat exchange at the floor. When arriving at the wall, the air temperature in the boundary layer at the wall, warmer than the cold air near the floor, will be warmer than the air at the centre profile and the same height. A positive temperature difference is observed.

In the simulation, the temperature difference is higher. The air temperature in the lower volume, perfectly mixed throughout the sub-volume, is lower as in reality, where a greater part of the cold air does not reach the centre, due to a re-circulation effect at the fan coil unit. Then, since the wall is isothermal over the complete height of the room, the air temperature in the boundary layer at lower levels is higher than in the real case. As a result, the temperature difference between sensor and centre is larger. Nevertheless, even if the difference is much bigger, the tendency is the same for simulation and measurement.

In case two (Figure IV - 48), with the medium fan speed, a larger difference is observed in simulation, over the whole height. The reason can be that the temperature sensors in the measurements are at 5cm from the walls, while the boundary layer has a smaller thickness (c.f. also §3.3.1 in Chapter II). Differently to the measurements, the temperature in the sensor sub-volumes represents the mean temperature in the boundary layer and is thus different from the measured temperature.

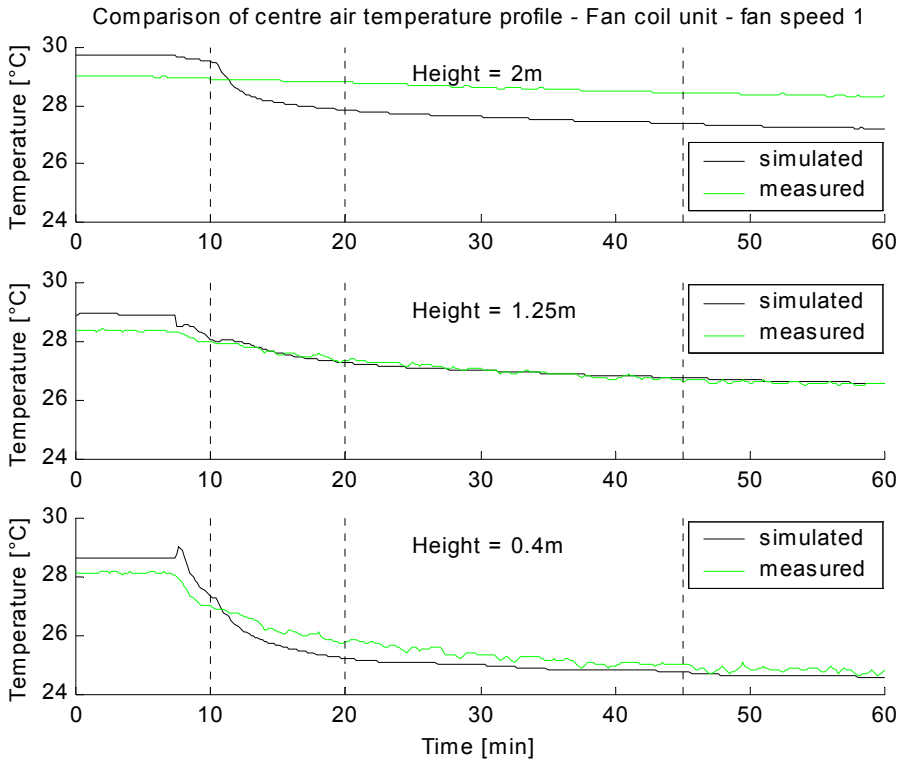

Figure IV - 45: Validation of the room model for the fan coil unit - centre temperature - fan speed 1

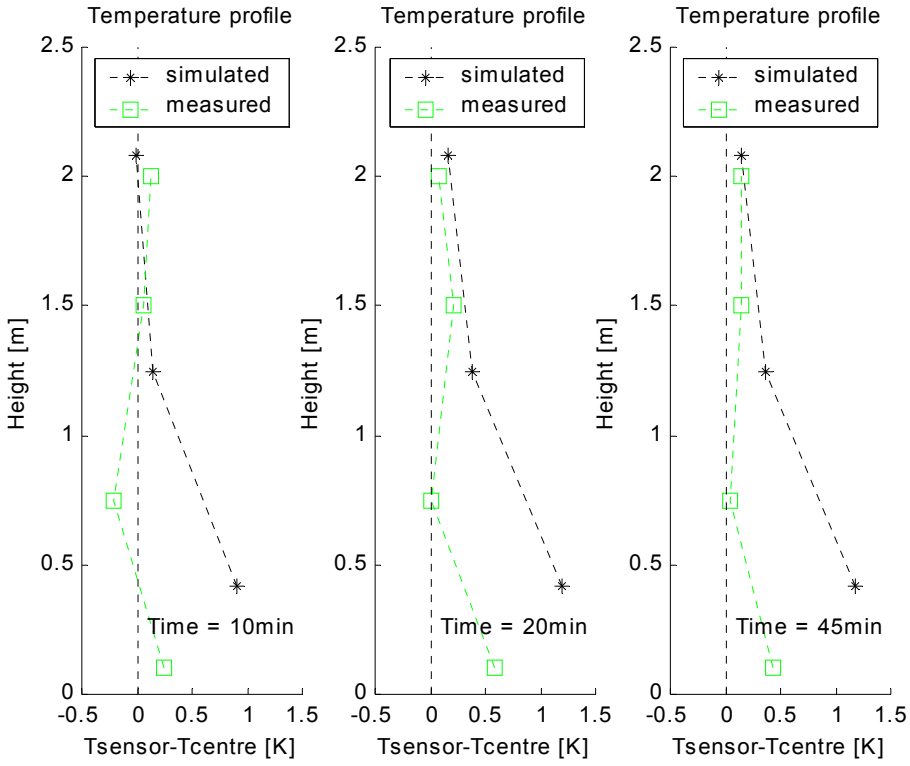

Figure IV - 46: Validation of the room model for the fan coil unit - sensor temperature - fan speed 1

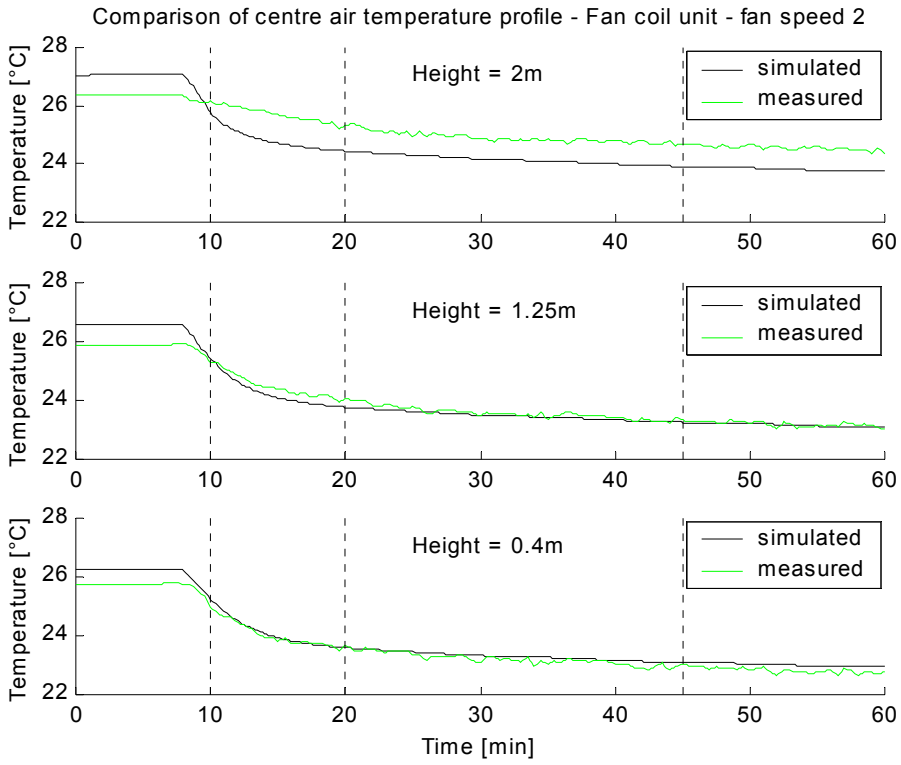

Figure IV - 47: Validation of the room model for the fan coil unit - centre temperature - fan speed 2

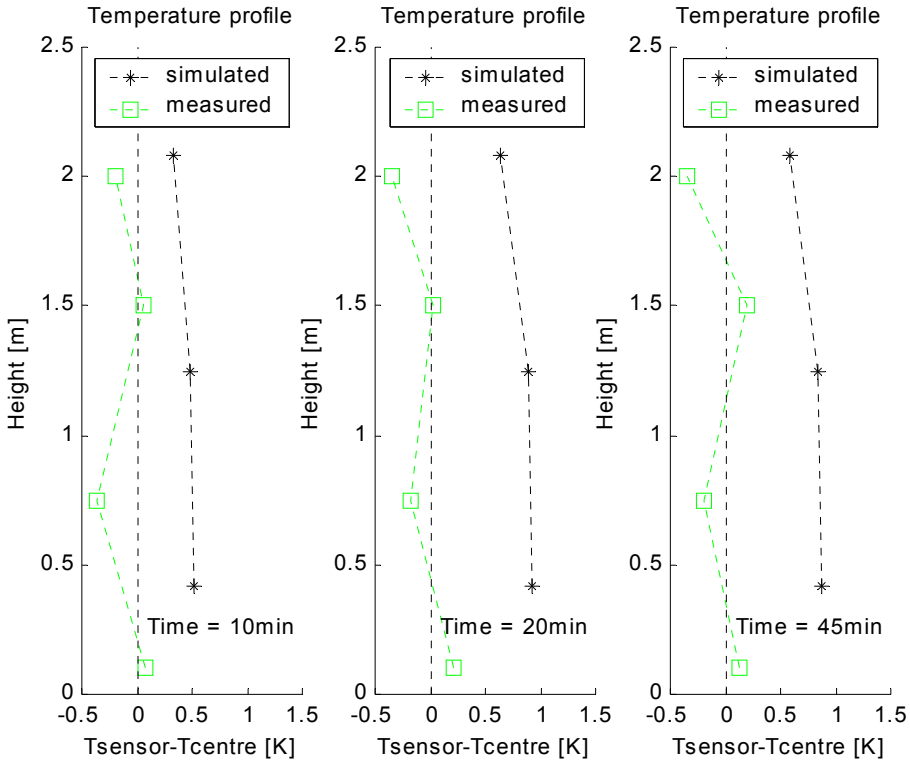

Figure IV - 48: Validation of the room model for the fan coil unit - sensor temperature - fan speed 2

6.4 CONCLUSION ON VALIDATION OF THE ROOM MODEL

In all heating cases, the results are in good agreement with measurements.

The simulated centre temperature follows the measurement quite closely. A difference in the temperature response at the centre profile is probably due to the time constant of the heat source for which the step is carried out.

The difference between sensor and centre temperature is also in good agreement with measurement. The phenomenon of negatively buoyant air flow at walls is well represented in the model. In some cases the difference is slightly overestimated. In the following section it is shown how to avoid an overestimation while keeping results close to reality.

In the cooling case results are slightly less acceptable than in the heating cases. The temperatures at lower and medium heights are well represented. The temperature response and value are different in the upper part of the room. If performance is assessed at a standard height in the room, this error at higher positions does not have an impact on controller tests.

Contrarily to the heating cases, the difference between sensor and centre temperature is higher in simulation. The reason for this remains in the modelling of the boundary layer in the wall jet while the sensors in the real tests are probably placed outside this boundary layer.

7. SENSITIVITY ANALYSIS ON IMPORTANT PARAMETERS OF THE ROOM MODEL

The sensor module is mainly based on the correlation for the maximum penetration of the negatively buoyant wall jet (equation (31)) in the heating case. The sensitivity of the used correlation on main parameters is studied. The following errors have an influence on the calculation of the downward travel of the jet:

- error in the air flow rate in the jet or the plume
- error in the air entrainment into the ceiling jet
- error in the length of the wall jet
- error in the initial jet thickness (without error in the flow rate)
- error in the initial jet temperature

In a first section, these parameters are studied on their influence on the results of the correlation. The error sources are studied, one by one, using equations of proportionality. Finally, a series of diagrams is proposed in order to estimate the addition of the possible errors and to help to keep the summation error as low as possible. The diagrams are based on proportional laws.

In a second part, the possible influence of the correlation for the negatively buoyant wall jet on the modelled difference between sensor and centre temperature is studied.

The theoretical conclusions about the error in the temperature difference between sensor and centre temperature are studied by simulation. In a third section possible errors are defined in order to study their real effect on the simulation results. Three simulations are carried out for negative errors, positive errors and without errors (compared to the values defined in the development paragraph) of the parameters of the correlations in order to estimate the impact of the correlation

7.1 SENSITIVITY OF THE CORRELATION FOR PENETRATION OF THE NEGATIVELY BUOYANT AIR FLOW AT THE INTERNAL WALLS

Proportional laws give the influence of the mentioned errors in correlations on the calculation of the penetration distance of the wall jet (equation (31)). These laws are given in the following sections.

7.1.1 ERROR OF AIR FLOW ENTRAINED INTO THE JET OR PLUME

The correlation for the flow rate in plumes or jets depends mainly on the constant used. A difference between the chosen constant and the "real" constant results in an error in the calculation of the air flow rate at the end of the plume, at the ceiling.

Separating the flow rate and the penetration distance in equation (33) gives the proportional influence of an error in the flow rate calculation on the wall jet calculation:

$$\delta_p \propto \dot{m}^{-2.402} \tag{53}$$

7.1.2 ERROR OF AIR ENTRAINMENT INTO THE PLUME OR JET AT THE CEILING

A jet correlation (29) is used for calculation of the entrainment of air into the ceiling jet. As for the plume or the jet, the constant of the correlation introduces an error in the air flow rate at the "virtual" origin of the negatively buoyant wall jet. Its influence on (31) is identical to that in equation (53).

7.1.3 ERROR DUE TO THE ESTIMATION OF THE LENGTH OF THE WALL JET

The total length of the wall jet (around the internal walls) can only be estimated. In Chapter II it has been shown that the wall jet is observed nearly all around the internal walls. Only close to the external wall the influence of the wall jet decreases. An error in the estimated length of this "virtual" diffuser at the top of the internal walls creates also an error in the calculation of the initial flow rate of the wall jet and thus an error in the initial velocity of the jet. It is supposed in the model that the warm air goes downward at all 3 walls opposite and next to the emitter. While an error at the opposite wall can be neglected (W_{zone}), the error can be sensible at the side walls L_{zone}, where an error of dL_{Zone} is introduced.

This error of dL_{zone} results in a final error for the penetration distance of:

$$\delta_p \propto \left(\left(1 + \frac{W_{zone}}{2\,L_{zone}}\right) + \frac{d\,L_{zone}}{L_{zone}}\right)^{-2.402} \tag{54}$$

The result depends on the room geometry. For long rooms, the error is less than for short rooms, if the same relative error of dL/L is assumed.

7.1.4 ERROR INTRODUCED BY THE ESTIMATION OF THE INITIAL JET THICKNESS

The penetration distance δ_p depends directly on the initial jet thickness D. The initial thickness of this wall jet is estimated to about 0.2m near the ceiling for the cases observed in the test in the EREDIS test room (electric convector and fan coil unit). The thickness is not known for the different emitters, it can only be estimated. The influence of this estimation on the value of penetration distance is studied. The laws used for the calculation of the penetration distance give:

$$\delta_p \propto D^{1-0.402} \tag{55}$$

7.1.5 ERROR DUE TO A FALSE TEMPERATURE DIFFERENCE BETWEEN THE AIR TEMPERATURE IN THE WALL JET AND AT THE CENTRE

An error in the temperature difference between the initial jet temperature and the ambient temperature is normally due to an error in the entrainment rate in the jet or plume at the external wall and the jet or plume at the ceiling. The magnitude of the temperature can thus only be estimated since the phenomena are coupled with the error introduced by §7.1.1 and 7.1.2:

$$\delta_p \propto d\vartheta^{-0.402} \tag{56}$$

7.1.6 ADDITION OF ERRORS

All error sources listed previously have to be considered simultaneously in order to assess the resultant error of the calculation of the maximum jet travel. For this, a series of 4 diagrams is constructed that permits the addition of the following errors:

- error in the constant of the plume correlation: dC_{plume}
- error in the constant of the ceiling jet/plume: $dC_{ceiling}$
- error in the estimation of the length of the wall jet: dL_{WJ}
- error in the estimation of the thickness of the wall jet at its origin: dD_{WJ}

The diagram is constructed using the relationships developed in §7.1.1-7.1.5 describing the relationship between the error in a parameter and the impact on the final result.

For all of these particular error sources, minimum and maximum error can be found in literature.

Starting from these data, three examples of parameter choices are selected in Table 15. They are combined in order to over- or underestimate the final result, the penetration of the jet.

Table 15: Error estimation for the wall jet correlation - three examples

	dC_{plume}	$dC_{ceiling}$	dL_{WJ}	dD_{WJ}
Bad choice with low error	+2.5	-15	0	+50
No error	0	0	0	0
Bad choice with high error	-2.5	+15	+30	-50

In a fist case, the reference case (No error), all parameters are assumed to be chosen correctly. The error in the calculation of the travel of the wall jet is zero.

In the two other cases, the values are chosen for bad cases of parameter selection. These examples show that the parameters can be chosen in an intelligent way. As a main factor influencing the jet travel the estimation of the wall jet length is observed.

The impact of these choices on the final result, the vertical penetration of the jet into the room, is represented in Figure IV - 49. For the three sets of parameter choices the error can be followed from the plume zone until the end of the jet.

Other combinations can be tried in order to estimate the error for other combinations of errors in the parameters.

From the obtained results the following can be concluded as rules for a choice of parameters

reducing the error:

- over-estimate the constant for the plume of the convector (in the case of the jet from a fan coil unit the constant should be under-estimated)
- under-estimate the constant for the jet/plume at the ceiling
- over-estimate the length of the wall jet at the top of the walls
- over-estimate the thickness of the wall jet

On the other hand, for other choices of parameters, as indicated in Figure IV - 49, the theoretical error in the penetration distance can achieve up to 90-100%.

The examples that have been presented in this section will be used in the following section, where the room model is used to estimate the real error obtained with the three parameter choices in terms of temperature difference between sensor and centre profile.

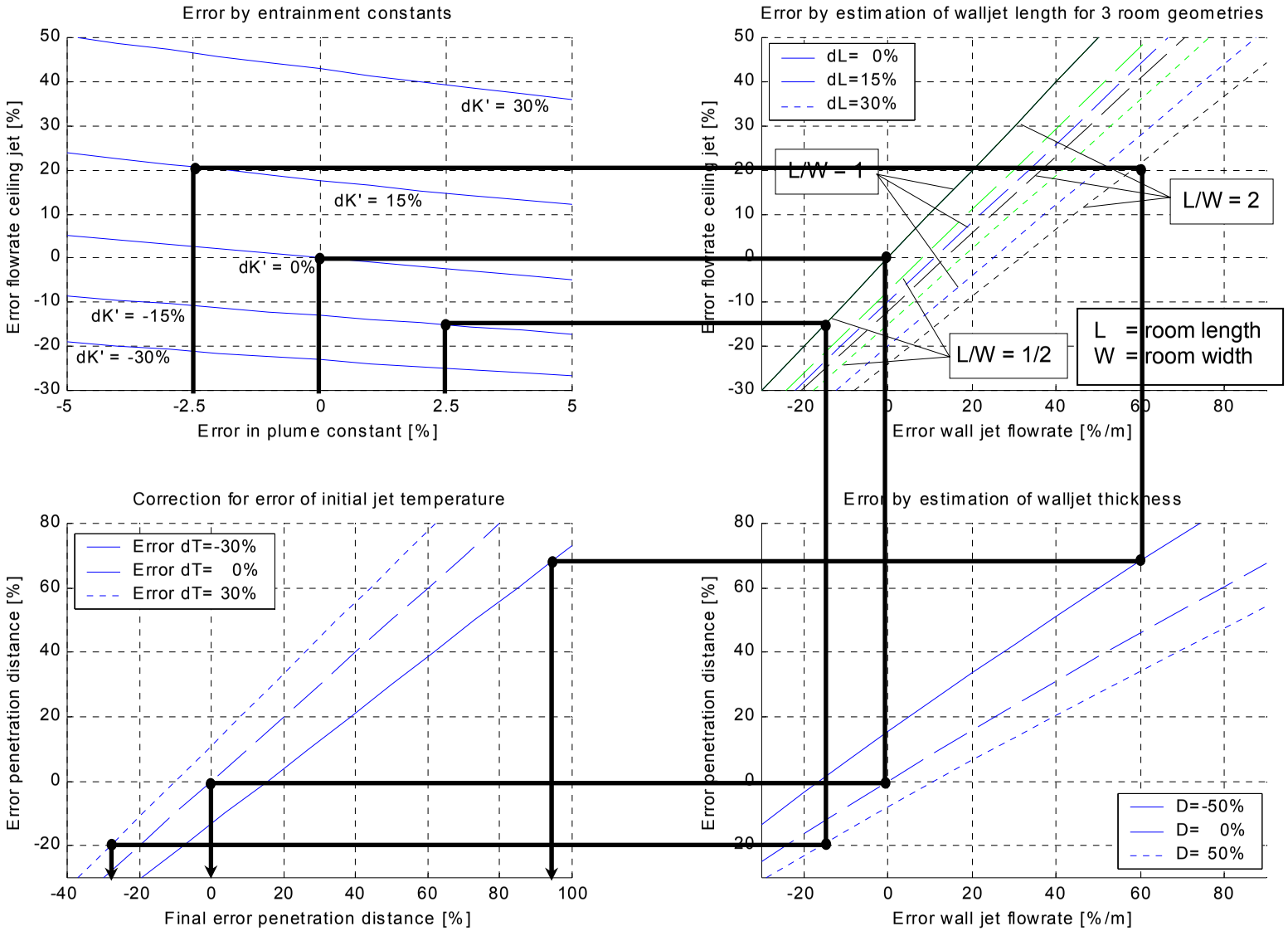

Figure IV - 49: Addition of errors of the correlation for the penetration distance

7.2 SENSITIVITY OF THE SENSOR MODULE ON AN ERROR IN THE IMPORTANT PARAMETERS OF THE WALL JET CORRELATION

The sensitivity of the correlation of the penetration distance on its main parameters, as demonstrated in the previous section, is only a theoretical way to show the impact of these main parameters. More interesting is the sensitivity of the model outputs, especially the temperature difference between sensor and centre zones, on these parameters. This is studied in this section using the proposed room model and a set of assumed errors in the main parameters of the model.

Considering that previous models do not represent the phenomenon of a negatively buoyant wall jet at all, the proposed model improves the result of the temperature difference between sensor and centre position in all cases where the penetration depth is underestimated.

In the case of an overestimation of the penetration depth, it is possible that the classic model gives better results than the new model since the proposed model would over-estimate the temperature difference between sensor and centre profile.

This is shown using an example of a simulation with three choices of the main parameters of the model. The same values selected for a high (overestimated penetration depth) and a low (underestimated penetration depth) error in Table 15 are used in a series of simulations. The case of the electric convector is chosen for this study. The heat emission is 1000 W; the room is identical to the EREDIS test room. Figure IV - 50 shows the results.

With the good parameter choice, the temperature difference between sensor and centre temperature profiles is nearly 0 in the higher sub-volume. In the lower sub-volume it is slightly positive. In the medium sub-volume, the temperature difference is about 0.7K.

When the bad parameter choice with the minimum error is chosen, the temperature difference at medium height is reduced to 0.4K. In the upper volume the difference is nearly unchanged. At lower height the difference is now slightly negative, identical with the result of a classic model assuming a boundary layer of natural convection at the walls. The result in temperature is, for all heights, improved compared to a classic model.

With the bad choice and maximum error, the temperature difference at medium height is increased to over 1.2K and over-estimated. The result can, in this case, depending on the wall temperature be better or worse than with the classic model.

An intelligent parameter choice will provide results between those of the best choice and those for the bad choice and low error. Using these parameters there is no risk for bad temperature estimation in the sensor volumes.

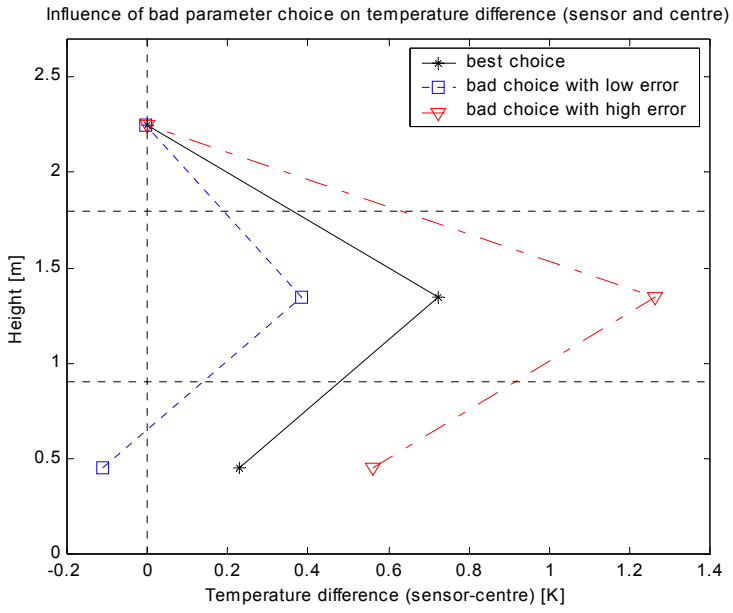

Figure IV - 50: Error in the temperature difference between sensor and centre temperature profile due to good and bad choice of the model parameters

8. CONCLUSION CHAPTER IV

Correlations have been selected for the implementation into a new zonal model. As far as possible, they have been represented in a general form, easy to use in a zonal model.

A new zonal model has been developed with a minimum number of sub-volumes, but adapted to a large number of HVAC systems. This has been possible after a detailed study of convective phenomena in Chapter II and with a division of the model in a classic, zonal model, dividing the room only into five sub-volumes.

A second model, a sensor module, has been developed in order to estimate the temperatures in the sensor zones. The superposition of both models provides all necessary data for performance assessment as well as for taking into account the effect of sensor position of the controller sensor.

The zonal model can be used separately for tests where the temperature at sensor positions is not of interest. In this case the sensor is assumed to measure the temperature at the centre part of the room.

The implementation of the model in the graphical environment has been adapted to this modular structure of the model. The zonal model and the sensor module are represented as separate blocks in order to use the modularity of the graphical environment and in order to give the user a better understanding of the model structure. The convective room model has been implemented, together with a model of radiation and of the envelope, into a complete room model.

Open loop validation has been carried out for the case of an electric convector and for a fan coil unit in heating and in cooling mode, for different heat emissions and fan speeds. The validation is carried out against measurements obtained in the EREDIS test room.

Two main aspects have been studied in the validations:

- *Validity of centre temperature profile*
- *Validity of the difference between sensor and centre temperature profile*

In the heating cases the results for both aspects are very promising. The representation of centre as well as of the sensor temperature is very good. Both parts of the model have been found to give good results.

In the cooling cases slight non-linearity has been observed for the case with a low fan speed. In this case, a re-circulation of the cold air can appear. The switch between re-circulation and no re-circulation creates this non-linearity. In cases of higher fan speeds, this problem is eliminated. The temperatures at centre position and low and medium height are acceptable; at the high air sub-volume a difference is observed. This difference could probably be eliminated with a more detailed model, but only with the restriction of longer simulation time. In the cooling case the sensor zones are always characterised by a boundary layer of natural convection. This is represented in the model, but the lumped model for the whole height of the internal walls introduces an error at lower and at higher heights. Since the temperature sensor near the walls were placed at 5cm from the walls, the air temperature is measured slightly outside the boundary layer, the results can thus not be directly compared.

The sensitivity of the main part of the model, the calculation of the wall flow with negative buoyancy, which can affect the controller's sensor in all heating cases, is studied. The influence of the main parameters is given as proportional laws and a series of diagrams has been developed in order to study the effect of addition of errors. These diagrams also permit an intelligent choice of parameters minimising the error in the model. Simulations introducing errors in each of the parameters are carried out. They show that a good choice of parameters guaranties acceptable results and that the new model gives, in all cases, a better representation of the system as the classic model assuming a natural convection boundary layer.

CHAPTER V

APPLICATIONS

In this last chapter the new room model is used to answer the following questions:

- *Is the use of a well-mixed model justified, when the sensor is assumed to be at the centre of the room?*
- *What is the impact of the sensor position on the results of controller tests?*

Controllers are therefore tested in a simulated building for the following HVAC systems:

- *Electric convector*
- *Fan coil unit in heating and in cooling mode*
- *VAV system in heating and in cooling mode for two types of air diffusers*

In a first step, the control of these HVAC systems is analysed in single room tests regarding the influence of model and sensor position. The tests are carried out using three types of controllers: proportional-integral, proportional and ON/OFF controller.

For cases where the HVAC system is supplied by a central unit providing water or air to the room level, the impact is analysed on both flow rate and heat emission since this can be important for whole building control performance.

A particular case is the VAV system. There is a significant interaction between control on the room and on the building level, due to the variable air flow in the system. Different models or sensor positions can thus have an impact on the test results. Therefore, a whole building is simulated to analyse this effect.

As a result, the differences obtained in the tests are presented depending on HVAC system and controller type.

Different performance indices are compared in a last part for the studied systems in order to show differences or similarities using these indices.

1. SIMULATION OF A BUILDING

A building is simulated in order to study the effect of the use of different room models and the position of the controller's sensor on the results of a controller test. The simulation is carried out for two cases:

- Tests of a single room under closed loop control with a step change in the internal heat gains (for different HVAC systems),
- Tests of a multi-zone office building using real weather data and internal gains (only for the example of the VAV system).

Different HVAC systems are used for the study. These systems and the building are described in the following section.

1.1 BUILDING STRUCTURE

1.1.1 BUILDING LEVEL

[Husaunndee01] and [Vaezi97b] used a virtual building for their studies. The same building is used here to carry out controller tests.

The simulated building (Figure V - 1) has a north-south orientation and can be divided into groups of rooms, here called zones. There are 9 rooms on the north and 9 rooms on the south side of each floor. All of the rooms have similar dimensions and structure. The zones with a south facade are zones 1, 3, 5 and the zones with a north facade are zones 2, 4, 6. Zone 3 and 4 include rooms with similar occupancy patterns on three of the five floors (each floor is identical). There is no glazing on the east and west facades.

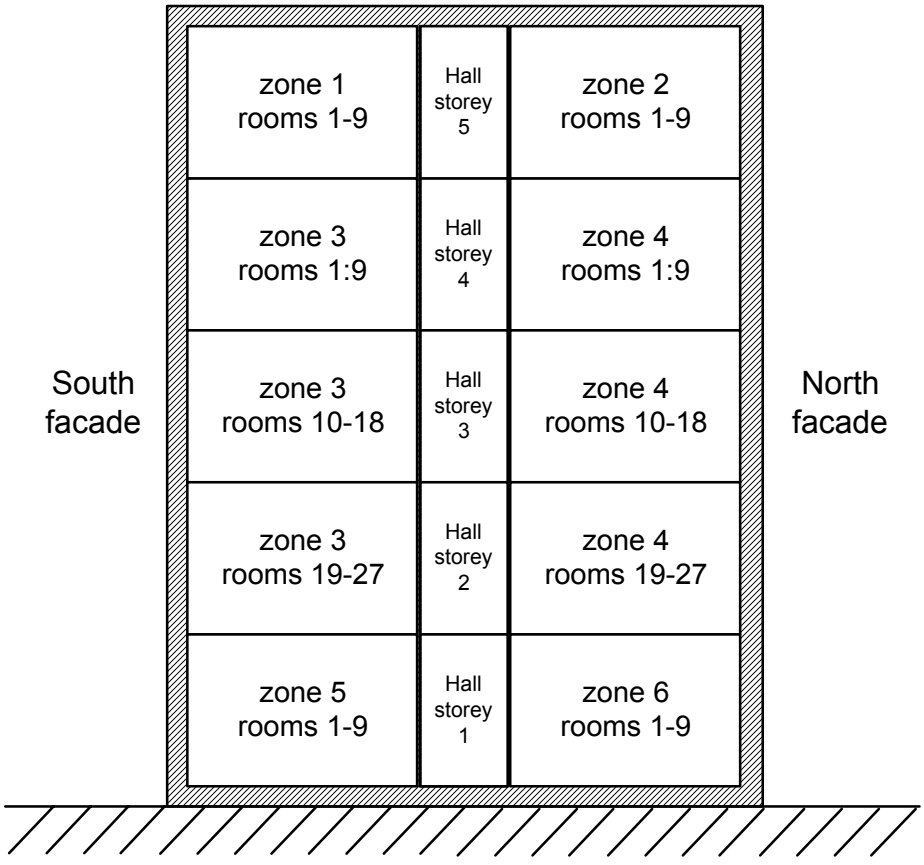

Figure V - 1: Division of the simulated building into six zones

A hall on each floor separates the zones on the southern and northern facades. It is assumed to be similar in temperature to the zones.

The building is equipped with an innovative lighting and shading control system ([Husaunndee01]).

1.1.2 ROOM LEVEL

The rooms are 5m in length, 5m in width and 2.6m in height. They all have one wall towards the external facades. The window at this wall has a size of 4.5m in length and 1.8m in height. The internal walls consist of two layers of plaster separated by a layer of mineral wool. A description of the structure of the rooms is given for the example of a room on an intermediate floor (zone 3 in Figure V - 1) in Table 16.

Table 16: Physical properties of the room

Surface	Material (Inside → outside)	Thickness [mm]	Density [kg/m^3]	Specific heat [J/(kg K)]	Conductivity [W/(m K)]
Window	Double glazing	4 / 6 / 4	U value: 3.85 W/m²/K		
Wall external	Glascal	55	2000	620	1
	Mineral wool	80	200	670	0.04
	Glass	10	2700	800	1.15
Wall internal	Plaster	10	1200	837	0.42
	Mineral wool	50	200	670	0.04
	Plaster	10	1200	837	0.42
Floor	Concrete	200	2100	653	1.75
	Air layer	380	1.2	1006	2.71
	Mineral wool	20	200	670	0.04
Ceiling	Mineral wool	20	200	670	0.04
	Air layer	380	1.2	1006	2.71
	Concrete	200	2100	653	1.75

The structure of floor and ceiling is slightly different on the first floor and on the fifth floor respectively. This difference is neglected in parametering the models.

Since the rooms are all similar, the simulations are based on one characteristic room in each zone of the building. The input- and output flows (air or water flow rates and heat flow) of this room are then multiplied with the number of rooms per zone.

1.2 BUILDING HVAC EQUIPMENT AND DESIGN

The impact of model type and sensor position is studied for the following systems:

- Electric convector
- Fan coil unit in heating and in cooling mode
- VAV system in heating and in cooling mode

The characteristics of the VAV system are found to be strongly dependent on the diffuser used (cf. §1.2.3). The VAV system is thus studied for two extreme cases of diffusers, a slot ceiling diffuser and a round ceiling diffuser. The extraction is, in these cases assumed to be placed at the ceiling.

The electric convector and the fan coil unit are identical to those used in the validation part in Chapter IV.

Figure V - 2 shows the different HVAC systems used for the study and their position in the room.

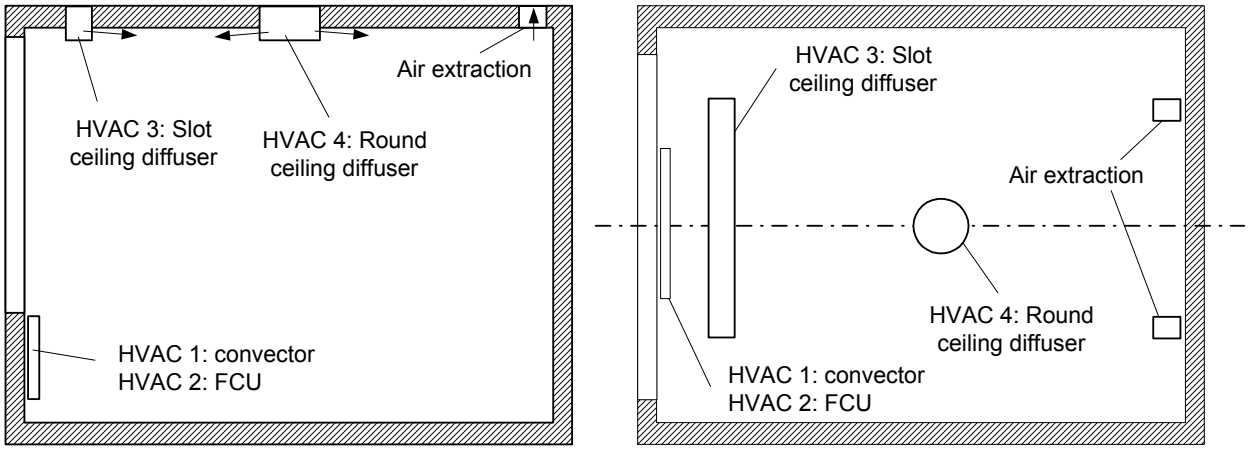

Figure V - 2: HVAC systems used for the study (left: vertical cross-section; right: plan)

The sizing and design of the mentioned systems are described in the following paragraphs.

1.2.1 ELECTRIC CONVECTOR

The electric convector (horizontal air outlet) is identical with that used in Chapter II (§2.2). It has a length of 0.75m and a height of 0.5m is placed at the external wall under the window, on the symmetrical axis. The nominal power of the convector is 1500W. The time constant of the electric heater element is about 200s.

1.2.2 FAN COIL UNIT

The fan coil unit is identical with that used in Chapter II (§2.2). It is also placed at the external wall. The nominal power of the electric heater element is 1200W; the fan itself has an emission of 28W - 59W, depending on the fan speed. The time constant of the electric heater element is 200s.

The cooling coil contains a volume of 0.79m^3. The time constant cannot be given here since it depends on the water flow rate through the coil. The cooling capacity is given from the manufacturer between 750W and 1800W depending on fan speed and water flow rate.

1.2.3 VAV SYSTEM

In the case of the VAV system, there are different types and positions of air diffusers that can be selected to distribute the air in the room. There is thus no "standard" case that can be considered as representative. At the same time there are different strategies to control the air flow in VAV systems. The following paragraphs deal with these points. Two cases of diffusers are selected there in order to get an idea of a possible impact of sensor position for these cases. The design and selection of a diffuser in a room is first discussed. Then, a control strategy is chosen.

1.2.3.1 Diffuser selection

The ASHRAE Handbook [ASHRAE97] provides information about air flow in jets for several different types of air diffusers, and rules for the selection and design of diffusers. According to

these rules, the diffuser should be selected, taking account of the entire flow range of the VAV system. The selection can be made using a number of different criteria: noise, jet mapping (throw, spread and drop), comfort (air diffusion performance index - ADPI). These criteria maximise the comfort of the room occupants while reducing noise and improving the conditions of the air in the occupied zone.

Class A diffusers [ASHRAE97] are selected for this study since most diffusers are mounted in or on the ceiling. The design of the diffusers is carried out using jet mapping. The throw of the jet (the distance from the outlet of the diffuser at which the centreline velocity is reduced to 0.25m/s) is selected so that it is slightly bigger than the characteristic length of the room (generally the distance between diffuser outlet and the next wall intersecting the jet trajectory, or the intersection of the jets from two adjacent diffusers) to prevent the jet dropping into the occupied zone when the system is in cooling mode (Figure V - 3). This corresponds to the selection of an acceptable ADPI in the occupied zone, in most cases.

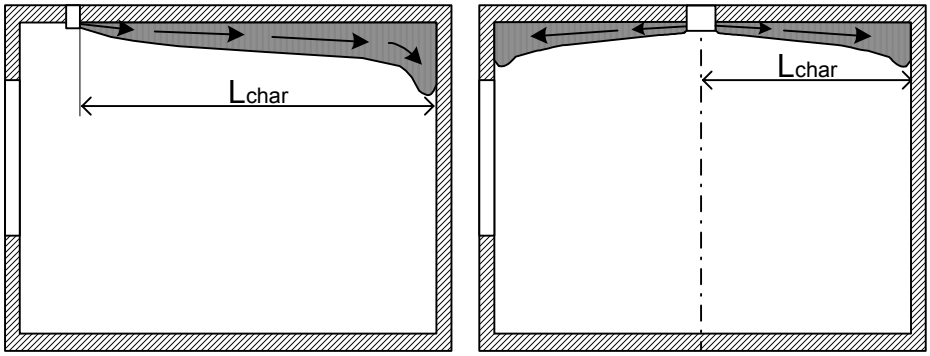

Figure V - 3: Diffuser design by jet mapping

As shown in Chapter IV, the law of velocity and flow rate in jets depends on the zone of the jet. There are diffusers distributing air following the second zone or the third zone of a jet. Depending on this parameter, the flow rate is either proportional to the square root of the distance to the outlet or proportional to the distance to the outlet.

Non-dimensional flow rate is plotted against non-dimensional distance from the outlet of a diffuser in Figure V - 4 using second and third zone laws. The possible range of flow rates, obtained using the range of constants K' given in [ASHRAE97], is plotted for each region.

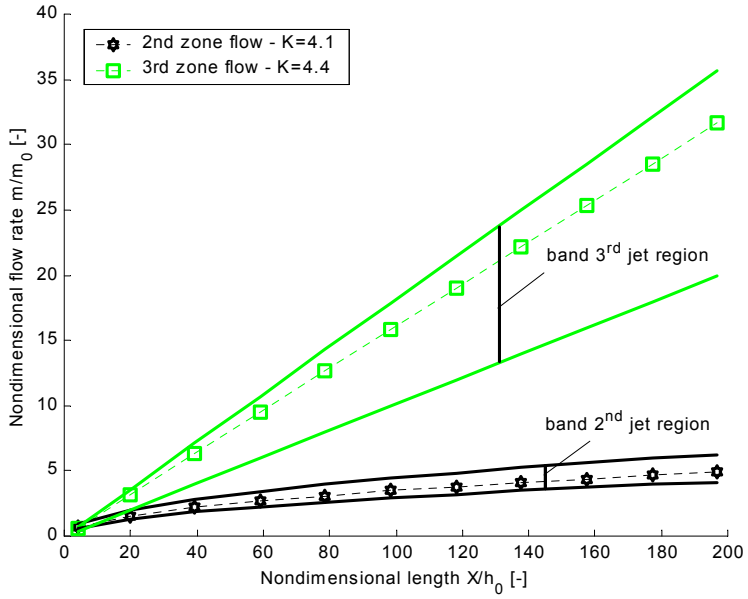

Figure V - 4: Airflow in a jet for second and third region flow characteristics

A slot diffuser creating a jet with second zone characteristics and a radial ceiling diffuser with creating a jet with third zone characteristics are selected for the study. The flow rates for these two chosen diffusers (dashed lines) are plotted in Figure V - 4 after determining the jet constant K' from manufacturer data. There is relatively little air entrainment for the jet from the slot diffuser while significant air entrainment occurs for the radial diffuser.

The two diffusers represent two cases near the extremities of the bands of flow rates for jets (Figure V - 4). For all other realistic cases, the air entrainment will probably be within these two bands.

1.2.3.2 The VAV control system

A central air-handling unit, with supply and return fans, provides air to all of the rooms in the building. “Pressure independent” VAV boxes with water reheat coils are used in the rooms, as shown in Figure V - 5:

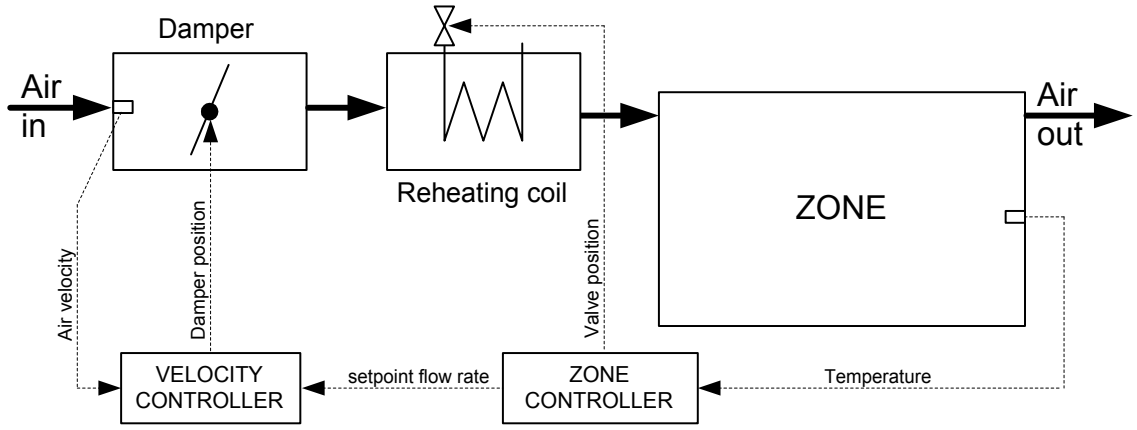

Figure V - 5: VAV system on the room level

In cooling mode, the room temperature controller varies the air flow rate set-point of the velocity controller. The velocity controller adjusts the damper position to control the air flow rate into the room (pressure independent control). This controller used the measurement of a differential pressure at a “grid” at the air inlet of the damper which can be converted into a flow rate. In heating mode, the air flow rate is held at its minimum value and the room temperature is controlled by varying the position of the valve controlling the water flow rate through the reheating coil.

1.2.3.3 VAV terminal box

The air inlet temperature to the VAV boxes is designed to 13°C for the cooling case and 18°C for the heating case.

The VAV terminal box includes the damper as well as the reheating coil. The damper has an opening time of 1 minute from fully closed to fully open. The dampers are sized depending on the load in the different zones of the building. The maximum air flow rate for a room in zone 3 (single zone tests) for example is 300m^3/h, the minimum flow rate is limited to 30% of the maximum flow rate.

The water temperature at the inlet of the reheating coil is 80°C. The maximum flow rate is 38l/h.

1.2.4 CONTROLLERS

Three types of controllers are used in the study:

- Proportional-integral (PI) controller
- Proportional (P) controller
- On/Off controller without hysteresis

The two first controller types are tuned manually, separately for each emitter type.

1.2.5 CONTROLLER SENSOR

In [Matsuba98] different time constants of the sensor have been used in order to analyse the stability limit of VAV control depending on sensor time constant. A standard value of six minutes for the time constant is assumed considering this study. The sensor measures the average of air and mean radiant temperature at the position of the sensor. The mean radiant temperature is, for all cases, defined as the mean radiant temperature at the centre of the room.

In the case of the zonal room model, the sensor positions as shown in Figure III - 3 are assumed.

2. SINGLE ROOM TESTS

The single room tests are based on the following assumptions:

- Constant external and adjacent temperatures
- Constant air and water conditions at the inlet of damper and coil
- No direct or diffuse solar radiation
- No air flow between adjacent rooms

The tests are carried out for a duration of 5 hours. In each test, at t = 180 min, the internal heat gains in the room are changed. The values of these heat gains before and after the step are chosen separately for each system in pre-simulations and for all three controllers in order to make sure control during the whole test.

For each HVAC system the following questions are answered:

- Is there a high discrepancy between the control results when the sensor is placed at different positions?
- Is the result using the well-mixed model within the band given by the results using the zonal room model with the sensor at different positions in the room (cf. Figure III - 3)?

As a result, it can be concluded, for each studied HVAC system, if a controller test (real or virtual) can be assumed as representative for all other cases of sensor position. The result of a controller test will thus also be meaningful in practice. If the result, using the well-mixed model, is within the band of results obtained using the zonal model, the use of the well-mixed model is justified for controller tests.

For all cases, the case of the zonal model with the sensor placed at the centre (position A) is taken as benchmark.

All controllers are tuned for each emitter system with the sensor placed at the centre (position A).

In the case of the VAV system in cooling mode, the possibility of an On/Off control is considered as well, even if this case is rarely observed in practice.

The results of the tests are shown for the resultant temperature at the centre of the room. In cases where the HVAC system in the room has also an effect on the whole HVAC system, for example the air flow in a VAV system or the water flow through the coils of VAV system or fan coil unit, the results are also shown for these flow rates and for the emitted heating or cooling power.

All results are discussed regarding the resultant temperature in the room since this variable has a comprehensible, physical meaning. The mean value and the maximum amplitude are compared considering two aspects:

- Is the controller performance for one controller the same, when different models/sensor positions are used?
- For each model type or sensor position, is the comparison between controllers represented in the same way?

2.1 ELECTRIC CONVECTOR

The boundary conditions during the test are listed in Table 17.

Table 17 Conditions single room test - convector case

Conditions	Heating Mode
Set point temperature [°C]	21
Temperature adjacent rooms [°C]	20
External air temperature [°C]	-10
Short-wave radiation [W/m²]	0
Internal gains before the step change [W]	0
Internal gains after the step change [W]	500
Nominal power of the convector [W]	1500

2.1.1 GENERAL BEHAVIOUR OF RESULTANT TEMPERATURE

Figure V - 6 shows the resultant temperature at the centre of the room for the well-mixed model and the zonal model with the three sensor positions for the different controller types.

Well-mixed model: The results are, for all three controllers, very close to the benchmark. The maximum temperature amplitude for the On/Off controller is underestimated compared to the benchmark with the sensor placed at position A.

Zonal model with sensor at position B: An offset in the resultant temperature is observed in the quasi-steady state periods. It is due to the impact of the warm wall jet on the temperature at the sensor position. The sensor is, in these tests, always placed in the warm wall jet. This leads also to a faster response of the temperature measured by the sensor on control action. The temperature response at the centre of the room is "anticipated". The amplitude of the resultant temperature is smaller than when the sensor is placed at the centre.

Highly non-linear phenomena are observed in this case. Figure V - 6 for the On/Off controller shows variable amplitude of resultant temperature for the period after the step. While the amplitude is larger directly after the step of the internal heat gains, it gets smaller from a certain time on (about 230min in Figure V - 6). This is due to the varying penetration of the jet near the internal walls.

Zonal model with sensor at position C: There is a small offset due to the positioning of the sensor in the boundary layer of natural convection. The results are similar to the benchmark in means of amplitude in all three cases.

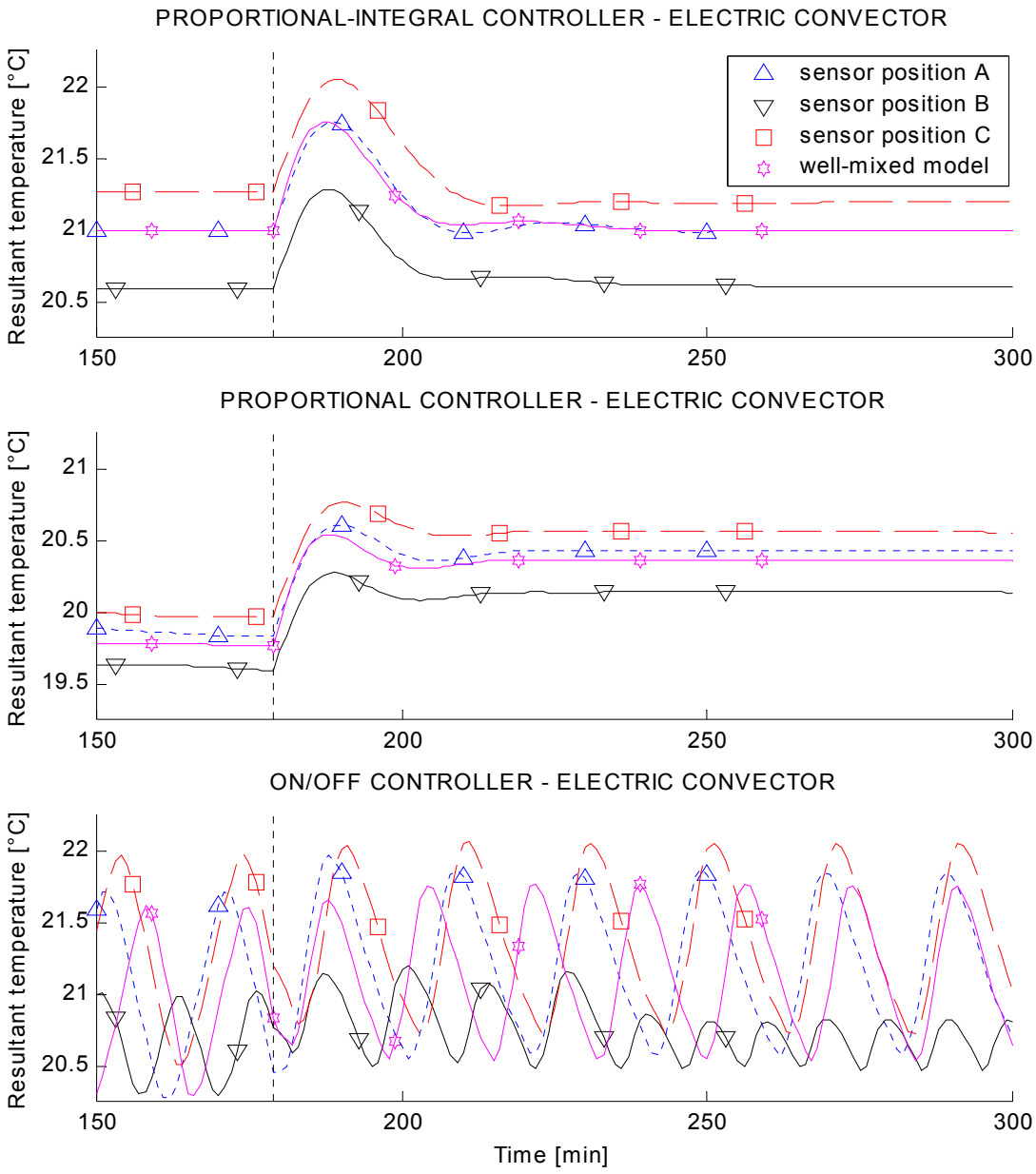

Figure V - 6: Resultant temperature - electric convector

2.1.2 POSSIBLE IMPACT ON RESULTS OF CONTROLLER TESTS

Analysis for one controller and changing sensor position/model type

The well-mixed model is nearly identical to the benchmark, the zonal model with the sensor at position A in terms of the resultant temperature. For the zonal model with the sensor at position B and C, the influence of the warm plume (position B) and the cold wall (position C) creates an offset. These differences from set point are qualitatively the same for the three controller types.

The maximum amplitude using the well-mixed model is close to that for the benchmark. When the sensor is at position B, the amplitude is significantly smaller small due to the warm plume around the sensor. All other differences are small.

Comparison of the three controllers for changing sensor position/model type

In terms of mean resultant temperature, except the offset characteristic for each model type/sensor position, the comparison between the three controllers shows similar results.

When the amplitude is studied, the results are slightly different for the well-mixed model and the zonal model with the sensor at position C. When the sensor is placed at position B, the On/Off controller would have a better classification compared to the benchmark and would have a similar performance regarding amplitude even if this is not the case as seen in the benchmark, (position A).

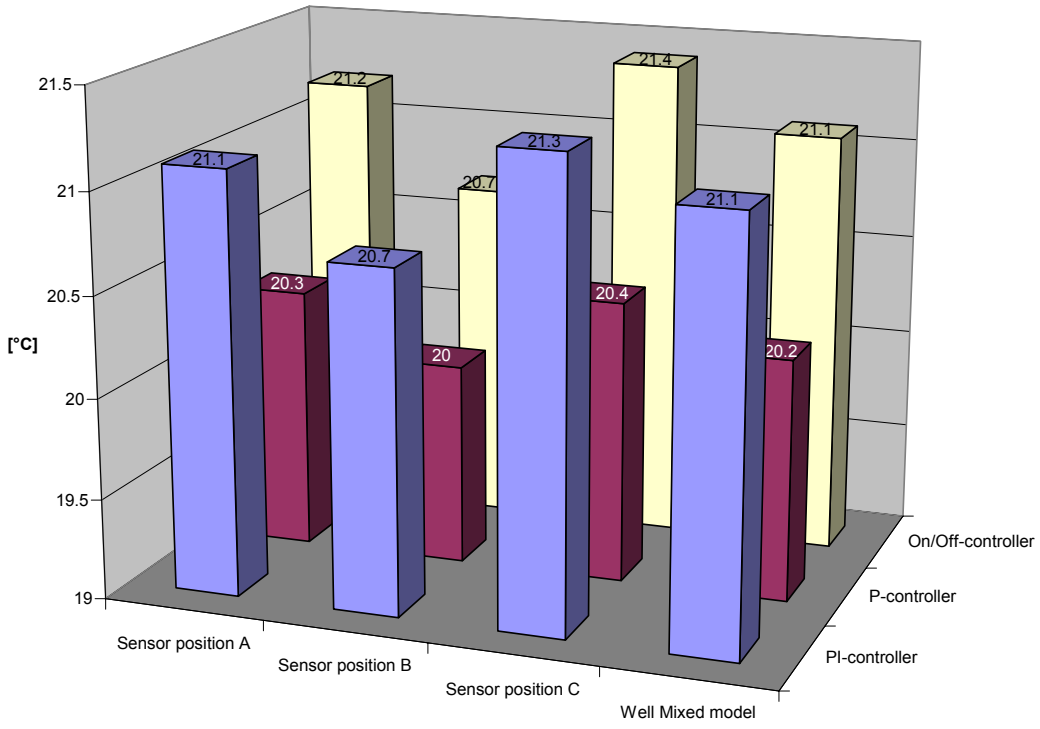

Figure V - 7: Mean resultant temperature - electric convector

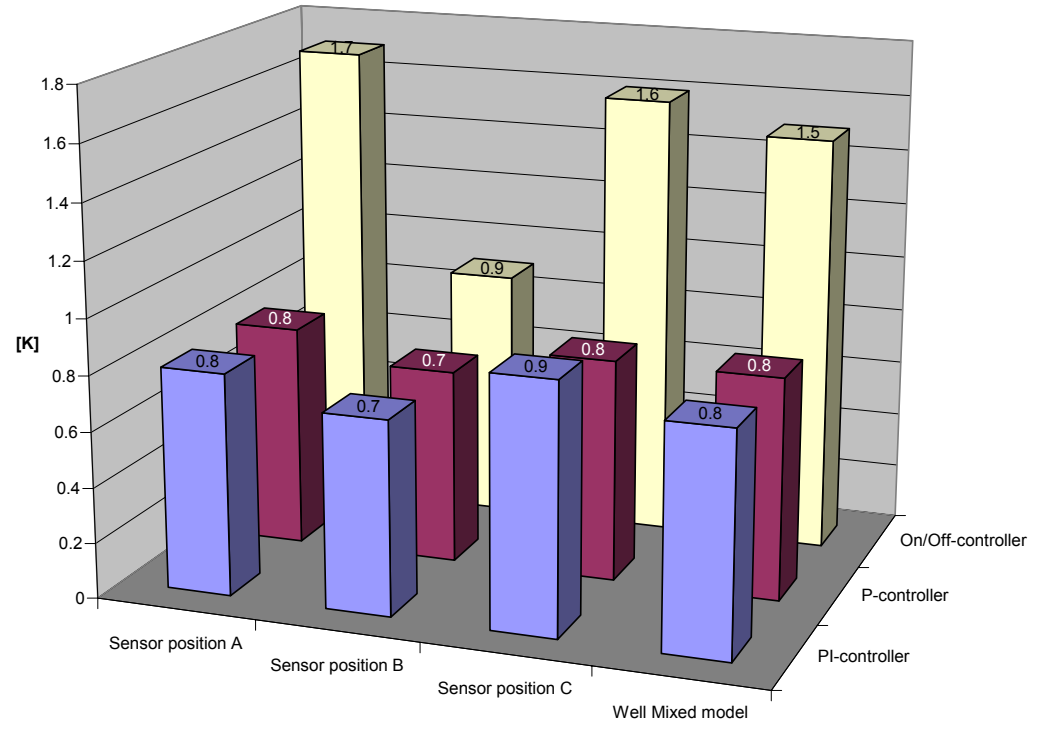

Figure V - 8: Maximum amplitude in resultant temperature - electric convector

2.2 FAN COIL UNIT

2.2.1 HEATING TESTS

The boundary conditions during the tests in heating mode are listed in Table 18.

Table 18 Conditions single room test

Conditions	Heating Mode
Set point temperature [°C]	21
Temperature adjacent rooms [°C]	20
External air temperature [°C]	-10
Short-wave radiation [W/m²]	0
Internal gains before the step change [W]	0
Internal gains after the step change [W]	500
Nominal power of the heat element [W]	1500

2.2.1.1 General behaviour of resultant temperature

Figure V - 9 shows the resultant temperature at the centre of the room for the well-mixed model and the zonal model with the three sensor positions for the different controller types.

Well-mixed model:

For all three controllers the results are very close to those of the benchmark. In all cases the temperature is within the band of results for different sensor positions and the amplitude is slightly smaller.

Zonal model with sensor at position B:

An offset is observed for all controllers due to the influence of the warm wall jet. This offset is increased for the On/Off controller, where the penetration of the warm wall jet varies significantly during the test. In this test, an amplification of the amplitude is observed. This is due to two effects: when the fan coil unit heater is switched off (while the fan is still switched on), the plume of the internal heat gains has an impact on the measurement of the controller sensor (high offset). When the heater in the fan coil unit is switched on, the high temperature differences between the wall jet and the room air diminish the downward penetration of the wall jet. The sensor is now placed at the end of the wall jet (lower offset).

Zonal model with sensor at position C:

An offset is observed due to the boundary layer of natural convection. The results are similar to those of the benchmark in means of amplitude.

General differences:

Low offset for cases of PI and P controller. For sensor position B, the offset is smaller than for the convector tests due to a smaller maximum jet penetration (higher buoyancy forces in the wall jet). The well-mixed model can be used for all three controllers. If the sensor is placed in the possible jet trajectory, the zonal model with sensor position B has to be used in order to represent wall the impact of the warm wall jet on the sensor measurement.

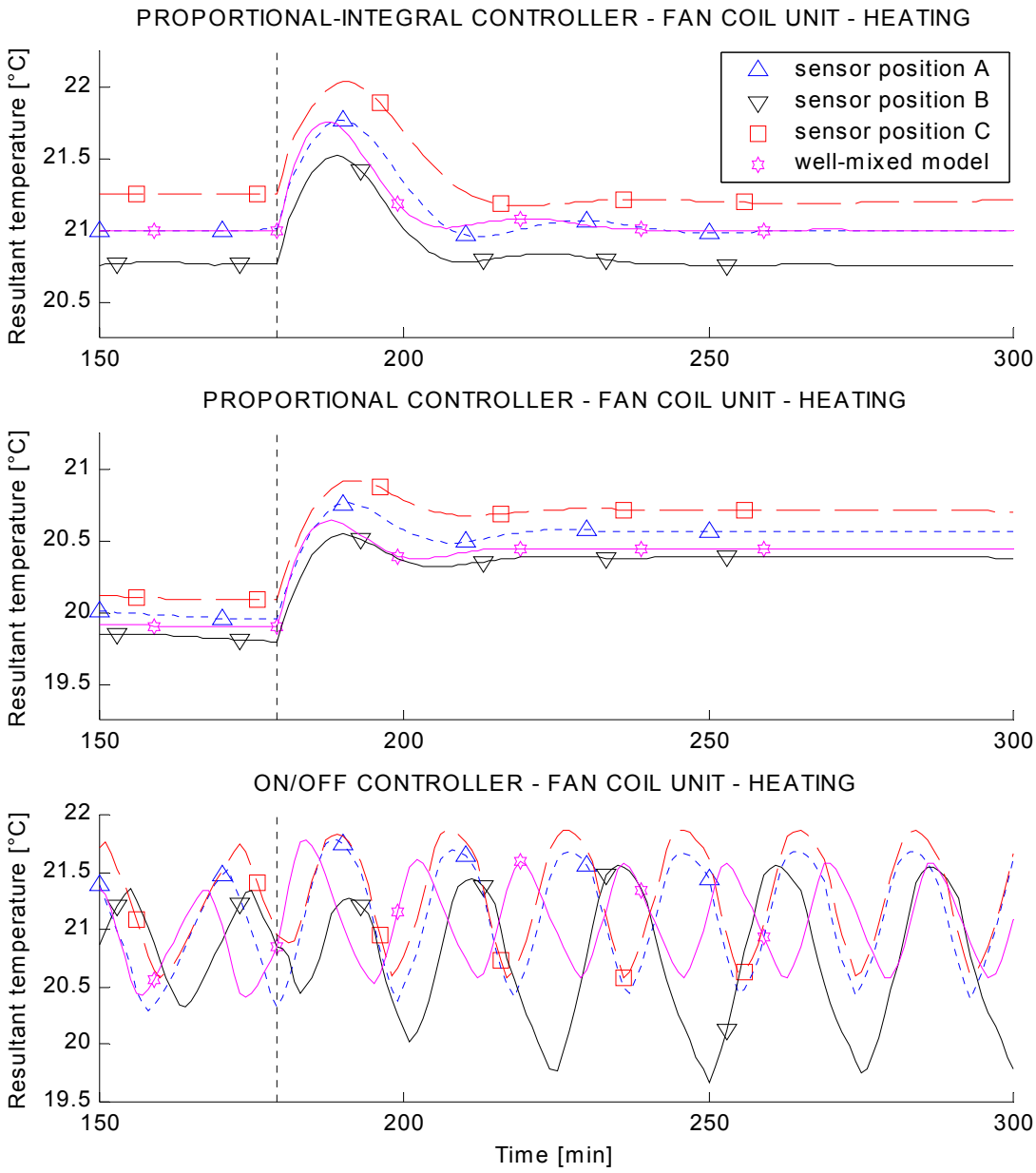

Figure V - 9: Resultant temperature - fan coil unit -heating

2.2.1.2 Possible impact on results of controller tests

Analysis for one controller and changing sensor position/model type

The well-mixed model is nearly identical to the benchmark, the zonal model with the sensor at position A in terms of the resultant temperature. For the zonal model with the sensor at position B and C, the influence of the warm plume (position B) and the cold wall (position C) creates an offset. These differences from set point are qualitatively the same for the three controller types.

The maximum amplitude using the well-mixed model is close to that for the benchmark. When the sensor is at position B, the amplitude is significantly larger due to the dynamic effect of the warm flow at the internal walls, which makes the control slightly unstable. All other differences are small.

Comparison of the three controllers for changing sensor position/model type

In terms of mean resultant temperature, except the offset characteristic for each model type/sensor position, the comparison between the three controllers shows similar results.

When the amplitude is studied, the results are only slightly different for the well-mixed model and the zonal model with the sensor at position C. When the sensor is placed at position B, the On/Off controller would have a worse classification result compared to the benchmark.

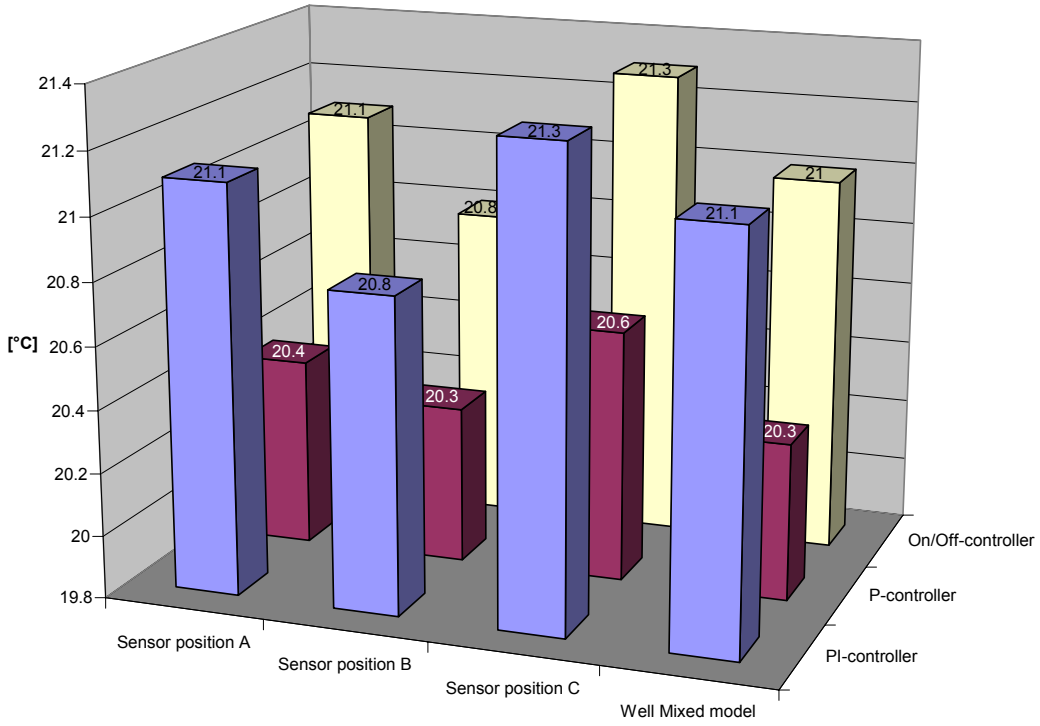

Figure V - 10: Mean resultant temperature - FCU heating

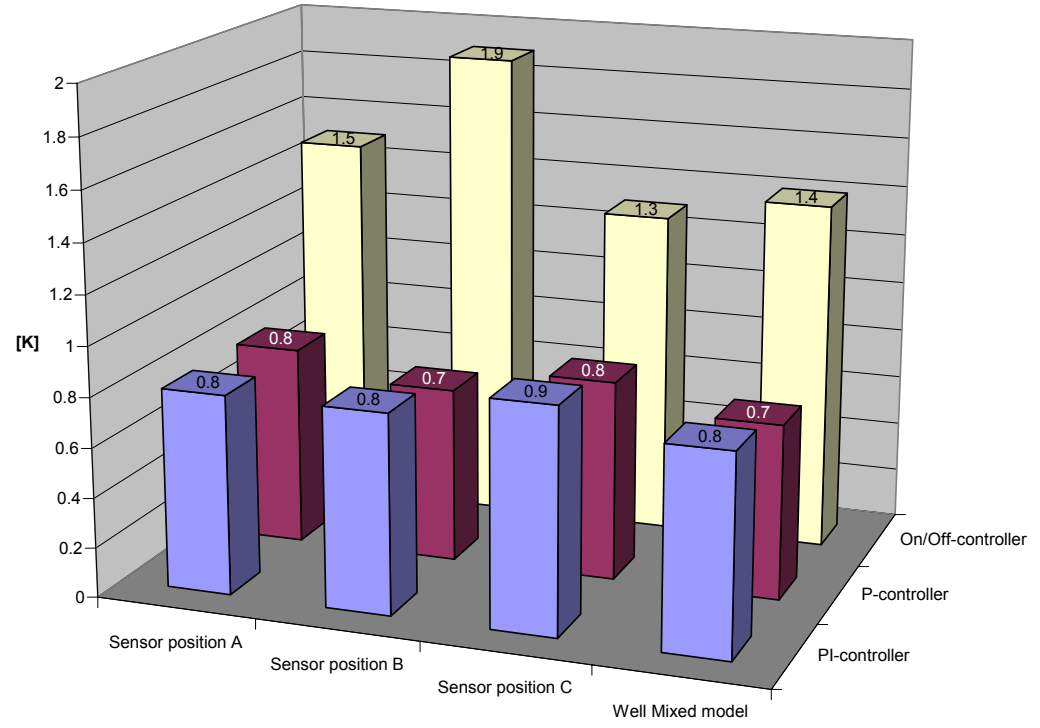

Figure V - 11: Maximum amplitude in resultant temperature - FCU heating

2.2.2 COOLING TESTS

The boundary conditions during the tests in cooling mode are listed in Table 19.

Table 19 Conditions single room test

Conditions	Cooling Mode
Set point temperature [°C]	24
Temperature adjacent rooms [°C]	25
External air temperature [°C]	35
Short-wave radiation [W/m²]	0
Internal gains before the step change [W]	0
Internal gains after the step change [W]	300
Inlet water temperature [°C]	8
Nominal water flow rate [kg/s]	0.075

2.2.2.1 General behaviour of resultant temperature

Figure V - 12 shows the resultant temperature at the centre of the room for the well-mixed model and the zonal model with the three sensor positions for the different controller types.

Well-mixed model:

Unlike the benchmark, the well-mixed model assumes perfect mixing of the air in the room. This results in a higher impact of the internal heat gains on the resultant temperature at the centre of the room. The maximum amplitude in the case of the PI and the P controller is thus higher. The load is higher in the case of the well-mixed model and the offset is thus higher for the case of the P controller. A bypass effect has been observed for the case of the fan coil unit. This effect is not represented in the well-mixed model. However, the mean temperature is close to that of the benchmark. In the case of the On/Off controller, amplitude, offset and the period are very different from the benchmark due to a difference in the load.

Zonal model with sensor at position B:

An offset is observed due to the boundary layer of natural convection at the internal walls. The results are close to the benchmark for PI and P controller. In the case of the On/Off controller longer periods appear, due to the higher load.

Zonal model with sensor at position C:

Identical to sensor position B.

General differences:

The offset for all cases can be neglected. The small differences might be explained by the small step of the internal gains. This low step has been necessary in order to keep control in all simulated cases.

For the selected gains, the differences in amplitude for PI and P controllers are acceptable. In the case of the On/Off controller differences are observed in means of temperature amplitude and period.

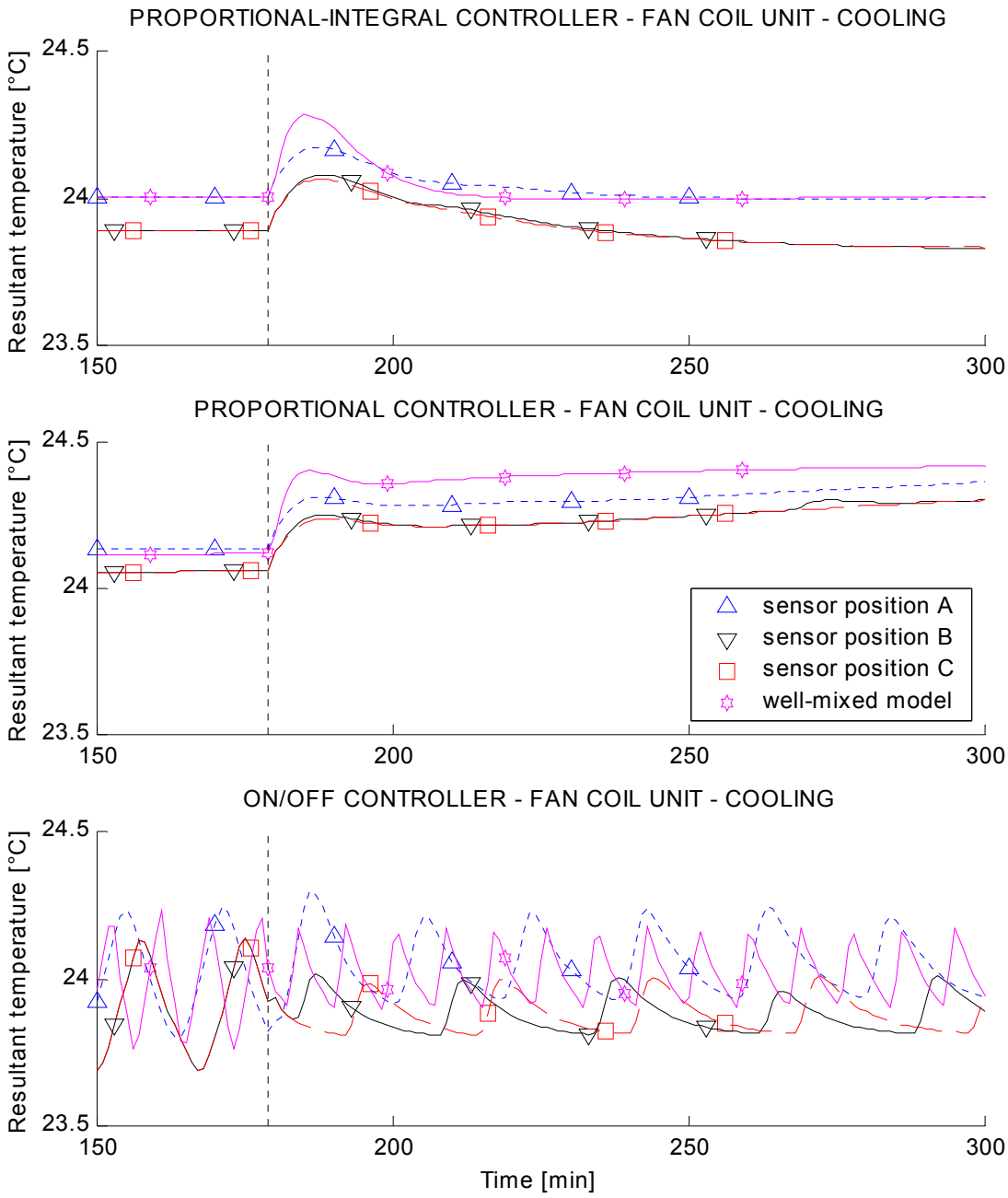

Figure V - 12: Resultant temperature - fan coil unit - cooling

2.2.2.2 Possible impact on results of controller tests

Analysis for one controller and changing sensor position/model type

The well-mixed model is nearly identical to the benchmark, the zonal model with the sensor at position A in terms of the resultant temperature. For the zonal model with the sensor at position B and C, the influence of the cold wall (position B and C) creates an offset. These differences from set point are qualitatively the same for the three controller types.

The maximum amplitude, small in this case, is close to that for the benchmark using all models and considering all sensor positions.

Comparison of the three controllers for changing sensor position/model type

In terms of mean resultant temperature, except the offset characteristic for each model type/sensor position, the comparison between the three controllers shows similar results.

When the amplitude is studied, very small differences are observed, which are also influenced by the rounding of the values. A classification would give the same results in all cases.

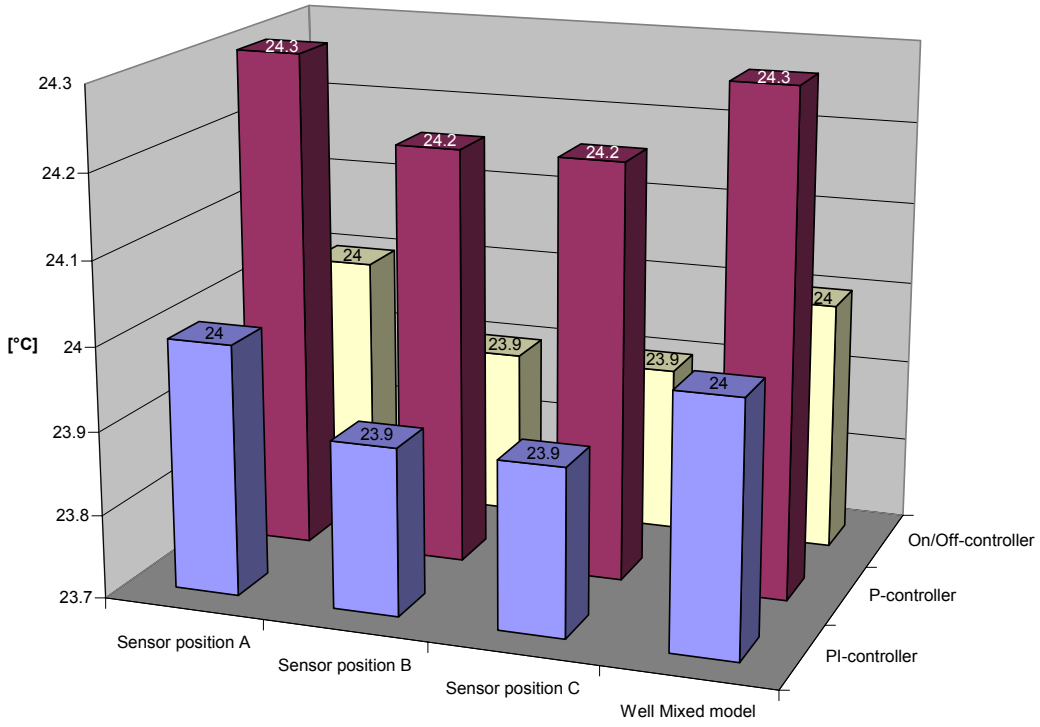

Figure V - 13: Mean resultant temperature - FCU cooling

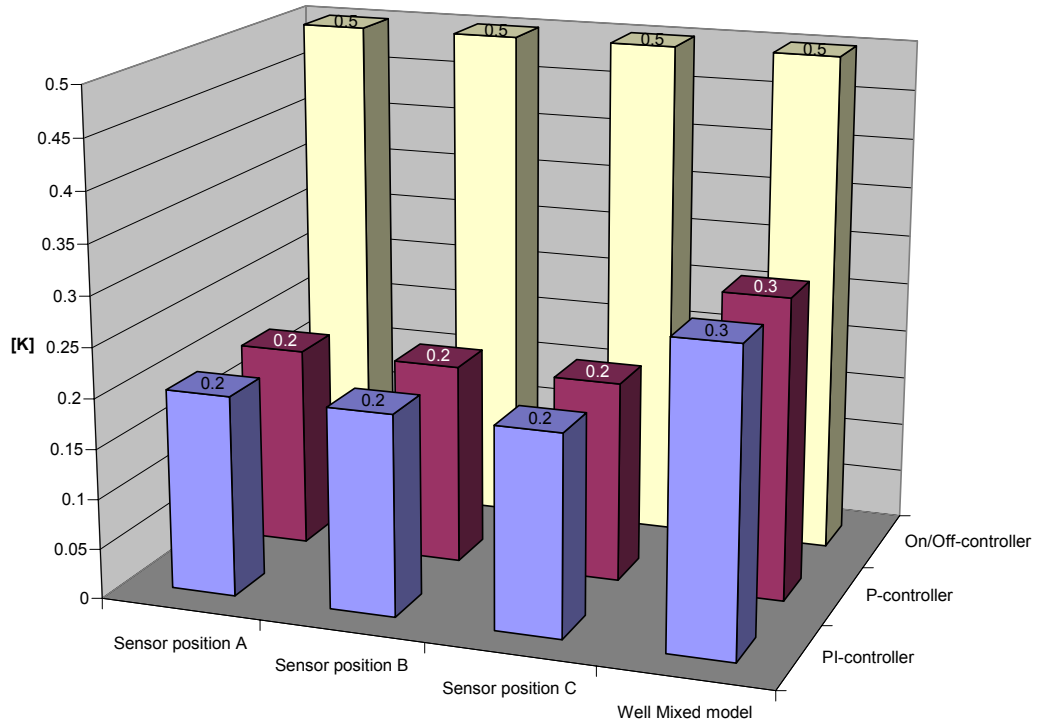

Figure V - 14: Maximum amplitude in resultant temperature - FCU cooling

2.2.2.3 Emitted power and water flow rate through the coil

For the sensor positions B and C, higher water flow rates are observed (Figure V - 15). This is explained by the effect of the warm wall on the sensor measurement.

With the zonal model, the cooling power, obtained by a heat balance on the air through the fan coil unit, is about 50% of that with the well-mixed model. This is due to a better representation of convective heat exchange at the internal room surfaces using the zonal model.

A bypass effect is also observed by the difference in the water flow rate through the coil in the case of the zonal model. Due to the low air temperature at the fan coil inlet the cooling power is only slightly increased for the higher flow rates in the case of position B and C compared to the benchmark (A).

These differences can affect the control in the central unit of the building. The differences in the water flow rate can affect the control of a variable speed pump for example. The differences in the cooling power on the other hand affect the control in the chiller. For these reasons the use of a zonal model seems to be necessary, especially for whole building tests.

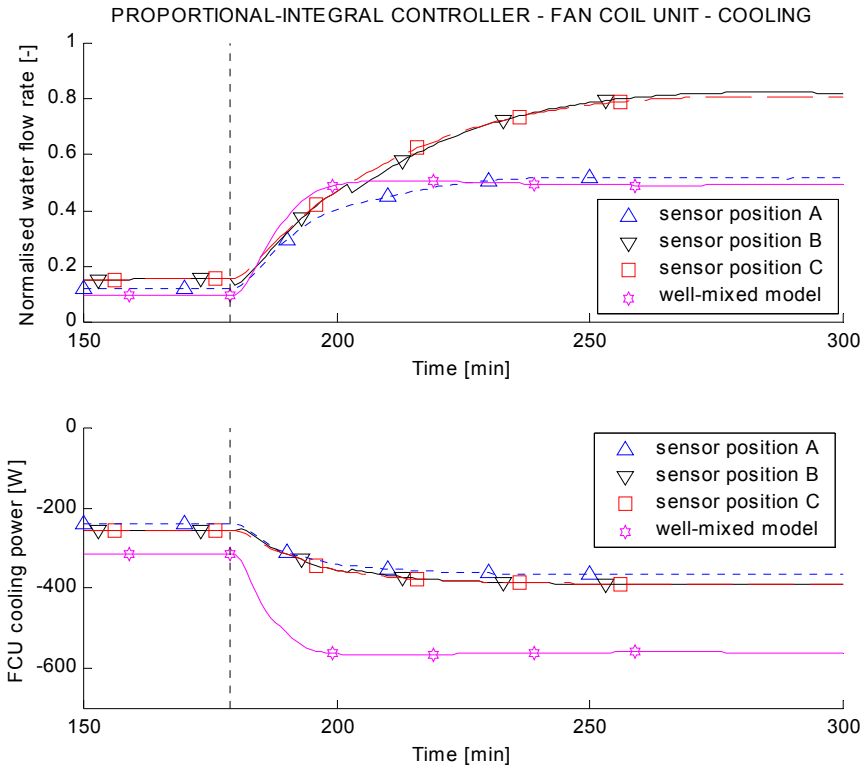

Figure V - 15: Normalised water flow rate through coil and FCU cooling power

2.3 VAV SYSTEM

2.3.1 COOLING TESTS

The boundary conditions during the test in cooling mode are listed in Table 20. The On/Off controller is not realistic since it appears rarely in practice, but however it is analysed here.

Table 20 Conditions single room test - VAV system - cooling

Conditions	Cooling Mode
Set point temperature [°C]	24
Temperature adjacent rooms [°C]	24
External air temperature [°C]	35
Short-wave radiation [W/m²]	0
Internal gains before the step change [W]	350
Internal gains after the step change [W]	850
Air supply temperature RHC [°C]	13
Maximal air flow rate [m^3/h]	280

2.3.1.1 Slot diffuser

2.3.1.1.1 General behaviour of resultant temperature

Figure V - 16 shows the resultant temperature at the centre of the room for the well-mixed model and the zonal model with the three sensor positions for the different controller types.

Well-mixed model:

There is good agreement with the benchmark for PI controller. In the case of the P controller there is significant offset and also higher amplitude. In the On/Off controller test the offset creates a difference in load and so higher amplitude and shorter periods.

Zonal model with sensor at position B:

The measurement of the controller sensor depends strongly on the cold jet from the slot diffuser. This results in an offset of the resultant temperature. The amplitude is similar to that of the benchmark for PI and P controller.

In the case of the On/Off controller, the high impact of the cold jet on the measurement of the controller's sensor changes significantly the test result. While the temperature response is similar to that in the tests with the sensor placed at other positions (the temperature response is in these cases approximately the same as in the open loop case), period and amplitude are reduced by factor 3-4 since the controller acts more on the temperature in the jet than that of the room.

Zonal model with sensor at position C:

There is a small temperature offset due to effect of warm walls. For all controllers the amplitude is close to that of the benchmark.

General differences:

The control with the sensor at position B depends strongly on jet characteristics (temperature, entrainment, etc.). These parameters define the offset to the set point. The use of the well-mixed model is not recommended since the different load leads to a different offset.

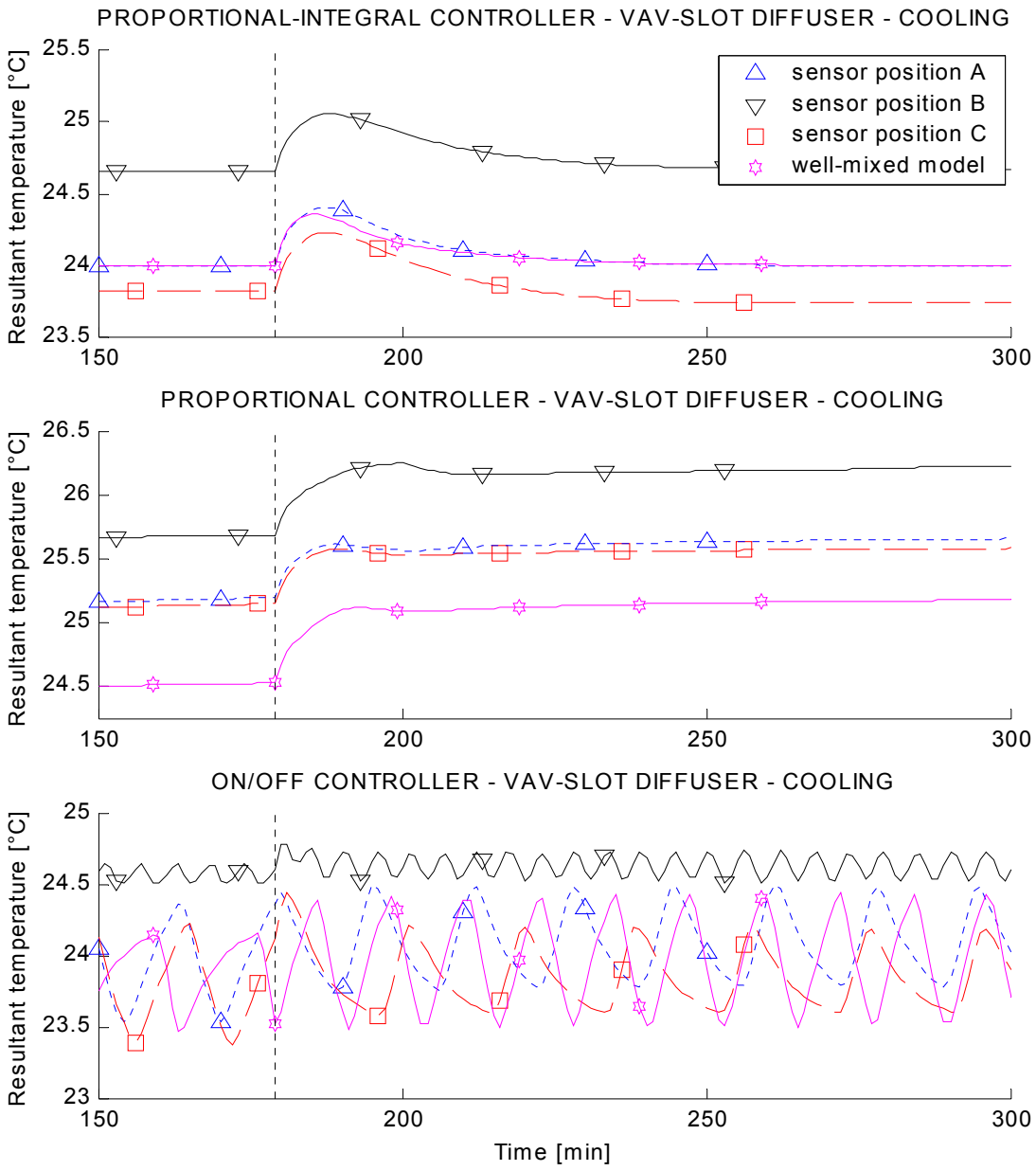

Figure V - 16: Resultant temperature - VAV system with slot diffuser - cooling

2.3.1.1.2 Possible impact on results of controller tests

Analysis for one controller and changing sensor position/model type

There is good agreement between the different models and sensor positions with offsets due to the cold jet (sensor position B) and the warm wall (sensor position C). The well-mixed model is nearly identical to the benchmark, the zonal model with the sensor at position A in terms of the resultant temperature.

The differences in maximum amplitude are relatively small except the case of sensor position B where the cold jet affects the sensor measurement and "anticipates" the control.

Comparison of the three controllers for changing sensor position/model type

In terms of mean resultant temperature, except the offset characteristic for each model type/sensor position, the comparison between the three controllers shows similar results.

The classification would give similar results in all cases in terms of amplitude, except that where the sensor is placed at position B. In this case, the On/Off controller would get better results than when the sensor is placed at the centre.

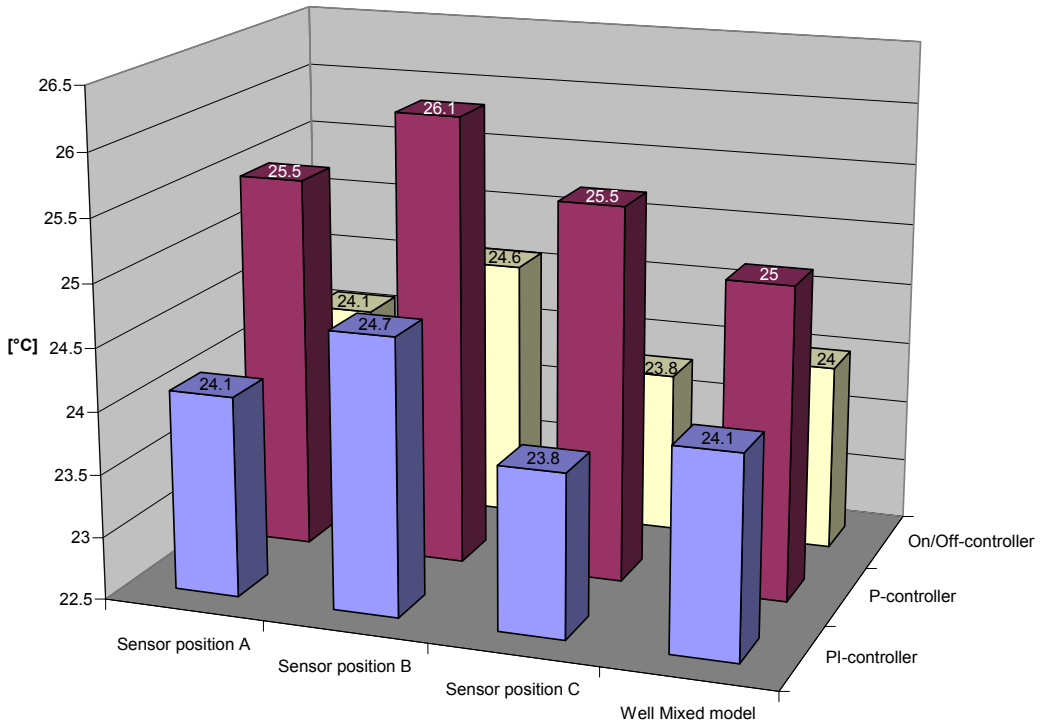

Figure V - 17: Mean resultant temperature - VAV slot diffuser cooling

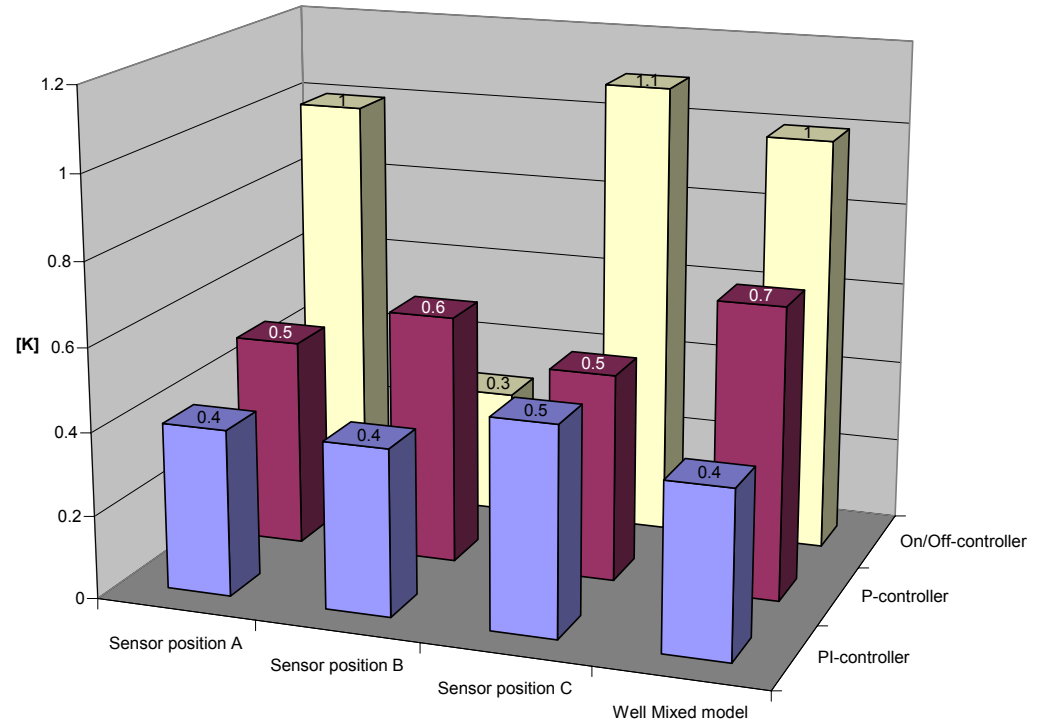

Figure V - 18: Maximum amplitude in resultant temperature - VAV slot diffuser cooling

2.3.1.1.3 Emitted power and water flow rate through the coil

Flow rate and cooling power are close to the benchmark when the sensor is placed at position C (Figure V - 19). For the sensor position B a lower air flow rate is observed due to the influence of the cold jet on the sensor measurement.

The well-mixed model underestimates the air flow rate as well as the cooling power of the VAV system due to differences in the convective heat exchange at the internal room surfaces.

The differences obtained can affect the control in the central air-handling unit. The demand of air flow at supply or extraction fan in a building simulation would not be represented correctly.

The use of a zonal model seems to be necessary from the point of view of the representation of the air supply to the rooms, especially for whole building tests.

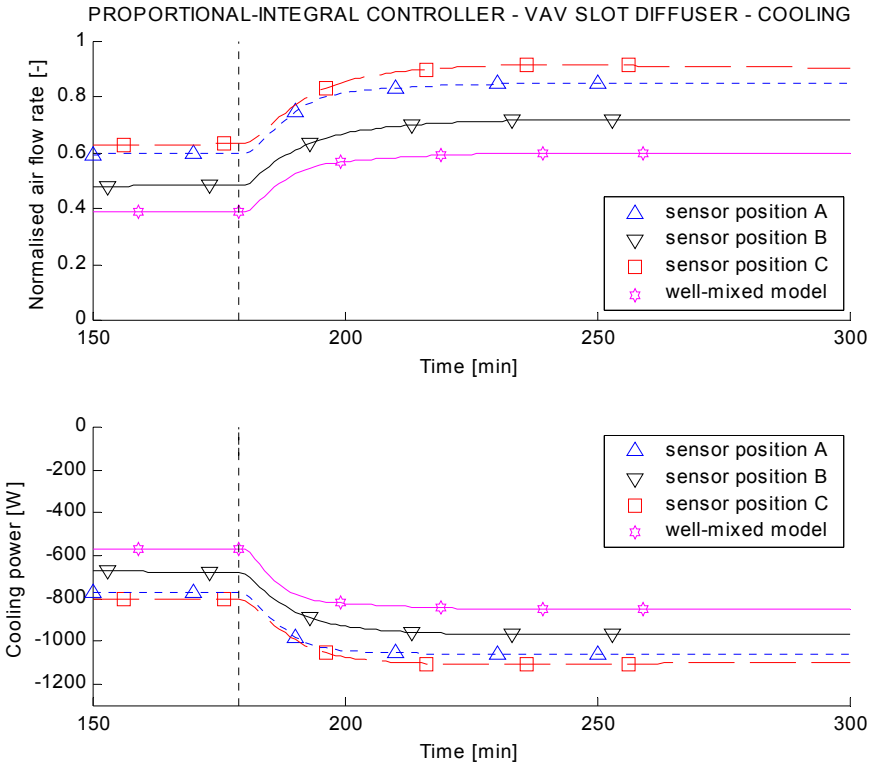

Figure V - 19: Normalised air flow rate through coil and VAV cooling power

2.3.1.2 Radial ceiling diffuser

2.3.1.2.1 General behaviour of resultant temperature

Figure V - 20 shows the resultant temperature at the centre of the room for the well-mixed model and the zonal model with the three sensor positions for the different controller types.

This case is similar to that of the slot diffuser. Lower temperature non-homogeneity due to better mixing between jet and room air creates closer results between the different models and sensor positions to the benchmark in all tests.

Well-mixed model:

There is good agreement with the benchmark tests. In the test with the P controller there is little disagreement (offset) due to difference in load.

Sensor position B:

A lower offset is observed since the jet from a radial diffuser is characterised by higher air entrainment and thus lower temperature differences. For the On/Off controller tests the cold jet leads to smaller amplitude (anticipation).

Sensor position C:

Slight offset due to effect of the warm internal walls. There is good agreement concerning temperature amplitude for all controllers.

General differences:

The offset can be neglected in all cases. The well-mixed model can be used without significant error. The use of the zonal room model is only proposed in the case that the sensor is placed in the trajectory of the cold jet.

Differences in air flow rate and cooling power:

The use of a zonal model might not be necessary due to a good mixing of the air in the room. The air flow rates and cooling power have been found close to the benchmark for the well-mixed model as well as for the different sensor positions.

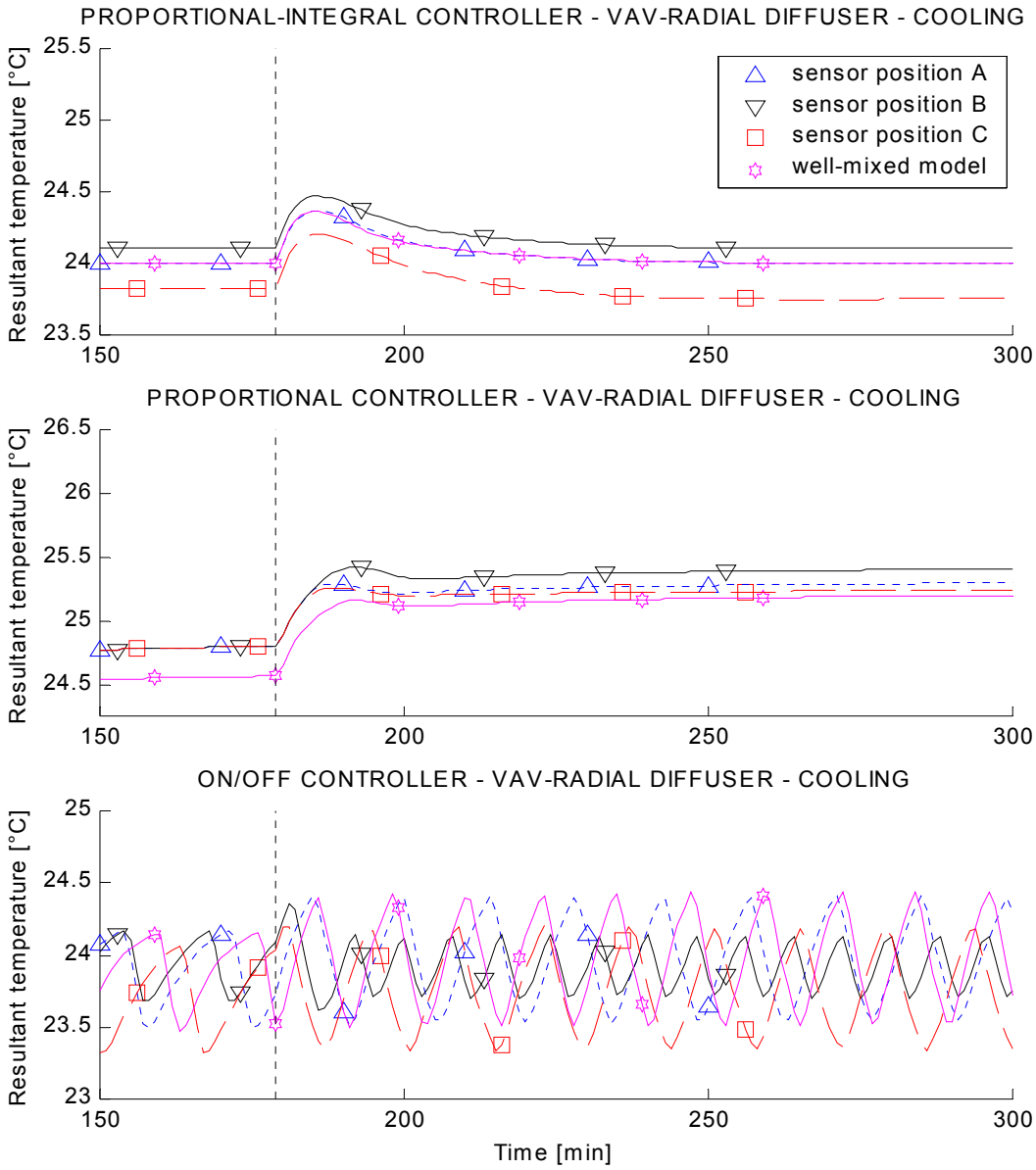

Figure V - 20: Resultant temperature - VAV system with radial diffuser - cooling

2.3.1.2.2 Possible impact on results of controller tests

Analysis for one controller and changing sensor position/model type

There is good agreement between the different models and sensor positions with small offsets due to the cold jet (sensor position B) and the warm wall (sensor position C). The well-mixed model is nearly identical to the benchmark, the zonal model with the sensor at position A in terms of the resultant temperature.

The differences in maximum amplitude are relatively small.

Comparison of the three controllers for changing sensor position/model type

In terms of mean resultant temperature, except the offset characteristic for each model type/sensor position, the comparison between the three controllers shows similar results.

The classification would give similar results in all cases in terms of amplitude.

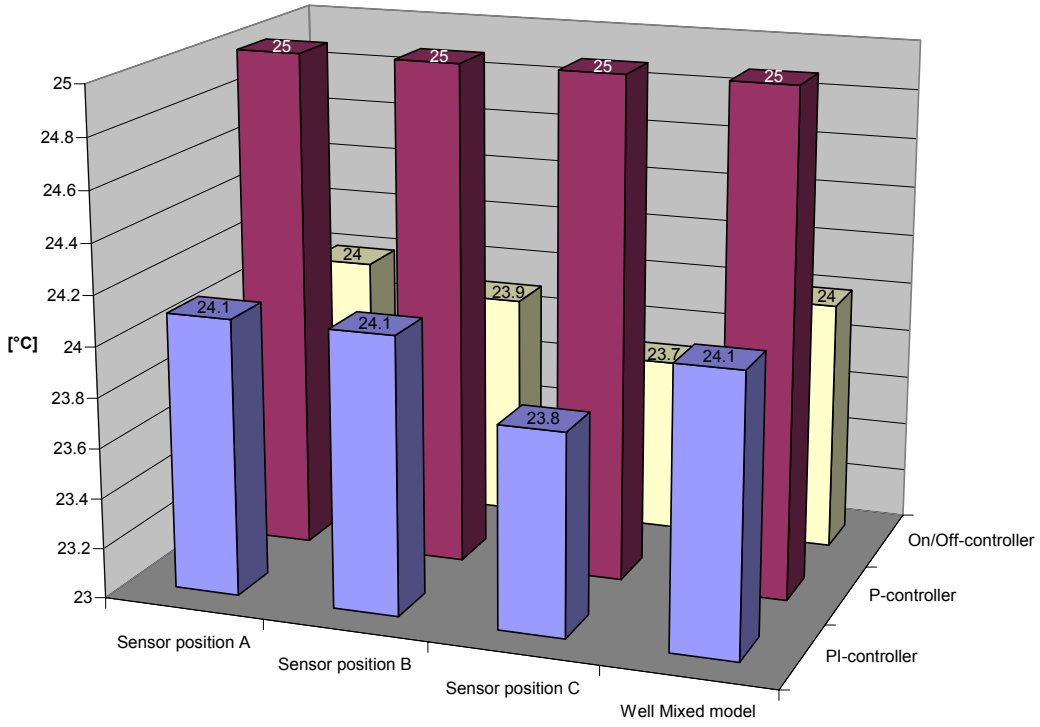

Figure V - 21: Mean resultant temperature - VAV radial diffuser cooling

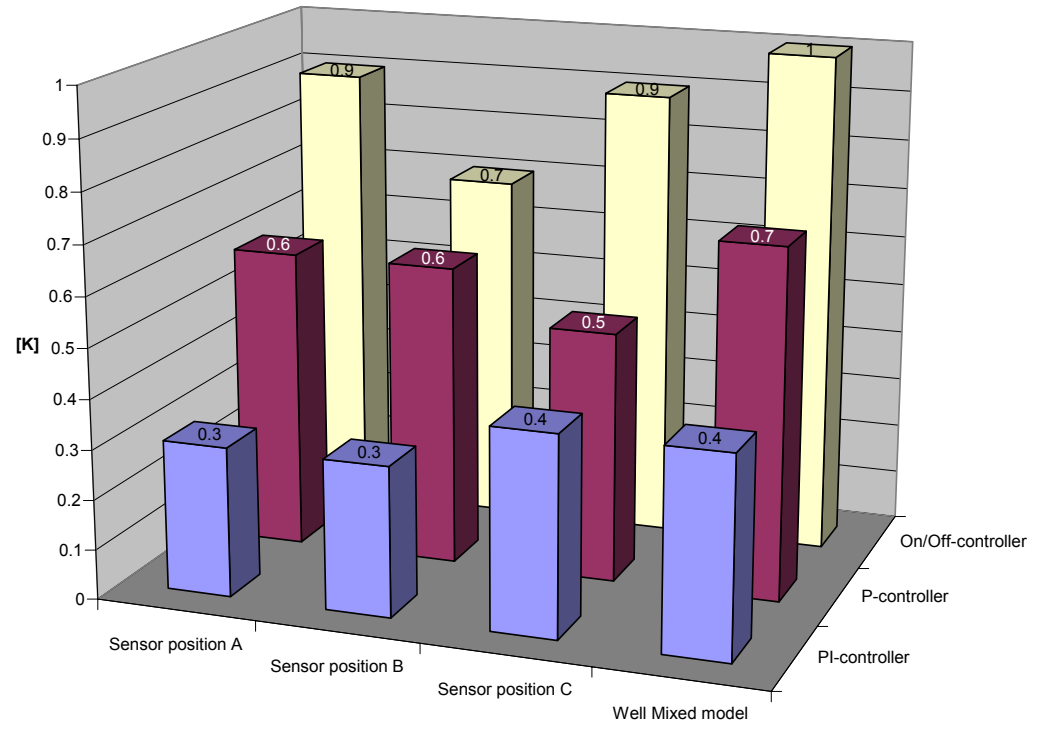

Figure V - 22: Maximum amplitude in resultant temperature - VAV radial diffuser cooling

2.3.2 HEATING TESTS

The boundary conditions during the test in heating mode are listed in Table 21.

Table 21 Conditions single room test

Conditions	Heating Mode
Set point temperature [°C]	21
Temperature adjacent rooms [°C]	21
External air temperature [°C]	-5
Short-wave radiation [W/m²]	0
Internal gains before the step change [W]	600
Internal gains after the step change [W]	50
Air supply temperature RHC [°C]	18
Air flow rate (30% of max. flow) [m^3/h]	85

2.3.2.1 Slot diffuser

2.3.2.1.1 General behaviour of resultant temperature

Figure V - 23 shows the resultant temperature at the centre of the room for the well-mixed model and the zonal model with the three sensor positions for the different controller types.

Well-mixed model:

Bypass effects of the warm air at the ceiling create a significant difference in the load, compared to the benchmark test. This is especially observed for the P controller (lower offset) and the On/Off controller (higher amplitudes and shorter periods).

Sensor position B:

Due to high temperature differences between the warm jet at the ceiling and the room air the warm wall jet does not affect the controller's sensor. The sensor is thus always placed in a boundary layer and identical to the sensor position C.

There is very little offset due to effect of cold walls. The amplitude is nearly identical with the benchmark for the three controller types.

Sensor position C:

Identical to sensor position B.

General differences:

Offset and amplitude for different sensor positions can be neglected.

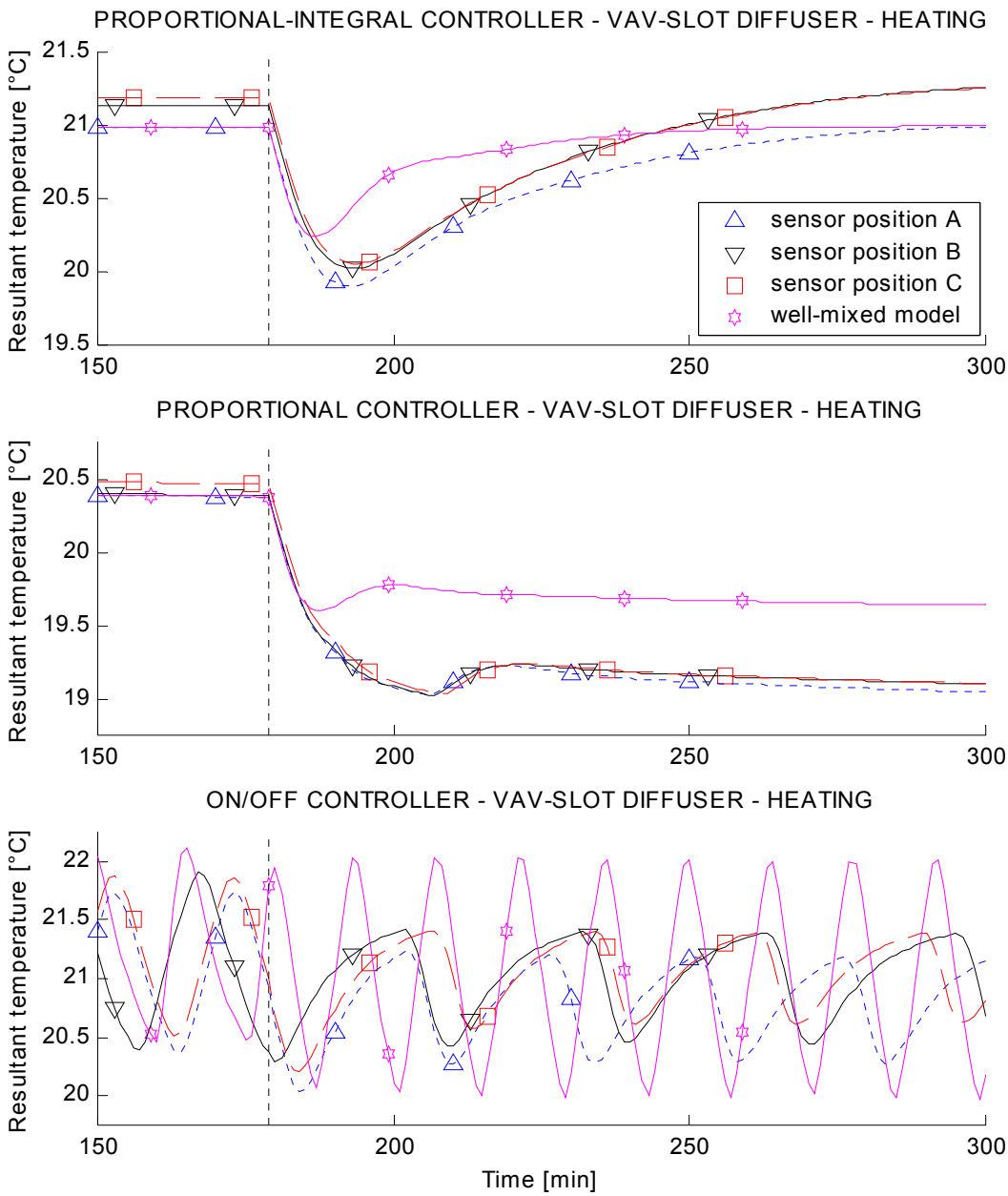

Figure V - 23: Resultant temperature - VAV system with slot diffuser - heating

2.3.2.1.2 Possible impact on results of controller tests

Analysis for one controller and changing sensor position/model type

There is good agreement between the different models and sensor positions with small offsets due to the warm wall (sensor position B and C). The well-mixed model shows some differences in terms of the resultant temperature.

The differences in maximum amplitude are relatively small for all cases of the zonal model, but significant in the case of the well-mixed model.

Comparison of the three controllers for changing sensor position/model type

When the zonal model is used and neglecting the offset due to sensor position, the comparison of the three controllers shows similar results in terms of mean resultant temperature. The well-mixed model provides significantly different results in terms of mean temperature and amplitude.

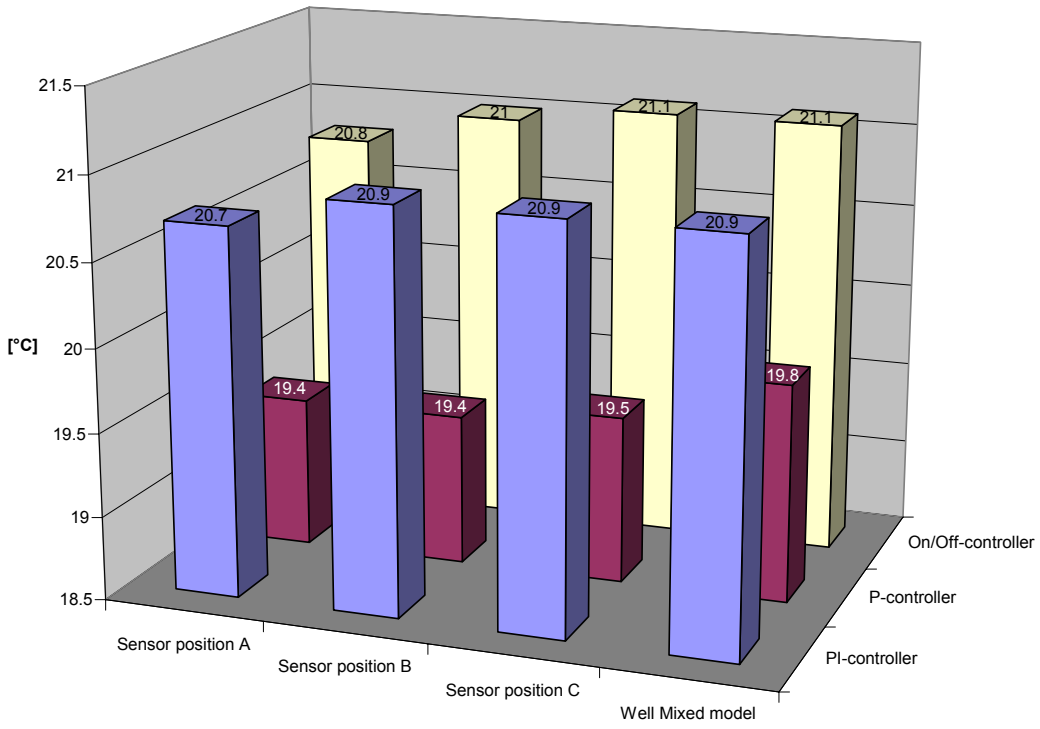

Figure V - 24: Mean resultant temperature - VAV slot diffuser heating

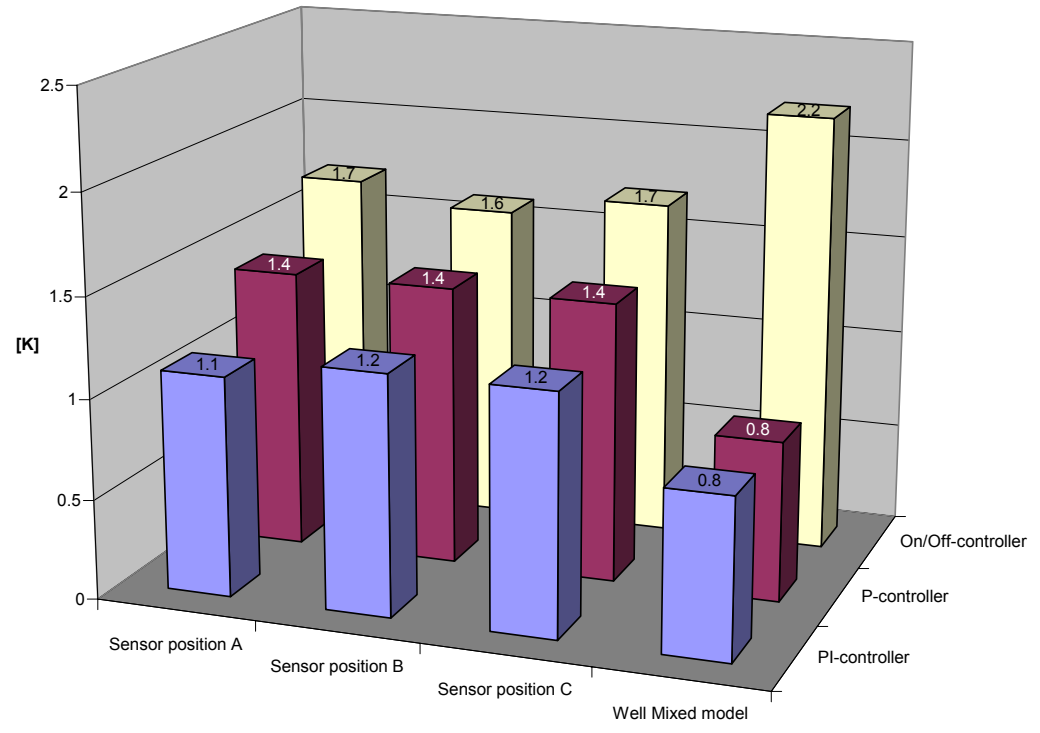

Figure V - 25: Maximum amplitude in resultant temperature - VAV slot diffuser heating

2.3.2.1.3 Emitted power and water flow rate through the reheating coil

When the sensor is placed at position B or C, very little differences in the water flow rate through the re-heating coil are observed (Figure V - 26). The heating power is also very close to that obtained benchmark, where the sensor is placed at the centre of the room.

Sensor position is thus unimportant for this case.

The use of a well-mixed model is not recommended here. The falsified convective heat exchange at the internal room surfaces (mainly due to stratification effects) makes the well-mixed model predict very different water flow rates and heating power.

The use of a zonal model is absolutely recommended in this case.

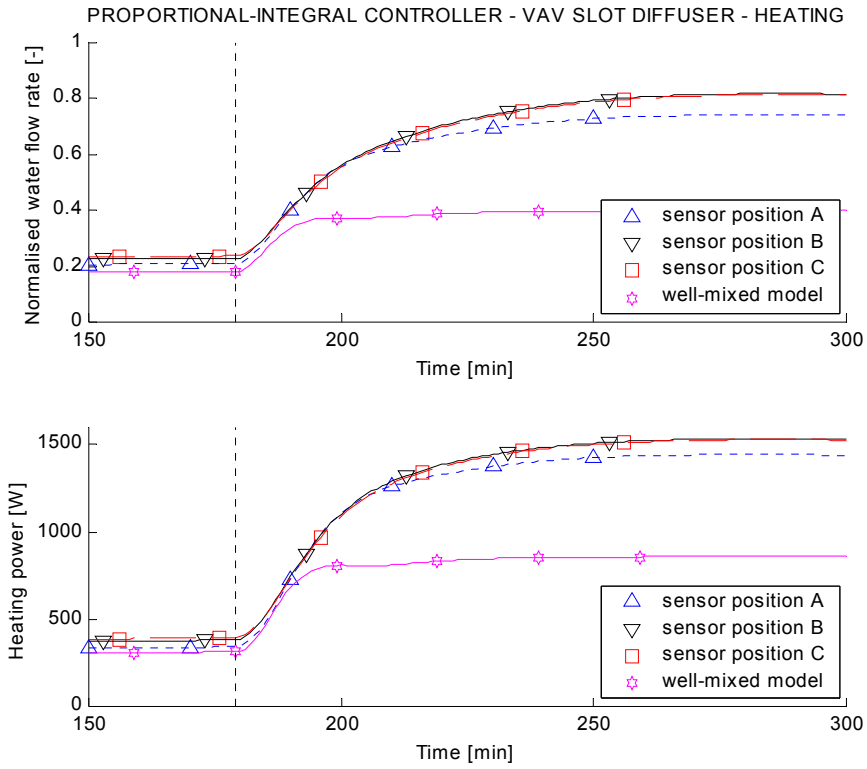

Figure V - 26: Normalised water flow rate through coil and heating power

2.3.2.2 Radial ceiling diffuser

2.3.2.2.1 General behaviour of resultant temperature

Figure V - 27 shows the resultant temperature at the centre of the room for the well-mixed model and the zonal model with the three sensor positions for the different controller types.

Well-mixed model:

Compared to the corresponding case with the slot diffuser, the well-mixed model predicts better the phenomena in the zone. The better mixing in the room creates more homogeneous conditions in the room diminishing the bypass effect in the room. The results are thus similar to those of the benchmark. Only in the case of the P controller the slight difference in load creates a small offset. The amplitude is only slightly larger than the benchmark case.

Sensor position B:

An offset is observed caused by the jet impact at sensor position. This impact is similar for the three controller types. The amplitude in the case of the On/Off controller is underestimated due to the direct effect of the warm wall jet.

Sensor position C:

A slight offset compared to the benchmark is observed caused by the temperature difference at the internal walls. The amplitude is similar to that of the benchmark.

General differences:

There is an offset when the sensor is placed in the jet trajectory (B). When the sensor is placed at this position the use of the zonal room model is necessary.

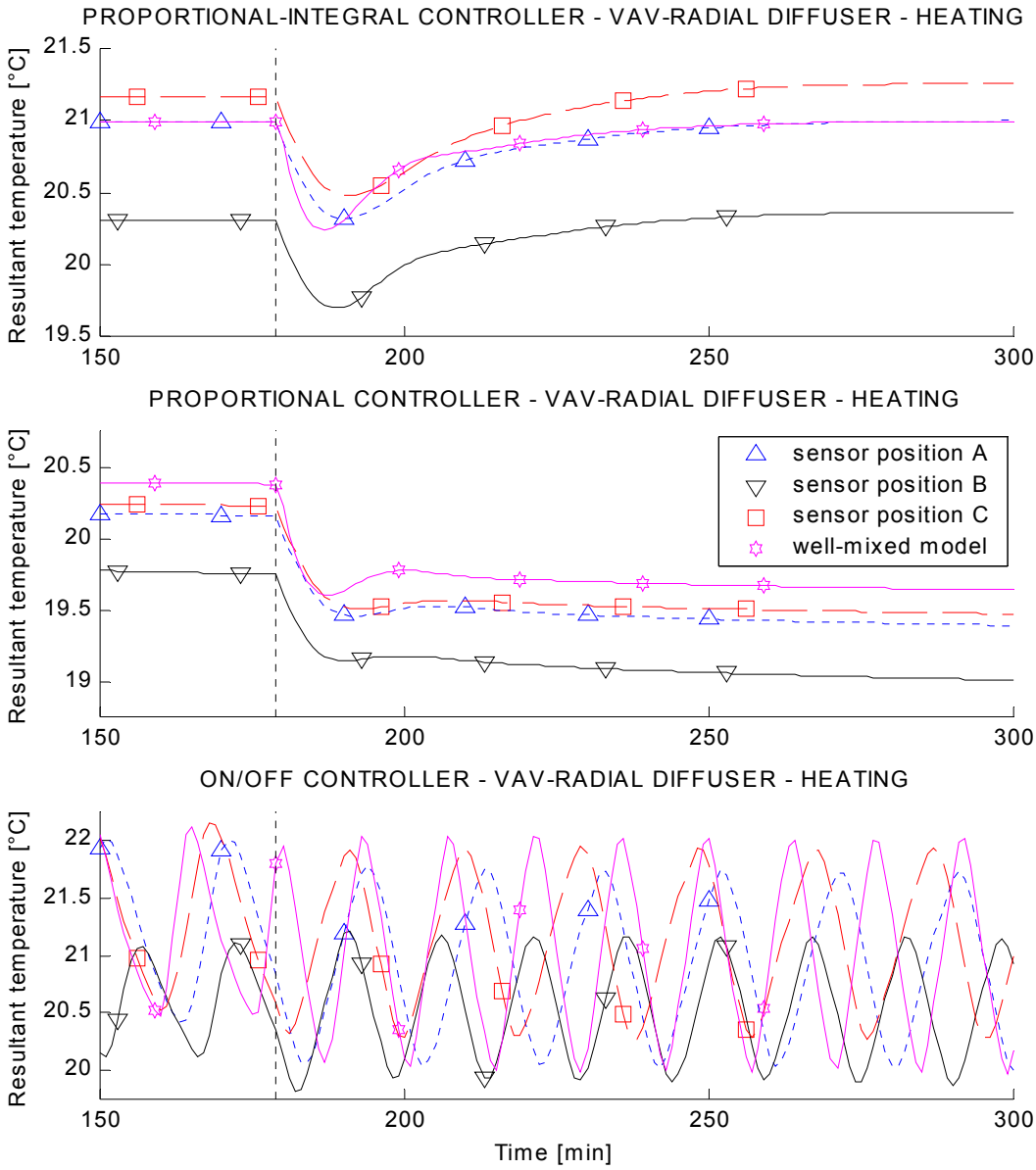

Figure V - 27: Resultant temperature - VAV system with radial diffuser - heating

2.3.2.2.2 Possible impact on results of controller tests

Analysis for one controller and changing sensor position/model type

There is good agreement between the different models and sensor positions with small offsets due to the warm jet and the warm wall (sensor position B and C).

The differences in maximum amplitude are relatively small in all cases except that where the sensor is placed at position B. The jet influence reduces the maximum amplitude.

Comparison of the three controllers for changing sensor position/model type

In terms of mean resultant temperature, except the offset characteristic for each sensor position, the comparison between the three controllers shows similar results. The well-mixed model would provide significantly different classification.

In terms of the maximum amplitude sensor position B would result in a better classification for the On/Off controller. The other results are similar.

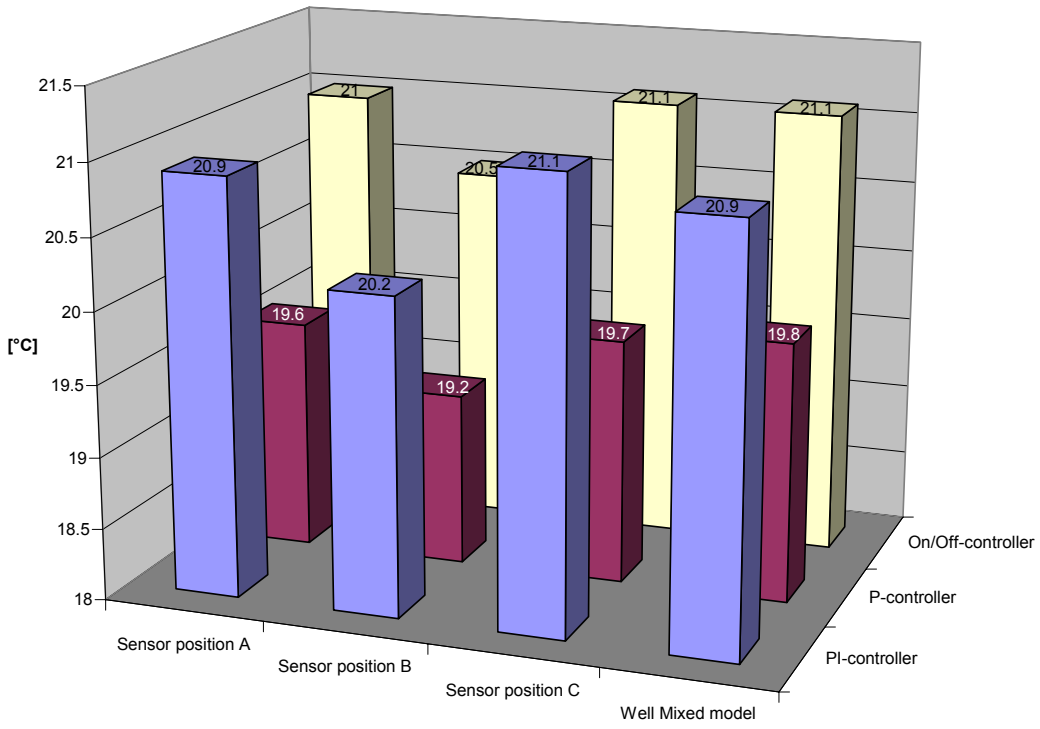

Figure V - 28: Mean resultant temperature - VAV radial diffuser heating

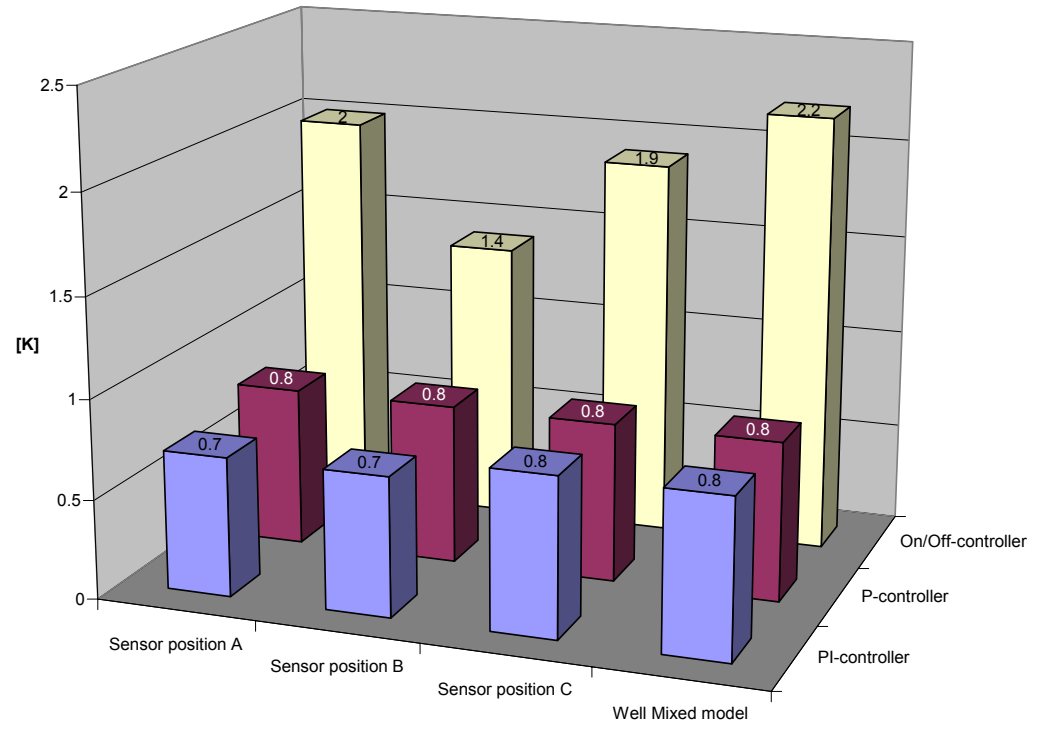

Figure V - 29: Maximum amplitude in resultant temperature - VAV radial diffuser heating

2.3.2.2.3 Emitted power and water flow rate through the reheating coil

For the sensor placed at position C, similar results are obtained compared to the benchmark (Figure V - 30).

The well-mixed model predicts the water flow rate and heating power slightly better than in the corresponding case with the slot diffuser. However, the difference is still significant and the use of the zonal model is recommended.

When the sensor is placed at position B, the warm wall jet affects the measurement of the controller sensor. As seen in Figure V - 27, the resultant temperature is controlled to a lower value. This leads to smaller water flow rates and lower heating power. The results are similar to those when using the well-mixed model.

The use of the zonal model is recommended when whole building control with variable fan speeds is to be studied.

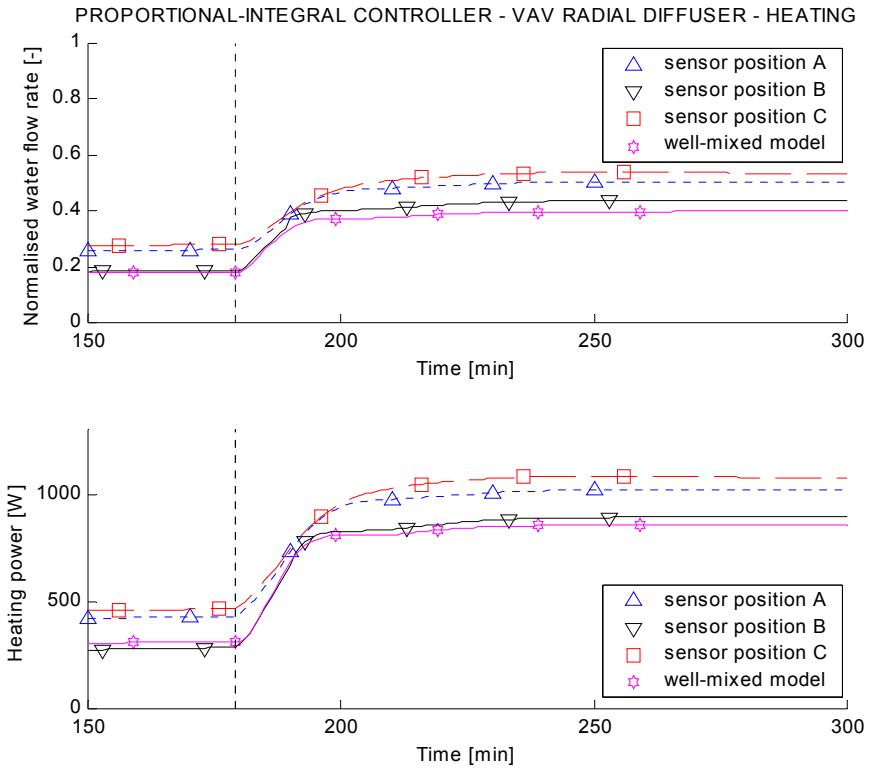

Figure V - 30: Normalised water flow rate through coil and heating power

3. VAV WHOLE BUILDING PERFORMANCE TESTS

In this analysis the building is equipped with a VAV system including primary plant (boiler, chiller, etc), a single air-handling unit (including supply and extract fans as well as a mixing box) and pressure-independent terminal boxes with reheat coils in each room. The building also has an innovative lighting and shading control system. The model of the VAV system and its central plant was developed for testing the performance of integrated building control strategies [Husaunndee01].

The behaviour of all of the rooms in the same zone will be very similar and, to simplify the simulation, only one room in each zone of the building is simulated. The design heat gains and air flow rates associated with each zone are therefore divided by the number of rooms in that zone. Six rooms are therefore simulated, each representing a typical room in each of the six zones of the building. Real weather data are used to simulate summer and winter conditions. The internal gains follow a predefined profile during an occupancy period that extends from 8 am to 6 pm. This profile assumes a constant heat gain during the whole occupancy period.

The VAV system is simulated with both slot and radial diffusers.

3.1 IMPACT OF ROOM MODEL AND SENSOR POSITION ON THE PERFORMANCE ASSESSMENT

The control performance tests are carried out for one typical day in summer and one typical day in winter. Representative results in the figures are presented for zone 3, a zone with southerly orientation. All other values of resultant temperature and energy consumption in the tables are presented as average over the whole building. As for the single zone tests, a comparison of mean and maximum values for the results is listed in the appendix.

3.1.1 SUMMER CASE

During the summer test period, the greatest differences are observed when the slot diffuser is used (Figure V - 31). When the sensor is at position B, the cold jet has a significant influence on the measured temperature and the behaviour of the simulated zone. The results are similar for all other sensor positions. Note that the airflow predicted by the well-mixed model is higher due to differences in the calculated heat flows at the internal surfaces and the calculated ventilation heat losses.

The values of the resultant temperature, which were obtained during the summer test period, are given in Table 22 and Table 23.

As for the single room tests the mean resultant temperature ϑ_{res} and the maximum peak-to-peak value of resultant temperatures $\Delta\vartheta_{res}$ are tabulated for both types of diffuser. The means and maxima are taken over the occupancy period and over all six zones.

The single room tests showed a high difference to the benchmark, sensor position A, when the sensor is placed at position B and when the slot diffuser is used. This difference is observed also in the building test. The maximum amplitude of the resultant temperature in this case is about 70% different to that of the benchmark.

The performance predicted by the well-mixed model is similar to that predicted by the zonal model, when the control sensor is placed at position A or C. The well mixed model can thus be used without introducing significant errors in these cases.

When the sensor is at position B, the use of a zonal model is recommended due to the steady state error caused by the impact of the cold wall jet.

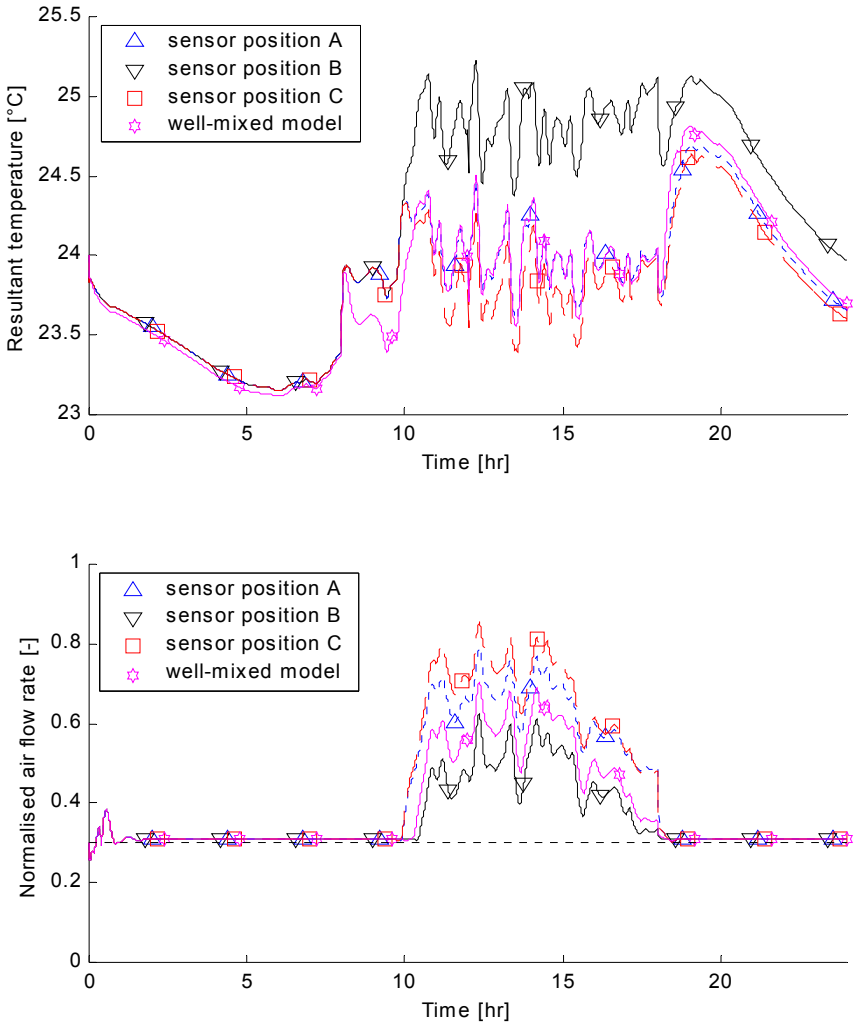

Figure V - 31: Building test -cooling - slot diffuser - resultant temperature and air flow rate in zone 3

	Mean ϑ_{res} [°C]	Max $\Delta\vartheta_{res}$ [K]
Sensor position **A**	24.0	1.0
Sensor position **B**	24.6	1.7
Sensor position **C**	23.8	0.8
Well **M**ixed model	23.9	1.1
Max. difference	0.6	0.7
Difference [%]		71
Worst case	B	B

Table 22: Assessment of control performance for VAV slot diffuser - cooling - building test

The round diffuser permits much better mixing of the jet with the room air. The conditions in the room are more homogeneous. When performance is assessed the differences between the two

models and the different sensor positions get smaller. Table 23 shows the result of a performance assessment in this case.

	Mean ϑ_{res} [^{o}C]	Max $\Delta\vartheta_{res}$ [K]
Sensor position **A**	23.9	1.0
Sensor position **B**	24.0	1.2
Sensor position **C**	23.8	0.8
Well **M**ixed model	23.9	1.1
Max. difference	-0.2	-0.2
Difference [%]		-20
Worst case	C	C

Table 23: Assessment of control performance for VAV radial diffuser - cooling - building test

The highest differences are obtained when the sensor is placed at position C, but they are very small.

3.1.2 WINTER CASE

As can be seen in Figure V - 32, two major effects are observed when the tests are performed in winter. Firstly, the resultant temperature predicted by the well-mixed model rises much more quickly, at the start of the preheating of the production, than that predicted by the zonal model (for all positions of the control sensor). The zonal model is able to predict correctly the significant temperature stratification that occurs in the room when the terminal box is in heating mode. The control sensor is located in the intermediate main zone 2 and there is therefore a smaller initial temperature rise following the step change in the zone temperature set point to 21^{o}C at the start of occupancy. Stratification is also the reason why the reheating coil valve begins to close nearly two hours later than is predicted by the well-mixed model. The zonal model therefore predicts the room temperature will overshoot the set point for several hours more than is predicted by the well-mixed model. Sudden increases in the internal gains and the solar radiation are responsible for the second rapid change in the resultant temperature predicted by the zonal model at the start of the occupancy period.

The second effect is the lower value of the resultant temperature predicted by the zonal model after 13.00, when the sensor is at position B. The most likely explanation is that the warm, negatively buoyant wall jet only begins to increase the temperature measured by the control sensor after midday, and only then does the resultant temperature at the centre of the room drop below the values obtained for other sensor positions.

The values of the performance, which were obtained during the winter test period, are given in Table 24 and Table 25.

There are some differences in the assessment of the control performance when the well-mixed model is used or the control sensor is in position B. However the differences are again relatively small, particularly those associated with the sensor being located at position B.

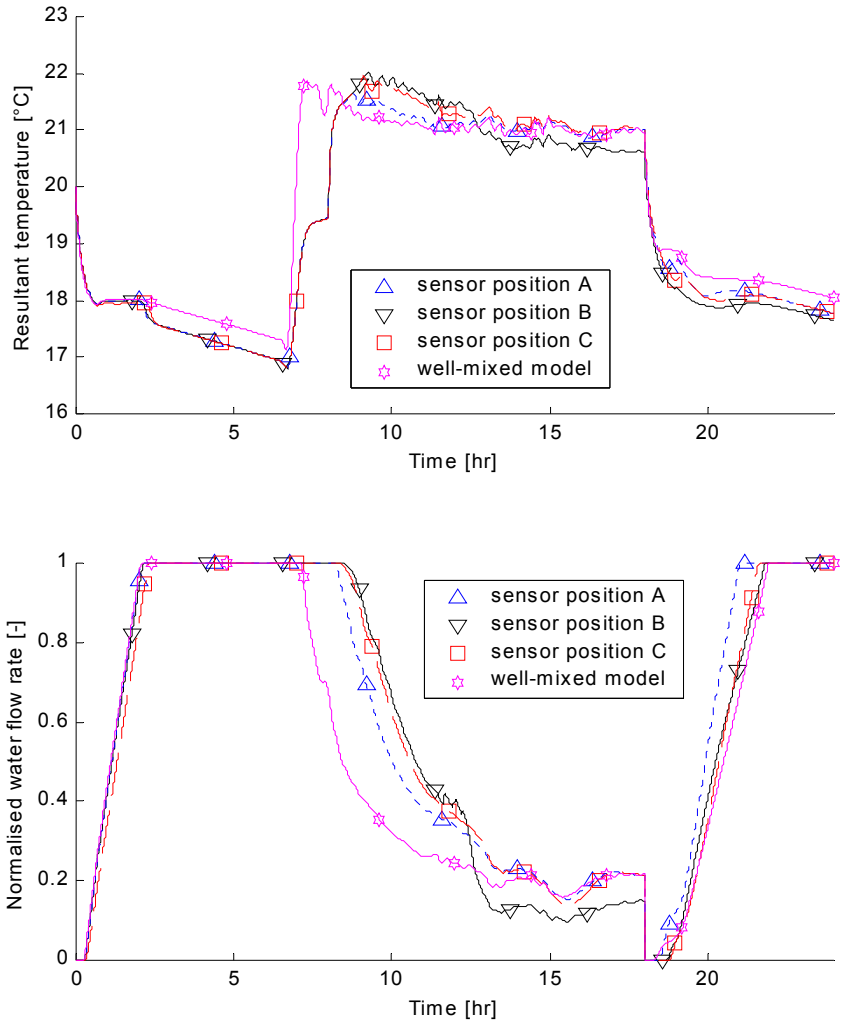

Figure V - 32: Building test -heating - radial diffuser- resultant temperature and water flow rate in zone 3

	Mean ϑ_{res} [°C]	Max $\Delta\vartheta_{res}$ [K]
Sensor position **A**	21.1	1.2
Sensor position **B**	21.4	1.5
Sensor position **C**	21.3	1.4
Well **M**ixed model	21.1	1.0
Max. difference	0.2	-0.3
Difference [%]		-23
Worst case	B	WM

Table 24: Assessment of control performance for VAV slot diffuser - heating - building test

	Mean ϑ_{res} [^{o}C]	Max $\Delta\vartheta_{res}$ [K]
Sensor position **A**	21.2	2.2
Sensor position **B**	21.1	2.5
Sensor position **C**	21.3	2.4
Well **M**ixed model	21.1	1.0
Max. difference	0.2	-1.2
Difference [%]		-56
Worst case	C	WM

Table 25: Assessment of control performance for VAV radial diffuser - heating - building test

3.2 IMPACT OF ROOM MODEL AND SENSOR POSITION ON BUILDING ENERGY CONSUMPTION

A comparison is made of the total energy consumption of the building predicted by the zonal model with different sensor positions and by the well-mixed model. The results are obtained for one day in winter and one day in summer, and for both types of diffuser. Table 26 shows the results obtained during the summer test period.

Sensor position	Slot diffuser	Round diffuser
Sensor position **A** [kWh]	538.6	509.2
Sensor position **B** [kWh]	494.2	500.8
Sensor position **C** [kWh]	549.4	523.1
Well-**M**ixed model [kWh]	526.7	526.7
Maximum difference [%]	8.2	3.4
Worst case	B	WM
Band of difference [%]	10.2	5.1

Table 26: Energy consumption - summer test day

For both types of diffuser, the energy consumption predicted by the well-mixed model is close to the mean of the four predicted values and to the values obtained using the zonal model with the sensor placed at the centre of the room (position A) or in a boundary layer (position C). Not surprisingly, the lowest energy consumption is predicted by the zonal model with the sensor placed at position B, where the cold jet influences its measurement.

The energy consumption is higher when the control sensor is placed at position C because the sensor measures a temperature that is higher than the temperature at the centre of the room. This effect will depend on conditions in the adjacent zones.

Table 27 presents the results obtained during the winter test period. In heating mode, the energy consumption predicted by the well-mixed model is significantly lower than those predicted by the zonal model. The main cause of the differences is the well-mixed model's assumption of homogeneous conditions throughout the zone, which has a major impact on the calculation of the heat losses at the surfaces and the ventilation heat losses. The convective heat exchange at the internal surfaces of the room is sensitive to the unmodelled spatial variations in the air temperature. The "bypass" effect, which is especially important in the heating case, is also not taken into account.

Sensor position	Slot diffuser	Round diffuser
Sensor position **A** [kWh]	571.7	567.2
Sensor position **B** [kWh]	629.4	579.7
Sensor position **C** [kWh]	610.6	606.1
Well-**M**ixed model [kWh]	531.1	531.1
Maximum difference [%]	10.1	6.9
Worst case	B	C
Band of difference [%]	17.2	13.2

Table 27: Energy consumption – winter test day

The highest differences are observed when the controller is placed at position B (slot diffuser) and position C (round diffuser). The obtained differences of 10.1 and 6.9% demonstrate the need for the use of a zonal model in this case.

4. IMPACT OF SENSOR POSITION AND ROOM MODEL ON THE TUNING OF CONTROLLERS

Room temperature controllers are sometimes supplied with pre-defined control parameters. The manufacturer usually specifies the values of these parameters to avoid the risk of oscillatory or unstable operation. The choice of room models or sensor positions can have no influence on the tuning of the controllers in such cases. However, in situations where simulation is also to be used to tune the parameters of the controllers, the type of room model and the assumed control sensor position can have a significant influence the outcome of the tuning process. The impact on the resulting control performance will be particularly important if the controllers are tuned to give tight control. Differences in the predicted temperature responses become larger and the risk of instability increases if the system has a relatively small dominant time constant or if low room ventilation rates are to be used.

Large differences in the transient responses have for example been observed in VAV systems in heating mode where significant temperature stratification in the room is observed. In these cases, aggressive tuning might even result in an oscillatory control loop. Figure V - 33 shows an example of this phenomenon in the case of the single room heating mode test using a radial ceiling diffuser. The controller was tuned manually using the zonal model and with the sensor at position B. The tuning process resulted in the selection of a value of 0,55 for the proportional gain of the controller, compared to a proportional gain of 0.12 for the well-mixed model.

The test conditions are the same as those given in Table 21 for the heating mode tests. Three effects are observed when the controller uses this value of gain:

- the response predicted by the well mixed model is highly oscillatory and the controller takes much longer to stabilise.
- the responses predicted by the zonal model are reasonably similar when the sensor is at the centre of the room or is in the boundary layer (position A and C).
- the resultant temperature predicted by the zonal model with the sensor in position B is not at its set-point before the step decrease in the internal gains occurs, because the control sensor is initially in the warm jet. After the step change in the internal gains, the sensor is no longer in the jet.

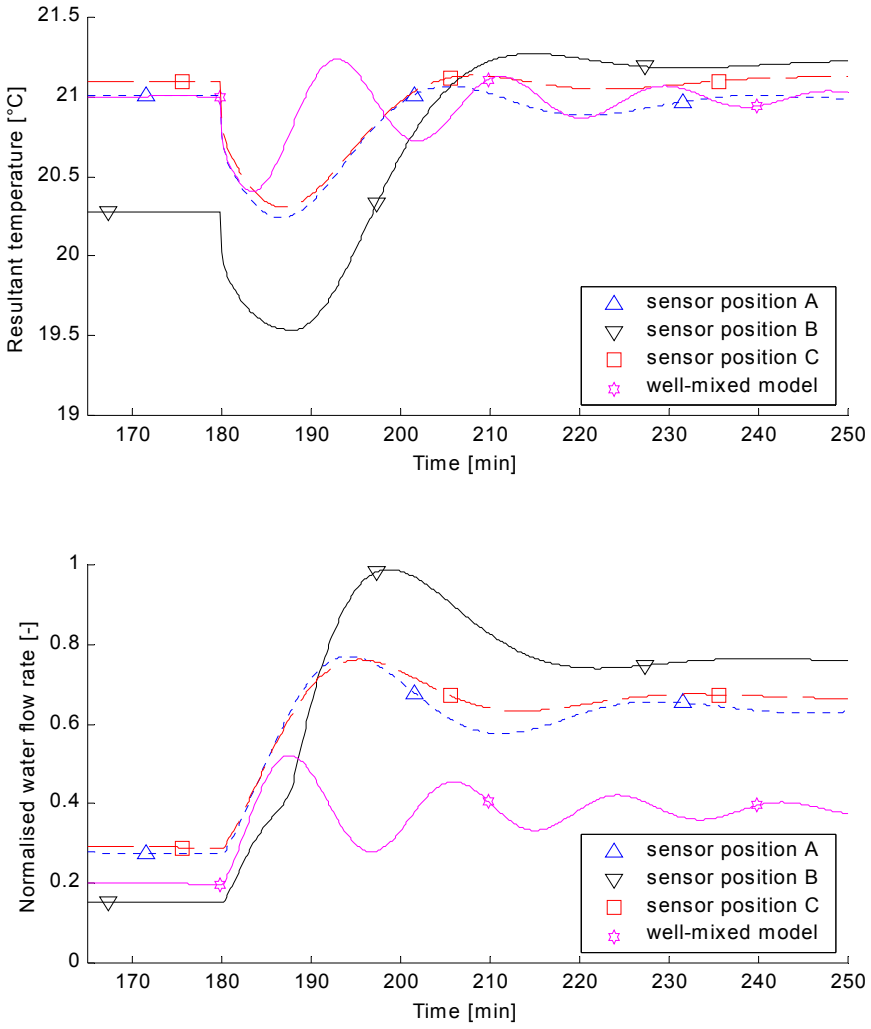

Figure V - 33: Single zone simulation after tuning of the controller using zonal model and sensor position B

Similar results can be obtained for other HVAC systems where effects of bad mixing of the room air or jets appear. In these cases the possible instability has to be considered.

5. CONCLUSION CHAPTER V

Results of performance assessment based on computer simulation will depend on the room models used and the method of performance assessment applied. The type of HVAC system is a main factor in this problem since it defines the convective phenomena throughout the room.

A second factor is the controller to be tested. P and On/Off controllers generally amplify differences between the models or sensor positions.

Problems can arise when the simulation is based on a well-mixed model of the room. The more the conditions in the room are non-homogeneous, the more differences to the benchmark (zonal model with sensor placed at the centre) appear. These differences are significant for cases where bypass effects interact on the heat emission in the room. Heating cases of a VAV system or cooling cases of a fan coil unit are typical examples.

The position of the control sensor can also have an influence on the predicted behaviour when the zonal model is used. The results have demonstrated that there are only slight differences in the predicted behaviour if the control sensor is placed at the centre of the room or outside of the possible trajectory of a jet. If the sensor is placed in the jet trajectory, a steady state difference is observed in cooling mode and both steady state and transient differences are observed in heating mode.

Similar conclusions can be made as far as the predicted energy consumption is concerned. Large differences are observed for all cases of bypass effects (e.g. fan coil unit in cooling mode and VAV system). In these cases the use of well-mixed models is not recommended.

In general it can be concluded that the more homogeneous are the actual room conditions, the more accurate will be the results obtained using a well-mixed room model.

The use of a zonal model is therefore recommended when there is significant temperature stratification, or if the control sensor is located in the trajectory of an air jet with a temperature very different from the mean room air temperature. When the sensor is located at a wall in a boundary layer of natural convection, the zonal model can be used for high temperature differences between the wall and the room air.

The following table lists the model recommendation for the studied systems (WM=well-mixed model; Z=zonal model). Whenever possible, the well-mixed model is proposed in order to minimise simulation time.

Sensor position	*Convector*	*FCU heating*	*FCU cooling*	*VAV system cooling*		*VAV system heating*	
				Slot diffuser	*Radial diffuser*	*Slot diffuser*	*Radial diffuser*
A	*WM*	*WM*	*Z*	*Z*	*WM/Z*	*Z*	*Z*
B	*Z*	*Z*	*Z*	*Z*	*WM/Z*	*Z*	*Z*
C	*WM/Z*	*WM/Z*	*Z*	*Z*	*WM/Z*	*Z*	*Z*

In the case of the convector or the fan coil unit, when the sensor is placed at position C, the well-mixed model should only be used when the temperature difference at the internal walls is small. For higher differences, the zonal model is proposed in order to take into account the effect of the colder walls.

When different performance indices are used to assess controller performance, contradictory results might be obtained. The results of three indices have thus been presented in this Chapter in order to avoid false conclusions about performance of controllers.

CONCLUSION

A room model, suitable for the study of the influence of the sensor position in building thermal control has been developed.

The important phenomena, to be represented in the model, have been analysed experimentally and by detailed simulation considering a large number of tests in this thesis with respect to two main aspects:

- *Conditions at the sensor positions for the sensor measurement*
- *Conditions at the occupancy zone for the performance assessment*

Taking into account both thermal phenomena in a room and methods of performance assessment of controllers, the zonal model approach is selected, dividing the air of the room into several sub-volumes, and is then adapted to fit the requirements of controller tests.

The model is split into two coupled parts, able to distinguish between three typical sensor positions and the conditions in the occupant zone:

- *Zonal model representing the conditions in the occupant zone,*
- *Sensor module representing the temperatures in three zones near the internal walls, where a controller's sensor is usually placed*

For the development of the zonal model, available correlations of convective phenomena in a room have been studied and existing correlations have been chosen for the implementation in the zonal model.

The second part, the sensor module, has been developed since the available correlations for negatively buoyant flow have not been found to be acceptable in the treated case. With this module, the temperature at typical sensor positions is estimated using a simple but valid approach.

The development of both zonal and sensor model has been carried out for a fixed division of the room into sub-volumes that has been found to be adapted to all studied cases of HVAC systems. If needed in the case of other HVAC systems, this division can easily be changed.

This new model has been coupled with models of conduction and radiation and structured in the graphical environment.

It has been validated for different HVAC systems and operating modes. Very good agreements have been obtained for heating cases. In cooling cases some discrepancies appeared but the results obtained were still satisfying the requirements in controller tests.

Sensitivity analysis has been carried out for the main parameters of the model estimating the conditions at the sensor positions. It has been found that an intelligent choice of parameters can minimise the errors to an acceptable level.

The model is finally used to analyse the importance of sensor position on the results of controller tests:

- *For a single room equipped with different HVAC systems, three types of controllers have been tested,*

- *For a whole building complete with its VAV system and other building services (e.g. sun-blinds, lighting etc.), controller performance and energy consumption are compared for cases of different sensor positions.*

The results are compared with those obtained using a well-mixed model.

A general conclusion about sensor position cannot be made since the importance depends on a large number of parameters, that are for example the HVAC system and its design, the room geometry, but also the controller type. The differences are generally small in terms of thermal comfort but can be significant in terms of overall energy consumption.

In general it can be concluded that the more homogeneous are the actual room conditions, the less important gets the position in the room and the less detailed room models must be. The use of the zonal room model is therefore recommended when there is significant temperature stratification, or if the control sensor is located in the trajectory of an air jet or plume or at a wall with a temperature very different from the mean room air temperature.

It has also been shown that sensor position has an effect on tuning of controllers in the case that no predefined controller parameters are available.

For different HVAC systems, either the new room model or the well-mixed model is proposed after a first study.

The developed model structure allows also an ease integration of new HVAC systems into the model in order to analyse the influence of sensor position.

The simplicity concerning parameterisation and usability makes the model interesting for manufacturers of controllers as well as for research laboratories carrying out studies in the control field. It can be used for controller tests either by simulation or by emulation.

In cases of changing of the general air flow pattern in the room the model still shows problems, especially in cases of bad design or abruptly changing loads. This problem has been eliminated in this thesis by well-designing the systems in the case of the VAV system and fixed air flow pattern in the case of the fan coil unit in cooling mode. Other, more appropriated solutions should be found in order to deal with this problem.

The model has shown good agreement for standard rooms. In the case of halls or atriums the applicability has not been proved. The division of each horizontal air layer in the model into several volumes could be more appropriated in such a case, but only at the cost of an increased complexity and greater simulation time.

REFERENCES

[Abramovich63] ABRAMOVICH G.N., The theory of turbulent jets, Cambridge (MA), MIT press, pp. 668, 1963

[Albright74] ALBRIGHT L.D., Scott N.R., The low-speed non-isothermal wall jet, J. agric. Engineering Res., N°19, pp25-34, 1974

[Allard87] ALLARD, Contribution à l'étude des transferts de chaleur dans les cavités thermiquement entrainées à grand nombre de Rayleigh, PhD Thesis, INSA Lyon, 1987

[Allard90] ALLARD F., Inard C., Simoneau J. P., Phénomènes convectifs intérieurs dans les cellules d'habitation, Revue Générale de Thermique, 1990, n°340, p.216-225

[Arditi98] ARDITI I., Husaunndee A., Mace E., Marchio D., Nannenberg S., Plokker W., Soethout L. et Visier J.C., SimTrain, a simulation package for BEMS education, SSB'98 System Simulation in Buildings Conference, Liège, pp 251-278, December 14-16, 1998

[ASHRAE97] ASHRAE Handbook of Fundamentals, SI Edition, American Society of Heating, Refrigerating and Air Conditioning Engineers, 1997

[Awbi98] ABWI, Hazim B., Calculation of convective heat transfer coefficients of room surfaces for natural convection, Energy and Buildings, 28, 219-227, Elsevier Science S.A., 1998

[Barles94] BARLES P., Dalicieux P., Inard C., Le panache des convecteurs électriques, Société Française des Thermiciens, Journée d'étude du 2 Février 1994 sur la Thermoaéraulique des Transferts couplés Emetteur de Chaleur - Bâtiments, 23p., 1994

[Bauer99] BAUER M., Methode zur Berechnung und Bewertung des Energieaufwandes für die Nutzenübergabe bei Warmwasserheizanlagen, Dissertation Universität Stuttgart, Mitteilung Nr. 3, 1999

[Beausoleil01a] BEAUSOLEIL-MORRISON I., The adaptive coupling of computational fluid dynamics with whole building thermal simulation, BS2001 conference, Rio de Janeiro, Brazil, 13-15 August 2001

[Beausoleil01b] BEAUSOLEIL-MORRISON I., Further developments in the conflation of CFD and building simulation, BS2001 conference, Rio de Janeiro, Brazil, 13-15 August 2001

[Beausoleil99] BEAUSOLEIL-MORRISON I., Modelling mixed convection heat transfer at internal building surfaces, Building Simulation 99 conference, Kyoto, Japan, September 1999

[Berglund78] BERGLUND L.G., Gonzales R.R., Application of acceptable temperature drifts to built environments as a mode of energy conservation, ASHRAE Transactions, Vol. 84:1, pp. 110-121, 1978

[Bjørn95] BJORN, E., Nielsen P.V., Merging thermal plumes in the indoor Environment, Proceedings of Healthy Buildings 1995, Fourth International Conference on Healthy Buildings, Milan, Italy, 11-14 September, Vol. 3pp. 1223-1228, 1995

[Blay93] BLAY D., Fleury B., Comparaison expérimentale de la diffusion de l'air suivant différentes bouches d'entrées d'air, Séminaire GREVRA, Sophia Antipolis, 20-21 octobre 1993, 12 p.

[Bouia93] BOUIA H., Modélisation simplifié d'écoulements de convection mixte interne, Thèse de Doctorat, Université de Poitiers, 1993, 110 p.

[Brau80] BRAU J., Modélisation thermique des bâtiments. Validation des modèles de calcul par une étude expérimentale en ambiance climatique simulée, Thèse de Doctorat, INSA Lyon, 1980, 295 p

[Buchmann95] BUCHMANN P., Modélisation numérique de la convection naturelle en cavité et d'écoulements libres de jets - application à la climatisation d'un local de grand volume, Thèse de Doctorat, Conservatoire National des Arts et Métiers, 1995

[CENTC247] CEN-TC247 Draft, Electronic Individual zone control equipment for applications: Fan coil and Induction Unit applications; Heating applications; VAV, CAV and chilled ceiling applications, Draft European standard submitted to CEN members for CEN enquiry, WI00247018

[Chen80] CHEN C.J., Rodi W., Vertical turbulent buoyant jets - A review of experimental data, The Science and Application of Heat and Mass Transfer, Oxford (U.K.), Pergamon Press, 83p, 1980

[Clarke85] CLARKE J.A., Energy simulation in building design, Adam Hilger Ltd, Bristol (UK), 1985

[Crawford62] CRAWFORD T.V., Leonard A.S., Observations of buoyant plumes in calm stably stratified air, Journal of applied Meteorology, Volume 1, pp 251-256, 1962

[Davies75] DAVIES A.E., Keffer J.F., Baines W.D., Spread of a heated plane turbulent jet, The physics of fluids, Vol. 18, pp 770-775, 1975

[Dexter94] DEXTER A., Haves P., Building control systems: evaluation of performance using an emulator, Building Services Engineering Research and Technology, 15(3), pp.131-140, 1994

[Doe89] Overview of the DOE-2 program, Version 2.1D. Simulation Research Group, Lawrence Berkeley Laboratory, LBL-19735, 1989

[During94] DURING H., Consommations énergétiques et confort thermique des locaux chauffés: approche par les modèles zonaux, Thèse de Doctorat, INSA Lyon, 1994

[Eckert51] ECKERT E.R.G, Jackson T.W., Analysis of turbulent free convection boundary layer on flat plate, NACA Report 1015, 1951

[Fang98] FANG L., Impact of temperature and humidity on perceived indoor air quality, Ph.D. thesis - 1998

[Fanger67] FANGER P.O., Calculation of thermal comfort: introduction of a basic comfort equation, ASHRAE Transactions, Vol. 73, N° 2, III.4.1

[Fanger70] FANGER P.O., Thermal comfort analysis and applications in environmental engineering, McGraw-Hill, New York, 1970

[Fanger72] FANGER P.O., Thermal Comfort, Mac Graw Hill Book Company, New York, 1972

[Fauconnier85] FAUCONNIER et al., Simulation thermique détaillé des bâtiments: Présentation du modèle BILGA, Rapport de recherche UTI/CEBTP E51.84, january 1985

[Fisk81] FISK D.J., Mean square error as a criterion for temperature control, Building Services Engineering Research & Technology, Vol. 2, N° 3, pp 127-132, 1981

[Fitzner96] FITZNER K., Displacement ventilation and cooled ceilings, results of laboratory tests and practical installations, INDOOR AIR 96, Nagoya, 1996

[Fluent98] FLUENT User's Guide, Version 5.3 (1998), Fluent Inc., Lebanon – NH, USA

[FranceAir91] FRANCE AIR, La Diffusion - Guide Technique de la diffusion de l'air, France 1991

[François92] FRANCOIS C., Maalej, Etude d'un profil de qualification des ambiances thermiques adapté à son suivi au cours du temps et aux besoins du GREC, Rapport de Recherche, convention CSTB/ADEME, N° 91-565, 15p., 1992

[Gagge67] GAGGE A.P., Stolwijk J.A.J., Hardy J.D., Comfort and thermal sensations and associated responses at various ambient temperatures, Environmental Research, N° 1, pp. 1-20, 1967

[Gagge71] GAGGE A.P., Stolwijk J., Nishi Y., An effective temperature scale based on a simple model of human physiological regulatory response, ASHRAE Transactions, 1971, Vol. 77, part 1, p. 247-262

[Goldmann86] GOLDMANN, D; Jaluria, Y., Effects of opposing buoyancy on the flow in free and wall, J. Fluid Mechanics, 1985, Vol. 166, p. 41-56

[Gordon74] GORDON R.G., The response of a human temperature regulatory system model in the cold, PhD thesis, University of California, Santa Barbara, CA., 1974

[Griffins74] GRIFFINS I.D., McIntyre D.A., Sensivity to temporal variations in thermal conditions, Ergonomics 1974, 17(4), p. 499-507

[Grimitlyn93] GRIMITNYN M.I., Fundamentals of optimising air distribution in ventilated spaces, ASHRAE Transactions, Symposia, N°SA-93-12-2, pp 1128-1138, 1993

[Gruber86] GRUBER P., Duppenthaler A., PVHS – Ein Simulator von polyvalenten Heizsystemen, Viertes Schweizer Status-Seminar, Energieforschung im Hochbau, 2/3 Oktober 1986, ETH Zürich, 1986

[Hardy49] HARDY J.D., Heat transfer, Physiology of heat regulation and science of clothing eds. L.H., Newburgh and W.B. Saunders Ltd., London, 78

[Hardy61] HARDY J.D., Physiology of temperature regulation, Physiological Reviews, N° 41, pp. 521-606, 1961

[Hassani97] HASSANI A.V., Kirkpatrick A., Sforza P.M., Flow and separation characteristics of three-dimensional negatively buoyant wall jets, HVAC&R Research, Vol. 3, N° 2, 1997

[Haves98] HAVES Ph., Norford L.K., DeSimone M., A standard simulation test bed for the evaluation of control algorithms and strategies, ASHRAE Transactions, 1998, Vol. 104, Part 1

[Hediger01] HEDIGER M., SIMTEST VAV Lab Tests Cooling and Heating, - Results and documentation of tests in HVAC Laboratory, N° HemR01.68, 19p., 2001

[Hemmi67] HEMMI P., Temperaturübertragungs-verhalten durchströmter Räume, Dissertation, ETH Zürich, 1967

[Hensel81] HENSEL H., Thermoreception and temperature regulation, Academic press, London, (Monographs of the physiological society, N° 38, 1981

[Hensen90] HENSEN J., Literature review on thermal comfort in transient conditions, Building and Environment, Vol. 25, N° 4, pp 309-316

[Hensen91] HENSEN J., On the thermal Interaction of building structure and heating and ventilation system, PhD Thesis, TU Eindhoven, 1991

[Hong97] HONG T., Zhang J., Jiang Y., IISABRE: an integrated building simulation environment, Building and Environment, 1997

[Horwarth80] HORWARTH A. T., Temperature distributions and air movements in rooms with a convective heat source, PhD, University of Manchester, 1980, 226 p.

[Horwarth85] HORWARTH A. T., The prediction of temperature variations in naturally ventilated rooms with convective heating, Building Service Engineering Research and Technology, 1985, vol.6, n° 4, p. 169-175

[Husaunndee00] HUSAUNNDEE A., Bolher A., Jandon M., Millet J.R., Visier J.C., Improving the SIMBAD toolbox for the development and assessment of integrated control strategies, Proceedings of sustainable building, Maastricht, Netherlands, October 2000, pp494-496

[Husaunndee01] HUSAUNNDEE A., Integrated control of HVAC system, lighting and blind in a building zone, Clima2000 conference, Napoli, Italy, 15-18 September 2001

[Husaunndee97] HUSAUNNDEE et al, SIMBAD: A simulation toolbox for the design and test of HVAC control systems. Proceedings of the 5th international IBPSA conference, Prague, CZECH REPUBLIC, 2 : 269-276

[Husaunndee98] HUSAUNNDEE A., Riederer P., Visier J.C., Coil modelling in the SIMBAD Toolbox - Numerical and experimental validation of the cooling coil model, System Simulation in Buildings SSB, Liège, 1998

[Husaunndee99a] HUSAUNNDEE et al, The building HVAC System in control engineering- A modelling approach in a widespread graphical environment, ASHRAE transactions, 1999, Vol. 105, Part 1

[Husaunndee99b] HUSAUNNDEE, Modélisation des installations de génie climatique en environnement de simulation graphique, Thèse de Doctorat, Ecole nationale des ponts et chaussées, 1999

[Hutter81] HUTTER E., Etude du comportement thermique des galéries couvertes par simulation en régime varié avec prise en compte de la stratification d'air, Thèse de Doctorat, Université de Paris VII, 1981, 207 p.

[Inard87] INARD C., Molle N., Allard F., Etude expérimentale du comportement thermique d'un local avec un système de chauffage convectif, Third Int. Congress on Building Energy Management, Lausanne, 1987, vol3, p. 202-209

[Inard88] INARD C., Contribution à l'étude du couplage thermique entre un émetteur de chaleur et un local, Thèse de Doctorat, INSA Lyon, 1988, 440 p.

[Inard90] INARD C., Expérimentation et modélisation dans le cadre du GREC; Synthèses des dispositifs expérimentaux et présentation des modèles zonaux, Rapport du contrat AFME/INSAVALOR, 1990, 382 p. n°0.04.0036; INSA Lyon, CETHIL Equipe Equipement de l'Habitat

[Inard92] INARD C., Essais comparatifs d'un corps de chauffe à eauc dans le cadre du GREC, Additif au rapport final, N° AFME 0.04.0036; INSA Lyon, CETHIL Equipe Equipement de l'Habitat, 1992

[Inard97] INARD C., Meslem A., Depecker P., Barles P., Structure moyenne et analyse intégrale du panache thermique des convecteurs électriques, Revue Générale de Thermique, N° 36, pp 495-509, 1997

[ISO7730] NF-ISO7730, Ambiances thermiques modérées - Détermination des indices PMV et PPD et spécification des conditions de confort thermique, Norme Internationale, X35-203, 1986

[Kapoor88] KAPOOR K., Jaluria Y, Heat transfer from a negatively buoyant wall-jet, Int. J. of heat and mass transfer, 1988, Vol. 32, p. 697-709

[Kast98] KAST, Dynamischer Anlagensimulator für Heiz- und RLT-Anlagen, Gesundheitsingenieur, 119, 1998

[Kherrouf95] BRAHIM-DJELLOUL KHERROUF S., Contribution à l'étude de l'interaction entre un jet d'air et le milieu ambiant dans les locaux climatisés, Thèse de Doctorat, Conservatoire National des Arts et Métiers, 1995

[Kirkpatrick91] KIRKPATRICK A.T., Malmstrom A.T., Knappmiller K., Hittle D., Miller P., Hassani V., Anderson R., Use of low temperature air for cooling in buildings, Proceedings of Building Simulation Conference, Sophia Antipolis, pp 62-66, France, 1991

[Klinger99] KLINGER, Bedarfsgerechte Regelung des Raumluftzustandes in Wohngebäuden – Teil 1-2, HLH, Bd. 50, 1999

[Knabe92] KNABE G., Gebäudeautomation, Verlag für Bauwesen, Berlin/München, 1992

[Knudsen90] KNUDSEN HN, Fanger P.O., The impact of temperature step-change on thermal comfort, Proceedings of the 5th International Conference on Indoor Air Quality and Climate - INDOOR AIR 90, p. 757-761

[Koestel57] KOESTEL A., Jet velocities from radial flow outlets, ASHRAE conference, Murray Bay, Canada, June 1957

[Kofoed91] KOFOED P., Thermal plumes in ventilated rooms, PhD Thesis, Instituttet for Bygningsteknik, Dept. Of Building Technology and Structural Engineering, University of Aalborg, Denmark, 1991

[Kubota91] KUBOTA H., Ogasawara K., Ijichi T., Horii T., Matuo T., Kamata N., Thermal sensation on atmosphere, INDOOR AIR, pp 257-262, 1991

[Lahrech01] LAHRECH R., Gruber P., Riederer P., Tessier P., Visier J.C., Simulation models for testing control systems for HVAC applications, BS2001 conference, Rio de Janeiro, Brazil, 13-15 August 2001

[Laret80] LARET, Contribution au développement de modèles mathématiques du comportement thermique transitoire de structures d'habitation, Thèse de Doctorat, Université de Liège, 1980

[Launder74] LAUNDER B.E., Spalding D.B., The numerical computation of turbulent air flows, Computer Methods in applied mechanics and energy, Vol. 3, 00.269-289, 1974

[Launder83] LAUNDER B.E., Rodi W., The turbulent wall-jet. Measurement and modelling, Ann. Revue Fluid Mech., 1983, Vol 15, p. 429-459

[Lebrun70] LEBRUN J., Exigences physiologiques et modalités physiques de la climatisation par source statique concentrée, PhD thesis, University of Liège, Belgium, 1970

[Lin00] LIN Z., Chow T.T., Liu J.P., Fong K.F., CFD simulation of transient cooling in a typical Hong Kong office, Proc. ASHRAE/CIBSE 2000 conference, Dublin, Ireland, 2000

[List82] LIST E.J., Turbulent jets and plumes, Ann. Rev. Fluid Mech., Vol. 14, pp 189-212, 1982

[Maalej94] MAALEJ J., Emetteurs de chaleur dans les bâtiments: comportement thermique et étude des performances, Thèse de Doctorat, Université de Valenciennes, 1994

[Madison95] MADISON R.D., Elliot W.R., Throw of air from slots and jets, Heating, Piping and Air Conditioning, 11:108, 1995

[Mathews99] MATHEWS E.H., van Heerden E., Arndt D.C., A tool for integrated HVAC, building, energy and control analysis Part 1: overview of QUICKcontrol, Building and Environment, 34, pp.429-449, 1999

[Matsuba98] MATSUBA T., Kasahara M., Murasawa I., Hashimoto Y., Kamimura K., Kimbara A., Kurosu S., Stability limit of room air temperature of a VAV system, ASHRAE Transactions, 1998

[McIntyre74] MCINTYRE D.A., Griffins I.D., Changing temperatures and comfort, Building services Engineer, Vol. 42, pp. 120-122

[Morton58] MORTON B.R., Forced plumes, Journal of Fluid Mechanics, Vol. 5, pp 151-163, 1958

[Moser88] MOSER A., Low Reynolds number effects in single room air flow, IEA Annex 20, Research Item 1.1, Working Report, ETH Zürich, Switzerland, 1988

[Musy99a] MUSY M., Wurtz E., Winkelmann, Allard F., Generation of a zonal model to simulate natural convection in a room with a radiative/convective heater, Building and Environment 36, p. 589-596, 2001

[Musy99b] MUSY, Génération automatique de modèles zonaux pour l'étude du comportement thermo-aéraulique des bâtiments, Thèse de Doctorat, Université La Rochelle, 1999

[Nevins75] NEVINS R. et al., Effect of changes in ambient temperature and level of humidity on comfort and thermal sensations, ASHRAE Transactions, 1975, Vol. 81, part 2

[Ngendeku88] NGENDAKUMANA, Modélisation simplifiée du comportement thermique d'un bâtiment et vérification expérimentale, Thèse de Doctorat, Université de Liège, 1988, 210 p.

[Osman96] OSMAN A., Model-based control of Laboratory HVAC Systems, Doctor of Philosophy, University of Wisconsin, 1996

[Özisik85] ÖZISIK M.N., Heat Transfer - A basic approach, McGraw-Hill Publishing Company, ISBN 0-07-047982-8, 1985

[Peng95] PENG X., van Passen, Simplified modelling of indoor dynamic temperature distributions, Clima2000, Brussels, Belgium, 1997

[Peng96] PENG, X., Modelling of indoor thermal conditions for comfort control in buildings, PhD thesis, Delft, University of Technology, 1996

[Phoenics91] PHOENICS, Reference manuals, CHAM Company, UK 1991

[Rajaratnam76] RAJARATNAM N., Turbulent jets, Amsterdam, Elsevier Scientific Publishing Company, pp. 304, 1976

[Ratnam98] RATNAM E., Campbell Th., Bradley R. Advanced feedback control of indoor air quality using real-time computational fluid dynamics, ASHRAE Transactions, 1998, Vol. 104, Part 1

[Redares86] REDARES C, Contribution à l'étude du comportement thermique des bâtiments en régime transitoire: proposition de différents modèles simplifiés, Thèse de Doctorat, Université de Perpignan, 1986, 245 p

[Regenscheit59] REGENSCHEIT B., Die Luftbewegung in klimatisierten Räumen, Kältetechnik, 11. Jahrgang, Heft 1/1959, 1959

[Riberon83] RIBERON J., Contribution expérimentale à l'étude de la diffusion de l'air dans un local, Thèse de Doctorat, Université Pierre et Marie Curie, Paris VI, 1983, 221 p.

[Riberon90] RIBERON J., Qualification des ambiances thermiques intérieures par mesures thermoanémométriques, Cahiers du CSTB, livraison 314, cahier 2450, 1990

[Riederer00] RIEDERER P., Marchio D., Gruber P., Visier J.C., Lahrech R., Husaunndee A., Building zone modelling adapted to the study of temperature control systems, ASHRAE/CIBSE conference 2000, Dublin, Ireland

[Riederer01a] RIEDERER P., Couturier S., Marchio D., Visier J.C., Influence of sensor position in building thermal control: Criteria for zone models, Clima2000 conference, Naples, Italy, 15-18 September 2001

[Riederer01b] RIEDERER P., Marchio D., Visier J.C., Husaunndee A., Lahrech R., Influence of sensor position in building thermal control: Development and validation of an adapted zone model, BS2001 conference, Rio de Janeiro, Brazil, 13-15 August 2001

[Riederer01c] RIEDERER P., Husaunndee A., Vaezi-Nejad H., Bruyat F., Development and quality improvement of HVAC control systems in virtual laboratories, BS2001 conference, Rio de Janeiro, Brazil, 13-15 August 2001

[Rohles80] ROHLES F.H., Milliken G.A., Skipton D.E., Krstic I., Thermal comfort during cyclical temperature fluctuations, ASHRAE Transactions, Vol. 86:2, pp. 125-140, 1980

[Rohles85] ROHLES F.H., Laviana J.E., Wei R., Wruck R., The human response to temperature drifts in a simulated office environment, ASHRAE Transactions, Vol. 91:1A, pp. 116-123, 1985

[Rouvel97] ROUVEL, Ein regelungstechnisches Modell zur Beschreibung des thermisch dynamischen Raumverhaltens, Teil 1-3, HLH, Bd. 48, 1997

[Roux84] ROUX J.J., Proposition de modèles simplifiés pour l'étude du comportement thermique des bâtiments, Thèse de Doctorat, INSA Lyon, 1984, 201 p.

[Schwartz61] SCHWARTZ W.H., Cosart W.P., The two dimensional turbulent wall jet, J. Fluid Mechanics, 1961, Vol. 10, p. 481-495

[SIMBAD01] SIMBAD - Building and HVAC Toolbox - version 2.0, document number, DDD-AGE-01-103S-ah_v200

[Simoneau89] SIMONEAU J. P., Draoui A., Allard F., Problèmes posés par la convection mixte dans la climatisation de l'habitat. Première approche en régime laminaire, Revue Générale de Thermique, jan 1989, n°325, p.31-39

[Simulink98] SIMULINK dynamic System Simulation for Matlab. Version 2.1 Mathworks Inc., Ma., USA, 1998

[Sprague70] SPRAGUE C.H., McNall P.E. Jr., Effects of fluctuating temperature and relative humidity on the thermal sensation (thermal comfort) of sedentary subjects, ASHRAE Transactions, 1970, Vol. 76, part 1, p. 146-156

[Stateflow98] STATEFLOW, For use with Simulink - User's guide, Version 1.07, Mathworks Inc., MA, USA, 1998

[Stolwijk70] STOLWIJK J.A.J., Mathematical model of thermoregulation, Physiological and behavioral temperature regulation, ed. Hardy J.D., Gagge A.P., Stolwijk J.A.J, pp. 703-721, Thomas Books, Springfield, IL., 1970

[Togari93] TOGARI S., Arai Y., Miura K., A simplified model for predicting vertical temperature distribution in a large space, ASHRAE Transactions: Research, Vol. 3630, pp 84-98, 1993

[TRNSYS96] TRNSYS, A transient Simulation Program. Solar Energy laboratory of the University of Wisconsin; Madison, USA, 1996

[Vaézi00] VAEZI-NEJAD H. et al, Projet QUALISIM: QUalité Assistée par la SIMulation – Définition du Cahier des charges et réalisation d'une première version d'un laboratoire virtuel, CSTB, Marne-la-Vallée, November 2000

[Vaézi91] VAEZI-NEJAD H. et al, The use of building emulators to evaluate the performance of building energy managment systems , IBPSA Simulation 91 , Conference proceedings building simulation 91 pp. 209-213

[Vaezi97a] VAEZI-NEJAD H., Jandon M., Visier J.C., Clémençon B., Halleur L., Lusson O., Real time simulation of a building with electrical heating system or fan-coil air conditioning system, Proceedings of Clima2000 conference, Brussels, Belgium, 1997

[Vaézi97b] VAEZI-NEJAD H. et al, Real Time Simulation of a Building with Electrical Heating System or Fan Coil Air Conditioning System, C, CLIMA 2000, BRUXELLES, 31/08-2/09/97

[Visier00] VISIER, Virtual laboratories used for climatic engineering, International Journal of HVAC&R research, Volume 6, number 6, October 2000

[Wallentén99] WALLENTEN P., Heat transfer coefficients in a full scale room with and without furniture, Building Simulation 99 conference, Kyoto, Japan, September 1999

[Walton80] WALTON G.N., A new algorithm for radiant exchange in room load calculations, ASHRAE Transactions, Vol. 86:2, pp. 190-208, 1980

[Wang99] WANG S-W, Dynamic simulation of building VAV air-conditioning system and evaluation of EMCS on-line control strategies, Building and Environment. 34, pp.681-705, 1999.

[Weinhold69] WEINHOLD K., Dannecker, R., Schwiegk U., Über Auslegungsverfahren von Lüftungsdecken, Luft-und Kältetechnik, Vol. 2, pp 78-84, 1969

[Wurtz95a] WURTZ E., Musy M., Allard F., Modélisation d'un panache d'émetteur de chaleur pour le logiciel de simulation énergétique des bâtiments SPARK, Int. J. Them. Sci. 39, p. 433-441, 2000

[Wurtz95b] WURTZ, Etienne, Modélisation tridimensionnelle des transferts thermiques et aérauliques dans le bâtiment en environnement orienté objet, PhD thesis, Ecole Nationale des Ponts et Chaussées, Paris, 1995

[Wyon71] WYON D.P., Bruun N.O., Olesen S., Kjerulf-Jensen P., Fanger P.O., Factors affecting the subjective tolerance of ambient temperature swings, Proc. 5th Int. Congress for Heating, Ventilating and Air-Conditioning, Vol. 1, pp. 87-107, Copenhagen, 1971

[Wyon73] WYON D.P., Asgeirsdottir T., Kjerulf-Jensen P., Fanger P.O., The effects of ambient temperature swings on comfort, performance and behaviour, Arch. Sci. Physiol., Vol. 27, pp. A441-A458, 1971